THE EFFICIENT USE OF DATA FROM DIFFERENT SOURCES FOR PRODUCTION AND APPLICATION OF DIGITAL ELEVATION MODELS

by

Eleftherios I. Theodossiou

A Thesis

Submitted for the Degree of Doctor of Philosophy

of University of London

Department of Photogrammetry and Surveying

University College London

Gower Street, London WC1E 6BT

U.K.

January 1990

ProQuest LLC.
789 East Eisenhower Parkway
P.O. Box 1346
Ann Arbor, MI 48106 – 1346

Abstract.

The emphasis of the investigation reported in this thesis is on the use of digital elevation data of two resolutions originating from two different sources. The high resolution DEM was captured from aerial photographs (first source) at a scale of 1:30,000 and the low resolution DEM was captured from SPOT images (second source). It is well known that the resolution of DEM data depends a great deal on the scale of the images used. The technique for capturing DEMs is static measurement of the spot heights in a regular grid. The grid spacing of the high resolution DEM was 30 m, and of the low resolution DEM was 100 m.

The aims of this thesis are as follows:

1. To assess the feasibility of using SPOT stereodata as a source of height information and merged with data from aerial photography.

This is carried out by comparison of the elevation data derived from SPOT with the digital elevation data derived from aerial photography. From the comparison of these two sources of height information, some results are derived which show the possible heighting accuracy levels which can realistically be achieved. A systematic error in the estimated average of the elevation differences was found and many tests have been carried out to find the reasons for the presence of this systematic error.

2. To develop methods to manipulate the captured data.

2.1. Gross error (blunder) detection.

Blunders made during the data capturing procedure affect the accuracy of the final product. Therefore it is necessary to trap and to remove them. A pointwise local self-checking blunder detection algorithm was developed in order to check the grid elevation data, particularly those which are derived from the second source.

2.2. Data coordinates transformation.

The data must be transformed into a common projection in order to be directly comparable. The projection and coordinate systems employed are studied in this project, and the errors caused by the transformations are estimated.

2.3. Data merging.

Data of different reliability have to be merged into a single set of data. In this project data from two different sources are merged in order to create a final product of known and uniform accuracy. The effect of the lower resolution source on the high resolution source was studied, in dense and in sparse form.

2.4. Data structure.

To structure the data by changing the format in order to be in an acceptable form for DEM creation and display, through the commercially available Laser-Scan package DTMCREATE.

3. DEM production and contouring.

To produce DEMs from the initial data and that derived from the two merged sources, and to find the accuracy of the interpolation procedure by comparing the derived interpolated data with the high resolution DEM which has been derived from aerial photography. Finally to interpolate contours directly from the "raw" SPOT data and to compare them with those derived from the aerial photography in order to find out the feasibility and capability of using SPOT data in contouring for topographic maps.

All things exist as they are, but move into higher forms.

There must be a *summum bonum* or highest good.

Aristotle (384-322 BC)

Dedication.

To my parents
and
my brother.

Acknowledgements.

Many people have helped and contributed in their own way to the initiation and completion of this thesis. I wish, therefore, to thank the following for their help.

Professor I. Badekas of the National University of Athens, who was my supervisor in Greece, for his instructions and the friends and lecturers of the same university for their discussions.

Dr. I. J. Dowman who supervised this project. I wish to acknowledge my sincere gratitude for the instruction and encouragement which I have received from him. It could not have been completed without his constant and lively interest on any odd problem during the course of this work. His broad experience in both the areas of Photogrammetry and Remote Sensing has given me the chance to learn a lot about SPOT imagery. His help throughout this period of study was invaluable.

Dr. E. Kapokakis for the directions that he gave to me in the very early and most difficult stages.

I would like to thank my parents for their patience, the encouragement that they gave to me and for the trouble of arranging every time my educational permission. I would like to thank also my brother for his encouragement. This thesis is dedicated to them.

I acknowledge the Greek State Scholarship Foundation for continuous financial support during my study, without whose grant it would not have been possible for me to carry out these investigations.

All the staff and members of the Department of Photogrammetry and Surveying, University College London and in particular:

Mike Pitkin for the manual digital elevation measurements from aerial photographs, the three SPOT measured blocks, for the experienced operator measurements comparison test, and his useful comments.

Peter Muller, who offered the aerial photography derived elevation matrix data, measured for the ALVEY MMI-137 project on "Real time 2.5D vision

systems".

Tim Day, for the use of the two sets data comparison program and for general discussions.

James Pearson, for his advice on the VAX and who kindly responded to my demand for more computer space.

Francelina Neto, for the use of the second SPOT hardcopy and general discussions about SPOT.

V. Paramananda and Hugh Thomas for their correction of the manuscript.

All my other colleagues - Akif, Christine, Clive, Faustin, George, Giotis, Kamie and Philip.

All my relatives for their support. Particularly I would like to thank my friend in Greece for the continuous correspondence and the encouragement given to me from the beginning of this project till the end. All my friends in England for their support.

Also I would like to thank Dr. D. Rokos, Mrs E. Basilaki and all of the people in Greece who although they did not know me believed in my target and contributed in granting and/or extension of my educational permission for staying in England.

IGN (France) and SPOT image for supplying the SPOT images, the aerial photographs and the ground control in the SPOT-PEPS campaign.

Table of contents

List of tables

List of figures

Chapter 4.

Chapter 5.

Appendix H.

List of maps.

Chapter 7.

List of plates.

Chapter 9.

Introduction.

1. Introduction.

During the past 10 years the use of images of the earth obtained from space has increased dramatically. Starting with the Landsat Thematic Mapper in 1982 good high resolution satellite imagery has been obtained, and in early 1986 stereoscopic data from SPOT.

Photogrammetric investigations towards SPOT system abilities for cartographic products were made even before launching. Regular topographic mapping or map updating and digital elevation models are emerging. Present trends to meet the user's needs and requirements lead to the developments of new products with updated specifications, produced more rapidly and at lower cost. Improvements in photogrammetry and in digital techniques will lead to a positive evolution and new products will certainly contribute to a significant increase in basic mapping suited for development projects in the world.

1.1. Background.

At the present time the commercially operating satellites which can be used for cartographic purposes and the experimental satellites which have the potential for cartography are the following:

The Landsat satellite which provides Multi-Spectral Scanner (MSS) data with 80 m pixel resolution and Thematic mapper (TM) data with 30 m resolution. Tests showed that a planimetric accuracy of 20 to 30 m and a height accuracy of 40 to 50 m are possible. However, the 30 m pixel resolution and lack of stereoscopic coverage are the main factors limiting its application to topographic mapping.

The Soviet high resolution systems MKF-6M, KATE-140, KATE-200 and KFA-1000. Since 1987 the Soviet company Sojuzkarta is distributing the photos taken with the KATE-200 and KFA-1000 cameras from unmanned KOSMOS satellites. For the KFA-1000 photos, permission from the imaged country is necessary according to a UN resolution. Both these cameras have operational status.

The KATE-200 is a perspective geometry camera. It is an improved version of the KATE-140 which is not operational anymore. The image format is 180 x 180 mm, the focal length is 200 mm, the orbital height is 220 km, and the photo scale is about 1:1,000,000, with a ground resolution of 25 m. It operates in 3 spectral bands. Tests showed that a planimetric accuracy of 20 up to 30 m and a height accuracy of 25 up to 50 m are possible.

The KFA-1000 at an orbital height of 220 Km produces images with format 300 x 300 mm. The focal length is 1,000 mm, producing images at a scale of 1:270,000 . The ground resolution is 5 to 10 m. The photographs obtained are vertical or oblique. Tests showed that planimetric accuracies of about 7 m, and height accuracies from 25 up to 35 m can be obtained.

The metric camera (MC) was a German experiment. A normal perspective geometry camera was carried out on board a NASA spacelab shuttle flight with an orbital height of 250 Km. The image format is 230 x 230 mm. The focal length is 305 mm and the image scale 1:820,000. The ground resolution is 16-33 m. Tests showed that a planimmetric accuracy of 8 m and height accuracy of 20 m can be reached.

The large format camera (LFC) is a NASA perspective geometry experimental camera. Forward motion compensation has been used. The flying height is 225 - 352 km, the film format 460 x 230 mm, the image scale 1:740,000 to 1:1,150,000 and the ground resolution 10 m. Tests have shown that planimetric accuracies of 6 m, and 9 m height accuracy can be reached.

The SPOT satellite provides 10 m pixel resolution (panchromatic sensor), capable of resolving a majority of the ground features required for mapping at medium scales, and 20 m resolution (multispectral mode) for thematic applications. The availability of SPOT data significantly changes the way in which satellite images may be used. It can be used for applications in which only aerial photographs were used previously. Space, and particularly SPOT imagery, offers a real opportunity to speed up the mapping programs of the developing countries. SPOT imagery has several characteristics that enable it to be very useful for small-scale mapping; world - wide repetitive coverage, uniformity over wide areas, synoptic view (large area coverage), high geometric fidelity, good

resolution, stereoscopic coverage, superior definition of certain natural features and availability at relatively low cost.

The SPOT satellite has prompted the introduction and development of new techniques. It has been in orbit for three years and it is only in the last 2 years that we have seen the development and commercial availability of software for setting up stereopairs. Nowadays, most of the analytical plotter manufacturers have developed suitable software and sell it to the users. Users have progressively grown familiar with this new reliable spaceborne multispectral sensor. The programme is now well established with SPOT 2 ready for launch in 1990; SPOT 3 under construction authorised for 1992; SPOT 4 in 1995 and SPOT 5 at the end of the development phase for this century.

There are many advantages in using SPOT for topographic mapping. Doyle (1984) showed that mapping from space photography could be six times cheaper than mapping from aerial photography and that image maps could be two orders of magnitude cheaper. Some figures for comparative costs have been published by Hartley (SPOTUK87) who has estimated on the basis of work carried out at the Ordnance Survey (UK) that data acquisition costs reduced by 66%, control costs decreased by 25-30%, preparation and triangulation reduced by about 100% and plotting reduced by 20%, giving an overall cost reduction of 30%. However, Hartley does not include costs of field completion in his figures, and work by IGN in a similar area at Ghardaia has indicated that field completion costs could be twice as high in comparison to the field completion for a map derived from aerial photography.

Although the cartographical organisations know the significance of satellite images in map production, they do not appear to be flexible enough in adopting this new source and method of capturing data. However, the market share taken by SPOT products has steadily increased and the specific SPOT capabilities have attracted new customers not yet used to this source of information. The main market figures by geographical area which appeared in the conference held in Paris for SPOT1 (23-27/11/87) are France 23%, Europe (outside France) 28%, Middle East 9%, Asia 12%, North America 24%, Latin America 2% and Africa only 2%. Market share by application has research and academic institutions buying most data (25%) with cartographic intelligence units coming next with 22% of the

total. 43% are CCTs and 57% photographic products. Most of the big cartographic organisations have been supplied with the software for setting up SPOT, and the majority of them have tried to set up at least one model. However, most of these try to develop their national database of past or recent existing information mainly as a graphical product, rather than capturing data from a new source. Moreover, the majority capture the height information by digitisation following contour lines, rather than single points for DEM production. Some of them have produced maps by extracting planimetric and height information, such as the IGN (France), the Ordnance Survey (UK) , the US Geological Survey and the McDonald Dettwiler. IGN is the organisation most involved in this mapping task. IGN has so far produced and published the following maps derived purely from SPOT images :

1. The Spécimen map in 1:50,000 scale in March - April 1986 from the first SPOT stereoscopic pair recorded under good conditions. This map appears to be more for displaying purposes rather than a systematic production. The contour interval is 40 m with intermediate contours 20 m and 10 m.

2. The Ghardaia and environs (Algeria) map in 1:100,000 in 1987. It is the first systematic trial in order to produce, starting with SPOT images, regular maps at the 1:50,000, 1:100,000 and 1:200,000, developing methods and comparing them with normal mapping procedures based on aerial photographs. The produced documents have three different styles: line map, monochrome SPOT-background map, and colour SPOT background map. In this project the accuracy of a SPOT derived map at scale 1:50,000 with 20 m contour interval, was checked. Using a SPOT image for compilation with B/H=1.0 a RMSE of 7.1 m in x ; 7.2 m in y; and 4.4 m in height was achieved using 275 check points (Denis & Baudoin 1988). Denis (IGN) claimed that a 10 m contour interval in flat areas is possible, but this seemed to be inconsistent with the heighting accuracies.

3. The Manosque and environs in the French Alps in scale 1:50,000. The contour interval is 20 m.

4. The Aix En Provence and environs (SE France) updated map in scale 1:100,000. This map was published in 1983 and updated from SPOT images recorded on 12/5/86.

5. The synthetic geometric perspective view of Nice and environs. This is generated by combining the SPOT image with a digital elevation model of the area.

IGN has also experimented in Thailand and Mali but admits that, as yet, no operational environment exists for topographic mapping.

The maps produced by IGN using SPOT images give a very good impression. However there are several problems with plotting contours due to non-perspective images and tilted views. In the non stretched images the different scale in X and Y can cause the operator to make an incorrect setting, or at least make the operators task more difficult. The detail completeness is poor but the metric accuracy claimed to be good. The fact is, however, that there is no full report of the map accuracies which have been achieved so far.

Ordnance Survey (UK) and Yemen Arab Republic (YAR) have been involved in a long-term joint project. The whole country is being mapped for the first time. 173 sheets at 1:50,000 and 12 sheets at 1:100,000 are involved. Landsat Thematic Mapper band 5 data and SPOT panchromatic data are being used as the primary data source for the mapping of the remote NE part of YAR. OS published some results from the experiments using SPOT for 1:100,000 scale mapping of YAR. It turned to SPOT, tested a stereopair against existing 1:50,000 scale mapping and decided that plan accuracies of 12 m and height accuracies of 10 m are possible. These were not as good as those reported by other workers but reflect a low density of control and some difficulty in finding natural detail. The result of the trial has convinced OS that adequate 1:100,000 scale maps with a contour interval 40 m can be produced.

Nowadays there is a great effort and trend in measuring the height information for DEM production by automatic correlation techniques from big companies (INRIA - ISTAR, MDA, Geospectra). The targets of these projects are the extraction of elevation information very quickly, accurately, and without or with a minimum of operator assistance. The French - Canadian experiment where the MDA system is used gives some figures for the accuracies of DEM generated by digital image correlation methods using SPOT images. A systematic error appears in these studies in the estimated average of the elevation differences.

Generally, the algorithms developed so far present some problems in the quality of the height information and they are not sufficiently reliable to be commercialised. The published results relating to the achieved accuracies are still not completely satisfactory for mapping purposes, but they can be used very efficiently in flying simulation and terrain visualisation.

Also in the investigation stage there is a great effort and trend from the researchers in automated mapping (Hawkins et al, 1987) and measuring the height information for DEM production by automated techniques such as: Chen et al (1988), Fukushima (1988), Hannah (1988), Otto (1988) and many others. Again the algorithms developed so far present problems. Day et al (1988,1989) gives a comparison of three different stereo-matching algorithms, and a quality assessment of digital elevation models produced by automatic stereo-matchers. Chen et al (1988) in the Taiwan experiment and Fukushima (1988) in the Mt. Fuji experiment also give some figures for the accuracies of DEM generated by digital image correlation methods. In the Mt Fuji experiment three SPOT images are used. In these studies there again appears a systematic error in the estimated average of the elevation differences.

In the investigation stage, the researchers appear to be more active in adopting SPOT as a source for extracting spatial information. The research and assessment phase culminated with the SPOT1 International Conference in November 1987 where more than 150 papers demonstrated the usefulness of SPOT data in all fields of activity. There are several studies and publications for the use of SPOT data for mapping and DEM production such as Dowman et al (1988), Bégin et al (1988) etc.

Nowadays, SPOT images have opened the field of automation, because of their suitability in the application of automated techniques. Although automated techniques are processing steadily , for the moment manual techniques remain an important production method for capturing the height information.

1.2. Main points and targets in this work.

The objectives and motivations for this work are the following:

1.2.1. To assess the feasibility of using SPOT stereodata as a source of height information.

Generally, the procedure for setting up SPOT models is covered satisfactory by Dowman et al. (1988), Ducher (1988), Denis and Badoin(1989), Simard et al (1987), Konecny et al (1987) and OEEPE tests on triangulation using SPOT data (1989). The presented results do not seem to be very representative, because of the quality and quantity of the ground control points which have been used, but they give a clear idea of the achieved accuracies .

Almost none of the worldwide cartographic organisations give any information about the SPOT heighting accuracy which can realistically be achieved. A small number of manually captured data tests were carried out for DEM production and a few results of the accuracies found have been published. Grabmaier et al (1988) assess the accuracy of a SPOT produced DEM by comparing the map derived from the DEM with the existing topographic map. The experiment gave very low accuracy results due to the errors introduced by the procedure which had been followed. Ley (1988) in the southern Cyprus experiment gives a better image about the feasibility of SPOT data. Eleven 1x1 km^2 and three 1x2 km^2 small size samples were captured in a regular grid with 100 m grid interval. The elevations were compared with points in the same position derived from the digitisation of the 1:50,000 maps. Again, in this study there appears to be a systematic error in the estimated average of the elevation differences.

The facts are that :

1. A few projects based on manual measurements have attempted to assess the feasibility of using SPOT stereodata as a source for the extraction of height information.

2. The previous investigations do not give a clear indication of the heighting SPOT accuracy or address the question of why the systematic error appears in the measurements.

Consideration of these facts has imposed and directed a part of this study to be concerned with these problems, in order to estimate the heighting accuracy levels which can realistically be achieved, and the magnitude and the possible reasons for, or sources of, the error.

In this study a lot of tests have been carried out to find the reasons for the presence of systematic error. Examples of these tests are: remeasuring DEM blocks in which a large systematic error appears; estimation of the operator variance; terrain (slope) affect; vegetation affect; error examination in a dissection procedure; off line correction for the systematic error; remeasuring blocks by an experienced operator and remeasuring blocks from a second SPOT stereopair. Several Pascal programs were written at this stage such as: the elevation checking and statistical analysis program using data from two sources - aerial photography and SPOT imagery; the DEM block joining in one larger block program; and the error displaying program.

The determination of the SPOT heighting accuracy is very important for digital elevation model creation using manual measurements, for mapping production and other applications. The determination of SPOT capability is very important in mapping in order to achieve final products of known accuracy.

For the purposes of the project, the knowledge of the SPOT heighting accuracy is very important in the blunder detection study when applying thresholds (height limits) in the blunder trapping procedure, in the data merging procedure when estimating the relative accuracy factor (RAF) of the one source to the other, and in estimating the interpolation accuracy in DEM creation for pure data derived from SPOT or merged data, when the "raw" data accuracy is known.

A study has been carried out regarding the main characteristics of the SPOT satellite. A large number of problems and error sources (weak points) are pointed out, described, and some solutions outlined. These problems could be divided into two main categories, the physical and the technical problems. The vast majority of physical problems are inevitable and related to the earth, orbital dynamics, sun illumination and atmosphere. The technical problems are related to the satellite characteristics and the recording device (sensor). Some of them could be identified and solved during the satellite's life, and some others are going to be

considered in future planning, as in the case of SPOT2 for example. A problem which has been solved during the life of SPOT1 is the problem of images affected by horizontal and vertical stripes (effects of the pushbroom sensor). All the images originating after July 1986, can be corrected, but not before (Begni, 1988) . Also, better on-board data (orbital parameters) as header data are now available to the users.

Finally, the mapping procedure from SPOT satellite imagery introduces some errors, because of the measuring conditions, due to image physical quality, terrain roughness, operator error, atmospheric conditions affecting the particular image (clouds, haze), and vegetation coverage.

1.2.2. To develop methods of manipulating the captured data.

Any mapping project produced must conform to a set of standards. As such this introduces an obligation that the captured data should be:

1.2.2.1. Transformed into a unique coordinate system.

1.2.2.2. Having minimum possible error.

1.2.2.3. Merged into a known and unique set of data, if data from different sources are used.

1.2.2.4. Suitably structured.

In the data manipulation stage the captured data have to be arranged, examined and processed with different methods. Some of the data manipulation stages, methods and techniques which are examined are the following:

1.2.2.1. Coordinate transformation stage.

Usually, the coordinate system is chosen to be the same as that adopted by the national cartographic organisation, in order for the data to be ready for map production, or directly comparable. The test area used for this project is in France (Montagne Sainte Victoire). The projection system used in this work is that adopted for official mapping by IGN (Institute Geographique Nationale), Lambert

Conformal Conic zone III. A general earth centred Cartesian Geocentric coordinate system is used for setting up satellite imagery in order to avoid the effects of earth curvature caused by flattening (mathematically) of the earth surface to the map projection. In order to get output data from the DSR1 analytical plotter in a square regular grid, the UTM projection system was chosen, because the geographical system gives different interval value for Northings and Eastings; and the geocentric system is not used for mapping purposes.

Several Pascal programs were written in order to do the transformations in the forward and reverse way for these four projection systems (Geocentric, UTM, Lambert and Geographical systems).

All the data measured from the analytical plotter had to be transformed from UTM via geographic to Lambert zone III system. An error is introduced due to the multiple transformations, initially from control points transformation stage, through the output data from the analytical plotter and finally from the transformations during the data manipulation stage.

In this project the projections and the coordinate systems employed are studied, and errors caused by the transformations are estimated.

1.2.2.2. Blunder detection method and technique.

The errors which are involved in a data capture procedure are: the gross, systematic and random errors. In order for the data to have the minimum possible error it is necessary to apply techniques for eliminating and trapping. Erroneous data can be removed or corrected if the value of the error is known. Elimination of systematic error(s) is generally an easy procedure when the magnitude and the source(s) of the systematic error(s) are known.

Gross error detection is a much more difficult task, and as yet there is no complete remedy. Blunders are made during the data capturing procedure and affect the accuracy of the final product. Therefore it is necessary to trap and to remove them. The main characteristic of a blunder is that its magnitude is very large in comparison with the measured value itself. Blunders are subdivided further into

large, medium and small. Large blunders are introduced mainly in the automated procedures and are easily detected, while medium and small blunders are much more difficult. It is remarkable how blunders affect the nearest "correct" points and it is well known that after a statistical analysis, points which appear as large residuals are not necessarily or likely to be blunders.

In recent years much more attention has been paid to blunders by the international photogrammetric community, which is involved in the aerial triangulation process, but only a very few investigators have been concerned with the blunders involved in the data captured for DEM purposes. Some works were centred on global techniques such as: fitting polynomials to the data (Jancaitis and Junkins,1973), filtering in both the spatial and frequency domains (Johnson, 1978), with other known problems of the global techniques; and only one Hannah (1981) has developed some local methods using constraints on both allowable slope and the allowable change in slope in local areas around each point.

SPOT data contain blunders mainly due to the measuring conditions. In this work a study of the blunders involved in the SPOT data is carried out and a locally self-checking blunder detection algorithm is developed.

1.2.2.3. Data merging method and technique.

Data have to be merged if they are derived from different sources or acquiring methods (This presupposes different accuracies).

It is a fact that in the worldwide cartographic organisations there exist data from different sources. The most common sources are the existing maps, through digitisation procedures and the stereoscopic models by applying photogrammetric techniques. Photogrammetric techniques can be applied on aerial photography or satellite imagery, softcopy or hardcopy data, depending on the platform, the source, the media, and the method of the information being recorded. In this study two different sources are examined. The aerial photography and the SPOT satellite imagery. There are two main instances:

1.2.2.3.1. Collecting elevation data from SPOT as main frame (source).

Capturing data from SPOT imagery in a dense grid covering a large area as a main frame and then in one part of this large area we capture some additional data from aerial photography with the same or lower density of grid. This applies when a SPOT DEM exists and we want to fill a gap or to get better relief representation and terrain features over part of the area, keeping the SPOT information.

1.2.2.3.2. Collecting elevation data from aerial photography as a main frame.

The data are captured from aerial photography in a dense grid as a main frame and then some additional data from SPOT imagery are collected to fill a gap, or to get later relief changes, for the map updating procedure. It is not a realistic case, but it has some applications in countries with boundary problems. Also it can happen in the experimental stage as it did in this project where the aerial photography data was captured in a 30 m regular grid (main frame), while the SPOT data is in 100 m.

Generally it is hard to find references for merging data derived from different sources and in particular there are no previous references for merging data from the two different sources used in this project.

The commercially available Laser-Scan DTMCREATE software installed on a VAX/VMS work-station in the Department of Photogrammetry and Surveying at UCL and used in this project does not accept different reliability data (having different weights). In order to be able to process them and to achieve uniformity in terms of the final product, a data merging algorithm was developed. The merging algorithm allows two sets of data with different accuracy to be suitably merged into one set of data of uniform accuracy.

The two data sources were merged as follows:

1. In a 30 m grid interval (the high resolution source grid interval), by taking into account their relative accuracy depending on the source from which each was derived. This was carried out by applying the estimated relative accuracy factors (RAF) or weights for the aerial photography and SPOT data.

2. In a 60 m grid interval, which is derived by skipping the aerial

photography data, through the data skipping procedure.

The data in each of the above cases were merged as follows:

1. According to the estimated RAF and

2. As equivalent accuracy data, having the same RAF, which means that the SPOT data were merged as being as accurate as the aerial photography data.

After the merging procedure the data are checked directly with the initial high resolution data. A statistical analysis was followed in order to estimate how the lower resolution source data affect the high resolution data, in dense and in sparse form.

1.2.2.4. Data structure technique.

The design of a data structure is far too important to leave to chance or to pursue haphazardly. For almost all applications a poorly designed data structure can result in the failure of the application. It may be expensive in run time or in storage space. It may not be transferable to an updated hardware system, or in the worst case, the manipulation routines may never function correctly because of obscurity and unnecessary complexity in the data structure. The data structure should be sophisticated, satisfactory to the memory requirements and processing speed for a particular situation.

Nowadays the commercially available packages lead the way and the user simply has to follow the data structure which is recommended. In this work the data has to be structured by changing its format. Several Pascal and Fortran programs were written to change the data format and several Laser-Scan routines were used during the data manipulation procedure, from the initial output file from the analytical plotter (count number and string of coordinates), to the Laser-Scan Internal Feature Format (acceptable input form for the DTMPREPARE package), to DTI format suitable for displaying purposes, up to ASCII WORD or real data suitable for statistical analysis purposes.

1.2.3. DEM creation and contouring.

Initially the accuracy of the interpolation package, or more specifically of the smoothing application function, is examined. This was carried out by interpolating the data derived from the aerial photography, and the data merged from two sources. The interpolation was carried out in the same sidelength as the captured grid. Then the data are compared directly with the initial data (interpolated and non interpolated). A statistical analysis is followed, in order to estimate the accuracy of the smoothed data.

Contour maps at scale 1:25,000 and 1:50,000 were produced from the interpolation of aerial photography data (30 m grid) and the interpolation of SPOT data (100 m grid). The contour interval was 20 m. The two SPOT hardcopy data were used to produce contours in order to examine the quality of the contours in relation to the image quality.

The 1:25,000 aerial photography and the SPOT derived contour maps were overlayed using a different colour. The two SPOT hardcopy data were overlayed separately. A grid was overlayed in another different colour on top of the aerial photography derived contours. This procedure facilitated the quality assessment of the contours derived from SPOT compared to those derived from the aerial photography data.

1.3. Outline of the thesis - overview.

The thesis is organised into ten chapters.

Chapter 2. Digital elevation model, terrain description and data acquisition methods.

A brief outline is given in the first part on the meaning, the definition of the DTM; and the difference between the digital elevation model, digital ground model and digital terrain model. The significance of the DEM and SPOT imagery as a part of GIS/LIS follows; and all the steps for a DEM generation and creation are outlined.

In the second part there is a review on data acquisition which addresses the terrain type, terrain use, sample density, pattern and sampling mode.

At the beginning there is a description of, and approach to, the terrain (terrain type and use). The terrain is described and evaluated through parameters and approaches such as the geomorphometric and the mathematical approaches. Methods of terrain classification by photogrammetrists are described; adopted terrain types, slope categories and land classification which are suitable to the project requirements are estimated. Two Fortran programs were written. The first was to estimate the gradient and the aspect and the second to convert the estimated values in a raster form, in order to be able to display through the existing displaying module. The presentation in a raster form of the gradient and aspect for the two sources derived "raw" data give a very good indication of the data quality.

A review of the data collection follows. Sampling density, pattern, and mode, which are suitable for DEM data capture are examined. The sampling patterns are divided into three main patterns, the grid, the random and the combination of those. The advantages and disadvantages of those patterns are pointed out. The sampling density is examined in relation to the sampling pattern and the terrain type. The relation between density, economy and accuracy factors is pointed out. The crucial factors in choosing the data collection method and measuring point density are examined. Finally the data collection method and pattern used in this project are presented.

Chapter 3. Data collection implementation, sources, methods and techniques.

This chapter is related to the data capture methods and techniques; data collection implementation; data collection software; the problems and weak points of all the procedures; and the SPOT satellite imagery.

At the beginning there is a reference to the data acquisition methods and techniques.

The data collection implementation used in photogrammetry is explained. The analytical plotters are briefly described with emphasis on the Kern DSR1 analytical plotter which is used in this project. The data capture program used in the project is described and its accuracy is determined.

The problems and the weak points of all the procedure are pointed out starting from the major technical problems in photogrammetry, the implementation (particularly those which are related to the hardcopy used in the analytical plotters) and the SPOT satellite images. In this section there is a brief description of the SPOT satellite, the image quality - physical error sources (eg.

earth, orbital dynamic, platform, sun illumination, atmosphere) or reasons due to technical characteristics (ie sensor, mirror view angle) . Some solutions and corrections to be applied are outlined. A brief description of the software for setting up SPOT images follows, and the procedure for setting up SPOT on the analytical plotter (exterior orientation accuracy) by previous investigators is described.

A reference to the previous SPOT heighting accuracy for DEM generation experiments follows and some statistical figures are estimated.

Finally there is a brief presentation on the SPOT image utilisation, assessment and results as well as the significance of SPOT for topographic mapping.

Chapter 4. Test data.

This chapter describes the test area and gives the image characteristics of the two different sources: aerial photography and SPOT satellite. There are two SPOT stereopairs of the same area used in this project. A primary statistical analysis of the aerial photography source is given in terms of: control point accuracy, aerial triangulation accuracy and accuracy of the setting up procedure. Then the control point accuracy for the SPOT stereopairs and the accuracy of the setting up procedure on the analytical plotter are determined.

Chapter 5. Accuracy of captured data.

Chapter 5 is concerned with the estimation of the accuracy of the SPOT data. A review of the statistical methods applied to the data regarding the sources and types of errors is presented. Then the accuracy of the captured data from aerial photography is estimated. The aerial photography data is more reliable, so was used as the "ground truth" (high resolution) in order to evaluate the SPOT data (low resolution). The SPOT data accuracy (SPOT heighting accuracy) is estimated by direct comparison of the SPOT data with the high resolution elevation data derived from aerial photography. A lot of tests were carried out at this stage such as, remeasuring DEM blocks in which a large systematic error appears; estimation of the operator variance; terrain (slope) and vegetation effect; error examination in a dissection procedure; off line correction for the systematic error; remeasuring blocks by the experienced operator and remeasuring blocks from a second SPOT stereopair. Several Pascal programs were written at this stage such as, the elevation checking and statistical analysis program using data from the two sources; the DEM block joining into one larger block program; and an error

displaying program. Finally, discussion, conclusions and recommendations are given regarding the SPOT heighting accuracy achieved.

Chapter 6. Manipulation of the DEM data.

Chapter 6 looks at some aspects of the manipulation of the DEM data as follows:

Firstly the SPOT data have to be transformed from the UTM projection (output from the DSR1 analytical plotter) to the Lambert zone III projection, in order to be comparable with the aerial photography data. An inevitable error is introduced to the coordinates due to the multiple transformations, initially from the ground control points transformation stage, through the output from the analytical plotter and finally from the transformations during the data manipulation stage. The errors caused by transformation are examined and evaluated.

Secondly a local self-checking and trapping blunder detection algorithm is developed in order to check the data (particularly the SPOT data) for blunders which are apparent during the data capturing procedure.

Thirdly the aerial photography data with 30 m grid spacing and the SPOT data with 100 m grid interval are suitably merged. In order for this to be possible the relative accuracy factors (RAF) are estimated. Then the data are labelled with the various relative accuracy factors (RAF) and merged, bearing in mind the uniform data accuracy needed in order to have a known accuracy final product (eg. a contour map). The SPOT data were merged the first time with the application of the estimated RAF, while the second time were merged with RAF = 1.0, which means as equivalent to the aerial photography data. This was necessary because the Laser-Scan software does not accept different reliability data (with different weights).

Fourthly the aerial photography data with 60 m grid spacing (sparse data - data skipping procedure) and the SPOT data with 100 m grid interval are merged. Again the SPOT data were merged the first time with the application of the estimated RAF, while the second time were merged with RAF = 1.0, which means as equivalent to the aerial photography data. The variable grid density data are used in order to estimate how the SPOT data density affects the DEM accuracy and quality.

Finally the data was changed in format in order to be ready and in acceptable format for input to the commercially available Laser-Scan DTMPREPARE, DTMCREATE and displaying software.

The manipulation flow-charts of the aerial photography and SPOT derived data are shown in the figures 1.1 and 1.2.

Chapter 7. Accuracy of the DEM.

In this chapter the DEM accuracy considerations, the influence of the terrain structure, the relief representation through the interpolation methods, the predicted accuracy of a DEM, and the interpolation errors and contouring from DEM data are presented.

The influence of the terrain is examined by estimation of the semivariogram. The semivariogram of the test area is presented and the interpretation is given. This is followed by a study of fractals, and the fractal dimension of the test area is estimated.

The interpolation methods are presented. Two basic categories of interpolation methods are examined : grid-based and triangulation-based interpolation. Grid-based and triangulation-based categories are compared and the directing factors in choosing an interpolation method are outlined. The pointwise, global, and patchwise grid-based (random to grid) methods are further examined and compared. The required accuracy of the interpolation method is estimated as a key factor in estimating the optimum sampling interval.

The accuracy of the interpolation method, or more specifically of the smoothing interpolation function of the DTMCREATE package is estimated. The aerial photography and the data merged from two sources are interpolated in the same sidelength as the grid interval. A statistical analysis follows and the accuracy results are estimated in order to examine whether there is any effect of the smoothing function or of the generation of the imaginary points.

Finally the contouring interpolation methods (contour creation from grid and triangulated data) are outlined and the quality assessment of the interpolated contours at 20 m intervals derived from the SPOT DEM data, as compared to the contours derived from the aerial photography (background) is carried out.

Chapter 8. Automated techniques of capturing data for DEM production.

This chapter looks at the automated techniques of capturing height information for DEM production.

At the beginning there is a brief reference to the automated techniques applied to the photogrammetric instruments. Then a brief reference is made to the current techniques applied to the digital images.

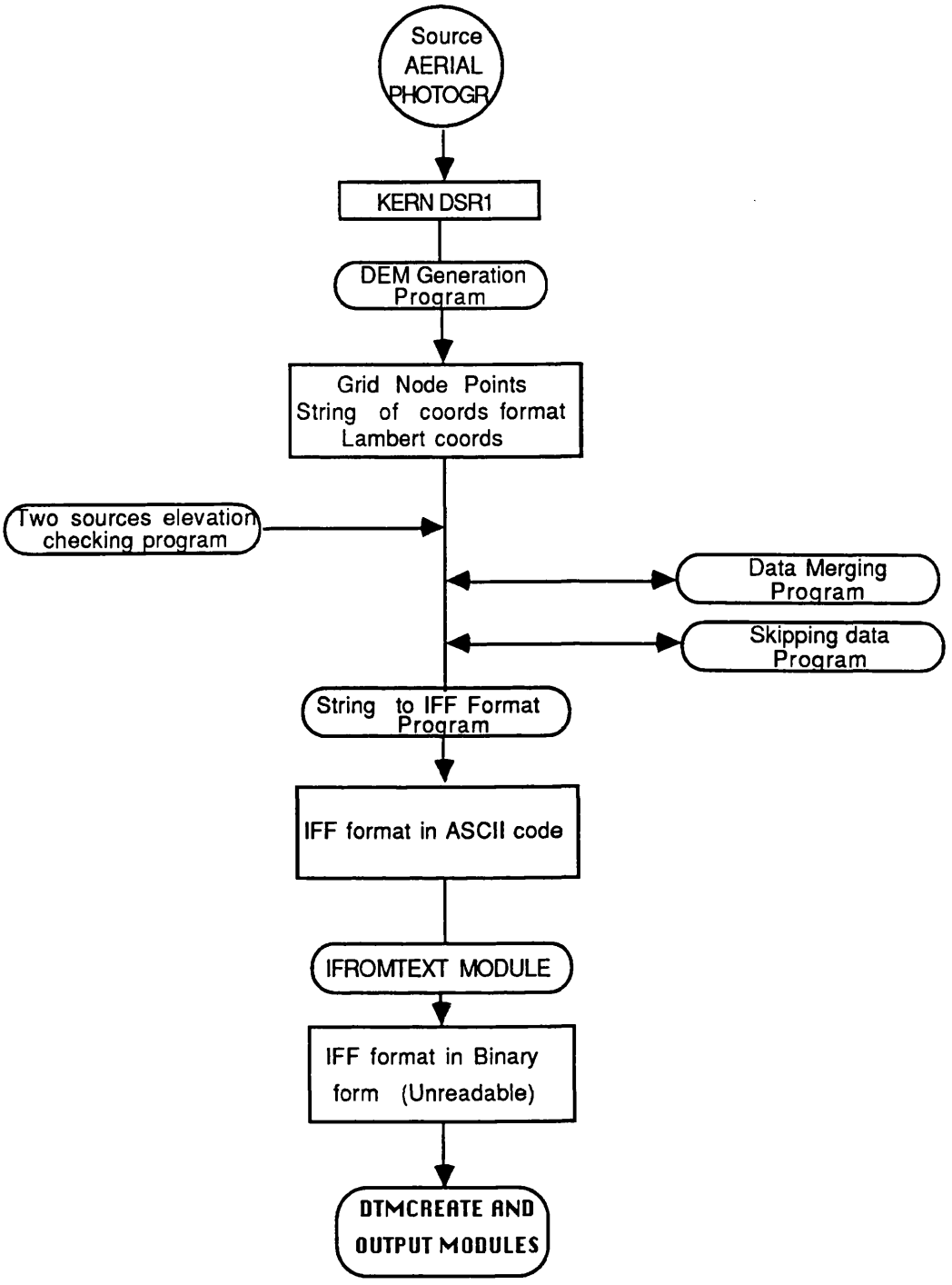

Figure 1.1. Manipulation flow-chart of the aerial photography data.

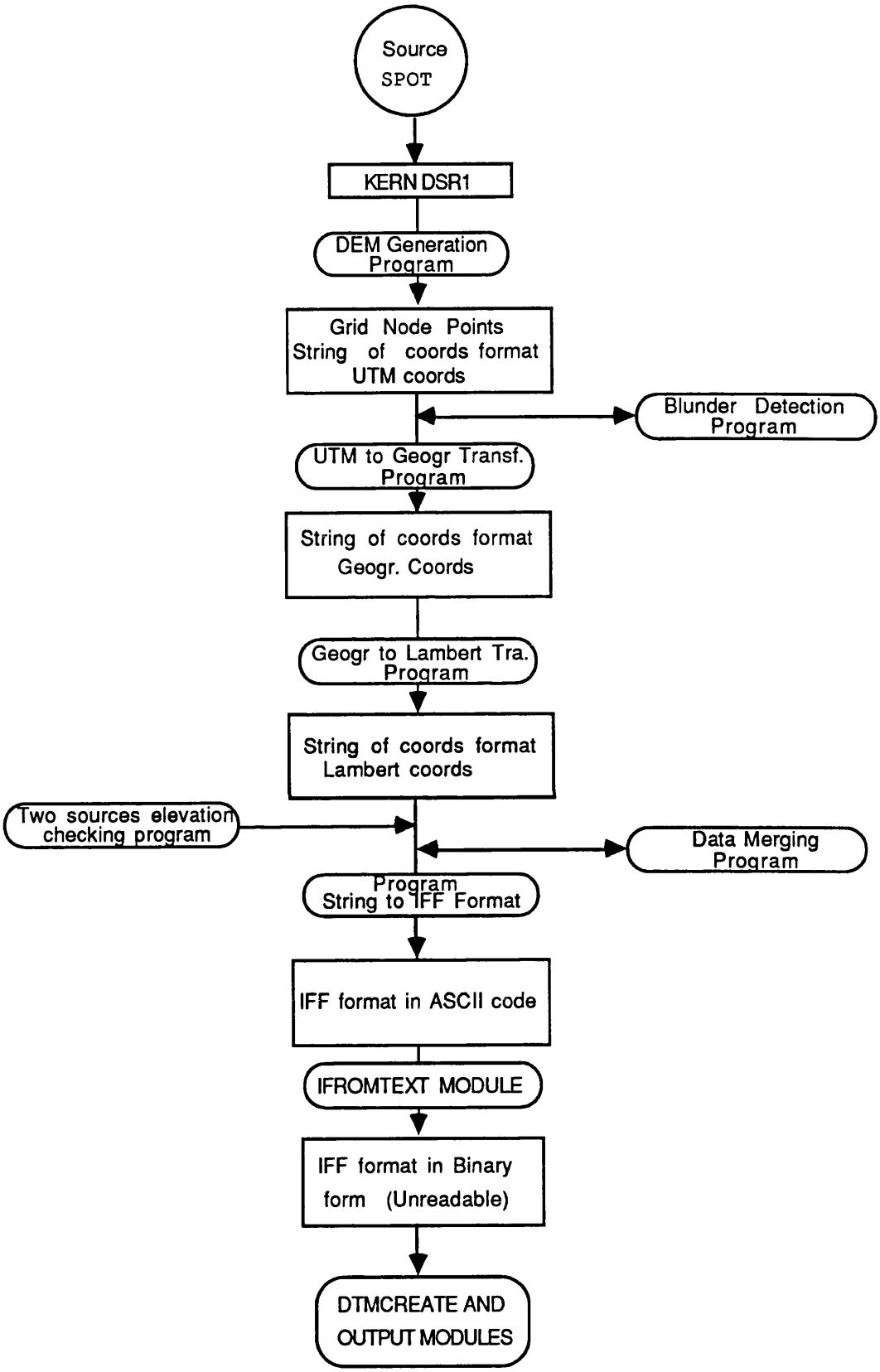

Figure 1.2. Manipulation flowchart of the SPOT data.

The automated techniques used in the Department of Photogrammetry and Surveying at UCL are examined. A brief description of the stereomatching algorithm and a quality assessment of the UCL experiment are given. The MDA system is outlined and a quality assessment of other experiments such as: the French - Canadian, the Taiwan and the Mt. Fuji experiment are presented.

The relation between the manually captured DEM data and that generated by stereomatching algorithms is examined. Finally the manually and the automated data capturing methods are compared.

Chapter 9. DEM applications.

This chapter is a general outline of the DEM applications, the uses of DEMs in topographic mapping, and the applications of the DEMs derived from SPOT imagery.

Chapter 10. Work summary, conclusions, discussion and recommendations.

This summarises the work and the results achieved. Then conclusions, and a discussion, recommendations for future work are made.

Chapter 2.

Digital elevation models.

2. Digital Elevation Models.

2.1. General - Definitions.

Landform is usually perceived as a continually varying surface that cannot be modelled appropriately by the choropleth map. A continually varying surface can be represented by contours and these contours can be effectively regarded as sets of closed, nested polygons. Although sets of isolines (contours) are very suitable for the display of a continually varying surface, they are not particularly suitable for numerical analysis or modelling. So other methods have been developed in order to be able to represent and to use effectively information about the continuous variation of an attribute (usually altitude) over space.

Surface modelling is a general term which is used to describe the process of representing a physical, or artificially created, surface by means of a mathematical expression. In order to generate the model, a set of samples (x_i, y_i, z_i ; i= 1,2,...,n) are obtained from a real surface. The x and y coordinates are associated with the spatial positions of sample values while the Z coordinates represent the values of the variable which is modelled. This variable can be elevation (most common), temperature, wind speed, population distribution, pollution distribution etc. So the digital surface can be applied to any surface for which numeric information can be obtained. Terrain modelling is one particular category of surface modelling which deals with the specific problems of representing the surface of the earth.

The concept of creating digital models of the terrain is a relatively recent development and the introduction of the term Digital Terrain Model (DTM) during the late 1950's is generally attributed to Miller and LaFlamme (1958).

Elevation is essentially an instantaneous point value. In a dense grid format DEM, each elevation value represents the basic phenomological unit of analysis and therefore, is analogous to pixel size in remote sensing imagery, or photographic resolution in photographs. The terrain is viewed as a two-dimensional signal where the pixel size or denseness of the grid is analogous to the sampling rate of elevation.

The DEM concentrated the interest of photogrammetrists when analytical plotters became commercially available, in relatively low price, because of the mass production and the analogue photogrammetric instruments were connected with encoder units, so it was possible for the direct contribution of the computer in data processing and mapping to be realised. DEMs provide the same sort of information as contour maps, but in a digital rather than analogue format suitable for processing by computer-based systems.

Three main terms (digital elevation model, digital ground model and digital terrain model) are used widely by the scientists in that field which have been coined to describe this, or closely related processes. Although in practice these three terms are often presumed to be synonymous, in reality they often refer to distinct products. Because a little of confusion rises in that point the following definitions are provide to simplify and to standardise the use of these three terms (Petrie, 1987).

Digital elevation model (DEM), refers to the creation of a regular array of elevations, normally in a regular or irregular grid. In other words digital elevation models refer to the creation of elevations array over the terrain and it has the feature that the elevation information may be composed of either regularly or irregularly spaced pattern.

Digital ground model is similar to a DEM but with the additional feature that it may be composed of either regularly or irregularly located data points. There is also presumed to be some connection between the elements which are no longer considered discrete. This connection generally takes the form of an inherent interpolation function which may be used to generate any point on the ground surface.

Digital terrain model (DTM) , is considered by some to include both planimetric and height information. However, unlike the previous definitions this representation may also include derived data about the terrain such as slope, aspect, visibility and so on. The data method of storage is the grid based method.

There are many definitions of DTMs. Some of them are the follows:

1. Blaschke's (1968) emphasised the importance of "storing measured coordinates X, Y, Z of characteristic terrain points in sufficient quantity and significance .....".

2. Leberl (1973) has given a more definitive definition, that a DTM is a set of representative points of the surface of the terrain stored in the memory of a computer, and algorithms to interpolate any new point of given planimetric location or to estimate other data.

3. Ayeni (1976) has given a rather comprehensive definition of a DTM as being the numerical (or digital) and mathematical representation of a terrain by making use of adequate elevation and planimetric measurements, which are compatible in number and distribution with that terrain, so that the elevation of any other point of known planimetric coordinate can be automatically interpolated with specified accuracy for any given application

4. Doyle (1978) finally gave the definition that digital terrain models (DTMs) are mathematical models representing in digital form the behaviour of a given variable associated with a terrain point.

From the above definitions it can be seen that a digital elevation model refers only to captured grid data, while the term digital terrain model is more general and includes grid data as well as other data.

In this work the data are captured in a regular grid. Because no other information about the terrain is included, the term digital elevation model is the appropriate term to be used in this thesis. Moreover the terms digital ground model and digital terrain model have to some extent been superseded by the term digital elevation model, which has become widely used in the scientific literature.

2.2. The DEM and SPOT imagery as a part of GIS/LIS.

A Geographical Information System (GIS) allows the integration, in a single data base, of information from several different origins, such as: thematic maps, DEM data, satellite images, statistical tabular data etc. Digital elevation modelling

has made a great contribution in mapping and it is an important part of the integrated GIS or LIS.

The collection of DEM data for the establishment of a digital data base is an enormous task. A well organised system is needed to establish a digital topographic data base for further use in a geographic information system because not only is collection of digital data involved but also a larger task of merging data into one single data base. A large DEM data base, therefore, needs a well organised system, both for production and utilisation of the data. Probably one of the most important stages is the integrating and merging stage with other data sources. This is not easy since capturing data in a regular grid mode is not practical, but preferable, because of its simplicity. The merging of data destroys this regularity. An attempt to interpolate grid data could be made, but the accuracy is reduced.

The use of digital satellite imagery in the field of GIS is becoming an important alternative method in the creation of GIS coverage, because of the widening availability of high resolution SPOT imagery, dramatic reductions in the cost of computer workstations and growth in the GIS market. Satellite imagery affords the user greater flexibility, in determining scale, time of analysis, level of detail, and most important what information the imagery should contain, for the user of hardcopy products only.

The most important of functions within the GIS is the production of base mapping particularly in scale 1:50000, reasonably complete from SPOT satellite images (Dowman et al, 1987) , the equal importance of map revision and the terrain visualisation in which the satellite imagery can be used with a DEM to produce a realistic perspective view of the ground.

More specifically in a Digital Cartographic Data Base, as a part of a GIS, the digital terrain data can be in DEM form only or in DEM form plus digital line graph (DLG) form which represents the hypsography and hydrography of the terrain. DLG data sets are composed of topologically structured nodes, lines and areas with related feature attributes and coordinates. The hypsography consists of information on topographic relief (primary contour data) and supplementary spot elevations. Hydrography consists of all flowing water features (breaklines), standing water, and wetlands. Apart from the features already mentioned it can include information

such as surface cover, nonvegetative surface features such as boundaries, transportation and other significant manmade structures. Existing topographic maps contain a large amount of terrain information. This information is useful and can be converted in digital form with the digitisation techniques. DEM data can be derived by interpolating elevations from DLG.

One example of such a recent creation is the Digital LandMass System (DLMS). It is a data base of terrain and associated cultural information. It consists of two independent components, - the digital terrain elevation data (DTED), which is used by the US Defence Mapping Agency (DMA), and the Digital Feature Analysis Data (DFAD).

At the moment the integration of SPOT satellite imagery within the GIS allows the full use of vertical satellite imagery (the sensor view angle should be as close as possible to zero). The image input is from computer compatible tapes (CCT). The image registration and transformation (rectification) to the ground is possible by means of control points (about four for the whole scene). The satellite image can be geometrically corrected (geocoded). Then the image can be used for map generation and revision. If a DEM is available the imagery can be draped over a perspective terrain view.

In the integration of the photogrammetric systems with GIS there remain some problems. The analytical plotter can supply a GIS normally with vector map data extracted from the hardcopy imagery. This a major barrier between photogrammetry and GIS. Recent developments however in digital photogrammetry have brought the two closer because it is now possible to perform a full range of photogrammetric operations on digital imagery, using a workstation that can also be used for conventional GIS applications.

2.3. Steps to create a DEM.

The creation of a DEM includes the following procedures:

1. Collection of the primitive data.
2. Conversion of the data information.
3. Representation of the relief in digital form which will be useful for

further use.

In order carry out the above procedures, the following factors have to be taken into account:

1. Desirable characteristics (prescribers) of the final product.
2. Characteristics of the object related to the survey.
3. Data structure.
4. Methods and instruments to collect the primitive elements.
5. Algorithmic conversion.

The creating and generating a DEM steps appears in the follows figure 2.1:

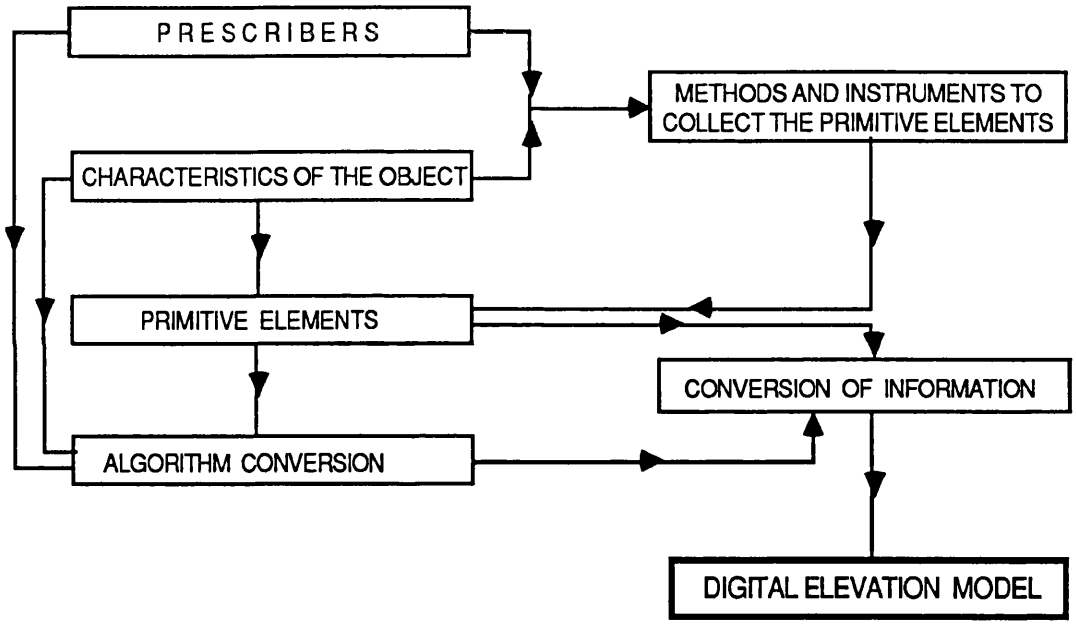

Figure 2.1. DEM generation and creation steps.

The desirable characteristics (prescribers) of the final products are very important and should be determined at the beginning of each project. During the exercise they are going to be the pilot line, in achieving the specified targets. These could be:

a. The type or the structure of the product, governed by compromise between sophistication, flexibility and production cost.

b. The quality, which means the accuracy and the measurements credibility (precision).

c. The cost of the DEM which is in inverse proportion to the quality (for a given accuracy).

The characteristics of the object related to the survey (terrain) is another important factor, in achieving the desired accuracy and adopting the suitable methods and techniques. From the characteristics and the conditions we can determine the best distribution and density in the spacing of the reference points which should be collected.

The determination of the surface problem could be solved in different ways, such as by carrying out sample measurements, during the data capturing procedure, or later by removing the redundant information. The selection of the method of primary collection of data or any algorithmic conversion should obey the structure and the details of the measured object.

The primitives elements (data) have a major part in defining the quality of the DEM. For example even if the most complicated algorithm is used, it will be impossible to describe a subject from which we have a deficit of reference points. The population of the reference points (ie. the height data) which have been collected or arranged should be, the minimum permissible (for financial reasons) in order to describe the object according to the prescribers. Moreover the data have to be manipulated (compressed, organised, transformed into the desired coordinate system etc).

The methods and instruments to collect the primitive information depend mainly on the desirable characteristics of the final product and the structure of the surveying object. However the existing instruments (hardware) and software may be restrictive. The information in general is not collected in one way (group of instruments or methods) but from many ways. These should give quick, accurate and cheap information.

The collection may be done by, direct methods (ie. land surveying), non direct methods (ie photogrammetry) or mixed methods. Each method gives speed, accuracy, flexibility and cost depending on the equipment and their combination. So we have the possibility to choose each time the equipment and methods which will give us better results.

The conversion of information. The term "interpolation" defines a conversion of the data structure with a foreseeable loss of information. Each conversion algorithm uses a mathematical model which fits on the measurement object. The mathematical model is the basis of the interpolation. The best algorithm for the conversion should have the following characteristics. The method must be fitted satisfactory in the reference points which constitute the exacting approach of the measurement object and to give the ability to the user to confine (filtering) the noises which are involved in the data collection.

2.4. Terrain description and approach - data acquisition methods.

2.4.1. General.

Many natural phenomena are so complex that attempting an exhaustive analysis is hopeless. Nevertheless the phenomenon-based approach should almost certainly be preferred over one based on an entire large data structure on a particular, small set of problems at hand, or worse still, on a convenient machine representation (Mark, 1979).

A data structure may be defined as a set of objects (data), together with the relations (if any) among them.

Relations between data elements may be three types: explicit, implicit, or algorithmic.

Explicit relations are just that : associated with the datum is a list (or other explicit indication) of the related elements.

Implicit relations are indicated by the position of the data element in storage. For example, in a list of elements, each item is related implicity to the preceding and following item in the list.

Algorithm relations are ones which are neither implicity nor explicity indicated, but which are nevertheless may be discovered through an analysis of some or all data. An example would be the nearest neighbour of a point among points distributed irregularly in space. Since this can be determined from an analysis of all point coordinates there is an algorithmic relation between such neighbouring points.

The problem structure in digital terrain modelling is very complicated, because there are several groups of specialists, each group examining the phenomenon (terrain) from a different perspective, and hence would have a different view of the "structure phenomenon".

The geomorphologist often views the terrain in terms of a land-forming process (past or present) combined with time (stage of development) and influences of geologic structure. The fluvial geomorphologist tends to see the terrain as a set of contiguous, hierarchically-arranged drainage basins, linked together by the drainage net. Other geomorphologists see the terrain as a set of slope units. The two dimensional analysis of slope profile form is well advanced, but extensions to three dimensions are less common.

The surveyor is concerned not with the explanation of the form of the earth(as the geomorphologists are), but with its accurate specification. The phenomenon is generally viewed as a polyhedral solid; the size of its facets can be adjusted to produce any desired degree of precision, within the limits of the instruments. This is already a mathematical model and so can be directly implemented as a data structure.

The photogrammetrists depending upon their training, see terrain structure as the surveyors do; in terms of contours, or drop lines.

The cartographers also claim interest in the terrain; their approach resembles that of the photogrammetrists.

Finally the mathematician says that the terrain would be presented as a particular mathematical surface.

2.4.2. Terrain types and ground categories.

In sampling the surface to establish a DEM, some problems are involved such as, the determining of adequate sampling density in order to meet given specifications and the evaluating of the accuracy of the resulting DEM. How accurately a topographic surface is represented by a DEM depends essentially on

several factors: sampling density, measuring errors, interpolation method and terrain classification.

Every spot on the Earth's surface has a multitude of varied but intricately interrelated attributes which make it unique and difficult to compare with any other. The more carefully we define types of terrain, the more difficult they will become to recognise and the more types there will be. However various efforts by researchers are made for the parametric description of the topography. The solution of the problem is not so easy because the form of the terrain surface is very complex.

Most methods which try to categorise the terrain consider a stretch of land from the complex earth surface with all that is made on it. The differences between them is the variation and the different name which is given in order to specify the terrain type.

Terrain type has a great importance in the economy of mapping. The terrain roughness is a dominant factor in the determination of mapping cost. The price per square kilometre will be from two to five times higher in mountainous areas than in flat terrain.

Relief peculiarities is one subject of special interest for photogrammetrists. This is the reason that it has grown rapidly in recent years. Since the photogrammetrists are concerned with the spatial information of the terrain, terrain is classified according to the degree of roughness. This problem is regarded as a problem of data reduction and feature extraction. More specifically the population of the height data which have to be collected or arranged should be the minimum possible (financial reasons) and to describe the object according to a pre-specified accuracy.

Relief study is necessary in order to:

1. Determine the appropriate grid interval (optimum sample size), to acquire the information (data) by photogrammetry and to describe terrain optimally with as little measuring effort as possible.
2. Determine the production time which is related to the economy and

3. To estimate the accuracy of the resulting map during the data processing. It is well known that flat or gently sloping relief could be represented better than rough and complex terrain.

2.4.3. Terrain evaluation (characterisation).

Terrain evaluation has developed in response to the need for an understanding of terrain by an increasing variety of disciplines concerned with its practical uses (scientific and applied).

Terrain evaluation (Beckett & Webster 1969) is defined as the " act or result of expressing the numerical value of; judging concerning the worth of " an object. This double meaning makes it somewhat more inclusive and thus preferable to such terms as analysis, classification, assessment, or appraisal.

These terms can describe the terrain evaluation as a process which involves:

1. Analysis. The simplification of the complex phenomenon which is the natural geographic environment.

2. Classification. The organisation of data distinguishing one area from another and characterising each.

3. Appraisal. The manipulation, interpretation, and assessment of data for practical ends.

Indications and rules help to distinguish the ground categories and terrain types. The terrain evaluation (characterisation) of the terrain type is subdivided in the following categories:

2.4.3.1. Terrain classification in photogrammetry.

2.4.3.2. Terrain description - Geomorphometric parameters.

2.4.3.3. Mathematical approach towards the terrain.

2.4.3.4. Land use and land classification.

2.4.3.1. Terrain classification in photogrammetry.

The photogrammetrists in classifying the terrain use a simple method. An accepted obvious quantitative terrain classification does not yet exist for the

purpose of studying the effect of terrain shape on the results of various photogrammetric processes. But even if it did exist, then there still remains the problem that terrain properties can vary strongly from one part to another. There are several simple methods such as:

The maximum height differences method according to Silar (1969).
The terrain classification is shown in the table 2.1.

CATEGORY	DESCRIPTION	tr = t / hectare
I	Regular, nearly plane surface	tr < 10
II	Regular, varying surface, oval shape	10 < tr < 20
III	Irregular surface	tr > 20
IV	Artificial, man made surface	Large number of artificial edges (tr >> 20)

Where t is the number of local extrema and/or terrain break lines.

Table 2.1. Terrain classification. After Silar (1969).

In this method the terrain classes are grouped at four terrain classes simply by counting the local extreme t_r (number of local extreme and/or terrain breaklines per unit area).

Makarovic (1973) presented a simple method in the progressive sampling method for DEM generation, in which the criterion is the second height difference. As this method utilises the progressive and composite sampling techniques, the stereomodel is divided at the beginning into several square patches. In each patch the height differences between adjacent sample points are calculated along each row/column. Second differences are then calculated along rows and columns with the additional possibility of along diagonals (Figure 2.2).

The chosen classifications are the follows:

I. Regular terrain with horizontal, slightly tilted and/ or slightly curved surfaces.

II. Semi-regular terrain, smoothly undulated with or without few

man-made objects.

III. Moderately rough terrain with some distinct morphological features.

IV. Rough terrain types with many abrupt changes.

The terrain belonging to the categories I and II can be covered exhaustively by plain progressive sampling. Composite sampling appears particularly feasible for the terrain category III. Terrain belonging to the category IV can be covered best by the selective sampling only.

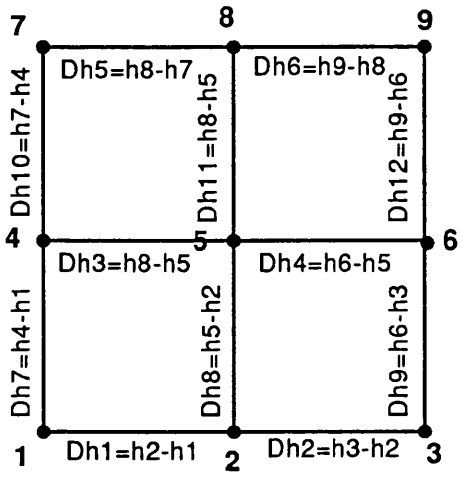

Figure 2.2. First and second height differences along row and column.

The second height differences give the information on the terrain curvature. If the second difference is larger than a pre-specified threshold, the local terrain is considered to be rugged and a dense sampling is required.

Tempfli (1980), attempted to evaluate the accuracy of the DEM, deriving quantities (eg. contour or volumes) to determine the adequate sampling interval and the method for reconstruction to meet given specifications. In this study he used synthetic data, but the criteria can be applied to real terrain. In this paper he classified the terrain in three different terrain types, for contour plotting at a scale of 1:50,000 with a contour interval 50 m.The slopes and the curvatures were calculated over a total area 8 by 12 Km and summarised as follows (Tempfli, 1980):

Flat terrain : elevation range : 300 m.

97% of the slopes are between zero and 10 degrees.

90% of the radii of curvatures are between 1000 m and ∞.

40% of the radii of curvature are between 2000 - 10000 m.

Rolling terrain: elevation range : 600 m.

96% of the slopes are between 0-25 degrees.

95% of the radii of curvature are between 100-50000 m.

40% of the radii of curvature are between 1000-5000 m.

Rugged terrain: elevation range : 1000 m.

91% of the slopes are between 0-30 degrees.

90% of the radii of curvature are between 200-1000 m.

40% of the radii of curvature are between 200-1000 m.

2.4.3.2. Terrain description - Geomorphometric parameters for approaching terrain.

Geomorphologists classify terrain by developing and applying complicated systems. There is a considerable number of different quantitative indices in terrain description or terrain roughness. Terrain roughness refers to the irregularity of a topographic (or other) surface (spatial variations of the terrain). These are (Mitchell, 1973 and Mark and Aronson, 1984):

Grain, texture, relief, average elevation, elevation relief ratio, slope parameters (slope or gradient, average slope, slope direction changes or aspect), and the curvature or wavelength.

Grain indicates in some way the scale of horizontal variations in the topography. It is used for the longest significant wavelength in the topography and is dependent on the spacing of major ridges and valleys. It is assessed by selecting a random point, drawing a series of concentric circles having diameter increments eg. of one mile and determining the maximum difference within each circle.

Texture indicates in the same way as the grain, the scale of horizontal variations in the topography. It is used to refer to the shortest significant topographic wavelength. It is very important in Geological studies.

Relief is used to describe the vertical dimension or amplitude of topography. It is the difference between the highest and the lowest elevations (extreme values) in the unit area equivalent to the grain size. Relief describes the vertical dimension of the terrain. Another concept is the relative relief introduced by (Frederiksen et al, 1984), in order to eliminate the dependence of the definition on this reference area, by dividing the local relief by the extent of the reference area (its diameter or perimeter). Relative relief is a dimensionless quantity; it depends on the extent of the reference area and its frequency distribution allows classification of terrain according to roughness and genesis.

Average elevation. Is derived from the mean of randomly chosen points within the unit area.

Elevation relief ratio. Is the relative proportion of upland and lowland. It is derived by subtracting the lowest elevation from the average elevation within the area and dividing the remainder by the relief. The resulting value therefore always falls between 0 and 1 and is expressed as a decimal.

Slope has two components - the gradient and the aspect. Slope is possibly the most important parameter of terrain forms, because it controls the gravitational forces available for geomorphic work. (Evans, 1972). Slope can be estimated in a number of ways. For example surface fitting has been used with digitised topographic map data, although with dense grid models there may be some difficulty in fitting a smooth plane to highly irregular elevation values. Mathematically the slope, tangent of the slope angle (tan a), is the first derivative of the elevation value in respect to the x (East/West) and y (North/South) directions and is defined as the maximum change of height, expressed in degrees (0^o-90^o).

$$\text{Slope} = \text{TAN}^{-1}\left(\sqrt{\left((\partial z/\partial x)^2 + (\partial z/\partial y)^2\right)}\right)$$

Slope is definable at any point of the terrain, except at break lines. A break line has been defined as a line where there is a sudden or abrupt change in slope. Break lines represent mathematically, lines where the spatial derivatives are discontinuous. Physically they are identified with the edges of ditches, dikes, cliffs and ridge lines.

In their macro structure slopes can be computed in any direction regardless of the format of the DEM data (random or regular). In other word, they include both low and high frequencies; therefore, they can be a representative parameter for the terrain roughness.

Aspect and gradient computation is based on the partial derivatives along the two perpendicular directions East-West and North-South symbolised as dx and dy respectively. They are assessed by counting the number of changes from rise to fall and vice versa along the same random traverses used for counting contours.

The gradient defines the first derivative (or else the slope vector) of a surface at a given point. The Gradient (G) can also be computed as a percentage of the vertical distance between two points with respect to their horizontal distance.

$$G = \sqrt{\left((dx)^2 + (dy)^2\right)}$$

Slope direction changes or aspect, denote the direction of an area. The aspect (pointing downslope) represent the direction of the maximum change of height, also expressed in degrees (0^o-360^o). Aspect points the downslope (toward the bottom of the valley), or upslope (toward the ridge) along the direction of the maximum rate of change of the slope. The aspect (A) as the directional component of slope can be calculated as the direction that slope faces:

$$A = TAN^{-1}\left((-\partial z/\partial y)^2 + (-\partial z/\partial x)^2\right)$$

Average slope is determined by counting the number of contours crossed by straight lines in directions NW-SE, N-S, NE-SW and E-W. across a circular unit area equivalent to the grain size.

Curvature, or wavelength or extent of the terrain form. The term wavelength has been adopted from the same term in electrical engineering provided that the terrain surface is similar to random signals and the terrain surface is equally sampled. It is the second derivative of the elevation in an arbitrary direction. The curvature in a terrain profile is defined as the average distance between successive (local) maxima or minima. This curvature is measured in length units (spatial units) and may be studied in various characteristic directions. Its relationship to

the terrain forms can be ideally studied using the Fourier Transform.

In a profile, if the DEM sampling is Δx and the profile L, the data may contain curvatures that range from a long curvature of L to a short curvature of 2(Δx). The curvature of a surface at a given point may be defined the spatial second derivative C given by:

$$C = \sqrt{\left((\partial^2 z/\partial x^2)^2 + (\partial^2 z/\partial y^2)^2\right)}$$

This "simple" curvature measurement is not invariant against rotations. Fritsch and Dusedau (1987) gives in addition five more complex curvature measures which may be used.

From the above geomorphometric parameters, the most important and widespread, for approaching terrain are the gradient, the aspect, and the curvature.

2.4.3.2.1. Terrain types and slope categories used in this project.

It is a fact that the photogrammetric operator sets the floating mark on the ground more accurately on the flat or gently rolling areas than on rough and steep terrain (relief), where the uncertainty is a dominant factor accompanying the measurements.

The terrain type in this work is described according to the slopes and grouped in 4 categories. This was carried out in preliminary measurements on the SPOT stereomodel, by the project operator. The terrain types and the slope categories used in this work are the follows:

0	- 6	Degrees	0	- 10%	Flat areas.
6	- 14	Degrees	10	- 25%	Gently rolling areas.
14	- 26.5	Degrees	25	- 50%	Semi-rough terrain.
above	26.5	Degrees	above	50%	Rough and steep terrain.

The slope categories were considered as a source of causing error in the SPOT elevation measurements and they are used on the estimation and the classification, of the caused error, in the applied statistical analysis. They are grouped in 4 categories to facilitate, in the statistical study, without losing the significance of the terrain roughness and its influence on the photogrammetric observations.

They are also used as the main criterion in applying the height limits during the blunder detection procedure.

2.4.3.2.2. The gradient and aspect estimation program.

Slope (gradient) and slope orientation (aspect) maps can be produced from DEM , and these are very useful for solving problems in many disciplines. Geomorphologists and Geologists pay a lot of attention to these products, while photogrammetrists do not. The reason is that until now it was difficult to produce these maps; the only way was to calculate the slopes from the contour map in an independent, tedious procedure. However, DEM offer the opportunity to produce slope and slope orientation maps easily.

Most people think that a map should normally be updated because of planimetric changes rather than morphological changes. Terrain surface changes considerably under certain circumstances. Melton's (1960) study in Wyoming (USA) showed (through the analysis of variance) that there was a significant difference between the steepness of north- and south-facing slopes . North-facing slopes were, on average, twice as steep as south-facing slopes (4.42^{o} as compared to 2.21^{o}). This is because the material moving down the south-facing slope 'pushes' the stream into the foot of the north-facing slopes, which hence become steeper.

Gradient and aspect maps with additional elements of ground material can give information on whether the relief representation needs to be updated or not. In addition, the representation of the gradient and aspect in a raster form gives a rough idea of existing blunders in the initial elevation data.

A program for aspect and gradient estimation SLOPE.FOR was written. The

main program calls the subroutines MENU.FOR, SET1.FOR and DEM_IO.FOR. The DEM_IO.FOR subroutine calls routines from the LSL$LIBRARY package. The SLOPE.FOR program reads a DTI file, output from DTMCREATE package, or the NE1.FOR program.

The program NE1.FOR, is linked with the subroutines NE2.FOR and DEM_IO.FOR. The DEM_IO.FOR calls routines from the LSL$LIBRARY package. The purpose of the program is to convert a file containing strings of coordinates, recorded in a regular grid, Point_Number, X, Y, Z, from the ASCII form, to the DTI form. The DTI files can be used as input in the ROVER Module, so the aspect and the gradient can be graphically displayed on the screen, or printed on the laser writer.

If the dx and the dy values are known quantities, the gradient (G) and the aspect (A) can be determined as follows:

$$G = \mathrm{SQRT}\ (\ (dx^2) + (dy^2)\ )$$

$$A = \mathrm{TAN}^{-1}(-\ dy/dx), \quad -\pi < A < \pi$$

IF dy <> 0 AND dx = 0 THEN

A --> $\pi/2$ OR A --> $-\pi/2$

IF dx = 0 AND dy = 0 THEN

G = 0 (Flat terrain) AND A is undefined.

The gradient is determined even when aspect is undefined. From the geomorphological point of view, rapid changes in the height values, means high gradient. On the other hand in flat areas, or nearly flat, the gradient is equal, or almost equal to zero.

The program asks the user through the MENU routine:

1. To specify the DTI filename, which contains the DEM or the label matrix stored in DTI form (the DTI files are stored in the DTI directory by default).

2. To specify the output filename to store the gradient and aspect DTI matrices. This is carried out calling a sub-menu, which contains two options, for storing the gradient and the aspect matrices in a separate file.

3. To choose an elevation smoothing. The user can, if he wishes, make a global

filtering of the DEM, to reduce the effect of the random noise, which is generated by the data collection system or other factors. This can be carried out by calling the elevation smoothing sub-menu. There are two smoothing options:

a. Smoothing based on distance from the centre 3 x 3 and

b. Smoothing based on a low pass filter 3 x 3.

4. Finally, if desired to compute the gradient , the aspect, or both. This can be carried out by calling the slope submenu, where the program asks the user :

a. To define the DEM spacing.

b. To define the gradient magnitude under which a terrain will be considered flat (1 < flat < 90). The threshold for the flat terrain (gradient) only affects the aspect estimation.

The program description algorithm is presented in appendix A.

The gradient and the aspect are estimated from the captured aerial photography and SPOT imagery elevation data. The description of the test area and the data elevation measurements from the aerial photography is described in § 5.2.3.2, while the data elevation measurements on SPOT is described in § 5.2.4.2.1.

The gradient and the aspect estimation from the SPOT elevations data for the entire captured area 14300 x 9900 m^2 (14400 points in 100 m grid interval) are shown in image form, in the figures 2.3 and 2.4. In the aspect and gradient estimation, no elevation smoothing has been carried out, while in the gradient and aspect estimation shown in image form in the figures 2.5 and 2.6 a smoothing of the elevation data was carried out based on a low pass filtering, in a convolution array 3 x 3 (see appendix A.2.2).

Figures 2.7 and 2.8 also show the gradient and the aspect estimation in image form, from the aerial photography derived elevation data for the area 6900 x 6000 m^2 (46200 points in 30 m grid interval). This gradient and aspect presentation represents the half of the test area.

SOURCE SPOT - GRADIENT

AREA 14300 x 9900 m^2

(Not to scale)

Figure 2.3. Gradient estimation in raster form from the SPOT elevation data.

SOURCE SPOT - ASPECT

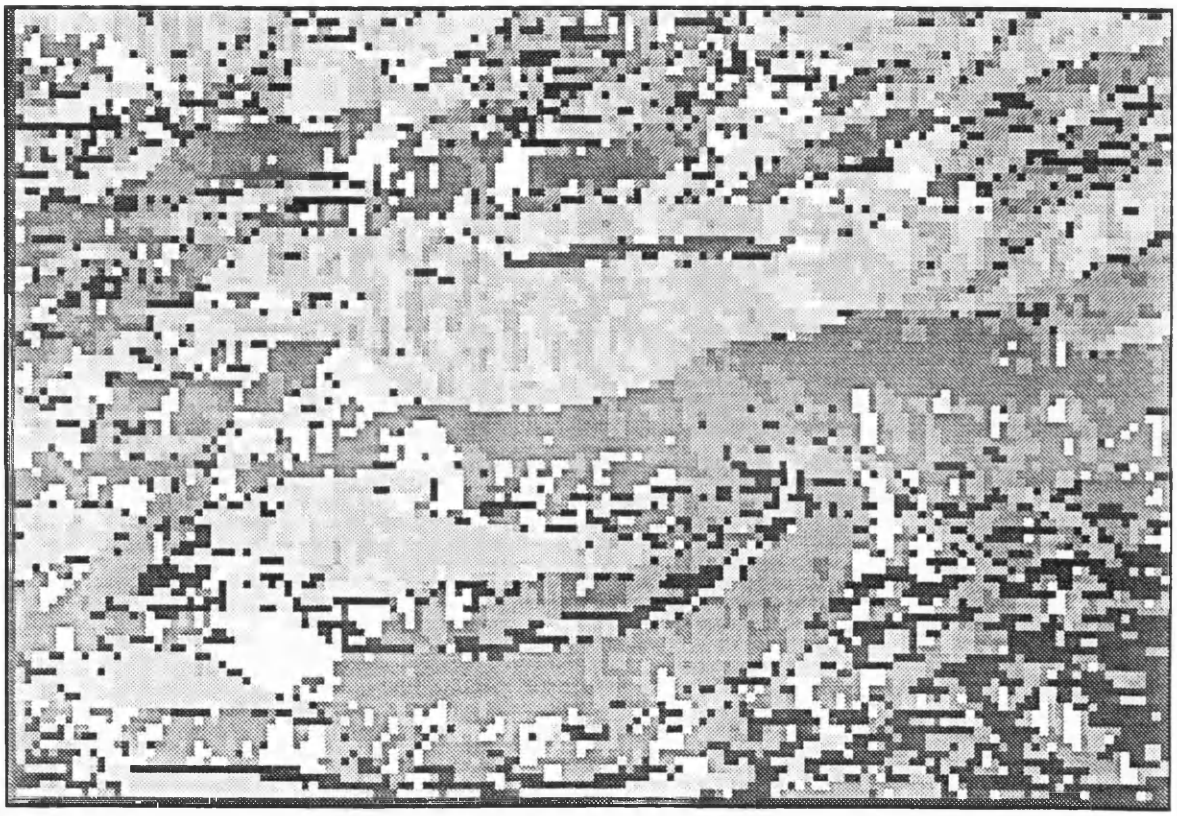

AREA 14300 x 9900 m^2

(Not to scale)

Figure 2.4. Aspect estimation in raster form from the SPOT elevation data.

SOURCE SPOT - GRADIENT

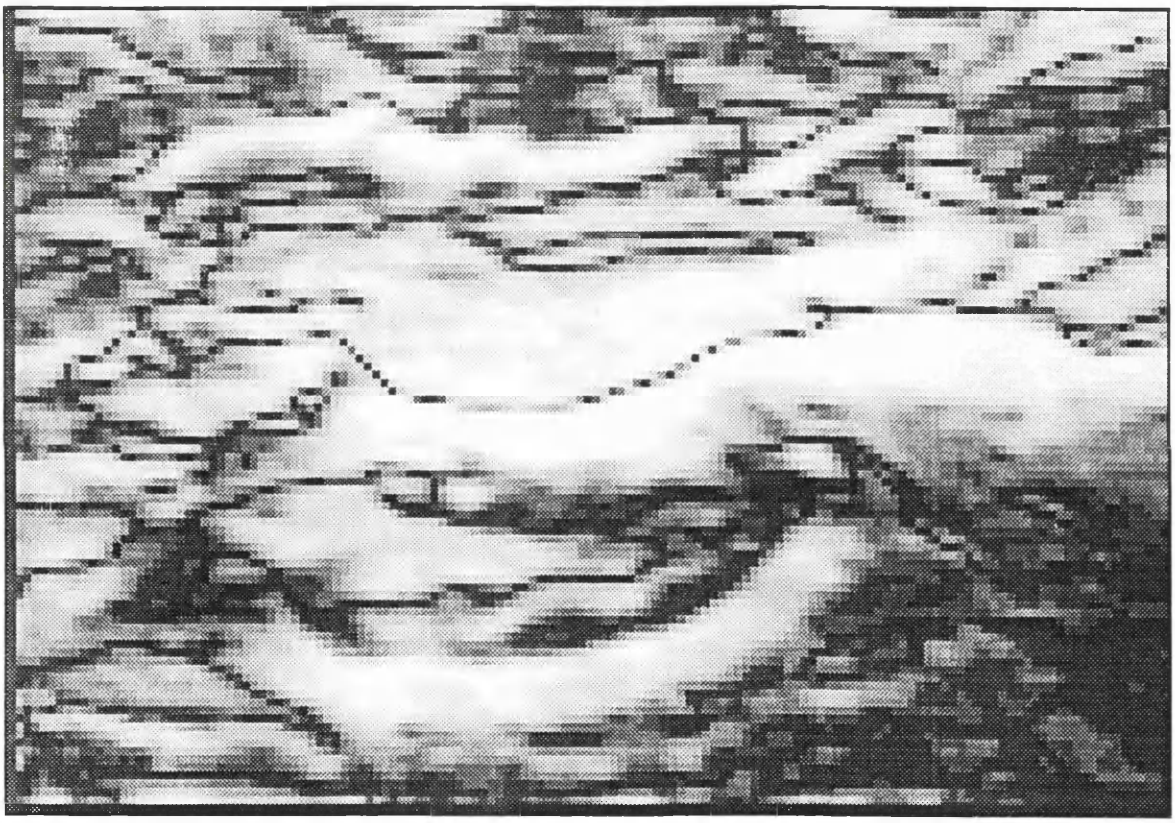

AREA 14300 x 9900 m^2

(Not to scale)

Figure 2.5. Gradient estimation in raster form from the filtered SPOT elevation data.

SOURCE SPOT - ASPECT

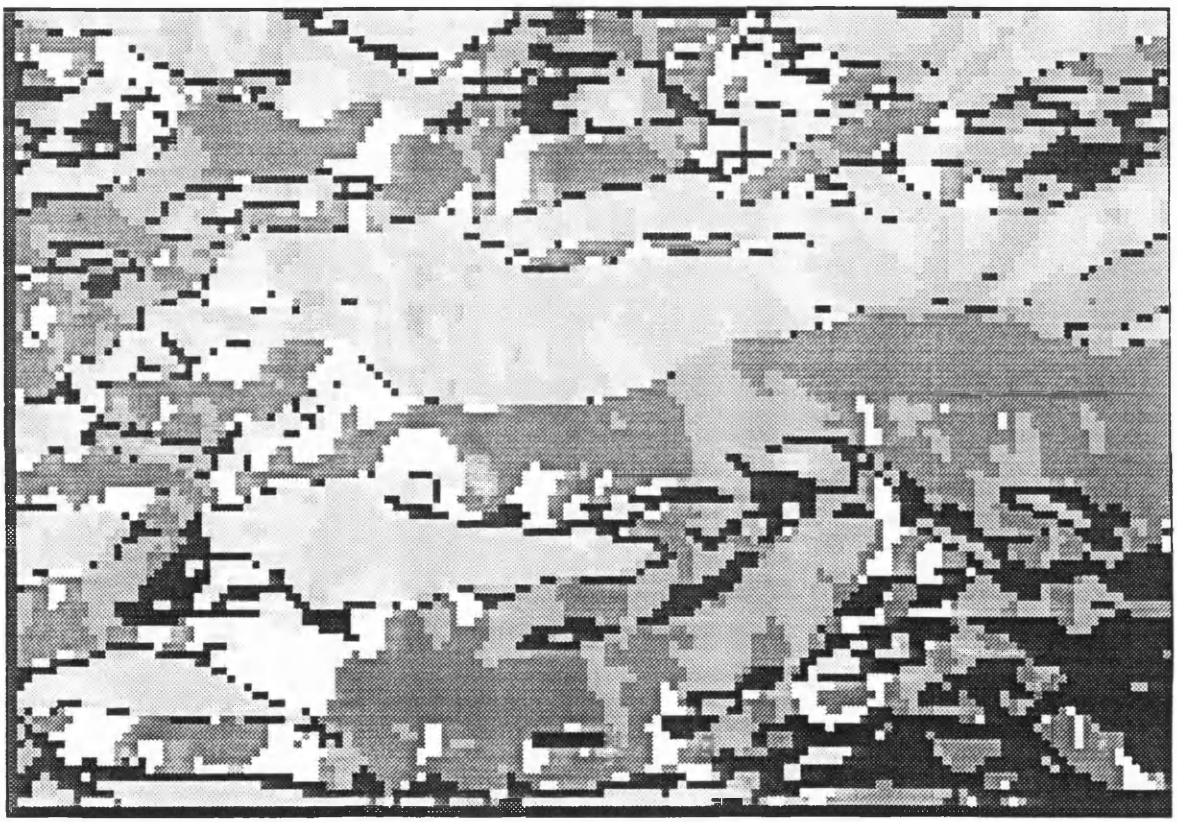

AREA 14300 x 9900 m^2

(Not to scale)

Figure 2.6. Aspect estimation in raster form from the filtered SPOT elevation data.

AERIAL PHOTOGRAPHY DATA

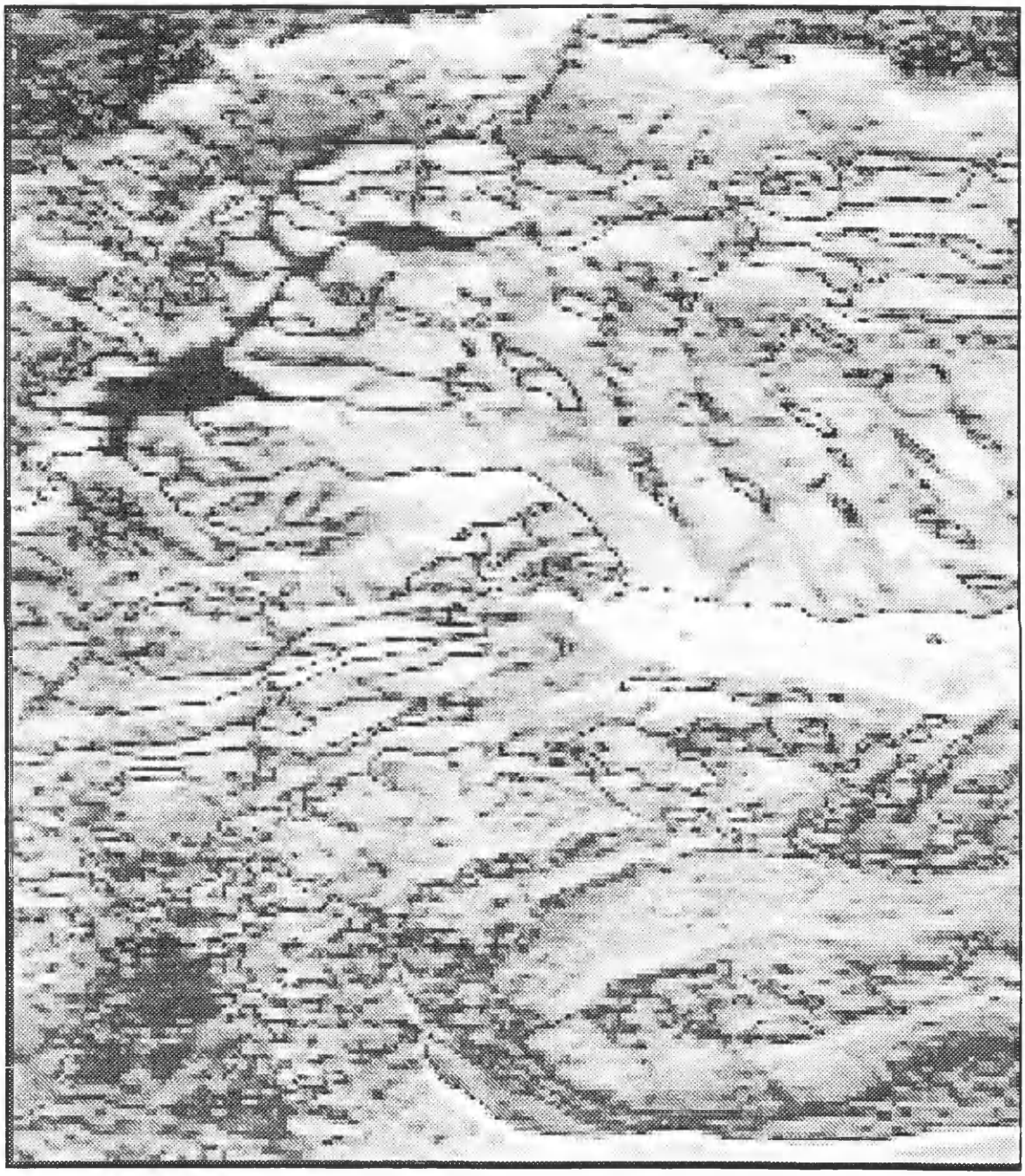

AREA 6900 x 6000 m^2

(Not to scale)

Figure 2.7. Gradient estimation in raster form from the aerial photography elevation data.

AERIAL PHOTOGRAPHY DATA

AREA 6900 x 6000 m^2

(Not to scale)

Figure 2.8. Aspect estimation in raster form from the aerial photography elevation data.

The presentation in a raster form of the gradient and aspect for the two sources derived "raw" data give a very good information of the data quality.

The aerial photography derived raster images give a very good sense of the data responce to the terrain features. However, the raster images which derived from the SPOT data give less good representation of the ground features as one can easily verify by comparing the presented SPOT area with the same aerial photography area.

2.4.3.3. Mathematical approach towards the terrain.

In recent years the investigators are oriented to the required procedures and densities for data capture (optimum sample size). The choice of the optimal sample spacing , meeting accuracy specifications for the DEM, can reasonably to be based on the selected statistical analysis of the selected terrain profiles in the projected area.

There are several techniques which use the terrain roughness parameters as criteria to determine optimum sample size. In all of them it is accepted that the terrain surface is effectively a continuous function. The method of measuring it however, renders it discrete; that is a finite number of ground points are actually measured to represent a continuous surface. Hence the concept of approximation or modelling is required (Segu, 1985).

Some of these techniques of mathematical approach towards the terrain are the follows:

1. Mathematical approach with the Fourier spectrum, frequency spectrum, power spectrum, Fourier spectra, harmonic vector magnitude (HVM), amplitude power spectrum, frequency domain-spectral analysis).
   (Ayeni, 1976; Frederiksen et al, 1978; Ayeni, 1978; Tempfli & Makarovic, 1979; Jacobi, 1980; Tempfli, 1980; Frederiksen, 1981; Tempfli, 1982; Ayeni, 1982; Frederiksen et al, 1984; Hassan 1986).
   Note: Extensive investigation has shown that a log-log scale of the power spectrum is linearly related to its Fourier frequency (Frederiksen, 1980; Frederiksen et al, 1984; Frederiksen et

al, 1985).

2. The Variogram (auto correlation function). (Matheron, 1971; Frederiksen & Jacobi, 1986).
3. Terrain models from random functions (Frederiksen et al, 1984).
4. Selfsimilarity and fractals (Mandelbrot, 1968, 1977, 1982; Frederiksen et al, 1984; Muller & Saksono, 1986).
5. Karhumen - Loeve expansion (Ostman, 1986).
6. Best Linear Unbiased Estimator (BLUE) or Kriging (Krige, 1951; Matheron, 1963).

From the high frequencies of the frequency spectrum, we can estimate the standard deviation between a digital elevation model and the terrain surface.

Either stochastic criteria (correlation functions or transition probabilities in the sense of stochastic process) or frequency spectra are suitable to describe terrain properties (Ackermann, 1979). The question is which covariance function can describe real terrain and which functions should be assigned to the different types of terrain. Makarovic (1972) describes the terrain by means of frequency spectra and Fourier analysis. If the frequency distribution of terrain is known all questions regarding point density interpolation method and accuracy can be answered.

Nowadays these theoretical techniques are limited in their applicability although they show some potential in the determination of sampling strategies for photogrammetric mapping over large areas (Balce, 1987) and the interpolation error.

In this work the variogram technique is used in finding the error introduced by interpolation according to the distance between the measured point and the point being interpolated. The description of the variogram, its estimation and the graphical representation for the test area are presented in sections 7.3.1 and 7.3.1.1 The estimation of fractal dimension from the semivariogram is presented in paragraph 7.3.2.

2.4.4. Land use and land classification.

There are many schemes for parametric classification of land. Land classification can vary from country to country and it is different in continental scale. Land classification differences for the same area can arise from each individual project point of view, ie land cover by vegetation or human land uses and activities. For Europe the most important and simple land classification elements contained in six classes (Stamp & Whillats, 1935).

1. Forest and woodland (deciduous, coniferous)
2. Meadowland and permanent pasture (grassland).
3. Arable or tilled land (cereals, roots, greenfodder).
4. Heathland, moorland, commons and rough hill pasture.
5. Gardens, allotments, orchards, and nurseries.
6. Land agriculturally unproductive.

The vegetation structure (two first categories of the first exercise) can be presented further in the following categories:

	Height (m)	Stem type	Form
1.	More than 7.0	Woody	Trees
2.	1.5 - 7.0	Woody	Young or dwarfed trees.
3.	0.5 - 1.5	Woody	Tall shrubs or dwarfed trees.
4.	Less than 0.5	Woody & non woody	Low shrubs, grasses, sedges, and mosses.

We can subdivide the fourth category of the previous exercise (second exercise) in more subcategories which specify better the land cover and vegetation in : grass, grass - scrub, scrub - bush, grass - bush, or one can subdivide according to human activities or human land uses in : pasture, partly cultivated, cultivated, pasture cultivated.

One other terrain classification which includes both terrain types - ground categories and land cover is the follows (Leupin and Cherkaoui, 1980) :

Covered flat terrain	Semi-covered flat terrain	Uncovered flat terrain
Covered semi-rough	Semi-covered semi-rough	Uncovered semi-rough
Covered rough	Semi-covered rough	Uncovered rough

2.4.4.1. Land categories used in this project.

The vegetation information for the Aix En Provence test area was extracted from IGN (1:25,000) maps. The categorisation of the land use in this work, was done according to the difficulties, or uncertainties that vegetation creates in the operator setting the floating mark on the ground. The main target was the generalisation and to keep it simple with as few categories as possible. The vegetation information were grouped in 3 categories as follows:

a. Foliage, coniferous and foliage + coniferous trees, grouped as group 1.
b. Bush, orchard, vine trees and rice crops, grouped as group 2.
c. Uncultivated areas, grouped as group 3.

The land categories were considered as a source of causing error in the SPOT elevation measurements and they are used in the estimation of the caused error in the applied statistical analysis.

2.4.5. Sampling density and pattern.

2.4.5.1. General.

Data collection demands the major time and the bigger cost from any other stage of the DEM creation. The optimum data sampling has two components, the optimum sample size and the optimum sample pattern.

The problem in DEM creation is how we can know that we have measured enough elevations during the process. The answer is not simple because it involves a proper assessment of the terrain roughness in relation to the size of the area occupied by the terrain.

Data selection can be controlled by the operator (selective sampling), by a computer (progressive sampling) and pre-defined patterns (in a regular pre-defined grid). To obtain a high quality DEM the measured points must be selected with respect to the topography. In production different sampling modes are often combined eg. selective sampling of breaklines with progressive sampling (Ostman, 1984).

There are a big number of sampling patterns, from which we may obtain the required terrain elevation information, but in reality we can distinguish only three patterns.

1. The grid pattern (systematic sampling).
2. The random pattern (random sampling).
3. A combination of the above (stratified sampling).

So digital elevation data can be produced on a regular grid, along terrain breaklines and points, or along contours or profiles.

2.4.5.2. The grid pattern (systematic sampling).

This is the simplest approach. It is applied by surveyors and civil engineers (cross sections) and in the acquisition of profile data measured photogrammetrically in stereoplotting instruments.

Photogrammetric data can be derived:

1. Automatically
2. Semi-automatically, during the production of orthophotographs or under computer control using an analytical plotter.

These are ordered points in intermeshing nodes which are formed in a regular geometric pattern (triangles, parallelograms or squares). From the grid determination for instance on the model, all the captured points are determined. The intermesh grid ordered points should cover all the area in which we are interested. The area is divided into square blocks which may have between them different dimensions. The advantages and the disadvantages of this pattern are:

Advantages:

It is necessary to store only the height information of the points which lie in the grid nodes. This presupposes that the origin is at bottom left. The orientation of the block (azimuth), the grid interval, and the number of rows - columns of the digital elevation matrix, are stored in the header.

It uses a simple interpolation method which in general reduces computer processing time.

As the position of the points is preprogrammed and fixed, the instrument automatically drives to the required grid node points under computer control.

It is the most promising application of automated photogrammetry.

We can use a small computer (PC or microcomputer).

Disadvantages:

The measured points do not always refer to the ground features. This may cause lack of height information in rough terrain or too much information in uniform and flat areas (embarrassing and unnecessary data redundancy). In this situation filtering of the measured data may need to be carried out as a preprocessing activity before the terrain model can be defined. Moreover depending on the pre-specified grid interval the finer but perhaps significant terrain features will not be measured specifically.

The interpolation procedure is quite simple and has a trend to simplify the ground. This becomes crucial in regions with variable relief, because the changes in ground slope are not well defined by the regular grid.

The interpolation result is a height which may be far from the real in amount of Dz. The error Dz is the difference between the interpolation surface and the real ground surface.

Although we measure only the height of the points which lie in the area of interest all the points are recorded in the computer (the nodes for which there is no measured height are automatically set to zero). This leads to disproportionate memory requirements, if the area of interest occupies only a narrow strip of the block.

2.4.5.2.1. Progressive sampling.

The above data shortcomings can be avoided with progressive sampling. This

method was originally proposed by Makarovic (1973,1975 and 1977). Progressive sampling techniques attempt to optimise automatically or semi-automatically the relationship between specified accuracy, sampling density and terrain characteristics.

The main idea is that one starts with a low resolution grid which gives a good general coverage of height points all over the area to be measured. An on-line computer attached to the photogrammetric instrument estimates the slopes and analyzes the terrain relief. Then it applies a progressive increase in the density of sampling (measurements) by halving the size of the grid cell in certain limited areas, matched to the local roughness of the terrain surface. Measurements of the height points at the increased density are carried out under computer control only in these pre-defined areas. A further slope estimation is carried out for each of these areas and the existing grid is halved according to the results. Further measurements of the height points under computer control only at the increased density are again carried out and so on.

Procedures have been tested for the use of test profiles in order to determine the optimum grid sampling density in a working area. (Balce, 1986). The contractors have not adopted the procedure as they consider that the selection of the location for the test profile within the stereomodel is also subjective. Although analytical stereoplotters are used, the progressive sampling method available with the equipment is not used and is considered slow.

2.4.5.3. The random pattern.

In this pattern the measured and stored points are completely randomly distributed (but specifically located) in the project area and completely independent. It is a common data acquisition technique, in land surveying operations. Sometimes it is employed by photogrammetrists by measuring heights selectively at significant points only ie. at the tops of hills, in hollows and along breaks of slope, ridge lines and streams. Thus all the points to be measured are identified by the photogrammetrist on the basis of his inspection and interpretation of the terrain features. From one defined area around a point, the interpolation surface is estimated and then the height of this point is estimated. The advantages

and disadvantages of the random pattern are:

Advantages:

The information collection method is completely independent of the relief variations. The terrain data will be collected in important positions in terms of terrain morphology or representation, ie on hill tops, in pits, in hollows or saddles, along breaklines (ridges), breaks of slope, rivers etc.

If the data collection system is sufficiently sophisticated then the number of points which are required for a given accuracy, is less than the number of the points from the other patterns (grid and the grid-random combination pattern).

Disadvantages:

Requires large computer resources.

It is possible to have in some area superfluous points and in others too few, so it is necessary to predetermine the type of interpolation surface to be used.

The interpolation procedure take a lot of computing time, if a random to grid interpolation is used.

Needs experience.

2.4.5.4. The combination of grid and random pattern.

Is the common approach to data acquisition taken by photogrammetrists. In this a relationship exists between some of the points forming the model.

The data is captured in the following general patterns:

1. Composite sampling.
2. Selective sampling.
3. Contours
4. Profiles
5. Characteristic lines
6. Joined triangles.

1. Composite sampling.

Composite sampling is the development of progressive sampling. This approach uses both selected and filling data. It is applied in the non-automated, operator controlled type of stereoplotting instruments. In this approach the

significant points are first measured in terrain and then additional points will be measured both along the centre line to give a longitudinal profile and at right angles to give a series of lateral cross-sections.

2. Selective sampling.

Selective sampling is a procedure using distinct morphometric features and "anomalous" terrain regions. Such data represent a geometric framework for subsequent manual, semi-automatic, or automatic non-selective sampling to form a complete DEM. Data on distinct morphometric features have high information content. In the latter case additional more homogeneous data have to be sampled, proving the so called "filling data". These can represent contour lines, parallel profiles or point grids.

3. Contours.

It is applicable in the analogue instruments. The operator follows the contour line and records points which lie on it. So a sequence of X, Y coordinates of points which lie in the same contour (constant Z) is recorded. Again this may be supplemented by spot heights measured in hollows and along terrain break lines, at the top of hills, ridge lines and streams etc.

4. Profiles.

In this case the pattern could vary from almost ordered points to nearly or completely random points. The profile is a sequence of measured points in a straight line.

Profiles could be:

Parallel and equidistant.

Parallel but not equidistant.

Not parallel and in changeable distances.

5. Characteristic terrain lines.

Is a sequence of X, Y, Z coordinates from one specific ground feature. This feature could be the top of an embankment or its base, or ditch and will define a change of slope. The points are usually stored sequentially along a terrain line. This method is used mainly in technical constructions because these have well defined (clear) surfaces (obvious slope changes).

6. Joined triangles.

The measuring heights lie on triangle apexes. The shape of the triangles is irregular. (random).

The advantages and disadvantages of the combination of grid and random pattern are:

Advantages:

These patterns are more flexible and come closer than the grid pattern to the segment topography. The profiles are flexible in terms of choosing the position, but less flexible in specifying the profile interval and direction.

The models easily are measured and the degree of experience required is not necessarily greater than that for the ordered points method.

There is a good accuracy-economy relation if the evaluation is good.

Disadvantages:

This pattern requires large computer resources.

When information is obtained from contours the accuracy is less (measure on the fly, dynamic measurements) than when information is obtained from a node pattern (where the instrument stops and waits for the operator to set the floating mark on the ground and then to record the point).

2.4.5.5. Sampling mode.

In data capture procedure we distinguish between static and dynamic.

In static sampling (point to point), the instrument is frozen while the operator records the coordinates of this point.

In the dynamic sampling (on the fly) the instrument moves (automatically or manually) and the points are recorded continuously. We can distinguish two kinds of dynamic sampling, the sampling in pre-specified time and the sampling in pre-specified equal distances. The sampling in pre-specified time is a difficult task for the operator, so the applications are very limited.

Comparing the static and the dynamic sampling, the static sampling gives better accuracy measurements, while the dynamic sampling is a quicker

procedure.

2.4.5.6. Examination of the relation between density, economy and accuracy factors.

DEM data are composed of mass points, breaklines and characteristic spot heights. The mass points are observed along parallel profiles and may or may not be in a grid pattern. Breaklines are classified as sharp and round. The former are edges of interpolated surfaces and when used in contour interpolation they produce a sharp jag in the contour. The round breaklines are used where extra information is needed but where a sharp jag is not required. The characteristic spot heights are observed on hill tops, depressions, saddles, water surfaces and road intersections.

Data density for mass points range typically from 1.6 mm to 2.3 mm at photo scale. Even the stereoplotter operator who has plotted contours for several years does not immediately know where to observe DEM data in order to produce a surface from which contours can be interpolated which correctly describe the terrain. He has to be trained by giving him interpolated contour plots so that he can see the result of his work. For this reason it would be preferable to have fast interpolation of a patch of DEM data and immediate presentation by superimposition in the stereoplotter optics.

Breaklines enable fewer mass points for a specified surface accuracy and they enable contours to be produced which are cartographically more acceptable. However, breaklines are time consuming, both in the time taken to decide where to observe them and in their actual observation. Experience has shown that it is easier to allow the observation of more points than necessary rather than the careful and time consuming selection of the essential points (Toomey, 1988). Later a computer program can be used to reduce the number of breakline points.

At first it was assumed that an increased geometric quality of the DEM would be achieved if the points to be measured were selected with respect to the topography. However this assumption was later found incorrect (Ostman, 1986). In this work it was found that regular grid measurements complemented with breaklines gave about equal standard error in interpolated elevations as compared

with operator selected points.

In another study Ostman (1987) examined if the operator selected points improve the geometric quality of the ground forms and, if this is the case, the amount of improvement. He believed that operator selected points contain more information than points in a regular grid, but what is the content of this information and how should it be used by the interpolation algorithm? Ostman (1987) agreed with Rudenauer (1978) that operator selected reference points did not give an improved overall standard error in elevations compared to grid measurements in which the same number of reference points were used.

The accuracy of the DEM depends on the identity of the initially captured points. In the case of capturing data in a regular grid, the grid interval is related to the density and consequently to the number of the captured points. The larger the number of collected points, the better relief representation (more accurate DEMs).

For many reasons the number of captured points should be reduced to the minimum because of the conflicting requirements of density, accuracy and economy factors.

It is well known that an increasing point density improves the standard error of the elevations of a DEM (Ostman, 1987). The standard errors of ground forms (slope and curvature) were studied theoretically. The conclusion reached was that only a slight improvement of standard error in slope occurs with increasing density of point measurements, but somewhat more slowly than the improvement of the standard error of the elevations (Forstner, 1983; and Ostman, 1987). This improvement was estimated to be proportional to the power 0.5 of the sampling distance (Forstner, 1983), while Ostman (1987) estimated the corresponding power to be 0.15. It is also shown by simulation that the standard error in curvature is almost independent of the sampling intervals that were used. In order to increase the quality of the ground forms, Forstner (1983) suggests taking additional form measurements, such as direct measurements of slope or curvature.

Balce (1986) captured sample profiles from large scale aerial photography:

1:4,000 with flat terrain and 1:8,000 with rough terrain. One stereomodel from each photo scale was sampled completely at various grid sampling intervals, in order to find out the optimum grid sampling interval. Profiles were captured with an analytical stereoplotter as follows:

1. From the 1:4,000 aerial photograph (flat terrain) in 3m grid interval as basis for comparison profile , using grid interval of 20, 51 and 62 m. Breaklines, hilltops and depressions were also measured.

2. From the 1:8,000 aerial photograph (rough terrain) in 4 m sample spacing as basis for the comparison profile, using grid interval of 7 and 12 m.

The roughness factors for each profile, which were going to be used for analysing the results of test comparison, were determined from the basic profiles.

Four interpolation programs were used : one based on Fourier transformation, one based on the self-similarity concept and two based on linear interpolation.

From each grid sampling combined with breaklines, hilltops and depressions, contour lines at 0.5 m interval were interpolated and plotted at 1:1000 scale. The discrepancies of contour lines were estimated. From the RMS's of discrepancies of contours, it was evident that they all met the required accuracies. From these, it was concluded that the true optimum grid sampling interval was 62 m for the flat terrain and 12 m for the rough terrain.

In another experiment (Balse, 1987), the same interpolated algorithms were used. The roughness factor in this test was defined to be the mean slope which was consistent, as was proved later.

The data were obtained from wide-angle aerial photography, at a scale 1:60,000, for compiling 1:20,000 provincial topographic series of the area with 10 metre contour lines. The profiles were sampled with 25 m spacing using an analytical stereoplotter. Profiles of varying sample spacing with spacing 50, 75, and 100 m were derived from the long profiles.

For the purpose of validating the observations one model was sampled three times at grid intervals of 75 and 130 m for the entire model, and 25 m for its southern part. Breaklines, hilltops, and depressions were also measured. From each grid sampling combined with breaklines, hilltops, and depressions, contour lines at a 10 m interval were interpolated and plotted at 1:20,000 scale. From the discrepancies of contour elevations, it was found that the contour plot from the 130 m grid sampling did not meet the specified accuracy (entire model), the

contour plot from the 75 m grid partially met the specified accuracy (accuracy suffered in the rugged portion), while contour plots from the 25 m grid met the specified accuracy with RMS of 3.2 m. On the other hand the 75 m grid interval for the rolling and flat terrain portion, and 25 m for the rugged portion met the specified accuracy.

Balse (1987) recommends that without progressive sampling, one has to be more conservative. The following profile attributes should be used with the most suitable programs:

Roughness of the terrain	Length of sample profile	Profile sampling rate
Rough terrain (R.F>=15)	Long (length>=1.75 model base)	High (Δd<=0.8 mm at image scale)
Flat terrain (R.F<15)	short (length<1.75 model base)	low (Δd>0.8 mm at image scale)

The varying width affects not only the data collection time but also data storage and computing time. In most cases the computing time depends linearly on the number of grid points, in perspective representations this is also true for the plotting time (derivation of contours). For DEM computations performed on a Harris H100 minicomputer, a 49% data reduction (varying grid size) had an effect of about 7% reduction of computing time, 49% saving in storage and a considerable reduction of 40% in both computing and plotting time (Kostli and Wild, 1984).

The Danish mapping firm Aerokort has investigated the price for generating DTMs. The price of measuring a grid DEM, including break - and structure - lines, is twice the cost of classical contour plotting. If only the grid is measured the price is almost the same. This is in accordance with investigations carried out by Toomey (1986). However, if the DEM is in established only to compute contours, it might be an unprofitable investment. So if it is possible to use breaklines, etc. in other applications the benefit of establishing DEM is improved. In urban areas DEM information is a part of the digital situation model (DSM). With the integration of the DEM and GIS it is possible to measure both models in one step (Sandgaard, 1988).

2.4.5.7. Forcing factors in adopting data collection methods and the density of the data points.

One central problem in photogrammetric data acquisition for DEM is the selection of the points to be measured. This selection can be controlled:

1. By the operator as in the case of selective sampling (manual selected points in which the human operator is needed to perform this selection.
2. By a computer in the case of progressive sampling or
3. By pre - defined patterns as in the case of sampling in a regular grid.

Manual selection of characteristic points is performed by an operator. The decision of where to increase sampling density is based on the topography of the terrain as judged by the operator. In order to obtain a high quality DEM, the measured points must be selected with respect to the topography. In production different sampling modes are often combined. We can combine the profiling or progressive sampling with the selective sampling of breaklines and other terrain characteristics.

Progressive and selective sampling are special algorithms which are developed to drive the analytical plotter to the estimated measuring point position. So special software is needed.

There are several factors which affect and impose the decision of adopting the data collection pattern. Some of them are as follows:

The sampling density and pattern should have a close relationship with the terrain type.

The specific type of equipment available for the photogrammetric measurements. If an automated or semi-automated photogrammetric instrument is available, the use of a regular grid is preferable (supposing that the appropriate software exists).

The required accuracy in the specific project. In static mode measured heights are 2 to 3 times more accurate than the dynamic (on the fly) mode of measuring heights (contouring).

The vast majority of the worldwide cartographic organisations use the the classical contouring method for measuring heights (dynamic mode). This method does not require special software, so it can be applied to analogue instruments,

which are still widely used on the production line.

Regular grid measurements complemented with breaklines, is of considerable importance in many situations. It is significant when designing the data structure for the storage of digital elevation data and is also of interest when carrying out progressive sampling. Is this approach more successful with respect to the overall standard error, or is the choice of point pattern in general of less importance?

In a practical situation, the setting of sampling parameters, for instance the grid spacing, can be a very difficult task. If the grid is too sparse, important features might be missed and if the grid is too dense, sampling is too expensive.

2.4.5.8. The data collection method and pattern used in this project.

In this project a regular (square) grid pattern for data collection was adopted. The author believes that for the terrain measurements the other regular grid patterns (such as the rectangular, hexagonal and triangular grid pattern) do not make any difference, but sometimes can create problems eg. in the stage of data manipulation.

The collecting of random data (operator selected points) was not carried out because:

1. It does not give an improved overall standard error in elevations compared to the grid measurements that the same number of reference points is used (Rudenauer, 1978 and Ostman, 1987).

2. It is always variable depending on the inspection and interpretation of the operator.

3. It is avoided for normal production because this method is time consuming, a smaller grid interval is preferable instead to maintain accuracy.

4. It is debatable whether random data are to be considered as more reliable than regular grid points under poor measuring conditions encountered in SPOT images of breaklines or steep-sided valleys (see § 5.2.4.5).

From aerial photography digital elevation measurements using a grid interval

of 30 m was carried out in order to offer a good background for checking the SPOT elevation data. Random data in terrain peculiarities are not measured, because the basic purpose was to provide a sufficient "ground truth" for checking purposes, rather than a perfect relief representation. The greatest possible distance of a SPOT point to a checking matrix node point is 21.22 m. An interpolation procedure was carried out taking into account the four nearest neighbour matrix points in respect of their distance from the point to be checked. If we consider the fact that 97,390 points were measured then the grid interval of 30 m was the appropriate one as it was a good compromise between accuracy and economy of data capture.

The grid interval for the SPOT measurements (100 m) was chosen with the criteria of 'averaging' the terrain relief, and also to do with the SPOT capability for manual data capture. This was satisfactory, because the test area includes most terrain variations. Although the SPOT panchromatic pixel is 10 m x 10 m, measurements in a grid interval less than 30 m do not make sense, because the operator can not see clearly the relief change in respect to the floating mark movement. A 30 m or 50 m grid interval is too dense for a 1 : 25,000 map, because 50 m on the ground correspond to 2 mm on the map. The 30 and 50 m grid interval are more suited to automated procedures. The grid interval of 100 m corresponding to 4 mm on the map (0.25 mm on the image scale) is adequate for gentle slopes as it 'averages' the relief, but in very rough and steep terrain a 100m grid is inadequate.

In this work the test area (12.4 x 6.9 Km^2) occupies only a small part of the satellite image. In other projects, and particularly mapping over large areas, it is necessary to make sure that the cartographic specifications of the earth's geoid are accurate, and to begin to address standard methods of storing and accessing the huge quantities of data. One major shortcoming of using satellite imagery is the ability to derive from the imagery accurate object space positions of geographic features. This problem is usually not significant for small geographic areas (3600 km^2 or less), where one monoscopic image or one stereomodel is all that is required; it is often easily solved by using an abundance of accurate photo identifiable ground control points. However, for large cartographic projects (particularly in areas of sparse control) the problem is much more significant. The derived object space positions between image boundaries will contain discontinuities, and a multiplicity

of ground control points will be required. This can limit the use of SPOT data in large mapping projects over sparsely controlled terrain, unless special measurements are taken.

Chapter 3.

Data sources, methods and techniques.

3. Data collection implementation, sources, methods and techniques.

3.1 Data capture methods and techniques.

Data capture is the encoding of data. In general the data information is not collected in only one way ie from one data source or method, but in many different ways. Combining different sources and methods should give us quick, accurate and cheap information.

The collection may be done by:

1. Direct methods ie land surveying.
2. Non direct methods ie photogrammetry.
3. Mixed methods.

The above can be explained by the Figure 3.1.

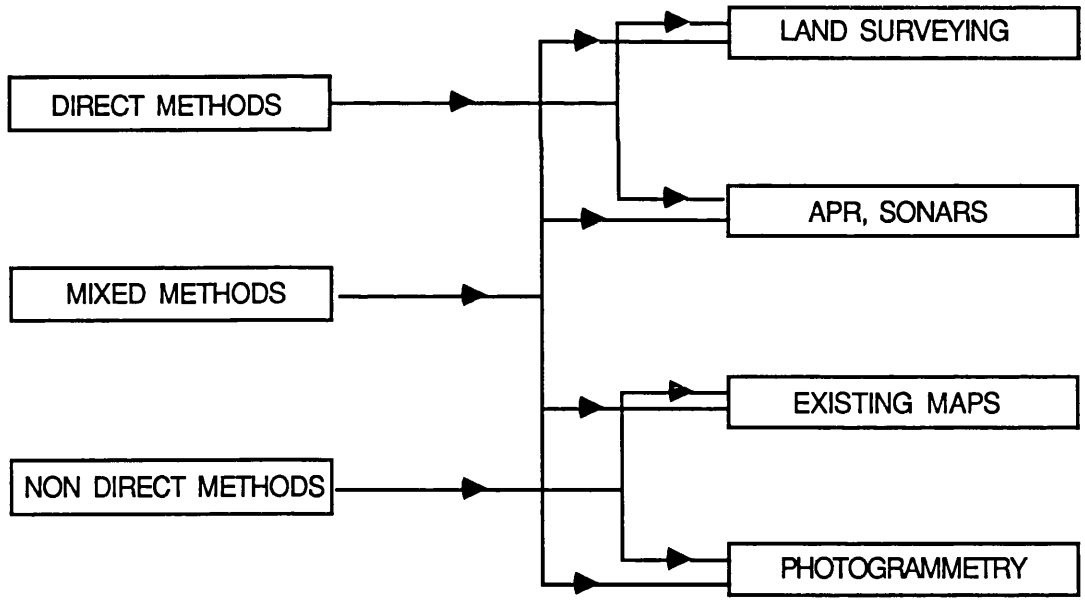

Figure 3.1. Data capture sources and methods

The data collection by photogrammetry may be done by:

1. Automatic photogrammetric instruments such as image correlator instruments.
2. Semi automatic photogrammetric instruments such as analytical plotters

or new digital plotters which accommodate softcopy (CCT) instead of hardcopy (film).

3. Non automatic analogue instruments with the operator assistance.

Digital mapping techniques include map digitising, direct encoding by electronic survey instruments, and the encoding of text and attributes by various means. So data can be drawn from many sources. Nowadays for each source we can extract the data using 5 methods and techniques:

1. Terrestrial survey.
2. Conventional photogrammetry.
3. Photogrammetry from space.
4. Use of scanner and array system (from existing graphics such as digitising a contour map, or an orthophotomap with contours).
5. Use of active scanner systems and RADAR.

Brief descriptions for the conventional photogrammetry and the photogrammetry from space cases are:

Conventional Photogrammetry.

Classical photogrammetry is based on conventional photography. Photogrammetric techniques are used to bring forth an almost endless variety of useful products that convey information about given surfaces and objects. A very important and perhaps the best known application of photogrammetry is the compilation of topographic maps and surveys complete with contour lines, based on measurements from aerial photographs. Orthophoto scanning is another less known but very useful application. Included in conventional photogrammetry are grid based techniques and raster techniques (photo-mapping)

Photogrammetry from space.

If the camera or sensing system is borne in a space vehicle, the process may be called space photogrammetry, or satellite photogrammetry. The increased use of high altitude aircraft and space vehicles for acquisition of basic imagery and other data has extended the range. In a parallel way the photogrammetric implementation

and techniques are adapted to the new approaches. New techniques and algorithms have been developed in order to reduce the amount of ground control, especially by the use of inertial position and height-finding systems to give the precise position of the sensor at any desired instant.

Some of the new advanced methods, techniques and applications developed in both photogrammetry from space and remote sensing are the following :

1. Manipulation of imagery from various sensors to accomplish theme extraction.
2. Automatic classification, or derivation of specialised information.
3. Geocoding of remotely sensed data.
4. Automatic height information extraction for DEM production (auto-correlation techniques). Automatic correlation techniques are applied on the SPOT, Landsat MSS overlaps and thematic mapper overlaps (the thematic mapper derived DEMs are low accuracy +/- 70 m RMS in height).
5. Automation techniques in the development of integrated , automated cartographic systems in which the photogrammetric system is a central element of a continuously automated mapping process.
6. New kind of products in graphical, digital, or image form.

3.2. Data collection implementation.

The methods and the instruments used to collect the information depend on:

1. The desirable characteristics of the final product.
2. The structure of the surveying object.
3. Existing equipment, measurement instruments and computer software.

The data collection may be done with:

1. Automatic photogrammetric instruments, or digital plotters.
2. Semi- analytical photogrammetric instruments (analytical plotters).
3. Non automatic photogrammetric instruments (analogue) with operator assistance.

Certain data structures are particularly suited to the data collecting,

processing and outputting techniques, but they must be capable of providing a certain type and level of data accuracy.

Stereoplotters typically produce segments or points which in a traditional procedure are not even coded, but only registered in an arbitrary manner.

Digitising by manual digitising tables create points, lines or polygons depending on the selected logic.

3.2.1. Analytical plotters.

An analytical plotter is a computer controlled stereoplotter. Basically it is a photogrammetric plotting system which solves mathematically in real-time the relationship between photographic image coordinates measured in the two dimensional photographic reference system and the ground coordinates of the object in the three dimensional 'real' world. Photo coordinates are measured by some form of stereocomparator. These are then fed directly into a suitably programmed high-speed mini (micro) - computer which solves the basic photogrammetric equations and provides a readout of model or ground coordinates. The control computer calculates the necessary corrections required in real time and implements them in real time.

The major difference between an analytical plotter and an analogue one is in the process of stereo restitution of a photogrammetric model. In an analogue plotter, the process of stereorestitution of a photogrammetric model is done by reconstructing the exact geometric relation of the image and the terrain in the instrument with the help of optical and/or mechanical devices. With the advent of electronic computers, the reconstruction of a stereomodel in an analytical plotter is computed based on two conditions which relate an image point, an exposure station and the corresponding object point through collinearity equations.

Analytical plotters have no limitations with respect to types of photography they can accept (focal length, film format size - not larger than the stage plate -, lens distortion, film shrinkage). The effects of these elements are compensated for in straightforward mathematical manner. They do not need fine mechanics and

optics for simulation, and a high degree of accuracy is obtained. A properly designed analytical plotter will permit accurate photographic scale measurements of two micrometers.

For the acquisition of terrain elevation data the analytical plotters can be programmed to drive to any desired position or series of positions corresponding to the required pattern and density of points in the stereomodel.

3.2.1.1. The Kern DSR1 analytical plotter.

3.2.1.1.1. Description .

The Kern DSR1 is a high precision stereoplotter, with a sophisticated distributed computing architecture.

The DSR1 without the peripherals is an optical-mechanical device, comprising coordinate input devices (handwheels/trackball, footwheel/handdisc, footswitches), four lead-screw servo-motor systems driving the stage plates, and a DEC LSI-11 processor (P2). This processor is devoted to driving the stage plates to maintain a stereo model in response to hand/foot wheels inputs, and to solving the collinearity equations. The departmental DSR1 is linked to a host computer, a DEC micro PDP 11/73 (P1) with memory capacity of the central unit of 64 K and running under RT11. P1 performs all other computational and input/output functions such as calculation of model orientations. Various peripheral devices such as a KERN GP-1 plotting table can also be attached to P1.

The software on the Kern (Cogan and Hunter, 1986) is written in a non-standard Pascal (Pascal 2, Oregon Software) language. Pascal language is used for reasons of transparency, self-documenting and fairly rigid program structures. It is highly modular in structure. P1 programs such as the orientation programs, make use of internal subroutine libraries of commonly used functions, and a library of subroutines for communicating with the plate processor. The library subroutines are available to users to develop their own host computer programs for driving the DSR for instance in stage plate or model coordinate systems.

The structure of the distributed computer facility is shown in the figure 3.2.

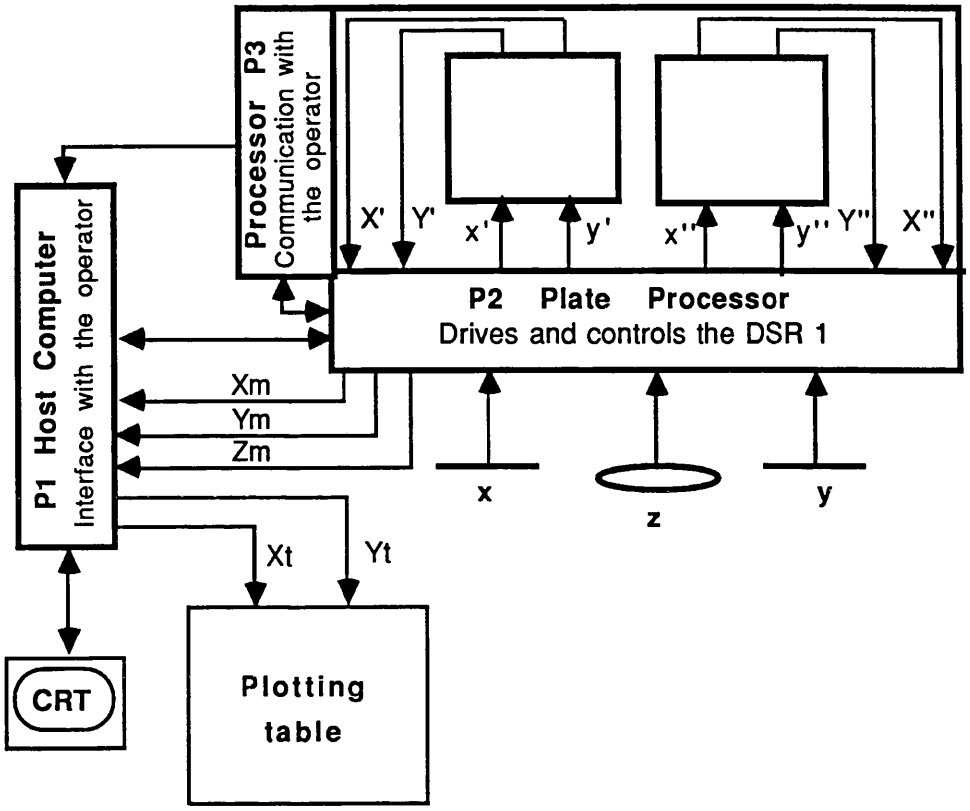

Figure 3.2. The Kern DSR analytical stereoplotter system.

3.2.1.2. Data collection software.

3.2.1.2.1. The DEM data capture program (DEM generation program).

This program (Saksono, 1988) was not supplied by Kern and is not official Kern software, but was written specifically for the requirements of the Department of Photogrammetry and Surveying at UCL. The program is installed on the PDP 11/73 microcomputer which supports the Kern DSR1 analytical plotter and it appears as an option to the main Kern menu. With this program the user can measure points lying on a regular grid with pre-specified grid interval, random points, or a combination. In the regular grid case, the instrument drives to the grid points at the specified grid interval and waits for the operator to measure the

height. Then it drives to the next grid point and so on. The manual planimetric control (conventional handwheels or the trackball) is disabled. That means the user can not move the floating mark (in plan) while he is observing the points, but the computer automatically drives the measuring mark to the next precalculated planimetric position of the defined grid node. The user can record the point by pressing the right foot pedal, or can discard the point by pressing the left foot pedal. The points may be discarded when the operator decide that he can not sufficiently interpret and measure them. The recorded points are stored in the PDP 11/73 hard disk (in the current logical device) and displayed on the screen. If a point is discarded then a message "skipped", following the point number, is displayed on the terminal, but nothing recorded in the file.

The program asks the user to give :

The number of the desired DEM rows and columns.

The grid spacing.

The initial point, the direction along X axis and the direction of the DEM block.

The user can either insert the above point coordinates from the terminal, or drive with handwheels to the desired position and record them.

The output data from the DEM generation program consist of:

A file which contains the generated digital elevation data as a string of coordinates (point identification, X, Y, Z ground coordinates).

A file for storing the corresponding image coordinates, with respect to the fiducial coordinate system, of each stored DEM point.

A file containing information of the starting points for the next block.

3.2.1.2.1.1. Accuracy of the DEM data capture program.

The accuracy problem of the semi-automatic methods of the DEM capture programs lies in the capability of a computer to drive the floating mark to the precalculated positions. Most of the existing packages follow a geometric pattern, most commonly a grid pattern. The most important consideration is avoiding an accumulation of error in the planimetric positioning of the floating mark. This can

be avoided easily if all the planimetric coordinates of the grid nodes are computed directly with respect to the starting origin. In this way the planimetric position of the floating mark is independent of the points being generated. The DSR1 data capture program follows this procedure.

In a sample of two blocks, the planimetric coordinates were checked with respect to the grid normality and the grid interval. The grid RMSE planimetric accuracy of the DEM data capture program was found to be less than 25 μm in the image scale or 1m in the ground (for the SPOT images).

3.3. Major technical problems in photogrammetry. Weak points of analytical plotters and SPOT images.

3.3.1. Problems in photogrammetry.

This section is not intended to cover all the problems facing the photogrammetrist in his effort to obtain precise measurements from imagery collected photogrammetrically or by other remote sensing techniques, but to give an idea or a sequence for dealing with the following problems on analytical plotters and with the SPOT images. The problems in photogrammetry can be grouped in three categories.

1. Obtaining the basic (raw) data.
2. Processing the data.
3. The nature of the earth's surface.

1. Obtaining the basic data.

One of the serious problems is that the conditions are rarely ideal for obtaining and preserving high quality original imagery. Some of these problems are related to the instant of exposure (ie. movement of the platform, sensor orientation etc), the camera or sensor, the film and the atmospheric conditions.

2. Processing the data.

Some of the operations which can cause difficulties at the stage of

transferring the quantitative information from the photographs to the map compilation sheet are:

The developing of the original film, making prints and operating the photogrammetric instruments.

3. The nature of the earth's surface.

The character of the surface of the earth itself causes difficulties for the photogrammetrist. Some of the problems are related to the earth curvature and the relief.

3.3.2. Weak point of analytical plotters related to the photographic material.

Apart from the high cost, analytical plotters suffer from one major disadvantage, related to the quality of the photographic image. The photographic emulsion is not of uniform thickness, it does not give infinite resolution and the film base is not perfectly dimensionally stable. In addition there are some problems due to the poor radiometric fidelity of the film writer. Image degradation occurs during the process of film writing, destroying the information fidelity.

High resolution space sensors record very large volumes of digital data at very close sampling intervals (13 microns on the SPOT focal plane). This resolution is degraded by the process of film writing the digital data onto photographic emulsion, due to poor dynamic response of the film.

Moreover digital SPOT image data (from which the hardcopies are printed) contain much information both as subtle grey level values and high frequency linear features, often less than 1 pixel in width. It is noticeable that a significant degree of degradation of this image information occurs during the process of film writing. Two main factors influencing the photographic image quality are: the transfer of the maximum grey scale range onto film ,and the preserving of the high frequency information. The first process relies on the histogram of the digital data being matched to the sensitivity range of the photographic film. The second process relies on adjacent pixels in the image being printed with different digital values. Laser film writers can do this, but continuously modulated LED film writers

cannot. The laser film writers are superior for high frequency detail, clearly printing individual pixels. Continuously modulated LED film writers are better for reproduction of subtle radiometric variations, preserving image texture. For linear feature following, predominant in topographic mapping applications, the preservation of the high frequency information was found to be more desirable than radiometric fidelity (if a choice had to be made), although the measurement of digital elevation models is probably better when the image texture is preserved. In other words the preservation of grey values improves the measurements of area features such as digital terrain models (Gugan & Dowman, 1988b).

Technology can not satisfactory solve these problems with film yet, and film parameter still remains as a limitation in classical photogrammetry. The only way to overcome the problem is the digital plotter, which uses a soft copy (Computer Compatible Tapes) as data source (instead of film) and the same software as in the analytical plotter.

3.4. SPOT satellite imagery.

3.4.1. Weak points of SPOT satellite images.

3.4.1.1. General characteristics of the SPOT satellite.

In this section it is not intended to explain the whole working mechanism of the SPOT satellite system, but to identify a few points which I think are relevant in understanding the foremost weak points.

SPOT (Systeme Pour l' Observartion de la Terre) satellite was launched by the French on 22 February 1986. The satellite orbits in a near circular, sun-synchronous, near-polar orbit at an altitude of 832 Km. The orbit was declared operational after a two-month post launch assessment. The revisit frequency is 26 days (that means the satellite will pass over the same point in 26 days , after 369 orbits), though the off-nadir viewing capability of the satellite enables more frequent coverage of a given area to be achieved if required. The satellite carries two identical and independent instruments, named HRV1 and HRV2

(Haute Résolution Visible) which are designed to operate in either panchromatic mode (λ = 0.51-0.73 μm) over a broad spectral band producing imagery at 10m resolution, or in multispectral mode within three narrower spectral bands producing imagery with a ground resolution of 20m.

Each HRV instrument is essentially a reflecting pseudo-Schmidt telescope. They have focal length 1082 mm, aperture f/3.5 and spherical corrector lenses. When SPOT uses the off-nadir viewing, swath width of individual images varies from 60 to 80 km depending upon the viewing angle. The vertical images cover an area 60 x 60 km^2, if the panchromatic mode is used. The swath width on the ground is 117 km (60 km per HRV and 3 km overlap).

The pushbroom method of imaging is a system composed of a linear array of detectors oriented perpendicular to the flight path, built in the focal plane of the sensor. The panchromatic SPOT images are really a composite of a succession of 1-D images (linear array), formed by a 6,000 element CCD array (Charge Coupled Devices), which transforms the incident light into a sampled video signal. These do not point exactly to the satellite nadir point. The array offset (constant parameter) for the panchromatic band is -0.476° (-0.00830777 rad), while for the multispectral band it is 0.476°. Each detector is 78 mm long and 13 μm wide. An image is comprised of the output from 6000 sequentially recorded lines of imagery, giving dimensions 78.0 by 78.0 mm.

These 1-D images are taken at 1.5 msec intervals (exposure time of the linear array sensor), as the satellite orbits the earth at ≈7.5 km/sec, so a complete image is formed about every 9.024 sec. Within one second, 667 lines can be recorded, which means the information of 667 x 6,000 pixels. Each pixel consists of 8 bits of information, that are compressed by pulse code modulation into 6 bits for transmission to the ground stations. For this reason, the recording data rate is around 25 Mbits/sec for each HRV.

There are four linear arrays, two within each HRV instrument. The linear array is approximately perpendicular to the satellite's track, and the plane formed by the array and the perspective centre is approximately vertical. For producing stereopairs and repeatability of observations, the array is frequently tilted

relative to the vertical by 45 steps, by increments of 0.6°, so that it is looking at angles off the vertical of up to 27° or so (B/H ratio from 0 to 1.1), but the plane formed by the array and the perspective centre remains approximately vertical and perpendicular to the satellite track. With this mirror it is possible to view any point within a strip 475 km either side of the ground track (Mather, 1987).

This technique provides a quick revisit capability on specific sites. For instance at the equator, the same area can be targeted 7 times during the 26 days of an orbital cycle (98 times in one year with an average revisit of 3.7 days). At latitude 45, the same area can be targeted 11 times in a cycle (154 times in one year, with an average of 2.4 days, a maximum timelapse of 4 days and a minimum timelapse of 1 day) The mirror movements are controlled by the ground control station. The projection is pseudo-cylindrical.

The advantages of a pushbroom scanner over a conventional multispectral scanner are: greater reliability, no moving parts, higher geometric accuracy, higher spatial resolution, higher radiometric accuracy, higher signal to noise ratio, lighter weight, smaller size, lower power requirement, longer life expectancy, and lower cost. The disadvantages are: there are many more detectors to calibrate, and cannot sense wavelengths longer than near infrared (Curran, 1985 pp. 155).

SPOT images are convergent images so a stereopair can represent almost the same area. The stereoscopic view in SPOT is achieved because of the different mirror view angle in which the image is recorded. That means that the one image is taken with an oblique view towards the east, the other one towards the west or the one could be vertical or near vertical. By contrast, in aerial photographs a stereoscopic vision is obtained when the stereopair has a common part of the same area (overlap area) usually 60%.

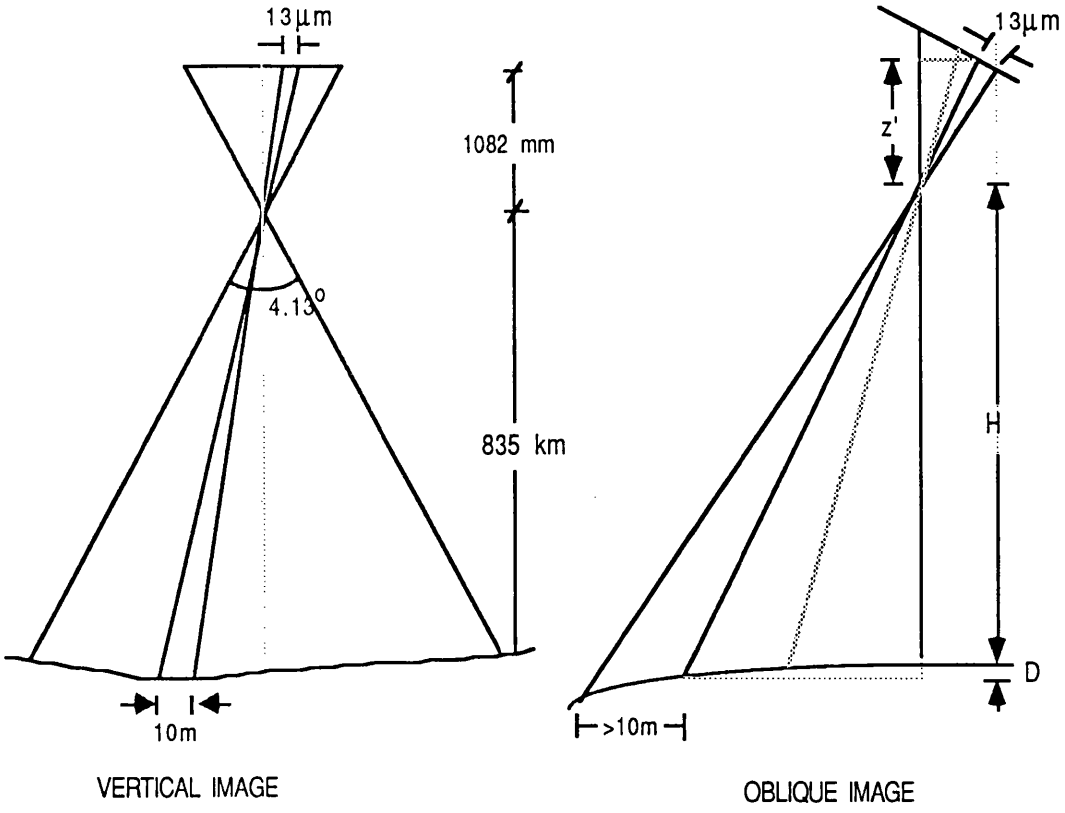

Figure 3.3. Vertical and oblique SPOT image.

The HRV instruments are carried on a platform. The platform itself helps to provide some basic services such as power supply, communication with the ground station and between various components within the system, attitude measurements and general control. Electrical power is generated by means of a solar panel. Power up to 1.8 Kw is generally generated which is quite sufficient for running the system.

The image data as collected needs to be transmitted to the ground station. The chosen communication frequency used by SPOT is X band, which allows the transmission of all the data recorded (Chevrel et al, 1981). In addition to this data, information about sensor calibration and platform attitude also needs to be transmitted to the ground. Thus the information to be transmitted is enormous and the ground receiving station needs to have a good management system to handle the data. The whole SPOT system is controlled by an on board computer which has a prime function of running a program which generates mirror pointing instructions for the two HRV instruments.

Throughout the mission, periodic on-board calibration of the CCD array is made and the amplifier gain can be adjusted by ground command. These adjustments permit compensation for large variations, along each orbit, of the angle of incidence of sunlight on the terrain. The sensitivity of the HRV sensor is such that reflectance steps on the order of 0.5 can be detected under suitable conditions of illumination, ie. sun higher than 30° above the horizon.

More details on the SPOT satellite system can be found in Begni (1982), Begni et al (1984), Chevrel et al (1981), SPOT User's Handbook (1988) and on the satellite orbit are available in Begni (1986).

SPOT data is either released on magnetic tape or on film positives. The type of data that is used has an influence on the results. Digital SPOT image data contains much information both as subtle grey level values and as high frequency linear features. SPOT images will produce several levels of processed imagery as standard products:

Level 1A : Is the photographic film for photogrammetry. This is printed from the raw data, with equalisation of the response of the detectors (known as CCD detector normalisation). Neither interband calibration nor geometric correction is applied (so neither GCPs nor on board attitude data are used). A level 1A images always comprises 3000 by 3000 lines in XS mode or 6000 by 6000 lines in panchromatic mode. Auxiliary data are supplied concerning the scene location, imaging geometry, and spacecraft attitude rates. The location accuracy is not specified. This product has some problems noted by investigators and users. In order to overcome these problems SPOT Image decided the release of a new 1AP product with the following specification and improvements:

1. Better fiducial marks, 8 thin marks exactly positioned at the centre of the corner and median pixels of the raw image.
2. Auxiliary data, which are going to be provided on CCT or MS-DOS floppy disk.
3. Better geometric accuracy.
4. Enlargement of the global scaling 1:350,000 instead of 1:400,000.
5. Observation comfort with the anamorphosis procedure, which is a linear

scaling along lines, in order to cancel the fictitious tilt of the stereomodel.

6. Better quality of photointerpretation, which is going to be achieved with the following procedures:

lower contrast, by non disturbing processing (stretching often unsuited) of the standard image.

edge enhancement by a specific filter, in order to improve the detection and interpretation of the linear items.

film density and contrast in accordance with the aerial photographs specifications.

Level 1B : Level 1A , corrected for known geometric distortion include along-line and along-column resampling to eliminate earth rotation, earth curvature and panoramic effect; mirror look angle and orbit characteristics (geometric system corrections), but not attitude errors. The outline of a level 1B image forms a parallelogram, instead of a rectangle. RMS location accuracy is 1,500 m for vertical scenes and 1800 m for oblique scenes. RMS local error is 17 m, 1.2 Km over the whole scene including relief errors.

The corrections to the level 1 products are made using only mathematical models and parameters estimated through payload telemetry or the orbit measurements.

Level 2 : This is a precision processed level. The radiometric corrections are as for level 1B. For geometric distortion, corrections involve bi-dimensional corrections by means of ground control points (6 or 9 GCPs per scene) and auxiliary data, but not a DEM. This means that parallax effects due to relief, particularly noticeable in oblique viewing imagery, are not corrected. Relief displacements remain. The image is rectified according to a given cartographic projection. The total number of pixels varies over wider ranges than is the case for level 1B data. The specification accuracy of position (RMS location accuracy) is 50 m for oblique to 30 m for vertical viewing.

Level S : The corrections applied to level S data are similar to those applied to level 2 data. The scene is rectified relative to another scene used as a reference. Distortions due to relief, are not corrected, but since the parallax effects are essentially the same in both reference scene and in level 1S scene, the two scenes can easily be superimposed using identifiable homologous points. RMS location

accuracy is 0.5 pixel ie 5 or 10m depending on the image mode.

Level 1P : Level 1A imagery printed with a diapositive size of 225 x 225 mm format size at 1:266,000 scale. The imagery is corrected for measured attitude variations in such a way that all linear and non-linear attitude biases (roll, pitch and yaw) are eliminated, and resampled to 9,000 x 9,000 pixels. In this way the product which obtained, has a constant orientation over the entire image. This version appears specifically oriented to photogrammetric applications. Level 1P is going to simplify the software for SPOT stereo restitution.

Moreover the following special products are made and distributed from SPOT Image: quick look films, quarter scenes, P + XS merged images and mosaics.

3.4.1.2. Image quality - Error sources.

The question of the image data quality is best approached from the user's point of view. An alternative might be a more scientific approach such as evaluating the radiometric and geometric quality derived from signal theory but this is the privilege of specialists. The user is generally more interested in one particular data property. Mapping applications, for example, demand a certain level of geometric quality, whereas the study of vegetation cover calls for radiometric quality.

Geometric quality describes the capacity of the data to give the exact location of imaged objects. Geometric quality depends on the geometry and dynamics, knowledge of any departure from anticipated geometry and dynamics, and the type of preprocessing performed on the raw data. Geometric quality can be split into intrinsic geometric quality and extrinsic geometric quality. Intrinsic quality concerns the image quality reference to external data. For a scene considered individually the most appropriate criterion may be the accuracy of shape reproduction, or in other words, the absence of internal distortion within the image. Extrinsic quality introduces the use of auxiliary data, e.g viewing angle and image orientation.

Four mathematical geometric quality criteria have been developed, describing both intrinsic quality and extrinsic quality of an elementary image:

1. Scene location accuracy. This is the difference between the actual and estimated positions of the scene centre.

2. Relative length distortion . This is defined by the ratio: (estimated distance - actual distance) / actual distance.

3. Anisomorphism. this is determined by the length distortion in two orthogonal directions.

4. Local coherence. This concerns the along-line (across-track) and along-column (along-track) regularity of the ground sampling interval.

Furthermore, three additional geometric quality criteria have been defined.

1. Multispectral (band-to-band) registrability. (when scenes acquired in different spectral bands).

2. Dual mode (P + XS) registrability (when scenes acquired in different spectral bands).

3. Multidate registrability (when scenes acquired on different dates).

Radiometric accuracy describes the quality of radiation measurements in the different spectral bands. By making certain assumptions, one can deduce from these measurements the spectral reflectance of imaged objects (terrain targets). The quality of these measurements depends on the atmospheric conditions (absorption and scattering), the characteristics of the HRV instruments (scanner optics) and the type of preprocessing performed afterwards (detection and conversion, scanner signal amplification and scanner calibration).

Geometric and radiometric quality requirements cannot be satisfied to the same degree at the same time for the simple reason that they are not always mutually compatible because of limitations imposed by the fundamental physics.

As a part of this thesis deals with the SPOT elevation data, the geometric accuracy is more important than the radiometric quality. Therefore, the radiometric quality will be described briefly, and particularly as a cause of difficulties in the operator factor, whereas the geometric quality requirements, particularly the major physical quantities or factors determining this quality, will be dealt with more extensively, bearing in mind that the following section is not intended to cover and to analyse all the possible error sources, but to examine some of those related to some of the essential problems of the SPOT satellite

imagery.

Analysis of the physical quantities which are involved during the recording procedure, acting as error sources, affecting the image geometric quality and some of the quantities which affect the radiometric quality are given below:

1. Due to the earth:

   Rotation, curvature, oblateness, morphology (relief displacement) and exposure angle.

2. Due to the orbital dynamics:

   Altitude variation, velocity variation, precession, tracking.

3. Due to the platform:

   Attitude, drift.

4. Due to the sensor:

   Misalignment, viewing angle, non linearities, exposure time (MLA), interframe deformation, calibration.

5. Due to the sun's illumination:

   Zenith angle, shining direction angle, sun-morphology interaction, sun-atmosphere interaction, shadow.

6. Atmosphere:

   Absorption and scattering, refraction, diffusion, clouds, haze.

In the following paragraphs some of the error sources which affects the image quality are examined.

The earth rotation effect.

While the SPOT satellite travels during the image acquisition of a complete scene, the earth revolves and both these angular changes combine in a composite motion which causes the satellite ground track to deviate from the nominal plane of orbit as shown in figure 3.4.

So the successive scanlines recorded by the linear array scanners shift westward as a result of the Earth's rotation. The amount by which successive scanlines shift is a function of the latitude. The shift is as its maximum at the equator as the following simple calculation shows:

$$\frac{9.024 \text{ sec}}{24 * 60 * 60 \text{ sec}} * 40{,}073 \text{ Km} = 4.185 \text{ km}$$

The total shift between first and last image line therefore is approximately 4.185 km in ground scale. In the image scale (1:400,000), the shift is approximately 1 cm. This is the reason that after post processing most images take the form of a parallelogram instead of square.

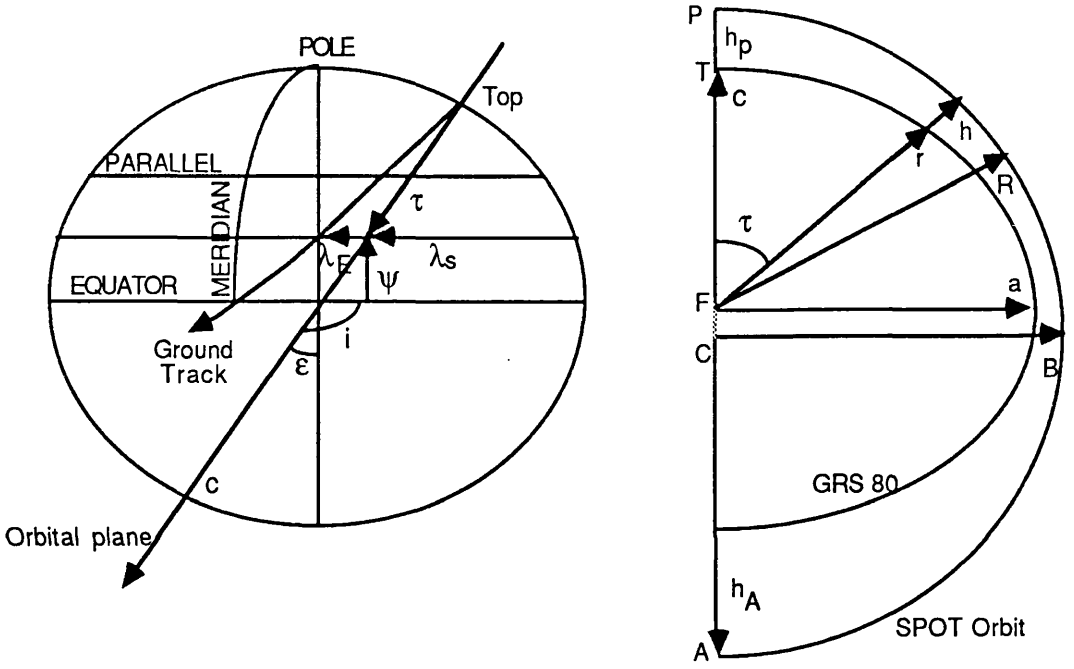

Figure 3.4. SPOT orbital relations. (After Kratky, 1987).

Corresponding geographical longitude slip λ_E increases linearly with time. The resulting change in the nominal orbit due to earth rotation is given by the formula $\lambda_E = \omega_E * t$, where $\omega_E = 2\ \pi/24/60/60 = 0.072722$ mrad/s is the constant angular velocity of earth rotation, and t is the time.

The nominal position of the satellite S_S is not affected by earth rotation position and therefore is defined by the orbital parameters τ and ε and by the geographical coordinates ϕ and λ_S. The earth rotation effects the actual position of

the satellite nadir point displacing it from S_S to S.

In this analysis the composite motion $\tau(t)$ and $\lambda_E(t)$ can both be assigned to the satellite as if it orbited around a stationary earth. The effect of travelled angle τ (fig. 3.4 and to derivations by Kratky, 1988), can be expressed by changes of geocentric latitude ψ and geographic longitude λ_S.

$$\sin \psi = \cos \varepsilon \cos \tau \quad , \quad \tan \lambda_S = \tan \tau / \sin \varepsilon \quad , \quad \lambda = \lambda_S + \lambda_E$$

Geographical latitude ϕ is derived from ψ by:

$$\tan \phi = a^2 \tan \psi / b^2$$

The earth curvature.

This not an error but is treated as an error source. The effect of earth curvature is relevant when satellite imagery is used for extracting height information, because of the large area of coverage. If a large area is mapped then care should be taken to solve this problem. This can be done either by applying a displacement to the image coordinates, or more effectively by employing the Geocentric coordinate system.

Given a distance (C) of a ground point (P) from nadir point (N) of an image, the difference (Δz) in measured elevations exhibit a negative trend. This trend (Δz) can be approximated by the formulae $\Delta z \approx - (C^2/2*R)$, where R is the earth's radius (R ≈ 6,378 Km). C then can be found from the follows:

From the sin rule (R/sinb)= (R+H/sinc) and hence

$c = \sin^{-1}((R+H)*\sin b / R)$

a = 180 - c - b and C=sina*R

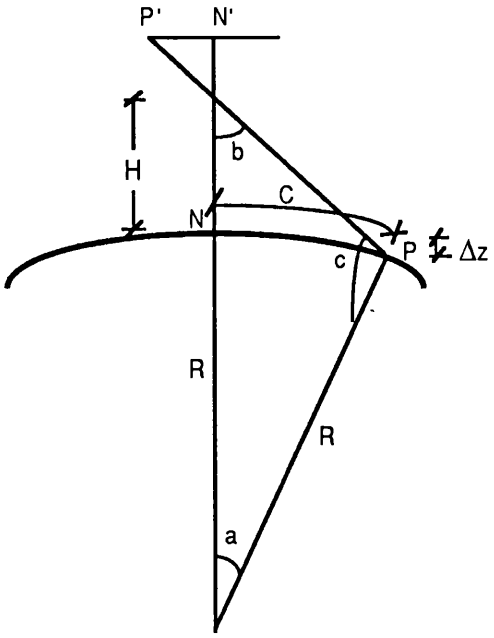

Figure 3.5. The earth curvature error.

For viewing angle 27° and H=835 Km, then C= 433 Km and $\Delta z \approx -14.7$ m.

The relief induced distortion.

The image distortion due to terrain can be dominant or comparable to the errors due to map inaccuracy in undulating and mountainous terrain. The distortion due to topographic relief depends on the sensor altitude and view angle, and it is in the form of slope forelengethening rather than foreshortening.

Topographic relief displacement is the shift in position of an object displayed in an image, caused by the elevation (topographic relief) of the object. The effect is to cause the scale to change throughout the image and to cause images to be displaced radically from the nadir, from the position at which they should appear, for objects whose elevations are above the datum. Relief displacement in terms of a radii distance from the nadir point r is given by the equation:

$$D = \frac{r * h}{H}$$

Where :

D : Is the relief displacement.
r : Is the distance on the image from Nadir to the displaced object.
h : Is the height of the relief.
H : Is the height of the vehicle above the datum.

The magnitude of relief displacement is given in the following example (Logan et al, 1988):

For an aircraft flying at an altitude of 4,572 metres (15,000 feet) an object 3,000 metres from aircraft nadir and 600 meters in elevation would suffer a 394 metre displacement from true location on the image. The displacement error increases with decreasing altitude (600 metres displacement at 3,048 metres altitude), and decreases at higher altitude (91 metres displacement at 19812 metres altitude).

For the SPOT satellite flying at an altitude of 835,000 metres:

For the vertical images. An object 30,000 metres from the platform nadir and 600 metres in elevation would suffer a 21.6 metres displacement (2 pixels).

For the oblique images, ie for an image with view angle 20°, an object 333.9 Km from nadir and 600 metres in elevation would suffer a 239.9 metres displacement (24 pixels).

The relief displacement in the pushbroom systems cannot be ignored as it can be ignored for normal relief on Landsat 1,2 and 3 image. The effect of the relief can be removed by using a rigorous three dimensional model of the geometry of two images, or by having a digital elevation model available in order to compute, and hence to correct, the effect of relief at any point.

Irregularities in sensor platform motions.

Irregularities of the platform can be distinguished in attitude and altitude variations. In the case of single exposure the platform can be considered to be stationary at the time of exposure. For SPOT the platform moves during formation of the image. In addition the satellite orbit is not stable.

Deviations in the platform attitude lead to a variety of distortions due to roll

f (ϕ), pitch g (ω), and crab or yaw h (κ) motions. Moreover there are forward movements on the space borne platform relative to the ground during the time of recording the image.

The effects of tilt can be considered in rigorous mathematical terms and the movement of the platform modelled by a matrix representing rotation. The elements of such a matrix can be found with the aid of ground control points (GCPs) or by measuring movements of the platform by sensors or by reference to fixed objects such as stars.

The attitude accuracy directly affects the registration accuracy. Error caused by attitude accuracy can not be completely removed by a ground data processing system without including other errors. Consequently, improvement of attitude accuracy and the development of an advanced attitude control system are needed to support subpixel registration accuracy without the use of control points. For image resolution of 10 metres or less, attitude accuracies of 10^{-4} degrees at the sensor with attitude drift less than 10^{-7} degrees/sec are essential to achieve subpixel registration accuracies without control points, provided other sources of positioning error are corrected to a pre-specified tolerance to support the required subpixel registration. The final registration accuracy depends on the number, the quality, and the distribution of the GCPs.

The ephemeris data are calculated every three days and the values are given for each scene to an accuracy of 100 m in each direction. The attitude of the satellite is determined to 600 m on the ground ($0^{o}.04$); change over a scene is given on the tape and is reported as being linear over a scene with a magnitude of 7 to 8 pixels.

The maximum drift in attitude is specified as 0.0006 Deg/sec, in 1.5 ms this could cause a movement of 0.013 m on the ground, so the accumulative change over an image 60 x 60 km could be 78 m. The lines will also be displaced relative to each other due to the rotation of the earth; this effect will vary according to the latitude. At 45^{o} N the change in heading is 2.75^{o} which means a shift between lines of 0.5m. The accumulative shift over 60 km is 3 km.

Variations in the platform altitude result in variations in the line scale in the recording direction. This is not significant, but observable when comparing different scenes. The column sampling interval is not affected. The spacecraft's altitude above the earth's surface is determined by three separate factors:

1. The oblate shape of the earth.
2. The eccentricity of the orbit.
3. The varying relief of the earth's surface.

The converging orbit, combined with the inclination of the orbit and earth curvature are particularly important factors.

Pixel offsets.

The interval of time between sampling the detectors is 1.5 ms, during which time the satellite will move forward 10m. With the axis vertical, adjacent lines will therefore join each other but the quality of the join will be affected by any change in altitude of the satellite or movement from the vertical plane passing through the centre of the earth or from a constant distance from the geoid. This overlap will also affect the radiometric resolution. Oblique lines will overlap each other as shown in figure 3.6.

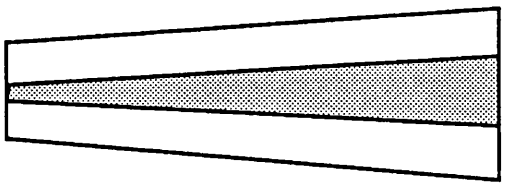

Figure 3.6. Lines overlap in an oblique image.

The panoramic effect.

The panoramic effect is introduced as soon as the strip selection mirror of an HRV scanner moves away from the vertical viewing position to acquire oblique imagery. This phenomenon is significant for extreme oblique viewing. In the extreme oblique viewing angle $\approx$ 27^{o} an oblique image covers a larger area in the across track direction (about 81 km) than along track direction which will remain the same as normal (60 km) and therefore the sampling interval increases from

10 to 13.5 m in panchromatic mode. The line sampling interval increases steadily as a result of:

1. The increasing distance between sensor and target.
2. The angle between the vertical and the viewing direction
3. Increasing effect of the earth's curvature.

The remedy adopted is to use a film format with different scales for the x and y axes.

Because of the panoramic effect, if a stereomodel comprising of a vertical and an oblique image is set up then the different scales in the stereoscopic base direction (across track) cause the model to appear to be sloping.

The problem with the images affected by horizontal and vertical stripes (effects of the pushbroom sensor) has been solved by SPOT for images originating after July 1986. Images produced before then apparently cannot be corrected (Begni, 1988).

Sensor noise and information recording device.

As stated earlier, the detection device on the SPOT satellite is based on the 'pushbroom' technique where a line on the ground in the cross-track direction is detected by a 6,000 pixels line within one electronic sweep. Although a pushbroom scanner has no moving parts during the recording procedure, it has moving parts in forming the view angle. Because of the moving parts, it is difficult to achieve perfect adjustment within the recording device, and thus these problems of mechanical scanning remain.

Distortions due to recording device.

The optical components of the recording device (camera) are not free from distortion. Each image line is recorded instantaneously by an assembly of four CCD (Charged Coupled Device) arrays with 1,728 CCDs per array. Each CCD generates one pixel. The complete assembly is known as DIVOLI and its function is to optically split each line into four groups of 1,500 points, with each point being recorded by an array. In panchromatic mode this results in a 6,000 pixel line whereas in multispectral mode a 3,000 pixel line is recorded for each spectral band by

combining the signals from adjacent CCDs.

Atmospheric absorption and scattering.

The earth's atmosphere has an effect on the path of radiation from the surface of the earth to the sensor. The main factors controlling the absorption and scattering are the angle of incidence, sun angle and the quantity of water vapour, ozone and aerosols in the atmosphere reacting to solar radiation reflected back by the ground and reaching the recording device after passing twice through the atmosphere. The two major effects resulting from these phenomena are attenuation of the useful radiation in the spectral band in question and a haze or blurring effect due to the atmosphere. SPOT CCD detectors require that observations of a point on the ground be long enough for photon flux reaching the detector to be significantly greater than the noise level of the system itself. (Gugan, 1987b).

Atmospheric refraction.

The effect of atmospheric refraction is that the path from the earth surface to the sensor is not a straight line but is curved according to the refractive index of the layers of the atmosphere. The atmospheric refraction has been carefully studied by applying techniques proposed by several authors (Schut, 1969; Saastamoinen, 1972 and 1974; Bomford, 1984; Forrest and Deroughie, 1974). Models of the earth's atmosphere have been constructed, and using these a correction can be calculated. The contribution of earth curvature to the refraction is said to be very small (Schut, 1969) and therefore it can be omitted.

Finally we can include the following atmospheric conditions as sources of causing problems in the image quality:

Shadow.

Shadow areas can be recorded in an image due to the look angle because the solar illumination does not coincide with the sensor viewing direction. Shadow creates problems on the photogrammetric observations. It is likely that imaged terrain which is not directly illuminated by the sun will not be completely dark because of diffuse sky illumination due to the atmospheric scattering.

Clouds.

From the 662,000 SPOT scenes acquired after two years of the SPOT 1 launch (22/2/1988) , about 25% are usable and present a cloud cover of under 10%, 30% present a cloud cover of under 25%, while 50% are difficult to use or are not usable at all (cloud cover up to 50%).

Haze.

Atmospheric haze varies from place to place and from time to time, depending on such things as industrial aerosols, dust, sea-salt nuclei and humidity. Haze is often much less in evidence in the early morning (0630-0900 local time), and late evening (1800-2000 local time).

Oblique images present larger distortions than vertical images. Off-nadir view influences the geometry of a SPOT scene. In the following paragraphs are outlined the most important distortions due to the off-nadir view images, with numerical examples.

The off-nadir view changes the geometry of a SPOT scene in across track direction. Assuming a mirror look angle of 8.6°, an instrument field of view (IFOV) of 4.13° and an altitude of 835 km, then a distance of 60 km on the ground, corresponding to a nadir view, is distorted absolutely to 61.2 km in a tangential plane.

The influence of the earth curvature increases with increasing off-nadir view in across track direction. With a mirror look angle of 8.6°, an already distorted distance of 61.2 km is stretched by a further 300 m.

The relief displacements in across-track direction also increase. With a mirror look angle of 8.6° and a maximal terrain height of 350 m, the displacement near the outermost pixel of a row is nearly 60 m.

While nadir viewing does not give a significant difference in height on the edges of the frame, the off-nadir frame shows, in addition to the well known perspective distortion across the track, an increment of about 50 m between the far edge and the near edge with regard to the ground track.

Moreover, SPOT images can exhibit a wide range of differences from the other satellites for a variety of reasons: (Swann et al and Kauffman et al, 1988).

1. The gain of the HRV sensors is such that a given scene may have a very narrow distribution of digital intensities, resulting in low contrast. When the imagery is radiometrically "stretched", quantisation effects become clearly visible.

2. The ability to point the sensors in a particular direction means customers have an input into the programming schedule. The arbitration of these requests sometimes results in acquisition of stereopairs days, weeks or months apart (the minimum lapse time is 1 day). The resulting multitemporal scenes can appear quite different due to agricultural, seasonal, and sun-angle changes (sun angle changes are always a likely problem).

3. Off-nadir viewing often results in a difference for the same ground areas between the two views. This occurs primarily when, in one view, the ground is between the satellite and the sun, while in the other both the satellite and the sun are one side of the ground area. Off-nadir viewing can even have the effect of making areas that are light-coloured in one image dark in the other.

4. Lastly, SPOT's sun-synchronous orbit is referenced to the nadir track of the satellite. With high off-nadir viewing, the satellite can be up to one-half a time zone away from the sun-time of the other pass. Shadows visible in the imagery will then have different orientations.

3.4.1.3. Treating of the SPOT imagery - corrections to be applied .

Several orbital simulation procedures have been developed in the last few years for geometric correction and registration, based on different analytical techniques. These have a common need for a significant number of ground control points. The simulation programs take into account all, or at least the most important and unavoidable, of the error sources such as the orbit dynamics (Earth-satellite dynamics), the satellite attitude, the sensor viewing geometry, the sun illumination and the atmosphere.

Vertical satellite imagery.

The vertical image can be handled easily. It contains mainly two types of distortion caused by the sensor orientation (tilt or movement during the image acquisition), and by the relief of the ground. The second source of distortion is negligible in most vertical satellite imagery, so in order to use the data it is necessary to correct the sensor distortion and register imagery to a ground coordinate system. It will be possible to automatically correct the image for the relief effects if a digital terrain model already exists of the area. This is a common process in remote sensing, known as geocoding. The procedure for producing a geometrically corrected orthoimage by registration to a number of ground control points (GCPs) is called rectification. This process requires the identification of points (GCPs) in the imagery for which ground coordinates are known. A number of coordinate pairs then allow the satellite image to be geometrically corrected to the ground coordinate system.

Oblique satellite imagery.

Oblique imagery contains larger distortions than the vertical image. It will again be possible to automatically correct the image for the relief effects if a digital terrain model already exists of the area, and to generate a geometrically corrected orthoimage after registration to a number of ground control points. This is possible for a level 1A scene by applying 2nd degree polynomials with sub-pixel accuracy (requires at least 6 GCPs). Accuracies of 0.6 to 0.8 pixels in along-track and 0.6 to 0.9 pixel in across-track can be achieved. The results showed that the distortions in the across-track direction can be described by this solution. An affine solution (requires at least 3 GCPs) is not possible because the distortions in across-track direction do not behaviour linear. Polynomials of higher degree should not be applied. With an increasing degree an increasing number of GCPs have to be measured , which can be very time consuming (ie. 3rd degree requires 10 GCPs, 4th degree requires 15 GCPs and 5th degree requires 21 GCPs) (Michaelis, 1987).

Stereoimagery.

Stereopairs can be used for 3D measurement and DEM generation. This requires the use of a specialised hardware system such as an analytical plotter, or a digital plotter. The image geometry of SPOT is classed as dynamic, because the position and the orientation of the sensor is changing throughout the 9 second

period. The collinearity equation represents the light path of a push broom sensor but the position and attitude parameters are constant only for recording a single line data. Thus, time dependent collinearity equations must be used to determine them with the aid of ground control, and linear or polynomial constraints must be used to link successive sensor positions. It is clearly impossible to store the exterior orientation elements of all perspective centre positions so some interpolation is required (Dowman, 1984). As a result it is not possible to form an error free model. Stereoscopic viewing is possible from any pairs taken from different angles but a better stereoscopic impression will be obtained with a greater separation between the orbits from which the images have been obtained, and also after corrections have been applied.

3.4.2. Software for setting up SPOT images.

The menu for setting up SPOT images appears similar to the user to that for setting up aerial photographs. It follows the same highly modular, flexible and maintainable structure.

The software suite is accessed from a special menu which contains the programs required by the SPOT system. These programs are for Camera management, Control point (coordinate) management, Coordinate conversion , Plate processor, SPOT orientation (Project definition, Inner orientation, Exterior orientation), Coordinate system control, DSR1/GP1 On-line definition, DSR1/GP1 On-line compilation.

When starting to use the instrument, the DSR1 is loaded with the plate processor program. This program receives the instructions sent by P1 and responds to coordinate input by driving the stage plates in one of several modes (eg. left plate, both plates, model system).

The SPOT image orientation procedure is basically a single image space resection (dynamic space resection), which allows for the dynamic motion of the satellite in its orbit during the 9 sec of image acquisition. Because of the basic instability of the dynamic SPOT imaging system, it is not possible to theoretically find an exact orientation of an image as it is with conventional aerial photography

(Gugan, 1987a).

The movements of the satellite along the orbit path and the rotation of the earth are the major components of the dynamic motion. The satellite orbiting around the earth in an elliptical orbit and its position (attitude) is described by the Eulerian parameters (orbital parameters) to a reference system (geocentric coordinate system). The earth is considered as one of the focuses of the ellipse, and the satellite position is defined by the true anomaly (F), which is the angle around the ellipse from the perigee (figure 3.7).

The dynamic motion (figure 3.8) is modelled as linear angular changes of F and Ω with time :

$$F = F_o + F_1 * x$$

$$\Omega = \Omega_o + \Omega_1 * x$$

where x is the along the track image coordinate, F_1 is the change in true anomaly, and Ω_1 is the ascending node per mm in the image.

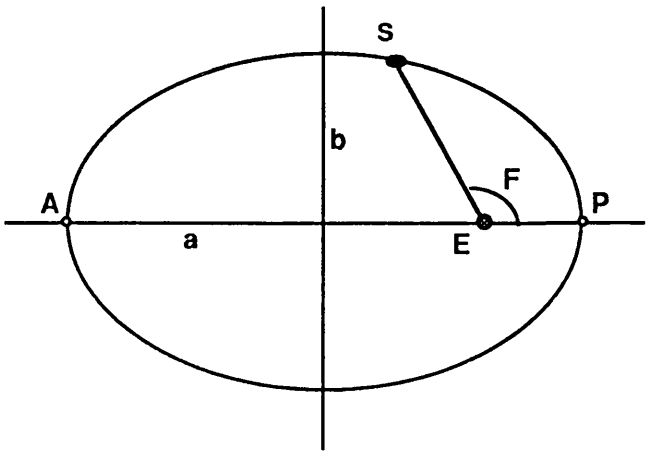

P : Perigee
A : Apogee
E : Earth
S : Satellite

Figure 3.7. Satellite orbit.

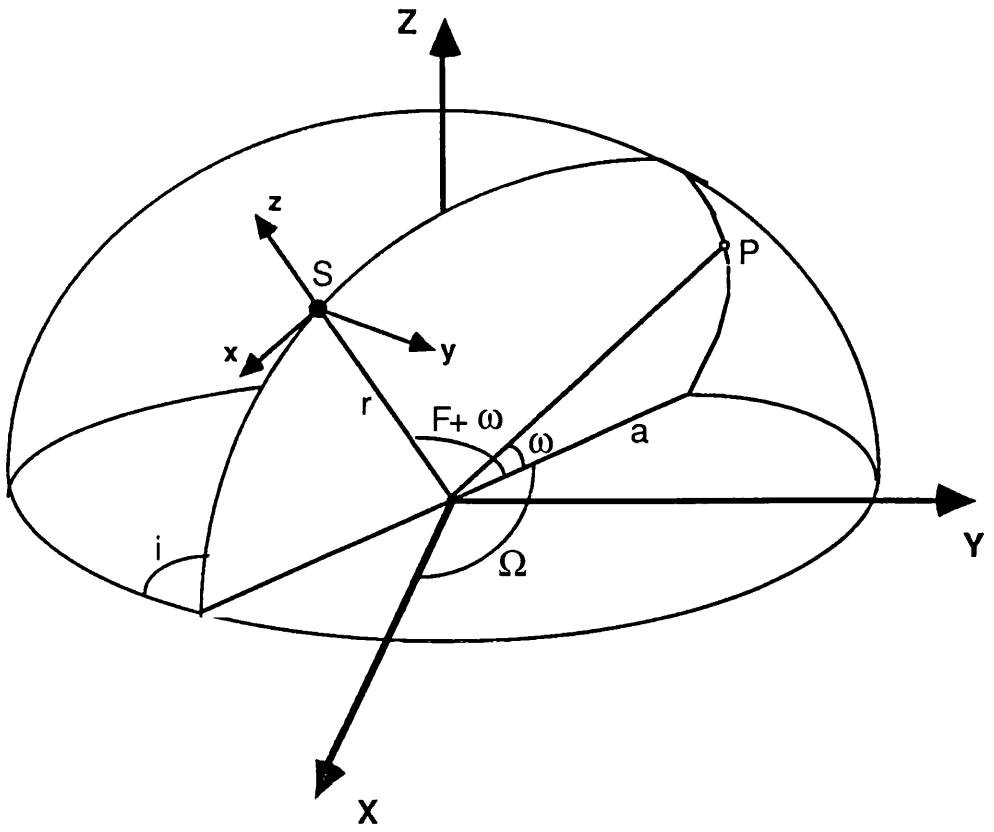

Figure 3.8. The UCL SPOT orbital model.

The F_1 and Ω_1 can be estimated from the SPOT orbit period and the earth rotation rate (Gugan, 1987a):

$F_1 = (2\pi / OP) * (ICT / PS)$

Where

OP : is the orbit period (sec), ICT : the instrument cycling time (sec) and PS: the pixel size.

$F_1 = (2\pi / 101.46 * 60) * (0.0015 / 0.013) = 0.00011906$ rad/mm.

Ω_1 is calculated in a similar way, where the period = (24 * 3600) =86400 seconds.

Thus $\Omega_1 = (2\pi / 86400) * (0.0015 / 0.013) = 0.00000839$ rad/mm.

The SPOT constant parameters are:

1. The mirror look angle (varies and given for each image).

2. The array offset (see § 3.4.1.1).
3. The argument of the orbit perigee (input 0.0 rad if not known).
4. The satellite orbit eccentricity (nominally for SPOT = 0.001).
5. The rate of change of true anomaly = 0.00011906 rad/mm.
6. The rate of change of ascending node = -0.00000839 rad/mm.
7. The focal lengths = 1082.0 mm.

The orientation software is designed to allow different levels of accuracy depending on the number of orientation parameters (unknowns). The number of parameters included in the solution varies (4, 7, 10 and in the new version up to 13 parameters). The parameters will depend on the number and distribution of the available GCPs. If 4 parameters - true anomaly (F), ascending node (Ω or AN), orbit inclination (i, nominally 98.698°)and semi major axis (a, nominally 7200000 m) - are used, then the minimum number of control points required in practice is 4. If 10 parameters - F, Ω, i, a, orientation parameters or sensor rotations (roll ω, pitch p, swing k), and rate of change of orientation parameters (ω', p', k') - are used, then the minimum number of control points required is 5, but in practice 7 are used. As a general rule, the more parameters used in the orientation, the better will be the orientation accuracy (smaller image coordinate residuals which affect the accuracy of stereomeasurements). On the other hand, fewer parameters used requires fewer control points. However some of the parameters have more effect on the accuracy than others. In the orientation software implemented at UCL on-board recorded data (satellite orbital parameters), provided with the images, are not used.

Currently developed software can handle a continuous strip of SPOT imagery for triangulation and mapping purposes. These models are based on a rigorous geometry and with the use of additional parameters and constraints. The improved orbital modelling using attitude ephemeris with level 1A data and the inclusion of higher orbital terms should improve the accuracy of a long strip of imagery, although it is not possible to find an exact orientation for this type of imagery and it may not improve the accuracy of a single model. Nevertheless it is likely that residuals could be minimised by using these models.

Rates of change of the satellite's attitude are recorded every 125 ms in orbit (73 times per image). Level 1P SPOT product has this image distortion corrected. This is very high frequency information, that could be included in the geometric model in place of the single values per image currently used.

Some of the developed models presented in the OEEPE test on triangulation of SPOT data (1989) are briefly as follows:

1. Physical modelling of SPOT system geometry (implemented by IGN).

The collinearity equations are written in a system linked to the instrument platform and HRV. The unknowns are ground coordinates for all the points measured, and orbit corrections (position and attitude) for the different tracks, i.e one per strip. The attitude correction is supposed to be constant. The positional correction is supposed to be linear (or constant) in time. The equations come from collinearity equations for all the measurements, from ground coordinates of controls and from assuming orbit corrections stay within CNES specifications (Veillet 1989a, 1989b).

2. Use of non-parametric parameters in the solution (BINGO SPOT).

This is the approach used by Konecny et al (1986 & 1987). Non-parametric parameters in the solution would be used to model residual image distortion and would be applied to image coordinates in a similar way to radial lens distortion with conventional photography. The development of a simultaneous bundle adjustment solution would be likely to improve the orientation results.

3. Bundle adjustment with orbit data (DGI, Queensland).

This model uses orbital equations to model the satellite path and polynomials plus on-board attitude measurements to model the variations of the satellite attitude with time (Priebbenow, 1989).

4. Bundle adjustment with constraints (CCM Ottawa).

The geometric model respects the physical reality of imaging, satellite orbiting and of the earth shape, instead of indirectly modelling their combined effect by empirical image fitting and warping, as frequently adopted in non-photogrammetric approaches. No auxiliary information from ephemeris and telemetry sources is needed, but may be utilised when available (Kratky,1988).

5. Use of CNES header data (UCL).

SPOT image is geocoded by rotation and translation of the line element of the CCD array relative to position determined by interpolation of the header data. The attitude information of the sensor is also used. This has the advantage of reducing the number of ground control. Three GCPs are enough for geocoding a single image (O'Neill & Dowman, 1988).

3.4.2.1. Exterior orientation accuracy.

The stereomodel accuracy which we can obtain from SPOT images depends on the B/H ratio, and the quality and distribution of control points.

The Department of Photogrammetry and Surveying at UCL (Dowman et al, 1987) provided some results of the SPOT stereomodel accuracy. The assessment has concentrated on the Aix En Provence images. A maximum of ten control points were used. The ground control were provided by the IGN and the check points were measured from the 1:25,000 map sheets of the area. The main results are summarised below:

Aix En Provence stereomodel - 10 control points used for orientation.

RMS plan accuracy (20 check points):	15.3 m.
RMS height accuracy (62 check points B/H = 0.73)	5.4 m.
RMS height accuracy (53 check points B/H= 0.32)	8.0 m.

Aix En Provence stereomodel - 6 control points used for orientation.

RMS plan accuracy (20 check points):	24.5 m.
RMS height accuracy (20 check points B/H = 0.73)	6.9 m.

Two level 1P images of Aix En Provence have also been measured. Control was not available over the whole stereomodel however.

Aix En Provence level 1P stereomodel - 8 control points used for orientation.

RMS plan accuracy (18 check points):	13.1 m.
RMS height accuracy (62 check points B/H = 0.73)	10.2 m.

IGN has used two sites in south - east France. 95 ground control points were actually used from 177 available and 16 good scenes from 31 available with viewing angles of +/- 27° and +/- 13°. A total of 608 measurements were made on control points and 653 on check points. The results for the accuracy of fitting the data to ground control using absolute orientation for models with the best Height/Base ratio, expressed as root mean square (RMS) errors, were as follows :

	X	Y	Z
On control points	4.5 m	4.1 m	4.1 m
On all check points	8.0 m	6.6 m	7.1 m

After rejecting points greater than 2.7σ the results became:

RMS_X= 4.7 m , RMS_Y= 4.5 m, and RMS_Z = 5.3 m.

Ducher (1989) from IGN published some later results from SPOT data for 100 to 120 well defined check points using from six to ten ground control points per model, including a standard level 1P version. The accuracy results for metric accuracy (Rodriguez et al, 1988; Denis and Baudoin, 1988) are presented in table 3.1.

	RMSE (m)					
	IGN in-flight acceptance tests (1986)			IGN recent tests (ADEF-87)		
	X	Y	Z	X	Y	Z
B/H=1.0 to 1.1, raw results Level 1A Level IGN-1P	8.1	5.5.	4.3	9.2 10.1	12.1 10.8	4.4 3.7
B/H=1.0 to 1.1,filtered results Level 1A	3.8.	4.2	3.4			
B/H=0.5 to 0.6, raw results Level 1A Level IGN-1P	7.8	7.2	8.3	10.4 9.9	12.3 11.6	6.4 4.1
B/H=0.5 to 0.6,filtered results Level 1A	4.6	4.4	6.7			
B/H=0.25 Level 1A Level IGN-1P				7.6 10.2	10.0 10.9	9.4 8.1

Filtered by rejecting points greater than a given value of residual (2.7xσ_o)

Table 3.1. Exterior orientation accuracy results from IGN of setting up SPOT models.

From the presented results we can see that the plan accuracy in the 1P level stereomodel has improved by the amount expected due to the removal of high frequency attitude measurement errors. However, the 1P data contained serious resampling artifacts. Some areas were undersampled due to satellite pitching, the resulting 1P image after resampling containing pixels with a ground size of about 30 m.

Simard et al (1987) gave some accuracy results from setting up three SPOT models:

1. Kananaskis test site. Images quality : very poor, poor.
   Base to height ratio 0.5

Points	Number	RMS residuals (m)		
		In X	In Y	In Z
GCPs	3	0.8	1.5	0.2
Homologous	19	0.5	2.4	- - -
Check	36	4.5	5.7	6.1

2. Chiang Mai results. Images quality : very good, very good.
   Base to height ratio 0.83.

Points	Number	RMS residuals (m)		
		In X	In Y	In Z
GCPs (1:50000 maps)	14	26.0	18.0	7.6
Homologous	13	0.1	0.7	0.0

3. Kedah results . Images quality : very good, very good.
   Base to height ratio 0.87

Points	Number	RMS residuals (m)		
		In X	In Y	In Z
GCPs (1:40000 aerial phot.)	13	9.1	6.2	6.4
Homologous	46	0.1	1.0	0.0

Instead of applying the dynamic space resection, Konecny et al (1987), University of Hanover, developed a mathematical model which avoids high correlations between the unknowns and is based on the use of photo coordinates

(abundance of collinearity equations). The unknowns of the orientations are approximated by the use of orbit data, and in the course of adjustment are partly formulated as additional parameters (maximum 32 parameters). The method has been implemented on Zeiss Planicomp and Orthocomp hardware and a bundle adjustment program, BINGO, has been modified to handle SPOT geometry. Test results of bundle adjustment are given in table 3.2.

NUMBER OF ADJUSTED POINTS	NUMBER OF CONTROL POINTS	INTERNAL ACCURACY			
		σ_{xy} MAX	σ_{xy} MEAN	σ_z MAX	σ_z MEAN
86	18	8.7	5.2	10.9	8.5
86	34	6.1	4.5	8.8	7.1
89	83	4.5	3.0	5.6	5.0

NUMBER OF INDEPENDENT CHECK PNTS	NUMBER OF CONTROL POINTS	MEAN DIFFERENCES			MEAN SQUARE DIFFER.		
		X	Y	Z	X	Y	Z
68	18	7.9	10.4	4.8	10.9	13.7	6.5
52	34	8.3	10.5	4.5	11.3	13.8	6.2

Table 3.2. Test results of bundle adjustment (in metres).
After Konecny (1987).

A consensus figure was declared by Denégre in November 1987 as a result of the various values for metric accuracy which were reported by different investigators at the PEPS closure meeting. It could be said that an accuracy of 5 m to 9 m can be achieved in x and y, giving a planimetric accuracy of 7 m to 12 m (RMSE), with maximum errors ranging from 15 m to 25 m. In elevation, the z accuracy ranges from 4 m to 8 m according to an approximate formula for z error (e_z) in metres such that $e_z \approx 2H / (B+2)$, with maximum errors from 10 m to 18 m.

Triangulation tests using SPOT data were carried out by OEEPE (1989) . A test site in the South east of France was chosen. The test area was divided in two zones (A and B strips). A SPOT strip is a series of images taken successively by the same instrument, the same day, along the same track of the satellite. Each strip was four images long. Five participants each carried out an independent procedure

for the triangulation using different mathematical models for sensor orientation and strip connections. In UCL each image was single set up (no bundle adjustment was used). They used variable numbers of control points (4, 6 10 and 20 GCPs for strip A; and 13 and 4 GCPs for strip B) and a variable number of check points. The overall residuals of the measurements made by each participant is shown in table 3.3.

PARTICIPANT	STRIP A					STRIP B				
	NUMBER OF CHECK	NUMBER OF GCPs	R M S (m) HEIGHT	PLAN	3D	NUMBER OF CHECK	NUMBER OF GCPs	R M S (m) HEIGHT	PLAN	3D
IGN	101	4,6,10 and 20	4.2	8.4	9.3	141	13, 4	4.9	12.8	13.7
UNIVERSITY OF HANNOVER	90	4,6,10 and 20	6.7	12.9	14.5	124	13, 4	4.7	13.9	14.8
CCM CANADA	72	4,6,10 and 20	9.9	16.0	18.8	—	—	—	—	—
UNIV. OF QUEENSLAND	108	4,6,10 and 21	8.5	13.4	14.6	123	14, 4	4.3	14.0	14.7
BRISBANE	105	4,6,10 and 20	6.9	12.7	15.4	122	13, 4	4.3	13.4	14.1
UNIV. COLLEGE LONDON	106	10 and 20	7.3	15.8	17.4	135	13, 4	8.5	13.0	15.5

Table 3.3. Results of OEEPE test on triangulation using SPOT data with 4 to 20 GCPs.

Most of the participants used 2 control points for the bundle adjustment of strip A and 2 to 3 GCPs for the bundle adjustment of strip B. These different results appear on table 3.4.

PARTICIPANT	STRIP A					STRIP B				
	NUMBER OF CHECK	NUMBER OF GCPs	R M S (m) HEIGHT	PLAN	3-D	NUMBER OF CHECK	NUMBER OF GCPs	R M S (m) HEIGHT	PLAN	3-D
IGN	101	2	10.4	21.5	24.1	141	2 and 3	6.3	23.2	24.0
UNIVERSITY OF HANNOVER	88	2	14.1	17.3	22.4	124	2 and 3	5.8	17.4	18.3
UNIV. OF QUEENSLAND	108	2	9.6	27.0	29.2	123	2 and.3	3.8	17.2	17.6
BRISBANE	106	2	9.6	27.0	29.3	122	2 and.3	3.9	16.5	17.0

Table 3.4. Results of OEEPE test on triangulation using SPOT data with 2 to 3 GCPs.

From this test we can conclude that:

a) accuracy of blocks same as single models.

b) the advantages of using more than 6 GCPs are very slight.

c) very little change between using 4 and 14 GCPs.

d) RMS in Z is less than by a factor of 0.5 - 0.7 in plan (identification of GCPs possibly explains why heights are better than planimetry).

e) height error less dependent on number of GCPs than planimetry.

3.5. SPOT heighting accuracy - Previous experiments.

A number of tests from SPOT generated DEM have been carried out. The results from 5 are summarised here:

1. In the southern Cyprus experiment (Ley, 1988) 14 grid elevation matrices were measured. The sizes were 1x1 km^2 for 11 areas and 1x2 km^2 for 3 areas. A SPOT stereopair with -23.77° and 21.18° look angles (B/H ratio = 0.96) was set up. 15 control points derived from maps were used to set up the SPOT model. The RMS error in orientation was 7.24 m in height, 15.65 m in Easting and 9.15 m in Northing (planimetric error 18.13 m). The results are presented in table 3.5.

AREA	MEAN DIFFERENCE	RMS	SD	AVERAGE SLOPE (%)
1	-7.20	17.35	15.78	24.0
2	-2.83	15.86	15.61	19.9
3	7.27	13.74	11.66	12.6
4	1.81	15.10	15.00	17.2
5	-0.80	8.48	8.44	2.0
6	15.63	28.29	23.58	28.6
7	20.49	35.69	29.22	26.9
8	15.37	19.15	11.43	14.2
9	20.02	23.40	12.11	16.0
10	3.60	12.24	11.69	18.1
11	15.55	19.01	10.95	15.3
12	16.40	19.67	10.87	11.4
13	22.72	24.70	9.67	9.4
14	19.62	21.03	7.58	3.8

Table 3.5. Statistical analysis of the southern Cyprus SPOT elevation measurements.

From the examination of the mean differences for each test area it was found that between the estimated map heights and the photogrammetrically measured SPOT, significant systematic errors occurred. The measured points were compared with points in the same position derived from the digitisation of the 1:50,000 maps after a contour interpolation.

The overall area average slope is 14.3%. The resulting errors were mean = +10.40m and standard deviation = 14.28 m. The largest mean difference was +22.72 m and the smallest -7.20 m. The largest standard deviation was 29.22 m and the smallest 7.58 m. The project operator was not experienced in photogrammetric observation .

The above experiment gave a strong positive systematic error in the mean. The standard deviation is acceptable.

2. In the Mt. Fuji experiment in Japan, 3 areas were tested (Fukushima, 1988). The objective of this study was to estimate the accuracies of DEM generated by digital image correlation methods using three SPOT images near Mt. Fuji. The descriptions of the tested areas are as follows:

Test area 1 : Mountainous with steep slopes. Some areas were covered with a little snow.

Test area 2 : The centre of the area is flat and each side of this area is mountainous.

Test area 3 : The eastern part of Mt. Fuji which is covered with coniferous forest. The slope is gradually changing.

The best results on the mean biases were -22 to -24 m and the worst were up to -28, depending on the test area and the correlation method. That means there is/are a source(s) that introduced a systematic influence or a systematic error in the measure of the central tendency of "average" in the data.

3. The Nepal experiment (Grabmaier et al, 1988). Contours from 1:100,000 map with an interval of 100 m were digitised. A SPOT stereopair with -25.1° and 29.3° look angles was set up. Contours were also interpolated from

the stereo SPOT DEM measurements. A superposition of the two contour maps allowed comparison of the two presentations. The differences between the two data sets are the accumulated errors of the map contours, their digitisation and the interpolation of grid points from the digitised contours, the orientation of the SPOT stereo scene, the measurements in it, and the interpolation of grid points from the SPOT stereomeasurements. A histogram of these differences shows 48% of all 16,895 differences to be between -25 m and +25 m, and 79% within -50 m and +50 m.

The above experiment gave very low accuracy results due to the errors introduced by the procedure which had been followed.

4. A small test has been performed on the Cyprus level 1A imagery (Gugan and Dowman, 1988c), from which a 108 point grid DEM was measured and compared with a reference DEM digitised from 1:50,000 map contours. A RMS error of 9.9 m was obtained, which reduces to 8.6 m if the error of 4.8 m inherent in the reference DEM is removed. This compares well with the results of spot height measurements from the Aix En Provence imagery (5.4 m) for a similar base/height ratio.

5. The UCL experiment (Day & Muller, 1988 & 1989) where automated techniques of capturing data for DEM production are used (see § 8.2.2.1). The quality assessment results derived from two tests are as follows: mean = 10.84 m and standard deviation = 18.19 m (see table 8.1) from one test; and mean = -3.19 m and standard deviation 12.17 m (see tables 8.2 and 8.9) from the other.

These studies show that DEMs derived from SPOT data are subject to systematic error and to a wide range of random errors in a way which is not normally expected from aerial photographs. In this project the use of large data sets derived from aerial photography and from SPOT allow a thorough investigation of these influences to be carried out.

3.6. SPOT image utilisation, assessment and results.

This section contains the results of the research carried out both within and outside the SPOT Preliminary Evaluation Programme (PEPS) and presented in the

conference held in Paris from 23rd to 27th November 1987. The conference, by its nature, therefore tended to be dominated by academic research results rather than by operational systems. In fact one of the very few operational environments described was the Ordnance Survey involvement in mapping in Yemen.

SPOT claim a 3-5 m RMS error in height for models with a base/height ratio of 1.0. This, of course, is dependent upon having plenty of excellent control (Hartley, 1988).

OS tested a SPOT stereopair against existing 1:50,000 scale mapping of Yemen Arab Republic and decided that plan accuracies of 12 m and height accuracies of 10 m were possible. These were not as good as those reported by other workers but reflect a low density of control and some difficulty in finding natural detail to use as that control which had not been distorted in some way by the pixel structure. The result of the trial has convinced OS that adequate 1:100,000 scale maps with a contour interval of 40 m can be produced. Information content will be less than would have been obtained from aerial photography but so, interestingly enough, will be the cost.

Denis and Baudoin (1988) from IGN described several widely distributed experiments. In Algeria, a RMS error in height of 4.4 m was achieved using 285 check points. He claimed that a 10m contour interval in flat areas is possible, but this seemed inconsistent with the heighting accuracies.

Photogrammetric tests have yielded consistent results with RMS plan accuracy of 6 m and height accuracy of 3 to 14 m being achieved, depending on base/Height ratio and control.

Image maps. Scales up to 1:24,000 can be supported with accuracies in the order of 10 m in plan and height. However the level of detail that can be extracted from the image is only equivalent to 1:25,000 scale specifications.

The Mapping and Charting establishment has assessed the ground modelling capabilities of the DSR1, I^2R and MacDonald Dettwiler and Associates system with heighting accuracies of 12 m, 12 m and 10 m respectively.

Priebbenow and Clerici (1987) from Queensland Institute of Technology described an analytical model to assess DEMs and line mapping. He reckoned that the total effect of roll in the model is 2-9 m, of yaw 1.8 m, and pitch 40.0 m. Model accuracies of 6.2 m in plan and 3.1 m in height resulted from a nine parameter solution and 27 control points. He gradually cut control down with no significant loss of accuracy until only 4 ground control points were present (residuals checked on 188 points). Good plotting results were obtained but tracks, fences and buildings had an 80 % omission rate for 1:250,000 scale mapping.

Jones (Nigel Press Associates) described Geospectra's DEM package. It requires two CCTs (Computer Compatible Tapes) and ground control as input and provides one ortho-image and a DEM as output. Level 1A SPOT images are corrected empirically for tilt, earth curvature and rotation and then resampled into epipolar space using eight GCPs. Elevation is extracted on a 10m grid using full grey scale correlation. Results on withheld GCPs indicate 18.4 m R.M.S.E elevation accuracy and 21 m in plan.

Renourd (INRIA) described very similar work on DEMs produced in France, again based on epipolar lines. A video of perspective views on panchromatic SPOT images was produced. It contained 5000 views and apparently took 200 hours of CPU time to create. The result was an excellent simulation of aerial movement around a SPOT model.

Bjerkes Joe (Satimage, Sweden) described the digital mapping capability set up in collaboration with the Swedish National Land Survey. They use Scitex to produce excellent hard copy results for printing originals. RMS errors of 6 m in plan and 5 m to 15 m in height have been achieved for experimental products.

There is a definite trend to support a belief that SPOT can provide an accuracy of 8 m to 10 m in plan and 4 m in height, given adequate control. USGS clearly believes that a 1:24,000 scale product is of interest to some users (Hartley, 1988).

3.7. Significance and advantages of SPOT for topographic mapping.

Mapping from satellite imagery offers advantages over conventional techniques, of the large area, coverage and that the number of required ground control points (GCPs) is substantially smaller. A user can obtain a soft copy (digital data) or a hard copy (image). They can also obtain a full image or a part (1 quarter of image).

In addition, SPOT provides the following advantages over the earlier Landsat satellites (Rosenholm, 1988):

1. SPOT can be programmed. A program request can be made in advance, at a reasonable cost, for one particular scene, large area or different season coverage.

2. The side-viewing capability. This offers two advantages. Firstly it is possible to observe a scene of a requested area more frequently, so the chances of obtaining a cloud free scene within a limited period of time increase. Secondly there is the ability to obtain stereo pairs of images. A very good base/height ratio is obtainable, slightly better even than for super-wide angle aerial photographs. (The larger the B/H ratio, the more precise height information can be).

3. Good spatial resolution. SPOT multispectral images have a pixel size of 20 metres and panchromatic images have a pixel size of 10 metres (in vertical viewing).

4. Well-adapted spectral sensitivity to aerial photographs. The multispectral images can be made very similar to infrared colour photos, and the panchromatic images can be produced as ordinary aerial photographs.

5. Good and stable geometry. The CCD linear arrays give high resolution and make the geometry of SPOT very stable and predictable, essential for accurate feature identification and location. This characteristic makes precision corrections of extremely good quality possible and precise matching. SPOT can be corrected extremely precisely to any coordinate system. The good geometric performances allow a geometric localisation accuracy of 500 m RMs for system corrected images

(no control points required). However, some problems of mechanical 'pushbroom' and CCD-technique may occur.

6. Good radiometric properties with a good signal/noise ratio and a limited point transfer function.

7. Can be resampled and enlarged to scales of about 1:20,000 or 1:25,000 when it is used as an orthophoto background.

8. The exposure time for each ground point imaged can be automatically maximised.

9. To form images without moving any mechanical part, which ensures excellent photogrammetric quality along the scan axis.

10. Simple conventional evaluation technique, although there are some problems arising from the data recording procedure. These are the following:

The sensor platform position and motion are not usually well enough known.

The collinearity equations represent the geometry, but the position and attitude parameters are constant only for recording a single line of data (Dowman, 1984).

3.8. Conclusions relevant to project.

In this project a non direct method (photogrammetry) of capturing data is used. The Kern DSR1 analytical plotter was employed for setting up the stereopairs. Two sources of data were used, the aerial photography and the SPOT imagery.

Photogrammetry as a technique of extracting information using a hardcopy as a source of information has some problems these concern:

- obtaining the raw, data due to the method and technique for registration of the information.
- information recording device (camera or sensor).
- the quality and the processing procedure of the photographic material,

which transfers the problems to the analytical plotter.

- the nature of the earth surface such as the earth curvature and the relief.

These problems become sharper in projects concerning mapping from space imagery. Many factors and error sources influence the image quality. For manual measurements and mapping the geometric accuracy is more important than the radiometric quality which only causes difficulties and uncertainties to the operator. SPOT satellite imagery is more sensitive than aerial photography with regard to the geometric quality, the radiometric quality and the operator comfort . Some of these factors affect both the geometric and radiometric quality while all of them affect the quality of the measurements made by the operator. These sources can be grouped according to the main quality factor that affects them, as follows:

Geometric quality:

exposure and viewing angle, irregularities in sensor platform motions and orbital dynamics (attitude variation, velocity variation, precession, tracking), refraction, interframe deformation, calibration.

Radiometric quality:

sun's illumination (zenith angle, shining direction angle, sun-morphology interaction, sun-atmosphere interaction, shadow), absorption and scattering, diffusion, clouds, haze, acquiring time, season (in forming stereopairs)

Geometric and radiometric quality:

pixel offsets, earth rotation, exposure time, sensor noise and distortion of information recording device (misalignment, non linearities)

Operator measurements and comfort:

all the previous sources mainly related to the radiometric quality and the panoramic effect.

All the above factors are related to the image quality and they should be considered if the quality of the captured information is examined. Some of these can be examined by being varied in an experiment and others will be constant. In this chapter an attempt is made to present some of the sources affecting the image quality rather than developing correction techniques which are beyond the aim of

this thesis.

In this project the image quality due to the photographic processing (three pairs of images were printed from the original CCP data) is examined. The illumination and atmospheric effects affecting the image quality are examined by measurements in a second better quality SPOT hardcopy. The panoramic effect is examined (the second SPOT stereopair is corrected for the panoramic effect, while the first copy is not). In addition there are some other sources related to the accuracy of 'raw' DEM data such as: the setting up procedure, the operator's experience, the relief effect, the ground coverage, and the projection transformations are examined in chapters 4, 5 and 6.

Chapter 4.

Test data.

4. Test data - Images used in this work.

4.1. Aix En Provence aerial photography.

4.1.1. Control point accuracy.

The control points for setting up the aerial photography models were provided by IGN. The control points are not all precise photo-identifiable positions. The planimetric accuracy is in the range +/- 2 m. Some points are fixed at the top centres of roof levels. These points are not easy to measure accurately. The estimated residual is up to +/- 2 m in the worst cases.

4.1.2. Aerial triangulation results.

The area was covered by two adjacent strips (series F86 300 3925) of 1:30,000 scale photography (North 8 models and South 7 models), from which 10 are covered by the SPOT image, with focal length 153.19 mm. The acquisition date was 24 May 1986.

In order to obtain a sufficient number of control points for setting up the aerial photography models, an aerotriangulation was carried out. The aerial triangulation was carried out by a Remote Sensing student for his MSc project requirements. This was carried out only for the study area and it was used as the base for controlling the photomodels for the DEM area.

The aerotriangulation and block adjustment, gave the results shown in tables 4.1,4.2 and 4.3:

	OBSER.	MEAN (m)	STANDARD ERROR (m)	VARIANCE (m^2)	STANDARD DEVIATION (m)
Dx	12	0.230	0.396	1.886	1.373
Dy	12	0.218	0.278	0.929	0.964
Dz	12	-0.007	0.314	2.076	1.441

Table 4.1. Aerotriangulation results of strip 1.

	OBSER.	MEAN (m)	STANDARD ERROR (m)	VARIANCE (m^2)	STANDARD DEVIATION (m)
Dx	10	0.023	0.237	0.564	0.751
Dy	10	-0.261	0.320	1.023	1.011
Dz	20	0.007	0.328	2.157	1.469

Table 4.2. Aerotriangulation results of strip 2.

	OBSERV.	MEAN (m)	STANDARD ERROR (m)	VARIANCE (m^2)	STANDARD DEVIATION (m)
Dx	22	0.136	0.238	1.241	1.114
Dy	22	-0.005	0.212	0.992	0.996
Dz	41	0.000	0.224	2.063	1.436

Table 4.3. Aerotriangulation results of strip 1 and strip 2 combined.

The aerial triangulation and block adjustment give a maximum residual in plan at a tie point of 1.16 m. The maximum residual in height at the same tie point was found to be 0.61 m. Height control points in the overlap area, were also observed on both strips of photography and the maximum error at these points is 2.84 m (at a point on the lower strip).

The results for control points used in the block adjustment give a maximum residual in plan = 1.23 m at one point and a maximum residual in height = -1.05 m at another point.

The residual errors in the area of overlap were acceptable, although some were at the limit of normal tolerance. The maximum residual in plan at tie points is 2.24 m and the maximum residual in height at tie points is 1.99 m. These accuracies are adequate for the present requirements for comparing SPOT data, but under normal mapping project conditions, using this scale of photography for 1:5,000 scale mapping, the maximum residual errors in both plan and height would need to be less than one third of the values of this adjustment.

4.1.3. Absolute orientation results.

The number of models observed for DEMs were 10, in two strips. Aerial photograph models were set up on the Kern DSR1 analytical plotter. The overall setting up procedure (absolute orientation) results are shown in the table 4.4:

	MEAN (m)	MEDIAN (m)	STANDARD ERROR (m)	STANDARD DEVIATION (m)
PLAN	1.029	0.666	0.225	0.711
HEIGHT	0.945	0.937	1.241	0.392

Table 4.4. Aerial photography models. Absolute orientation overall results.

From the above results we can estimate the mean RMS vector error, considering of course that plan and height have different weights.

RMS Vector Error = 0.467 m.

4.2. SPOT Aix En Provence imagery.

4.2.1. First hardcopy.

In the Department of Photogrammetry and Surveying at UCL there exist two SPOT stereopairs.

The first is provided for a collaborative test with IGN of SPOT imagery. IGN provided the SPOT data, underflight photographs (scale 1:30,000) and control through the aegis of the SPOT-PEPS campaign.

The second hard copy is provided for the OEEPE experiment on triangulation of SPOT data which was carried out in the Department of Photogrammetry and Surveying of UCL. The chosen test area is the European test site extending from Marseilles to Grenoble. The Aix En Provence area is a part of this European test site. Because of this test another SPOT hard copy pair is available.

4.2.1.1. General information.

The area to the north of Marseille, southern France, is a European photogrammetric test area, well mapped and controlled, and with a climate suitable for easy acquisition of imagery. The area was used for extensive tests of Metric Camera Imagery (Meneguette, 1985). The area has also been selected for collaborative tests with IGN of SPOT imagery. Details of the SPOT images used are given below:

Scene	Date	View Angle
50-262	18 - 5 - 86	22.6°
50-262	01 - 6 - 86	-17.5°

The Base/Height ratio is 0.84.

The preprocessing level is 1A level (raw data with detector calibration correction, radiometric equalisation, but no geometric correction).

The scene corresponds almost entirely to IGN 1:100,000 map sheet 67 (Marseille - Carpentras). The 01 - 6 - 86 scene is partial cloud covered. The image is affected by haze, about 1/3 of the scene being totally obscured . A few small completely opaque clouds are present on the 18 - 5 - 86 scene. The images are also affected by horizontal and vertical striping originating in the pushbroom sensor and uncorrectable by SPOT-Image, as these images were recorded before July 1986 (Begni, 1988) . There are a few noticeable differences in the images due to crop growth and sun glint on water surfaces (on the east viewing scene). These would be a problem for automatic image correlation, but are not serious for manual tasks.

The original hard copy data was provided by IGN. The film quality proved inferior to the original data. Inner orientation results were bad (residuals in x direction more than 10 µm in both images after the application of affine transformation). The images were reprinted. The Optronics film writer at Nigel Press Associates gave only a slight improvement but the MacDonald Dettwiler (MDA) Fire 340 at Hunting Surveys and Consultants gave a much superior film

image, with radiometric differences clear at pixel level (Gugan, 1987) (inner orientation residuals after affine transformation were found to be about 2 µm in x direction and 8 µm in y direction in both images). However it was also noted that the Optronics scanner had slightly better geometric fidelity than the MDA Fire.

The SPOT image corners are used for inner orientation and therefore should be clear and distinct from the border. IGN produces film data with fiducial crosses around the image. Unfortunately, no information was provided as to the coordinates of these features and so they could not be used for orientation.

It is strongly recommended that film data purchased is rigorously evaluated for radiometric quality before acceptance. Also the geometric fidelity affects elevation accuracy and it is important that inner orientation residuals to be much less than 10 µm.

A part of these scenes, showing the location of the 30 m digital elevation matrix derived from aerial photographs (§ 5.2.3.2), are shown in figures 4.1 and 4.2.

The term digital or grid elevation matrix refers to manual measurements in a normal grid providing 'raw' elevation data. That means that the data has not had any interpolation function applied.

4.2.1.2. Control point accuracy.

In order to set up the model 10 control points have been used to find the orientations of the sensors and a further 20 points have been used as independent check points. The control points have been selected to be well distributed over the whole model.

The control points have been provided by IGN and are photogrammetrically or geodetically derived (accuracy < 1 m).

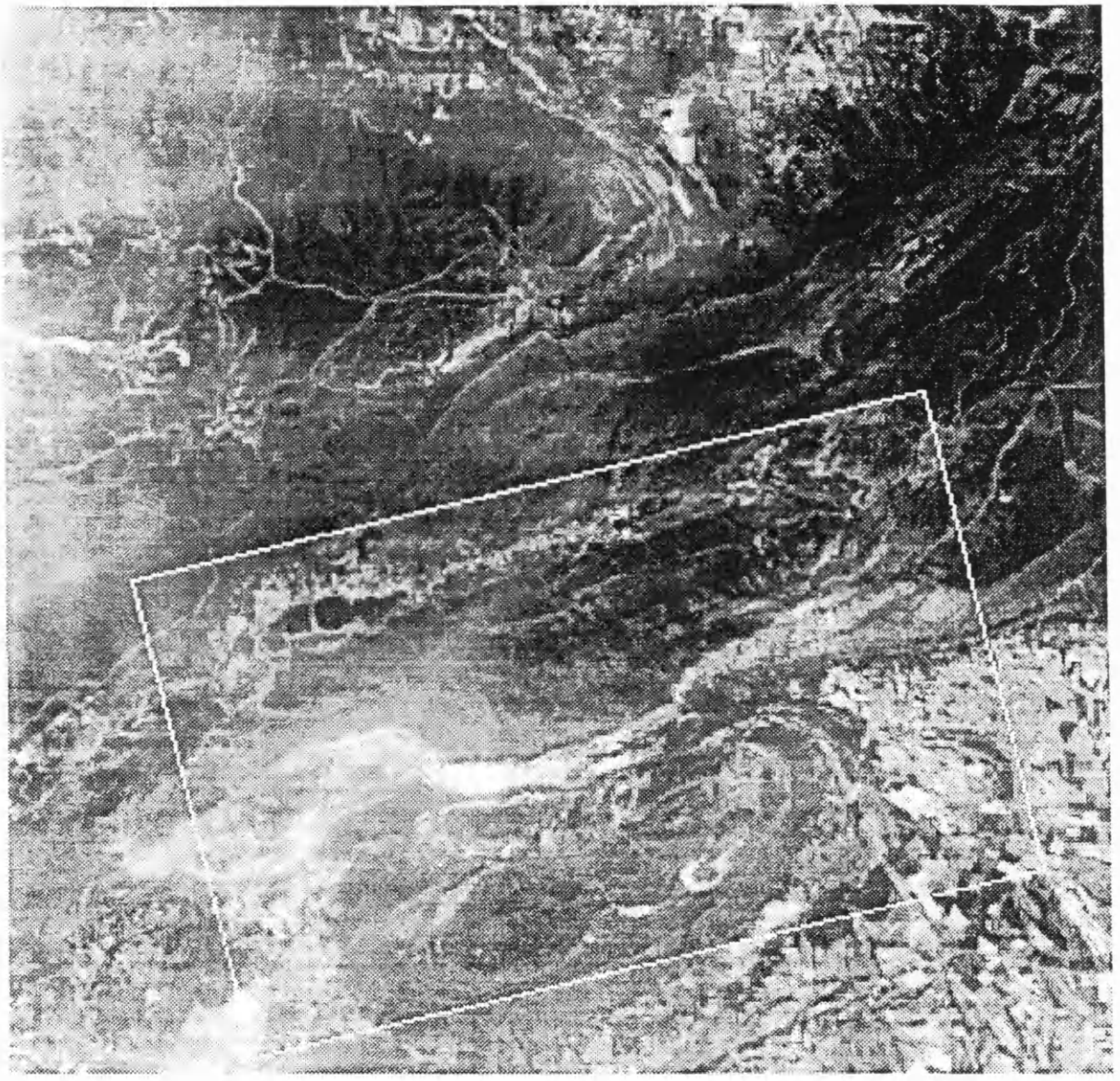

(Not to scale)

Figure 4.1. Part of left SPOT image, showing the location of the 30 m elevation matrix derived from aerial photography (© SPOT Image Copyright 1986 CNES).

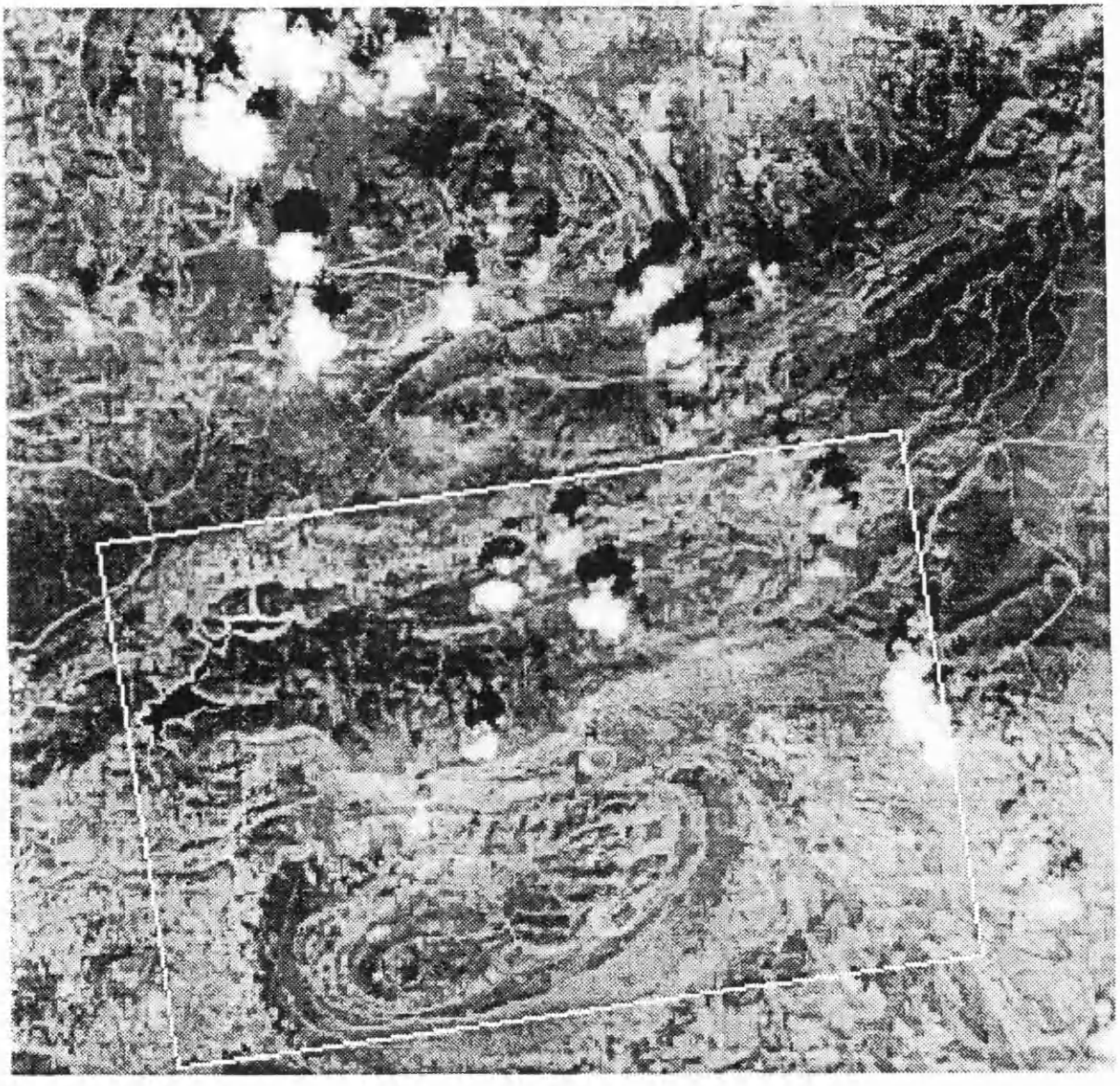

(Not to scale)

Figure 4.2. Part of right SPOT image, showing the location of the 30 m elevation matrix derived from aerial photography (© SPOT Image Copyright 1986 CNES).

The check points were digitised from large scale topographic maps (1:25,000). Coordinates were given in zone 3 of the French Lambert Conformal Conic map projection system and in the Geocentric system. (They are available in the Geographic coordinate system and Universal Transverce Mercator (UTM) after coordinate transformation). There is no a-priori information available pertaining to the accuracy of these check points. However as they were digitised from topographic maps 1:25,000, a planimetric RMSE accuracy of about 7 m (0.28 mm on the map scale) is expected and if we take into account the shrinkage of the map this seems to be reasonable. The height information of these points are obtained from the map contour lines, so normally a height accuracy of about 10 m is expected.

These points were not all suitable for use with SPOT; some were not identifiable , some topographical features were not precisely distinguishable (such as hill summits).

Ten well distributed ground control points, mainly road junctions, with geodetic coordinate accuracy were used for most of the orientation calculations. The accuracy of these control points may have a worse effect on the absolute orientation results owing to the fact that they are not signalised (premarked) points. Their detectability is therefore dependent on the scale and quality of the image. The accuracy (quality) of the control points is of major significance in the setting up the SPOT model procedure. It is found that the best control points in terms of detectability are main road junctions. Control points which are on the top of the hills or mountains do not give as good results as the points lying on flat or gently sloping areas.

It can be concluded the best control points for setting up SPOT images are on road junctions (main road and secondary roads) as these are easy to detect, to locate and to observe. It should be avoided to be in the crossing centre (centre of gravity) as it is difficult to be defined in planimetry. The best control points are on one edge of the junction, particularly if the roads are joined at an angle about 90 degrees. The control should be chosen in the valleys (lower level) as it gives better results than a control lying on the top of hills or mountains (upper level).

4.2.1.3. Exterior orientation accuracy.

The SPOT stereopair was set up on the analytical plotter in UCL with 10 control points well distributed over the model. The 10-parameter solution was chosen. Using all check points (20 points measured from the IGN map) this solution yielded RMS errors of 15.3 m in plan and 5.9 m in height.

Using only the 10 control points and discarding the check points the RMS Vector error on the ground control points is 8.7 m.

The planimetric and the height residuals on the control points are shown in figures 4.3 and 4.4. From these graphs we can see the following:

the GCPs are a great distance from the test area.

two of the GCPs (3040 and 8027) lie in the south-eastern part of the model. These points have a 5 m planimetric error and 8.6 m and -5.5 m error in heights respectively.

none of the GCPs lie in the test area.

the closest control point is 7.2 Km from the edge of the test area and the other control points are further than 15 km from the edges of the test area.

it can be seen by plotting the residuals for the 20 check points that while the height accuracies are random, the plan residuals have a pattern. This means that the residual patterns on each image from the independent space resections are similar (causing low residual x parallax). Similar results have been reported by Bahr (1978) using the collinearity equations with Landsat imagery.

The image RMS Vector error is :

In Left image $x = 4\ \mu m$, $y = 6\ \mu m$.

In Right image $x = 5\ \mu m$, $y = 6\ \mu m$.

The orientation software implemented at UCL does not provide the option of using on-board recorded data (satellite orbital parameters), which are provided with the images.

Comparing the model absolute orientation accuracy with those of Dowman et al (1987), Ducher (1989), Simard et al (1987) and Konecny et al (1987) (see § 3.4.2.1), we can say that the model setting up procedure gave very good results.

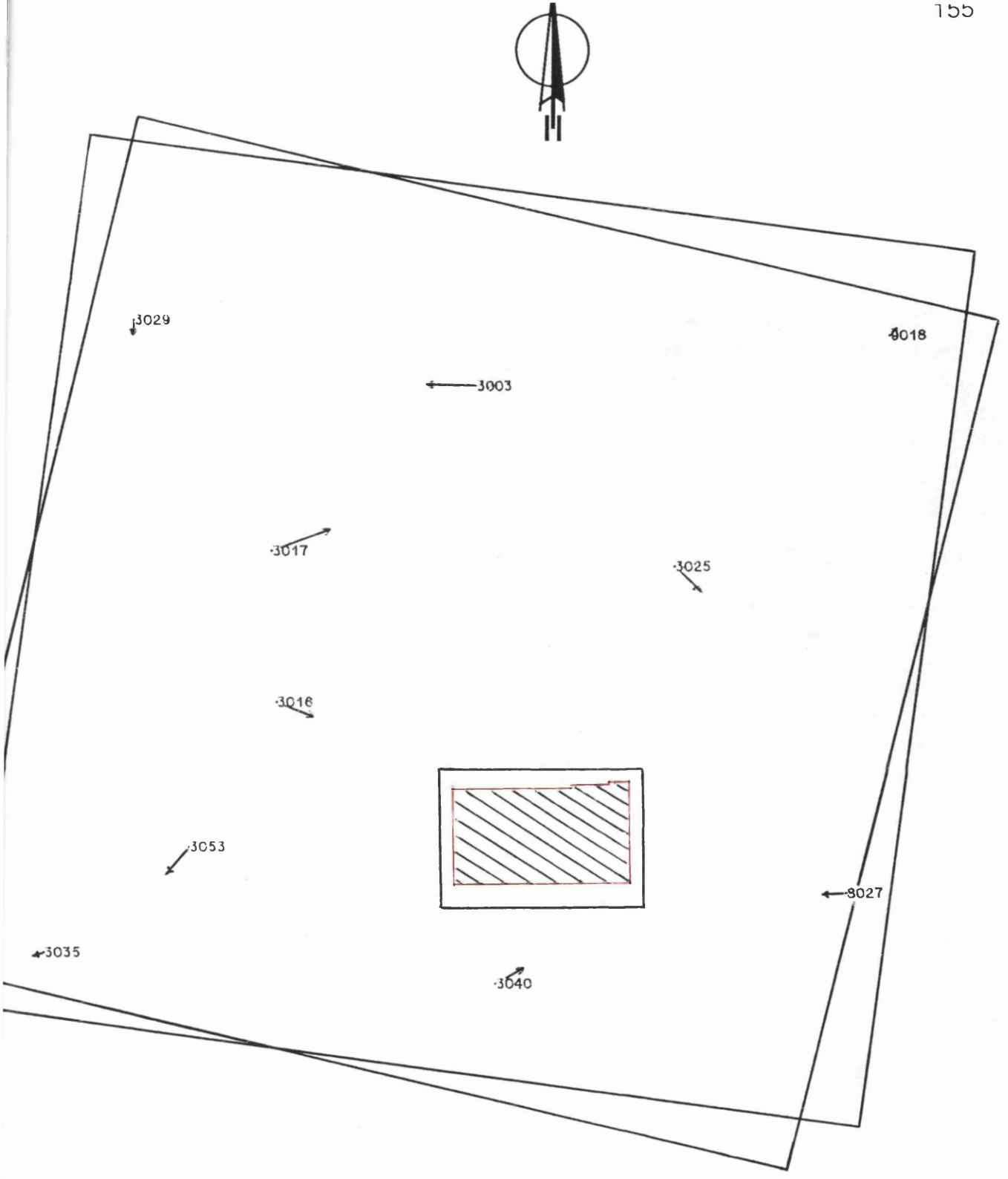

Scale 1:400,000 Residual scale 1 cm ÷ 10 m

Figure 4.3. Planimetric residuals of the first SPOT stereopair.

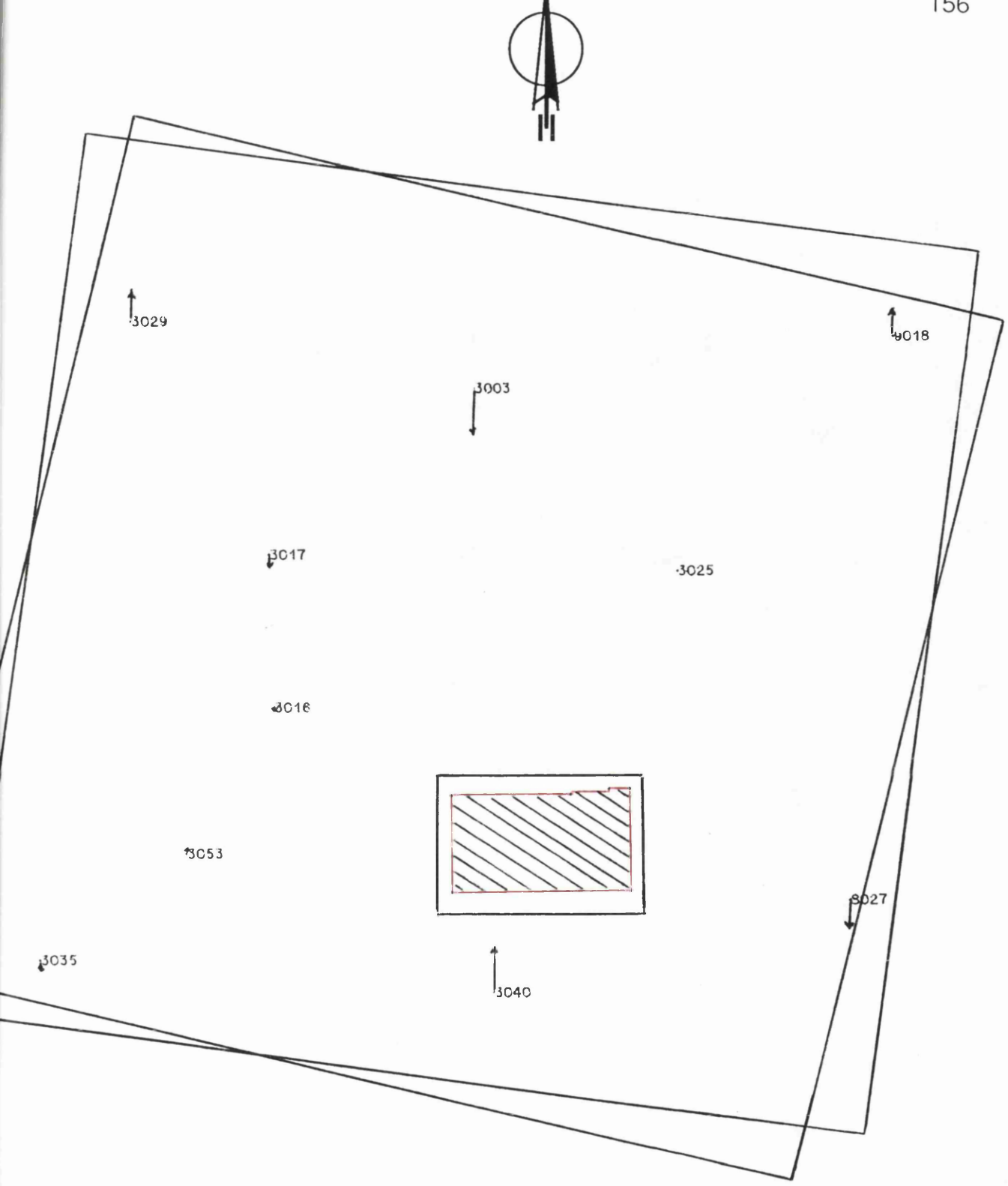

Scale 1:400,000 Residual scale 1 cm ÷ 10 m

Figure 4.4. Height residuals of the first SPOT stereopair.

4.2.2. The second SPOT hardcopy.

4.2.2.1. General information.

The available second hard copy was of better quality than that used in the original test. The scenes are clear from atmospheric effects. There were no serious illumination problems, no haze and almost no clouds. Only one scene has some cloudy parts, but these are far from the test area. Details of the second hard copy are given below:

Scene	Date	View angle
050-262	28-7-86	20.5°
050-262	30-8-86	-22.3°

So the B/H ratio is 0.91.

4.2.2.2. Control Points Accuracy.

In order to set up the model 15 control points were used to find the orientations of the sensors. The control points have been selected to be well distributed over the whole model. From those 8 GCPs were the same as those used in the first model and 7 new. The remaining two of the first model GCPs were out of the second SPOT model area.

The control points have been provided by IGN and derived from 1:60,000 scale aerial photography after aerotriangulation. The accuracy of those control points is estimated to be +/- 4 to 6 m for the computation of coordinates. The control was provided in the French Lambert Conformal Conic zone III coordinate system. It was transformed to Geographical and then to the Geocentric coordinate system. The error introduced in this transformation procedure is not significant (Dx=0.16 m, Dy = 0.31 m, Dz=0.22 m).

4.2.2.3. Exterior orientation accuracy of the second hard copy.

The SPOT stereopair was set up on the analytical plotter in UCL with 15 control points well distributed over the model. The resulting RMS vector error on the ground control points was 7.80 m.

The planimetric and the height residuals on the control points are shown in figures 4.5 and 4.6. From these graphs we can see the following:

the number of GCPs is increased from 10 to 15.

there are two additional GCPs, one close to the test area (3023) and the other in the test area (3042). These points have a 7.9 m and 9.7 m error in plan and a -4.9 m and -1.9 m error in heights.

the other control points are further than 15 km from the edge of the test area.

The image R.M.S vector error is :

In Left image $x = 7\ \mu m$, $y = 5\ \mu m$.

In Right image $x = 6\ \mu m$, $y = 6\ \mu m$.

Comparing the results of the exterior orientation of the setting up procedure for the second hard copy with those of Dowman et al(1987), Ducher (1989), Simard et al (1987) and Konecny et al (1987) (see § 3.4.2.1), we can say that the model setting up procedure gave very good results.

4.2.3. Exterior orientation accuracy of the first and second hard copy.

The RMS vector error on the ground control points of the procedure for setting up the first SPOT model using 10 GCPs was found to be 8.7 m, while the RMS vector error on the ground control points of the procedure for setting up the second SPOT model using 15 GCPs was found to be 7.8 m. Because most of the control points used in both stereomodels are the same this leads to the conclusion that the exterior orientation results become better when the number of control

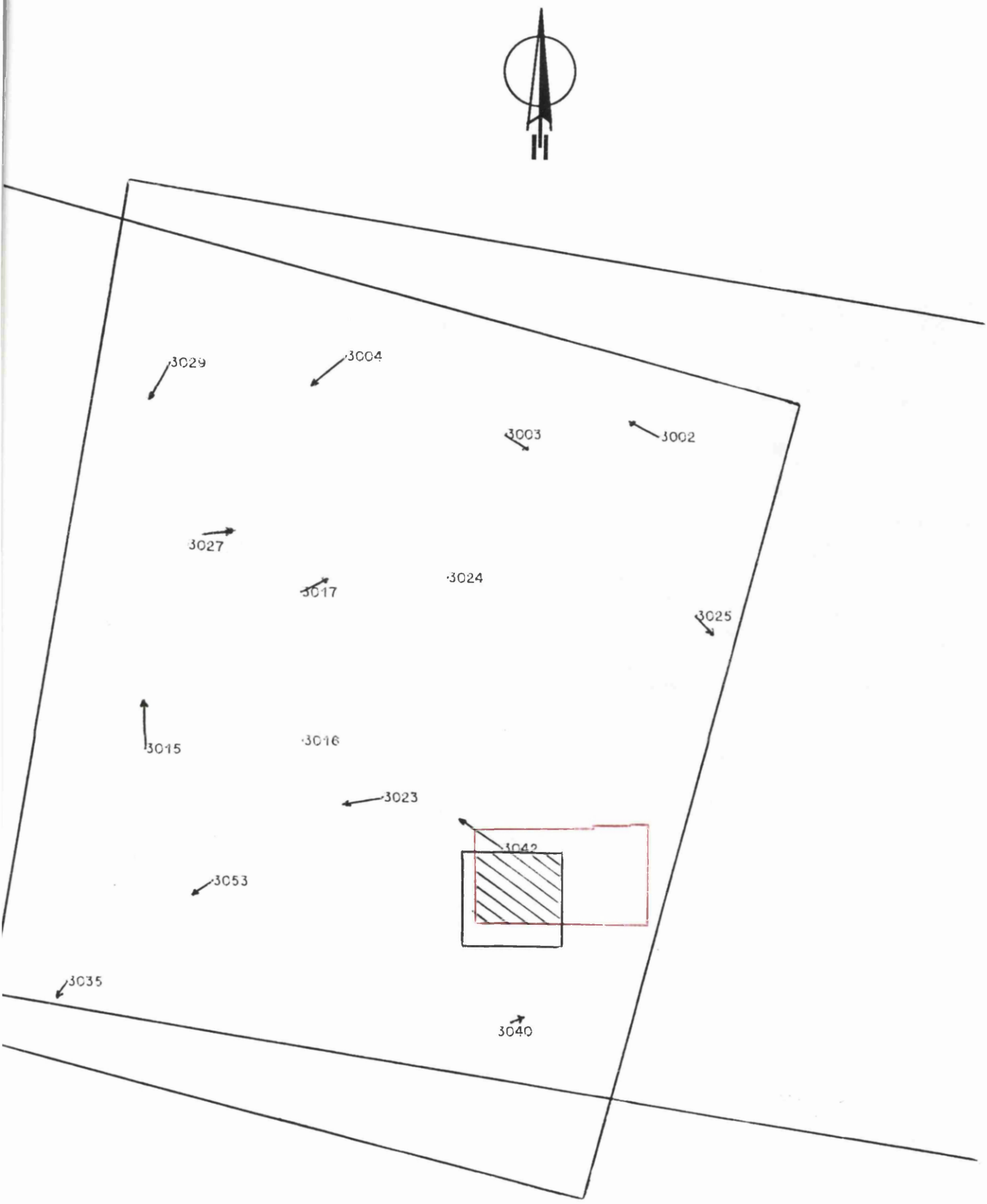

Scale 1:400,000 Residual scale 1 cm ÷ 10 m

Figure 4.5. Planimetric residuals of the second SPOT stereopair.

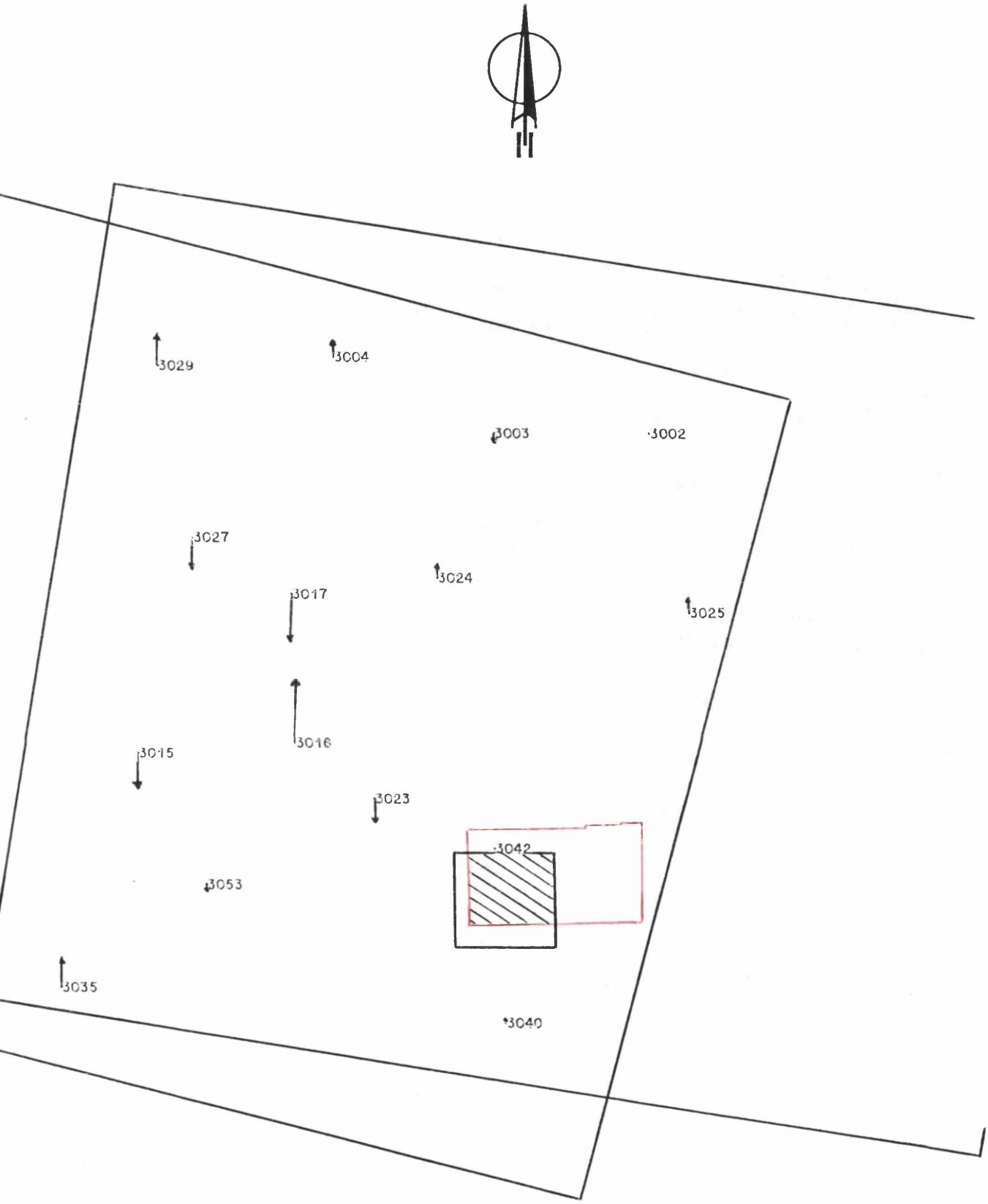

Scale 1:400,000 Residual scale 1 cm ÷ 10 m

Figure 4.6. Height residuals of the second SPOT stereopair.

points increases.

As we can see from these figures 33% more control gave 0.9 m better exterior orientation results. This means that the benefit of increasing the number of control points is very little. We can get the same conclusion by examining the results on the triangulation tests using SPOT data carried out by OEEPE (§ 3.4.2.1). However, the behaviour of a single SPOT stereopair is different to the behaviour of a number of stereopairs in a strip. It is a fact that for reasons of economy the ground control should be the minimum possible. However, the author believes that because of the application of the least squares adjustment in the estimation of the exterior orientation parameters the number of control should not be reduced below a certain limit. The larger number of control used in the second hard copy is possibly one of the reasons that the digital elevation measurements carried out on the second stereomodel have better accuracy than the same carried out on the first (see table 5.16).

Chapter 5.

Accuracy of captured data.

5. Accuracy of captured data.

5.1. General.

Accuracy is defined as the degree of closeness of an estimated value to its true value. However, the true or absolute value is not usually available in practice. Therefore the accuracy is normally redefined as the degree of closeness of an estimated value to its expected value (Davis et al, 1981, page 32). An accuracy measure is then given by the mean square error (MSE) as proposed by Gauss (Mikhail et al, 1976, page 45).

$$MSE = E\,[(p - E(p))^2]$$

where E is a statistical expectation operator; and p is an unknown parameter to be estimated.

In most practical work, the expected value is obtained from another estimate (or observation) which can be considered to have better geometry so that it has less bias in the process of the estimation (better accuracy).

Reliability has been a misleading term, in photogrammetry. In most work it mainly refers to an attempt to detect and to locate blunders. In fact reliability is concerned with the study of the sensitivity (quality) of the adjustment model with respect to the detection of errors in the functional or stochastic assumptions (ie. systematic errors or errors in the functional assumption or functional errors and weight error in the stochastic assumption) and detection of blunders (Gruen, 1980).

Precision is an indication of the spread of measured values of a quantity and describes the statistical quality of estimated parameters if a-priori assumptions of the adjustment in equations (in general a linear statistical estimation model such as least squares) are considered to be correct (Gruen, 1980).

Data collection accuracy depends both on the registration method and performance and on the source material. Each method gives a different accuracy (Kennie and McLaren, 1988) :

Ground survey gives very high accuracy.

Aerial survey in recording statically points gives high accuracy.

Aerial survey in recording dynamically points gives lower accuracy (contours).

Manual or automatic digitising of topographic maps gives low accuracy.

The relative accuracies (accuracy factor, AF) of digital elevation values as derived by various surveying techniques (adapted from Petrie and Kennie, 1988), are as follows (Kennie and McLaren, 1988) :

Ground Survey	
(1:500 map scale). Directly measured spot Heights	AF = 1
Aerial Survey	
(1:10,000 map scale). Spot heights measured in stationary mode	AF = 5
(1:10,000 map scale). Contours (measured in a dynamic mode)	AF = 15
Topo maps	
Medium scale (1:50,000). Generalised Contours	AF = 25
Small scale (1:250,000). Spot heights at grid nodes derived by interpolation from digitised contours	AF = 500

In this project the following sources are used for data capture :

1. Aerial photography at a scale of 1:30,000.
2. SPOT satellite imagery at a scale of 1:400,000.

The data capture technique is photogrammetry. The data were captured in a regular grid in stationary mode. One of the goals of this project is to find the accuracy of the SPOT elevation data in relation to the aerial photography derived data. For the two sources used in this project, the accuracy factor of the aerial photography derived data was assumed equal to 1.0. The SPOT accuracy factor was estimated relative to this factor and was found to be 0.10. (see §. 6.4.3).

5.2. Statistical methods applied to the data.

5.2.1. General.

Having suitably sampled the terrain and made the appropriate measurements we shall generally wish to examine the data derived so that we can make statements

about the terrain they represent with reasonable confidence. The subject of statistics is very large, and there are many techniques from which an investigator may choose. However, choosing the correct or the best technique in any given situation can be difficult.

Two rules are most important. First, to ensure that the sampling scheme is likely to produce the information that is required, and second to choose methods of analysing the data.

The following parameters can be used in the statistical analysis of the elevation data:

The first (numerical description), the arithmetic mean, (best estimate, best value, mean or average value), is the measure of the central tendency or 'average' in a sample. However, in some circumstances it can be misleading, and better measures might be the mode (the most frequently occurring value), or the median, (the middle value of those observed).

The second is the variance, which describes the the spread of values in the sample from the central value. The standard deviation (σ), gives the measure of the dispersion of the values about the mean. A small standard deviation indicates a close clustering of values about the mean, whilst a large standard deviation implies a wide scatter (indicates the degree of precision or degree of reliability of the mean). The root mean square (RMS) or quadratic mean, is the square root of the mean of the squares of the individual values.

The third is the skewness, the extent to which this spread is unequal about the centre.

The numerical values refer only to the sample from which they were derived. If we wish to use them to describe the terrain from which the sample was drawn, that is the sampling error, we need to know what confidence may be placed in the sample values as estimates of the terrain studied. So we have to make some assumptions.

In most simple applications we assume that the variation within classes is random ie the sampling error associated with one observation is quite independent of other observations. We often assume that these errors are distributed in a

certain way.

In the terminology of estimation the bias (figure 5.1) is equivalent to the systematic influence. It must be clear in mind that increasing the number of *n* observations will not eliminate the bias or even change it. The difference between the estimated value and the true value of any desired quantity is a measure of the bias. The accuracy is connected with systematic error ie. with bias. Thus we can say that the requirement for the best estimator to be unbiased means to be most accurate ie. systematic errors to be at the minimum possible level. In other words, if any bias exists with an estimator it should pass a certain statistical test before being accepted as the best estimator.

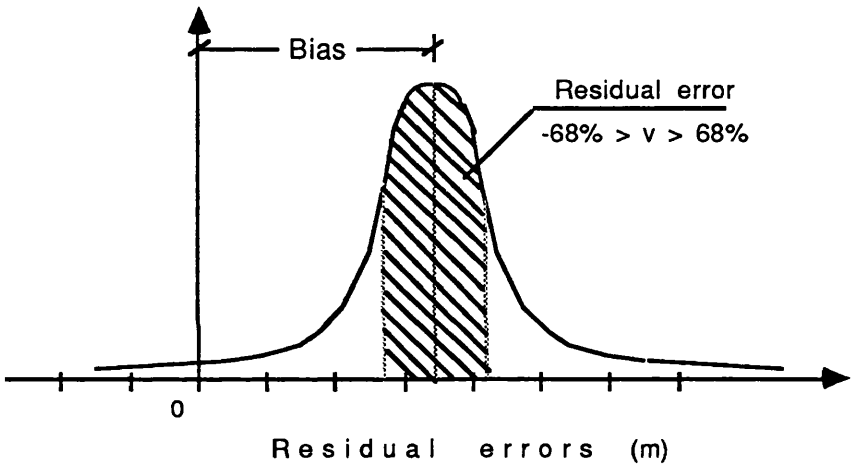

Figure 5.1. Shift of the Gaussian curve due to systematic errors.

If we have measurements we assume the measurements form a normal distribution. Statistics are most powerful when applied to normally distributed data.

Many tests are based on the assumption that the samples being analysed approximate to a normal distribution. To check the validity of this assumption on a set of data, a goodness-of-fit statistic between the sample and a theoretical normal distribution can be computed using a normality test. A number of tests may be used to check normality. The Kolmogorov-Smirnov one-sample test is used in this project because of its sensitivity, even with small sample sizes.

The Kolmogorov-Smirnov test gives the probability of obtaining the sample's

observed deviation from the theoretical, given that the underlying population is normal. If this probability is low, it suggests that the sample came from something other than a normal distribution.

No prior assumptions are made about the data except that the sample is from a continuous frequency distribution, that is, not categorical in nature. If the sample size is very small and there are a number of tied values (values that are assigned equal ranks) in the sample, then the test may be inappropriate. A fair number of ties can be tolerated with larger sample sizes.

For the normality test one variable name (set of data) is selected; the statistic and its two-tailed level of significance can be estimated. The significance level indicates the probability of obtaining such a sample from a population having a normal distribution.

The normality test (one sample Kolmogorov-Smirnov), sorts the observations into ascending order (H_1 to H_N). The observed frequency and expected frequency are estimated:

$$F_0(H_i) = F_{0,1}\left(\frac{H_i - \bar{H}}{s}\right)$$

$$\hat{F}(H_i) = \sum_{j=1}^{i} \frac{1}{N}$$

Two differences are calculated

$$D_i = \hat{F}(H_{i-1}) - F_0(H_i)$$

$$D_i' = \hat{F}(H_i) - F_0(H_i)$$

And the significant test is calculated as :

$$Z = \sqrt{N}\ {}^{\max}_{i}\left(|D_i|, |D_i'|\right)$$

and tested on a two-tailed basis

Rafferty et al (1985) pointed out that a significance level (of normality test) greater than 0.05 indicates that the distribution of the sample is normal.

Usually the elevation measurements made on the analytical plotter are normally distributed data, so statistical analysis can be applied directly on the data. However, the normality can be checked through the normality test.

Moreover the digital elevation models data are usually sampled under the same conditions of accuracy and precision, so all the observed elevations can be considered to have the same variance.

The variance-covariance matrices (v) provide the required information about the precision (deviation from the mean or scatter) of the variables in terms of their variances and covariances. However, in some cases it may be useful to have a single value to measure the precision, provided that we have a minimum number of observations (ie. 20 observations, otherwise we have problem of reliability). Two such values are:

1. The generalised variance : Determinant of (v)
2. The total variation : Trace of (v).

Generally large values of these measures indicate high degree of scatter or low precision, while low values represent concentration about the mean (Hassan, 1988).

Because of the unavoidable presence of gross and systematic errors in the result, not only a measure of precision but also a measure of reliability is required to assess the result, and later evaluating the gross and systematic errors.

Reliability is concerned with the bias, or the difference of the statistical expectation of an estimator from the true value of the estimated quantity. The reliability of a system describes the ability of the system to avoid biases, while the reliability of a result describes the biases inherent in the result.

The a-posteriori reliability measure reflects the calculated values of the additional parameters, so is more accurate than the reliability measure. The existing measure is just the maximum of the a-posteriori measure for a certain procedure of parameter selection or gives a function for determining weights (Huang, 1986).

5.2.2. Sources and types of errors.

Errors inherent in the measurements are inevitable. Repeated observations of the same quantity, taken under the same conditions, with the same instrument

and following the same procedure and care, are not going to be identical.

1. Sources of errors.

There are one or more of three sources of producing errors; personal, instrumental and natural.

1.1. *Personal errors.*

Operator errors can be due to carelessness of the operator involved in getting the measurement. Also, such error arises from the limitation in the human physical senses.

Some personal errors in photogrammetry may be due to:

The wrong setting of the floating mark on the surface of the model; pointing to the wrong control point target while setting up the model; reading or writing incorrect values etc.

Much of the personal errors could be minimised by employing well-trained and experienced staff.

1.2. *Instrumental errors.*

The instrumental errors are due to either imperfect construction or incomplete adjustment of the different components of the instrument.

The analytical plotters have a smaller number of mechanical components compared with the analogue instruments so the errors due to the first and the second factor are reduced. Example of the imperfect construction is unequal measurements of the stage movements due to the wrong encoder and the non-perpendicularity of the x and y axes. Most of the instrumental errors can be detected by careful testing of the instrument ie instrument calibration.

1.3. *Natural errors.*

The natural errors are produced by the continuous changes in the parameters constituting the physical environment which describe the field conditions, during the time of acquiring the observations.

Examples of such parameters include temperature, haze (humidity), wind pressure, atmospheric pressure, sun angle (refraction, absorption) etc. These affect our measurements, or our recordings. Wind speed results in a change of the flying direction. Sun angle is related with the atmospheric refraction, shadows and so on.

Earth curvature (which is not an error) can lead to errors in heights on a photogrammetric model if is not corrected.

2. Types of errors.

Errors have been traditionally classified into three types: gross, systematic, and random errors. The resulting error is actually a combination of one or more of these types of errors.

5.2.3. Data collected by photogrammetry from aerial photography.

5.2.3.1. General.

Data collection from a stereoplotter is a registration with interpretation because the information has to be classified, so skill and experience are needed. The planimetric and height accuracies which can be achieved using photogrammetric methods, the scale of the final product, the possible contour interval etc, are dependent on various interrelated factors. The most important of these being:

1. The scale and resolution of the image.
2. The base/height ratio.
3. The accuracy of the stereoplotting instrument.
4. Operator skills and experience (inaccuracy of setting the floating mark on the terrain model surface).
5. The accuracy of the model set up on the analytical plotter.
6. Terrain characteristics.
7. The registration procedure.

In addition the accuracy of height measurements depends on the altitude of the recording image station, which determines the size of the photogrammetric models.

The accuracy problem of the model set up in the analytical plotter is a problem of interior and exterior orientation (appropriate number, quality and distribution of ground control points, and restitution procedure of the

stereomodel).

The quality of the control points depends on :

a. The techniques ie. geodetic,photogrammetric (aerotriangulation), digitising from existing maps.
b. The implementation.
c. The calculation procedures.

Finally the accuracy of a dynamic profile scanning is lower than a static single point acquisition. (Sigle, 1984).

5.2.3.2. Data elevation measurements from aerial photography.

Ten aerial photograph models were observed (in two strips) for the necessities of the Alvey MMI-137 project on "Real time 2.5D Vision Systems". The DEM was produced in the department by manual photogrammetric measurement of spot heights from contemporaneous underflight aerial photography of 1:30,000 scale. The DEM covers the region of the Montagne Sainte Victoire, an area 12.42 km by 6.9 km with 30 m spacing. The range of elevations is 191.71 to 1010.99 m. This DEM is unusual in that the operator measured the top of the tree canopy, where it was present rather than attempting to estimate ground elevation. When the operator attempts to find the underlying ground level, the heighting accuracy will be based only on his interpretation which varies from time to time. It is well known that these variations sometimes occur not only between different operators, but also with the same operator if he attempts to measure the same points at different times.

From the scale of photography being used (1:30,000) ground surface points should be able to be heighted to an accuracy +/- 0.8 m; grass crop, bush and scrub level points (low level 2-3 m) to an accuracy of +/- 1.5 m, and tree heights to an accuracy +/- 3.0 m. The canopy is a highly curved surface with vertical sides, which may give variations of up to 5 metres in some places. In the cliff regions the change in height with very small (less than 1 metre) movements in plan could be as much as 15 m in height. Also the inability to spot-height a very steeply sloping surface consistently, could cause errors of up to +/- 3.0 m.

Water level (reservoir) reading were found to be accurate to +/- 1.0 m. The heighting on good hard surface points in level areas was found to achieve an accuracy +/- 0.25 m (Pitkin, 1988).

An overlap DEM area from different strip models was measured. The overlap DEMs (830 points) gave the following results (comparing values from the southern strip against the northern strip) :

Maximum difference	=	14.66 m.
% points less than 1m difference	=	51.1%
% points less than 2m difference	=	83.5%
% points less than 3m difference	=	91.6%
Mean difference of all points	=	0.51 m
Standard deviation	=	1.83 m

These differences appear to show a random distribution, and the accuracy is consistent with what could be expected from these sets of data.

The Lambertian shaded nadir view (see §9.1) of the DEM produced from the aerial photography data is shown in figure 5.2. In figure 5.3 is shown a positive digital terrain image (raster form) of half of the area (6900 x 6000 m^2) using the same data (46,200 points). In figure 5.3a is shown the negative image.

5.2.3.3. Observer's ability test.

Reobservation of the same DEM is a test of the observer's ability to consistently height the same planimetric positions. 990 points were reobserved by using the same model and the same orientation parameters. The statistical analysis results are the follows:

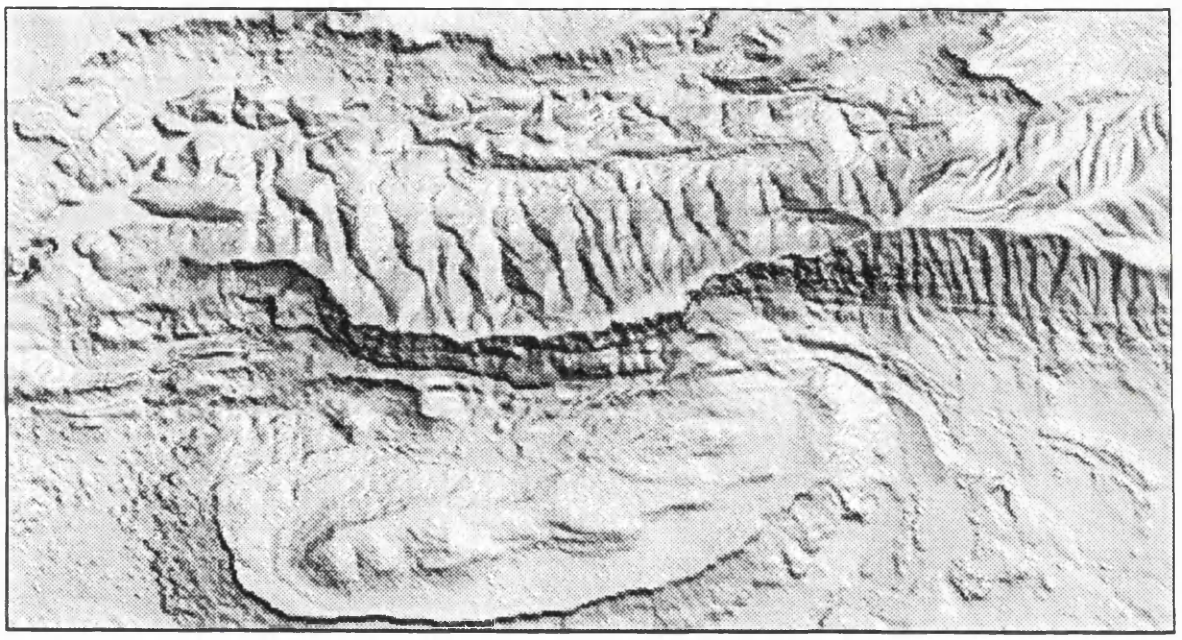

Figure 5.2. Lambertian shaded nadir view of the DEM produced from the aerial photography data.

AERIAL PHOTOGRAPHY DATA

AREA 6900 x 6000 m^2

(Not to scale)

Figure 5.3. Positive digital terrain image (in a raster form) of half area

AERIAL PHOTOGRAPHY DATA

AREA 6900 x 6000 m^2

(Not to scale)

Figure 5.3a. Negative digital terrain image (in a raster form) of half area.

Maximum difference	= 11.29 m
% points less than 1m difference	= 65.9 %
% points less than 2m difference	= 86.1 %
% points less than 3m difference	= 93.8 %
Mean difference of all points	= 1.14 m
Standard deviation	= 1.27 m

These results do show accuracy greater than the previous test, but fall short of the expected accuracy by 5 - 10%. It is not possible to fully evaluate the result of these tests without more information about individual points (particularly of the points not at ground level).

So, assuming these values are typical of all 95,865 points of the elevation measurements (through obviously the maximum absolute error can be expected to rise with more points), the 30 m digital elevation data should be adequate for testing elevation data derived from SPOT up to the specified target accuracy of an RMS error 5m in height.

5.2.4. Data collected by photogrammetry from SPOT satellite imagery - SPOT heighting accuracy experiments.

5.2.4.1. Purpose.

The availability of SPOT data significantly changes the way in which satellite images may be used. SPOT can be used for applications in which only aerial photographs were used previously. The determination of heighting accuracy is very important in applications such as DEM measurements for map production. Although automated techniques are at a good stage of development, at the moment manual techniques remain an important production method for capturing the height information for DEM construction.

Because the previous investigations do not give a clear idea of the SPOT heighting accuracy and particularly the reason for appearance of the systematic bias, the current experiment was carried out in order to estimate the heighting accuracy levels which can realistically be achieved, and also the magnitude and the

possible reasons or sources of error. The bias or deformation from the ideal normal distribution or systematic error distribution follows the "bell shaped" distribution. The errors are not White Gaussian noise because the expected value is shifted from zero.

The determination of the SPOT heighting accuracy is very important when a DEM derived from manual measurements is studied. For the purposes of this project, the knowledge of the SPOT heighting accuracy and the estimated height limits from the applied statistical analysis are used in the blunder detection study and the data merging procedure. Moreover the SPOT elevation data reliability is going to be useful in the estimation of the interpolation accuracy in DEMs, when pure data from SPOT or data merged from both sources are used for DEM construction.

The digital elevation matrix derived from the aerial photography is considered as absolute ground truth for the reasons that:

1. The scale of the SPOT scenes is 1:400,000 compared with the aerial photography scale of 1:30,000 (much higher resolution) and

2. The standard deviation of the aerial photography measurements was estimated as 1.3 m.

5.2.4.2. The main experiment - SPOT hardcopy measurements.

5.2.4.2.1. Description and procedure of deriving digital elevation data from SPOT.

The Aix En Provence SPOT model was set up on a DSR1 analytical plotter and twenty DEM blocks were measured. Of the 20 measured blocks 16 covered the same area as blocks derived from aerial photography. Each SPOT derived block contains 900 points in a normal grid with 100 m interval. The data were measured using the same exterior orientation parameters for all blocks. The output from DSR1 data capture program is a string of coordinates in UTM projection. The coordinates were transformed from UTM to geographical coordinate system (LLH) and then to the French Lambert Conformal Conic zone III map projection using the Clarke 1880 ellipsoid (see chapter 6). The SPOT derived spatial data cover a larger area

than that derived from aerial photographs. The following figure (Fig. 5.4.) shows the relative position of the two grid elevation blocks.

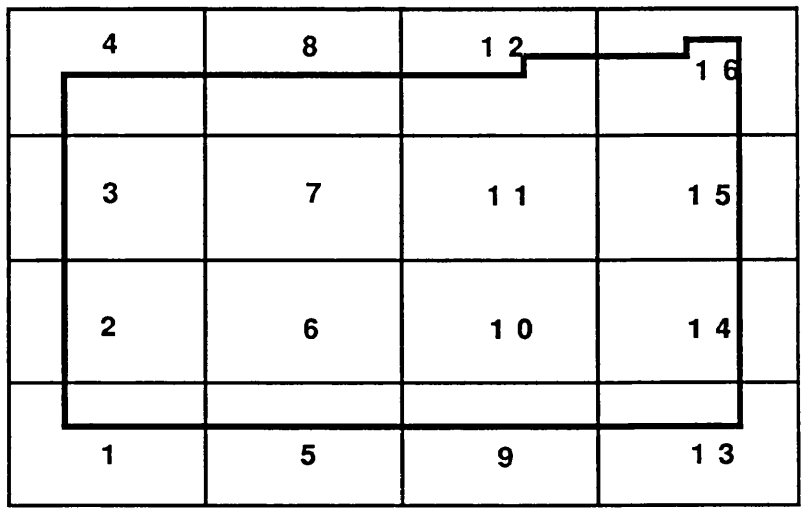

Figure 5.4. Relative position of the two sources grid elevation blocks.

Figure 5.5 is shown a positive digital terrain image (in a raster form), derived from the SPOT measurements (14400 points) of the whole 16 measured blocks (14300 x 9900 m^2), and figure 5.5a is shown the negative image.

The measuring conditions due to the physical image quality were not good. The 01-06-86 image is partly hazy in the test area and a few small opaque clouds (cumulonimbus clouds and their shadows) are present on the 18-05-86 scene. The surface illumination is poor. The southern site of the Montagne Sainte Victoire is in sunlight, but the northern part is poorly illuminated (in shadow).

The SPOT elevation data were compared directly with those derived from aerial photography, (the base data) utilising the nearest reference point, if this exists within a specified distance. The distance is chosen according to the criteria for minimising the additional error due to the variation of the terrain height. If we

AIX EN PROVENCE (SPOT)

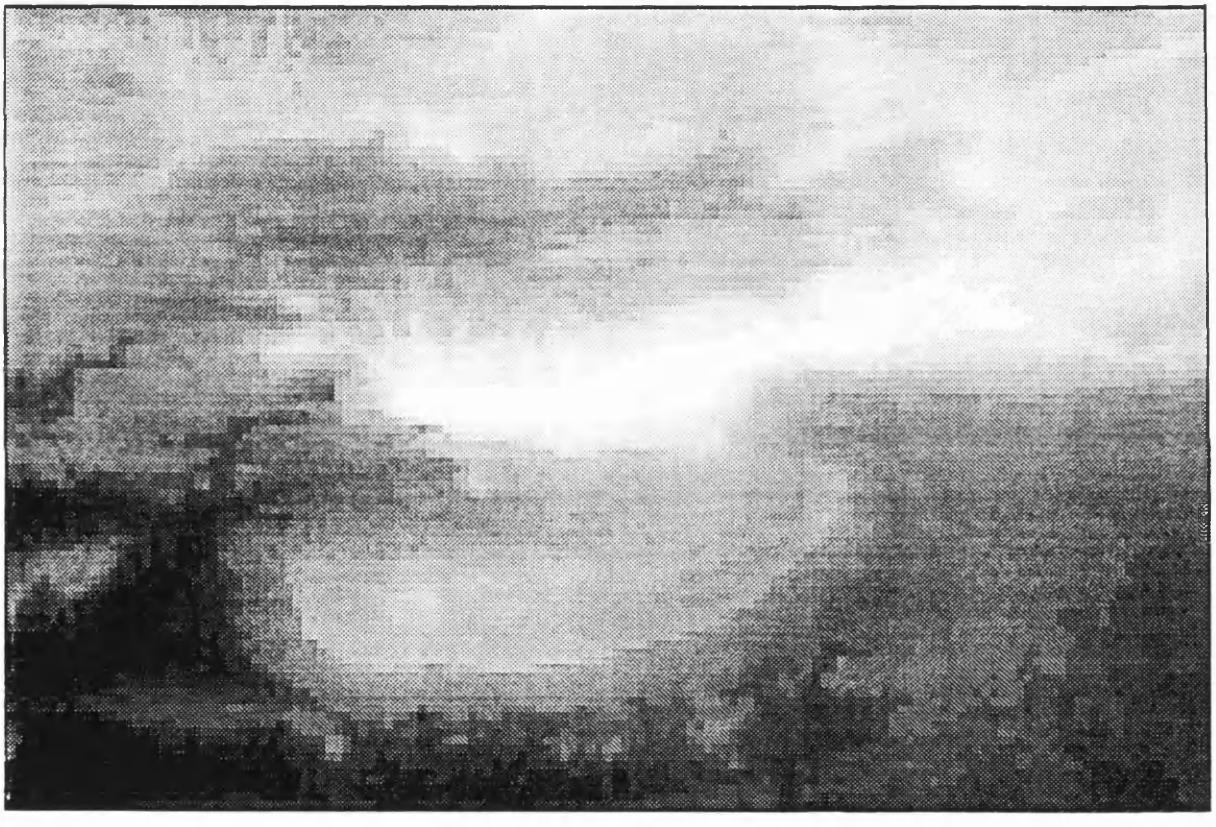

AREA 14300 x 9900 m^2

(Not to scale)

Figure 5.5. Positive digital terrain image (in raster form) derived from the SPOT measurements.

AIX EN PROVENCE (SPOT)

AREA 14300 x 9900 m^2

(Not to scale)

Figure 5.5a. Negative digital terrain image (in raster form) derived from the SPOT measurements.

would like to minimise the additional error due to variation of the terrain away from the manually measured reference point, the number of points to be evaluated is decreased. The introduced error due to the radius can be estimated from the terrain variogram (see § 7.3.1.1). In the following statistical analysis, the slope for the compared SPOT digital elevation matrix data was estimated as an overall block area average slope. The derived statistical results from the compared heights within radius 15 m, are shown in the table 5.1.

DEM BLOCK	NUMBER OF COMPARED POINTS	MEAN (m)	RMS (m)	SD (m)	AVERAGE SLOPE (%)
1	183	-3.88	11.21	10.52	26.1
2	514	4.80	16.88	16.18	35.5
3	514	-6.41	15.79	14.43	41.7
4	218	3.55	16.20	15.81	27.3
5	252	-3.81	9.67	8.89	30.3
6	708	4.35	19.44	18.95	43.3
7	708	16.03	28.17	23.16	64.6
8	300	4.56	12.60	11.74	35.4
9	249	-1.35	6.03	5.88	28.5
10	708	-3.53	8.80	8.07	36.4
11	708	11.78	27.53	24.88	66.4
12	301	9.37	17.97	15.34	38.6
13	185	2.97	5.68	4.85	7.6
14	531	-5.99	8.58	6.14	11.9
15	531	0.31	12.94	12.94	58.3
16	223	0.78	10.01	9.98	31.6

Table 5.1. Statistical analysis of compared heights within radius 15 m.

The RMS or quadratic mean is the square root of the mean of the squares of the height differences.

$$RMS = \left(\Sigma(dh_i)^2 / n\right)^{1/2}$$

The errors which are presented in table 5.1, are the combined errors which

analytical plotter).

The overall data statistical values are:

mean = 2.94 m, standard deviation= 15.82 m and absolute mean = 6.16 m in an area with an average slope 41.3%. The absolute mean is estimated from the summation of the absolute values of the residuals divided by the number of the observations. It is remarkable that although some blocks appear to show a strong systematic bias in the mean value, the overall mean is 2.10 m, which is good.

A goodness-of-fit statistic between the sample and a theoretical normal distribution is computed using the one-sample Kolmogorov-Smirnov test (§ 5.2.1).

The normality test gave the following results :

Statistic : 0.2237

Significance : 0.159

The significance 0.159 >> 0.05 indicates that the distribution of the sample is normal (Rafferty et al, 1985).

The line scattering diagram of all the height differences of the 6557 compared points is presented in figure 5.6. The class interval is every 4 m.

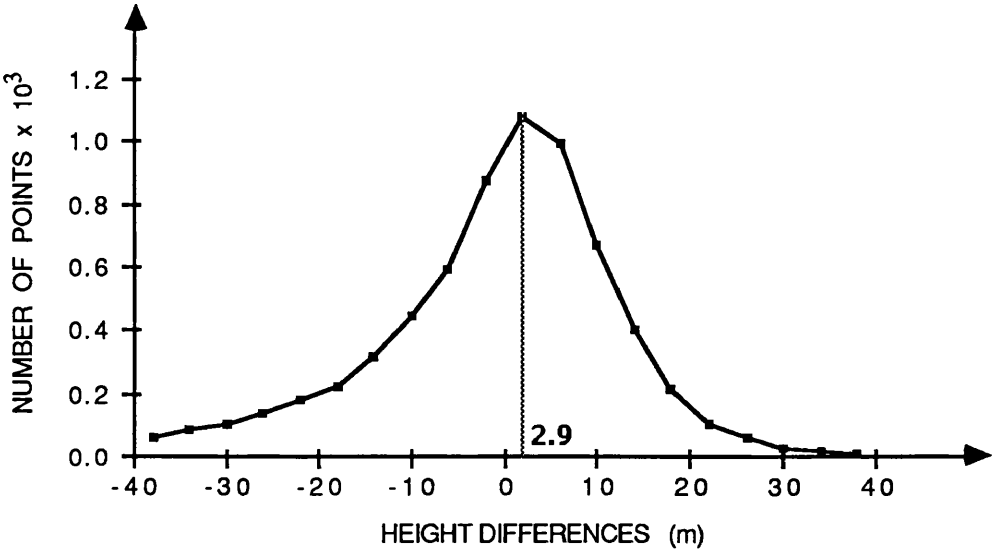

Fig. 5.6. Scattering diagram of height differences in the first SPOT hardcopy measurements.

This diagram does not include the points in which the height differences were

This diagram does not include the points in which the height differences were found to be greater than 2.7*(standard deviation of height differences). The number of those points is estimated to be 276 points in a total of 6833 points, or 4.04 %. In the above diagram we can see also that the observations follow the normal distribution law.

5.2.4.2.2. Observer's ability test.

The project operator has 5 years experience in plotting maps at large scales, but no previous experience in small scale mapping and SPOT images. It is also four years since he last carried out production work using photogrammetric instruments.

During the SPOT data capture procedure samples from four blocks were remeasured. This reobservation of the same data, was carried out to test the observer's ability to consistently measure height at the same planimetric position. From the two measured sets the height differences were estimated. Statistical analysis of the 1958 duplicated points is given in table 5.2.

If h_i' and h_i'' are two observations of the same point and dh_i is the difference $(h_i' - h_i'')$ then the mean difference (m) is: $(\Sigma dh_i / n)$ and the standard deviation is:

$$\sigma = \left(\Sigma(dh_i - m)^2 / (n - 1)\right)^{1/2}$$

DATA SET	NUMBER OF COMPARED POINTS	MEAN (m)	SD (m)	AVERAGE SLOPE (%)
1	709	-2.40	6.78	30
2	709	1.46	10.29	42
3	252	-0.88	11.75	45
4	288	4.22	3.57	10

Table 5.2. Statistical analysis of the 1958 duplicated points

The overall mean is 0.17 m and the standard deviation is 8.64 m. It can be seen that the mean value is not correlated with terrain roughness, whereas the standard deviation follows it.

The project operator measured a number of well defined (clear to observe) points on 4 different days with different inner orientation input files. The standard deviation of the measurements was found to be +/- 2.55 m.

From table 5.2. we can draw the diagram which shows the standard deviation changes in relation to the average slopes:

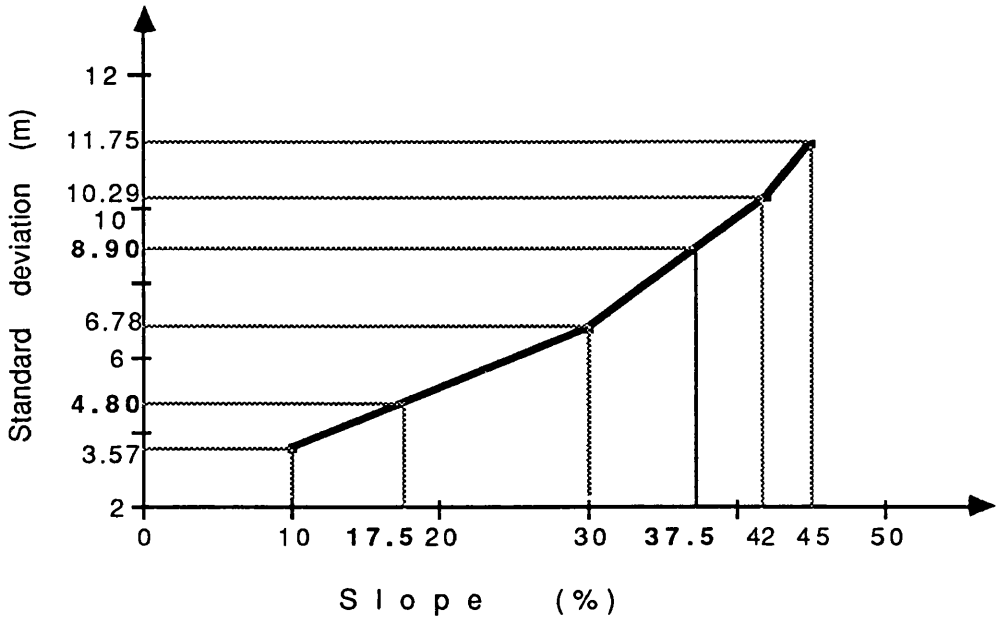

Fig. 5.7. Changes in standard deviation with slope.

Terrain types and slopes which are used in this work were grouped in 4 categories (terrain classification) (see § 2.4.3.2.1), so that each terrain type lies within a given slope range.

From Fig. 5.7, standard deviation values can be extracted for terrain type because of the relation between slope and terrain type. This will be useful for the estimation of the height limits (standard deviation of random error) which will have to be applied in further statistical analysis or in the blunder detection procedure.

The terrain classification and the estimated standard deviation (height limits) are shown in table 5.3.

Terrain classification	Height limits (m)
Flat areas	2.80
Gently rolling areas	4.80
Semi-rough terrain	8.90
Rough and steep terrain	14.00

Table 5.3. Terrain classification and height limits .

5.2.4.2.3. Remeasure the DEMs with large systematic bias.

The 7th and 11th of the DEM blocks (see table 4.1) with large systematic bias were remeasured again. The SPOT data were checked with respect to the aerial photography data. The old and the new mean and standard deviation values are given together in table 5.4.

DEM BLOCK	NUMBER OF POINTS	MEASURED FOR FIRST TIME		REMEASURED	
		Mean(m)	SD (m)	Mean(m)	SD (m)
7	708	16.03	23.16	17.79	23.16
11	708	11.78	24.88	21.71	34.95

Table 5.4. First and remeasured data statistical analysis values.

From table 5.4, we can see that in the 7th DEM block the results remained the same, while in the 11th DEM block there is a deterioration in the data.

The error display procedure (see § 5.2.4.4) allowed display of the errors of the first measured and remeasured 7th SPOT block. The comparison was done with the aerial photography data. The errors appear in figures 5.8, 5.8a (ungrouped errors) and 5.9, 5.9a (grouped errors).

In figures 5.8 and 5.8a the height differences (errors) grouping was carried out by the display software which used a default scale. Therefore 11 colours appear

on the display (each colour corresponds to a certain error magnitude) which are translated to grey scale on the laserwriter output. Because the interpretation is difficult even as a colour display and the grey legend does not appear on laserwriter output it was decided to group the errors into 5 categories (same as the estimated height limits) and then display. In figures 5.9 and 5.9a appear the total number of the compared points and the number of the height differences (errors) of the points which fall within each category.

Moreover a modification of the CHECK.PAS program (see § 5.2.4.2.4) allowed the comparison between the SPOT first measured and remeasured sets of data. The errors appear in figures 5.10 (ungrouped errors) and 5.10a (grouped errors) for the 7th block ; and 5.11 (ungrouped errors), 5.11a (grouped errors), for the 11th block.

All these procedures indicate that:

a. The operator measurements appear more or less stable.

b. The operator makes almost the same errors (mistakes) in some specific areas (see § 5.2.4.5 discussion).

TWO SOURCES COMPARISON

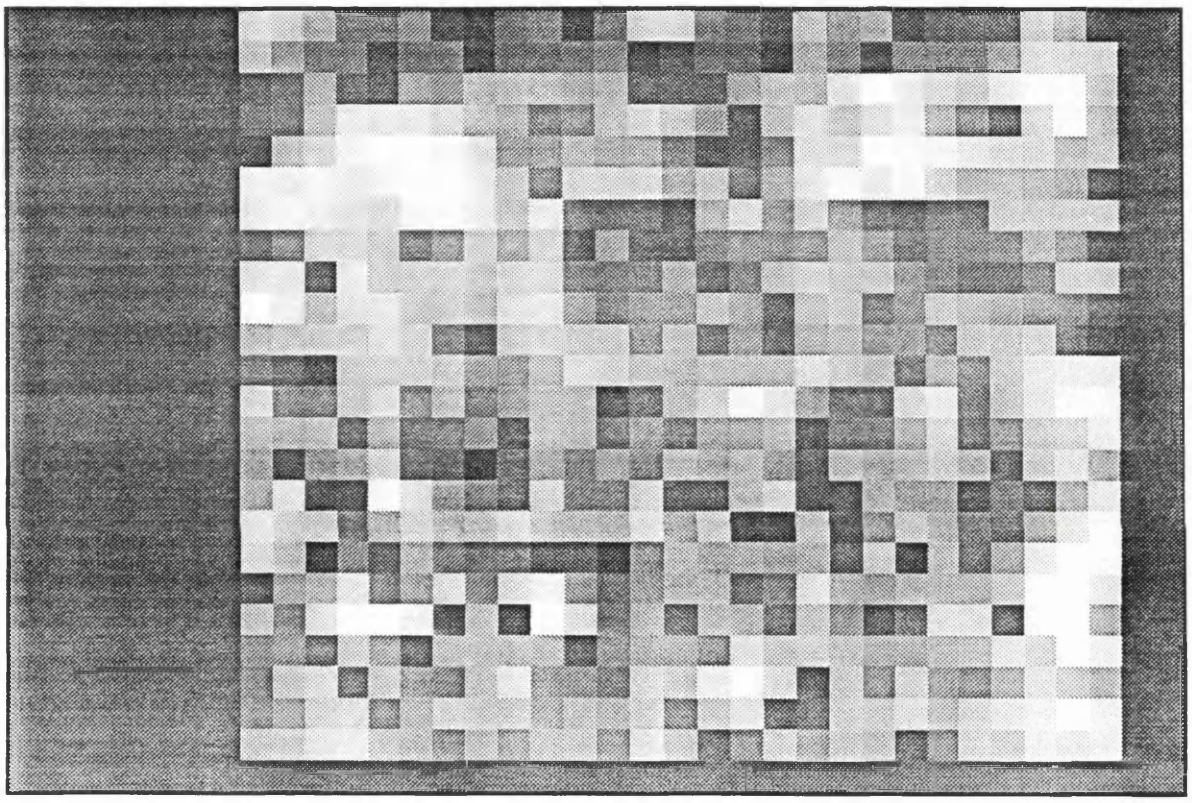

HEIGHT DIFFERENCES

(Not to scale)

Aerial photography and SPOT data comparison.

White parts correspond to large errors, while the dark appearance in the compared area means height differences (errors) ≈ 0 (less than 0.50 m). The same dark appearance part at the three edges means that there are no aerial photography data for comparison.

Figure 5.8. First time measured 7th SPOT block. Errors ungrouped.

TWO SOURCES COMPARISON

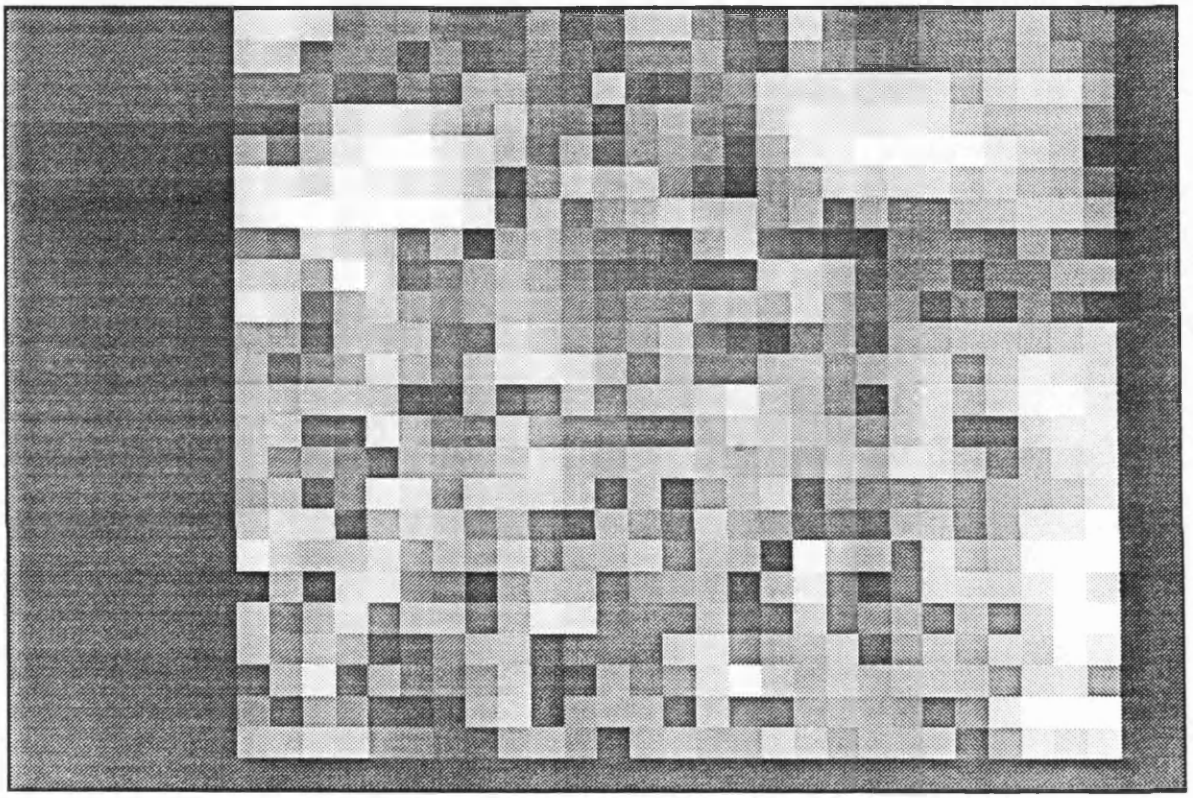

HEIGHT DIFFERENCES

(Not to scale)

Aerial photography and SPOT data comparison.

White parts correspond to large errors, while the dark appearance in the compared area means height differences (errors) ≈ 0 (less than 0.50 m). The same dark appearance part at the three edges means that there are no aerial photography data for comparison.

Figure 5.8a. Remeasured 7th SPOT block. Errors ungrouped.

TWO SOURCES COMPARISON

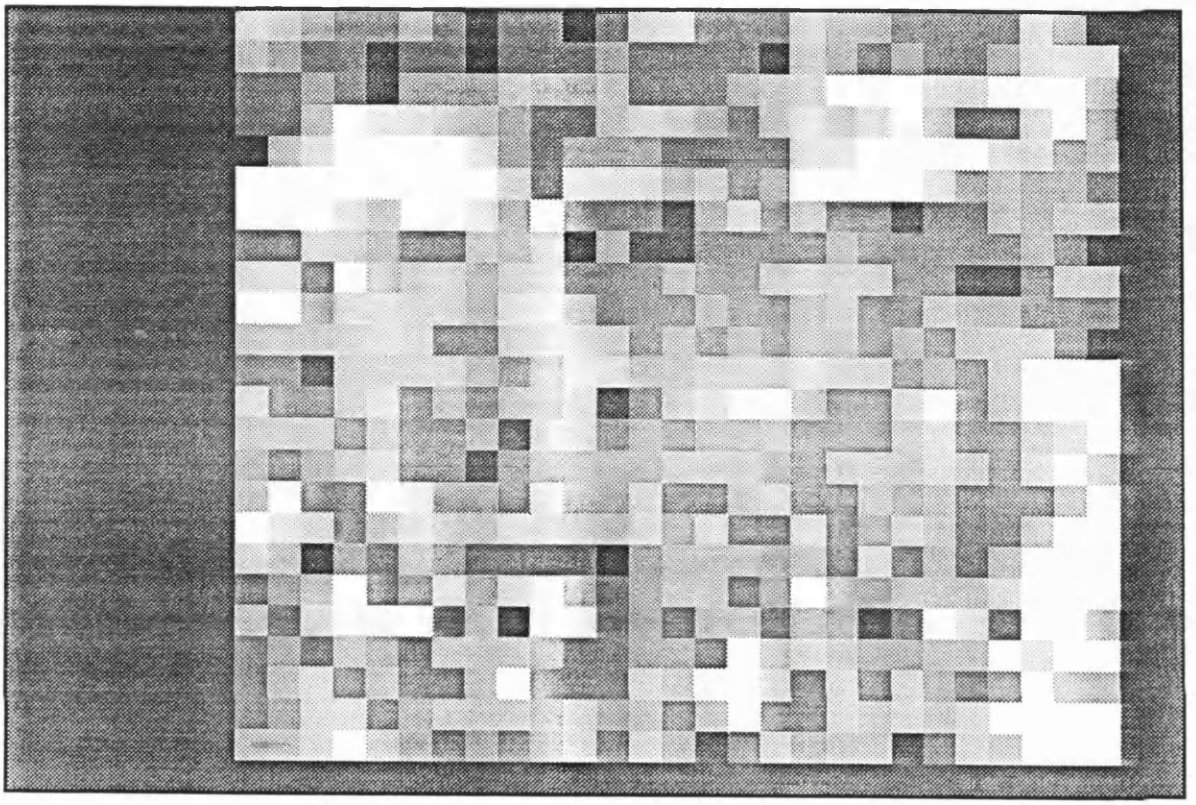

HEIGHT DIFFERENCES

(Not to scale)

Aerial photography and SPOT data comparison.
Height differences grouped in 5 groups for better visualisation.

Number of compared points 648

0.00 m	-	8.40 m	230	points
8.40 m	-	14.40 m	112	points
14.40 m	-	26.70 m	137	points
26.70 m	-	42.00 m	81	points
above 42.00 m			88	points

White parts correspond to large errors, while the dark appearance in the compared area means height differences (errors) ≈ 0 (less than 0.50 m). The same dark appearance part at the three edges means that there are no aerial photography data for comparison.

Figure 5.9. First time measured 7th SPOT block. Errors grouped.

TWO SOURCES COMPARISON

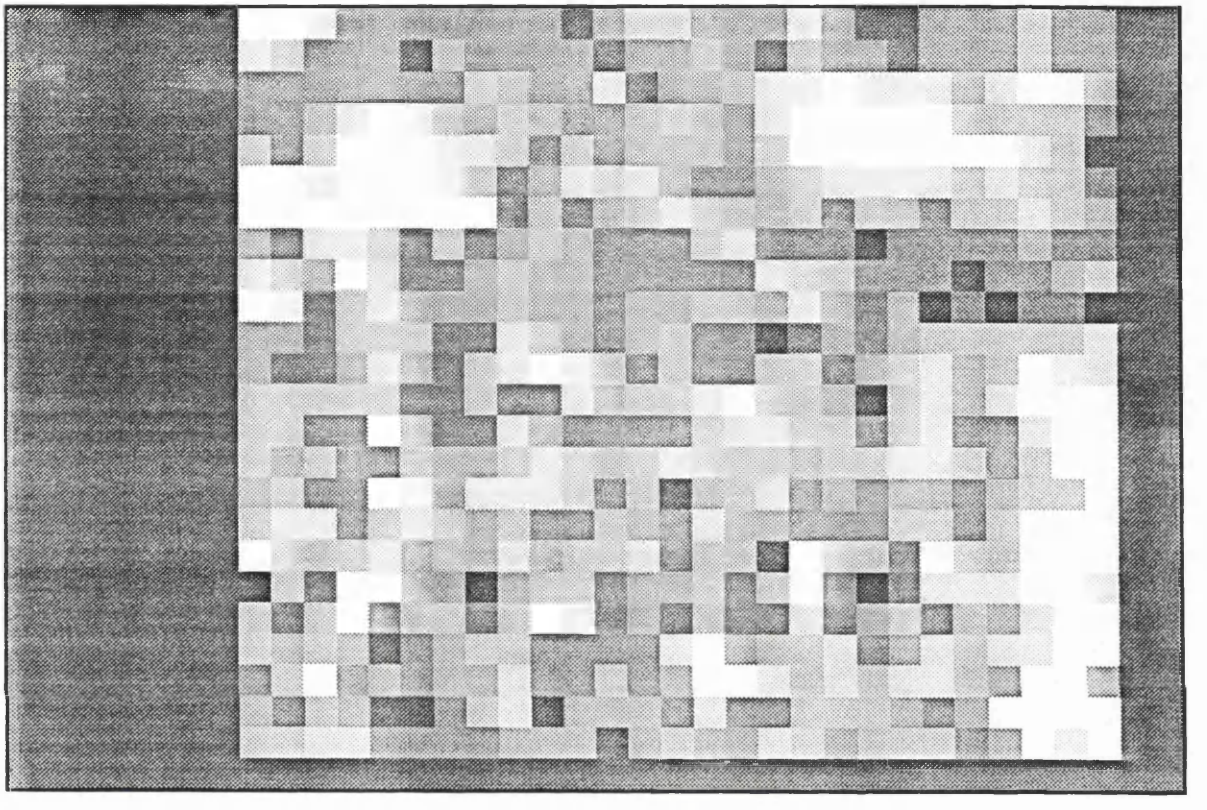

HEIGHT DIFFERENCES

(Not to scale)

Aerial photography and SPOT data comparison.
Height differences grouped in 5 groups for better visualisation.

Number of compared points			648	
0.00 m	-	8.40 m	239	points
8.40 m	-	14.40 m	110	points
14.40 m	-	26.70 m	140	points
26.70 m	-	42.00 m	77	points
above 42.00 m			82	points

White parts correspond to large errors, while the dark appearance in the compared area means height differences (errors) ≈ 0 (less than 0.50 m). The same dark appearance part at the three edges means that there are no aerial photography data for comparison.

Figure 5.9a. Remeasured 7th SPOT block. Errors grouped.

SAME SOURCE DATA COMPAR

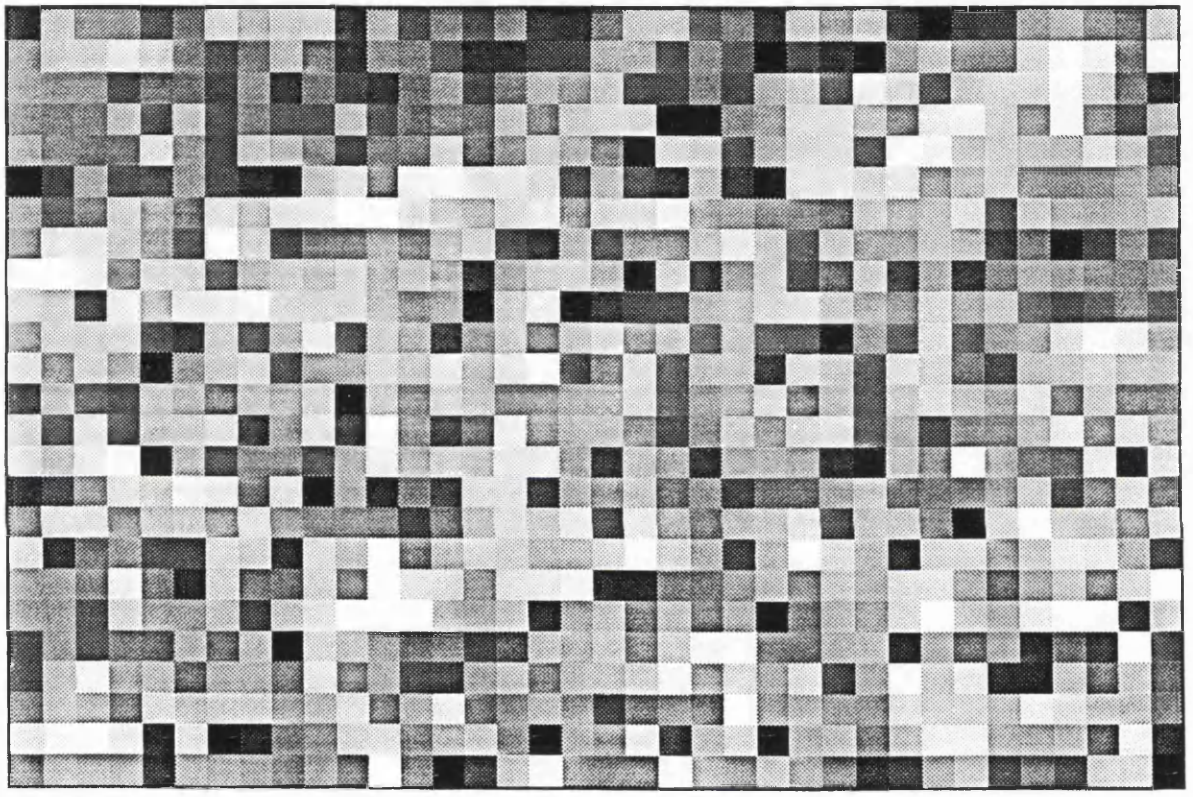

HEIGHT DIFFERENCES

(Not to scale)

Measured and remeasured data comparison.

White parts correspond to large errors, while dark appearance parts means height differences (errors) ≈ 0 (less than 0.50 m).

Figure 5.10. SPOT 7th DEM block. Errors ungrouped.

SAME SOURCE DATA COMPAR.

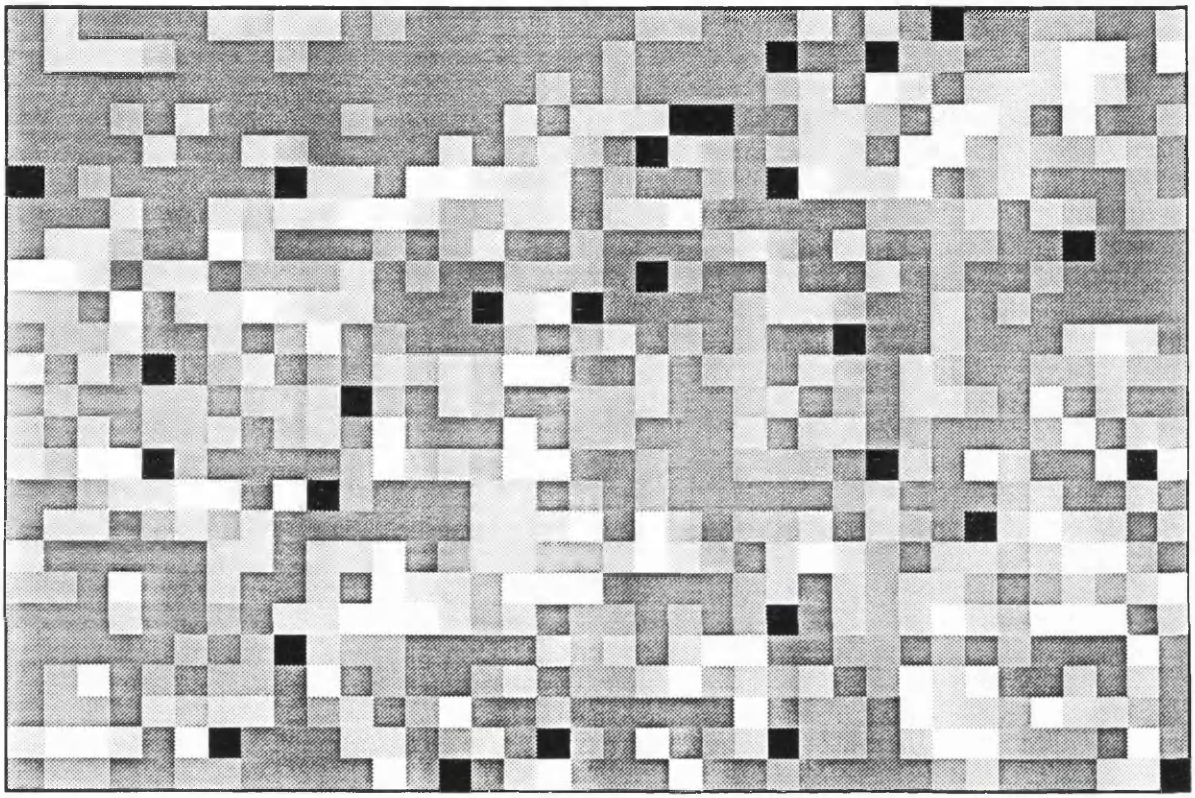

HEIGHT DIFFERENCES

(Not to scale)

Measured and remeasured data comparison.
Height differences grouped in 5 groups for better visualisation.

Number of compared points			900	
0.00 m	-	8.40 m	474	points
8.40 m	-	14.40 m	186	points
14.40 m	-	26.70 m	168	points
26.70 m	-	42.00 m	51	points
above 42.00 m			21	points

White parts correspond to large errors, while dark appearance parts means height differences (errors) ≈ 0 (less than 0.50 m).

Figure 5.10a. SPOT 7th DEM block. Errors grouped.

SAME SOURCE DATA COMPAR.

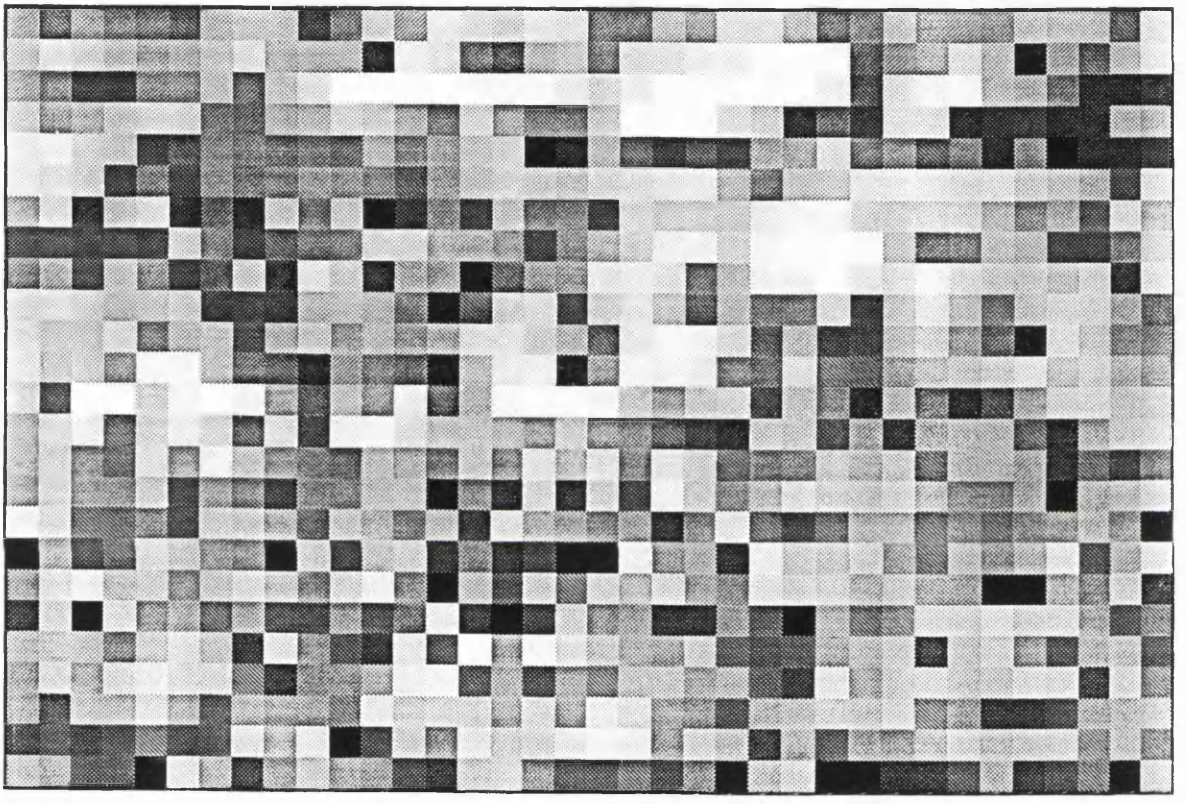

HEIGHT DIFFERENCES

(Not to scale)

Measured and remeasured data comparison.

White parts correspond to large errors, while dark appearance parts means height differences (errors) ≈ 0 (less than 0.50 m).

Figure 5.11. SPOT 11th DEM block. Errors ungrouped.

SAME SOURCE DATA COMPAR.

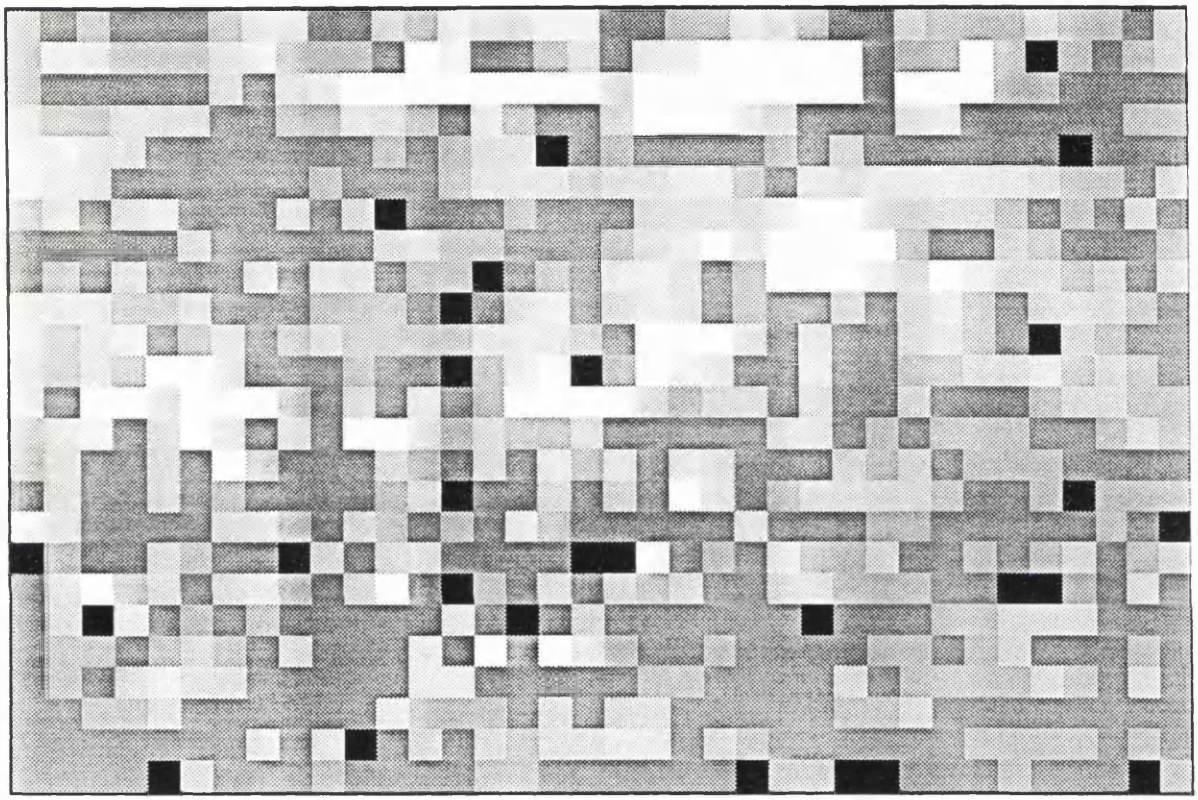

HEIGHT DIFFERENCES

(Not to scale)

Measured and remeasured data comparison.
Height differences grouped in 5 groups for better visualisation.

Number of compared points			900	
0.00 m	-	8.40 m	452	points
8.40 m	-	14.40 m	174	points
14.40 m	-	26.70 m	148	points
26.70 m	-	42.00 m	61	points
above 42.00 m			65	points

White parts correspond to large errors, while dark appearance parts means height differences (errors) ≈ 0 (less than 0.50 m).

Figure 5.11a. SPOT 11th DEM block.Errors grouped.

5.2.4.2.4. Program for pointwise comparison of the two sources of data.

A Pascal program CHECK.PAS was written in order to carry out the further statistical analysis. This is carried out by comparing a second source elevation point (SPOT) with the first source (aerial photography) four-neighbour elevations. The first source data are in a regular grid. Overlaying the two sources a second source point will lie in a grid cell surrounded by four first source elevation points. A simulated height (calculated height value) is estimated from the four-neighbour elevations derived from the aerial photography. This value is compared with the less accurately known height measured from SPOT. For more information about this program in pseudo - Pascal language see appendix B.

The above program aided the direct individual comparison of the elevation blocks derived from SPOT covering an area of 9 km^2 with the elevation blocks derived from the aerial photography covering (on average) 0.9 km^2. With this procedure a comparison of a small number of points is made. This was very helpful because the SPOT data were checked in small areas (patches) equivalent to the aerial photography derived blocks, so the statistical results refer to those small areas rather than in the whole SPOT derived block. The full statistical report provided by the program enabled erroneous points to be localised and certain conclusions (described later) to be drawn.

5.2.4.2.5. Partial comparison of DEM data from two sources.

Four out of sixteen SPOT DEM blocks were compared with the checking program (see appendix B). The check was made not all over the SPOT DEM, but partly in sub-blocks equivalent to the first source measured blocks (see § 5.2.4.2.4.). This partial comparison still can not give any information about the along- and across-track errors, because of the orientation of the test area in relation to the orientation of the scene.

SPOT DEM 1 : In the overlap area are 3 aerial photography derived DEM blocks (001, 002, 003) . 202 points out of 900 (22.4%) were compared.

SPOT DEM 2 : In the overlap area are 10 aerial photography derived DEM blocks (004, 005, 006, 006a, 007, 008, 009, 010, 011, 012). 565 points out of 900 (62.8%) were compared.

SPOT DEM 3 : In the overlap area are 9 aerial photography derived DEM blocks (012a, 013, 014, 015, 016, 017, 018, 019, 020). 572 points out of 900 (63.6%) were compared.

SPOT DEM 4 : In the overlap area are 4 aerial photography derived DEM blocks (021, 022, 023, 024). 260 points out of 900 (28.9%) were compared.

Slope and vegetation information is given after the statistical analysis for the interpretation of the results. Statistical analysis of slope and vegetation effects will be presented later (§ 5.2.4.2.6 and 5.2.4.2.7).

The first SPOT DEM gave the following overall statistical results (for the 24% overlapping area) : mean = -3.88 m and standard deviation = 10.52 m. These results appear acceptable.

In order to apply the height limits an average categorisation of the terrain was applied within the sub-block as follows:

1. DTM001.DAT. Flat terrain σ = 2.80 m, 3σ = 8.40 m.
2. DTM002.DAT. Flat terrain σ = 2.80 m, 3σ = 8.40 m.
3. DTM003.DAT. Gently rolling terrain σ = 4.80 m, 3σ = 14.40 m.

Taking further the sub-blocks statistical analysis it found negative mean values over all the sub-blocks as shown in table 5.5.

DEM SUBBLOCK	NUMBER OF COMPAR- POINTS	POINTS WITH HEIGHT_DIF >= LIMIT	AREA MEAN HEIGHT (m)		STATISTICAL RESULTS			
			FIRST SOURCE	SECOND SOURCE	OF ELEVATION DIF		OF ABSOLUTE ELEVATION DIF	
					MEAN(m)	SD(m)	MEAN(m)	SD(m)
001	50	13 (26%)	251.55	253.30	-1.75	9.09	7.14	12.77
002	77	28 (36%)	260.63	261.48	-0.85	10.35	8.47	13.97
003	75	25 (33%)	277.67	284.65	-6.98	11.04	11.31	21.47

Table 5.5. Partial comparison of first SPOT block and aerial photography data.

Regarding the slopes, 2/3 of the area has slopes <10% and 1/3 has slopes >50%. The vegetation coverage is 22% trees, 36% bushes and 42% uncultivated.

The second SPOT DEM gave the following overall statistical results (for the 72% overlapping area) : mean = +4.80 m and standard deviation = 16.18 m. It can be seen that there is a small positive bias in the mean.

In order to apply the height limits an average categorisation of the terrain was applied within the sub-block as follows:

DTM004.DAT, DTM005.DAT, DTM006.DAT, DTM006a.DAT, DTM007.DAT, DTM008.DAT and DTM009.DAT were classified as gently rolling terrain with σ = 4.80 m, so 3σ = 14.40 m.

DTM010.DAT, DTM011.DAT and DTM012.DAT were classified as semirough terrain with σ = 8.90 m, so 3σ = 26.70 m.

Taking further the sub-blocks statistical analysis it found a positive bias in some sub-blocks as shown in table 5.6.

DEM SUBBLOCK	NUMBER OF COMPAR POINTS	POINTS WITH – LIMIT >= HEIGHT_DIF >= LIMIT	AREA MEAN HEIGHT (m)		STATISTICAL RESULTS			
			FIRST SOURCE	SECOND SOURCE	OF ELEVATION DIF		OF ABSOLUTE ELEVATION DIF	
					MEAN(m)	SD(m)	MEAN(m)	SD(m)
004	78	6 (8%)	286.86	287.55	-0.69	8.87	6.89	11.71
005	50	7 (14%)	297.40	296.26	1.14	9.68	7.70	11.74
006	52	15 (29%)	306.82	300.58	6.24	17.39	12.11	18.37
006a	52	14 (27%)	297.15	285.60	11.56	23.91	16.04	24.33
007	50	14 (28%)	281.42	267.56	13.86	26.68	17.15	26.89
008	52	8 (15%)	273.86	270.27	3.60	10.76	8.31	11.77
009	77	14 (18%)	293.30	290.88	2.41	11.40	8.43	12.91
010	51	8 (16%)	326.48	316.80	9.67	22.26	14.23	22.73
011	78	4 (5%)	317.29	313.79	3.50	11.92	9.11	13.20
012	25	1 (4%)	330.79	326.96	3.83	10.56	8.68	11.66

Table 5.6. Partial comparison of second SPOT block and aerial photography data.

Regarding the slopes, 1/3 of the area has slopes <10% and 1/3 has slopes 10-50%. and 1/3 has slopes > 50%. The vegetation coverage is 56% trees, 19% bushes and 25% uncultivated.

The third SPOT DEM gave the following overall statistical results (for the 72% overlapping area) mean = -6.41 m and standard deviation = 14.43 m. These results appear acceptable.

In order to apply the height limits an average categorisation of the terrain

was applied within the sub-block as follows:

DTM012a.DAT, DTM013.DAT, DTM014.DAT, DTM015.DAT, DTM016.DAT, DTM017.DAT, DTM018.DAT, DTM019.DAT and DTM020.DAT were classified as semirough terrain σ = 8.90 m, so 3σ = 26.70 m.

Taking further the sub-blocks statistical analysis it found a strong negative bias in some sub-blocks in table 5.7.

DEM SUBBLOCK	NUMBER OF COMPAR POINTS	POINTS WITH – LIMIT >= HEIGHT_DIF >= LIMIT	AREA MEAN HEIGHT (m)		STATISTICAL RESULTS OF ELEVATION DIF		OF ABSOLUTE ELEVATION DIF	
			FIRST SOURCE	SECOND SOURCE	MEAN(m)	SD(m)	MEAN(m)	SD(m)
012a	26	1 (4%)	341.93	350.12	-8.18	10.65	11.10	22.37
013	52	0 (0%)	388.60	397.88	-9.29	9.93	11.93	23.62
014	130	8 (6%)	408.37	412.39	-4.02	13.66	11.15	20.45
015	52	4 (8%)	397.10	398.17	-1.07	14.66	11.96	19.70
016	52	0 (0%)	379.04	382.65	-3.61	6.28	5.67	11.28
017	78	7 (9%)	388.57	386.73	1.84	16.55	13.49	20.28
018	52	10 (19%)	379.41	381.73	-2.32	20.65	16.88	28.33
019	52	2 (4%)	368.40	380.85	-12.45	10.46	13.79	28.49
020	78	11 (14%)	379.62	393.88	-14.26	11.51	15.45	32.04

Table 5.7. Partial comparison of third SPOT block and aerial photography data.

Regarding the slopes, 1/4 of the area has slopes <10% and 1/3 has slopes 10-50%. and more than 1/3 has slopes > 50%. The vegetation coverage is 63% trees, 11% bushes and 26% uncultivated.

The fourth SPOT DEM gave the following overall statistical results (for the 30% overlapping area) : mean = 3.55 m and standard deviation = 15.81 m. The Mean value overall for the block is small but if we look through the sub-blocks we can see positive and negative bias which give finally a small overall mean.

In order to apply the height limits an average categorisation of the terrain was applied within the sub-block as follows:

1. DTM021.DAT, DTM022.DAT, DTM023.DAT.and DTM024.DAT were classified as semirough terrain σ = 8.90 m, so 3σ = 26.70 m.

Taking further the sub-blocks statistical analysis it found a strong negative bias over all the sub-blocks as shown in table 5.8.

DEM SUBBLOCK	NUMBER OF COMPAR POINTS	POINTS WITH LIMIT >= HEIGHT_DIF >= LIMIT	AREA MEAN HEIGHT (m)		STATISTICAL RESULTS			
			FIRST SOURCE	SECOND SOURCE	OF ELEVATION DIF		OF ABSOLUTE ELEVATION DIF	
					MEAN(m)	SD(m)	MEAN(m)	SD(m)
021	52	4 (8%)	389.46	393.33	-3.87	10.72	9.74	17.42
022	52	3 (7%)	400.31	405.46	-5.15	10.43	9.64	18.21
023	78	4 (5%)	428.88	423.01	5.87	19.48	14.37	21.28
024	78	0 (0%)	477.72	465.41	12.31	13.69	13.99	13.80

Table 5.8. Partial comparison of fourth SPOT block and aerial photography data.

Regarding the slopes, 1/5 of the area has slopes <10% and 4/5 has slopes > 50%. The vegetation coverage is 72% trees, 9% bushes and 19% uncultivated.

From the partial data comparison above presented we can see that the systematic error appear to be random, changing magnitude and sign from one strip to the other. The main reason is not easy to see, because of the several sources of error which are involved in the image recording procedure (see § 3.4.1.2).

5.2.4.2.6. The slope effect.

The terrain type and surface structure of the terrain is a very important factor which affects the accuracy of the photogrammetric measurements. All the researchers chose their test area to include all the relief peculiarities or consider different terrain areas, in order that their results be general and representative. eg. Ackermann (1979) represented the DEM accuracy as a function of ground slope (see § 7.5).

In this test one of the SPOT DEM blocks ie. the third DEM was chosen randomly (mean = -6.41 m standard deviation = 14.43 m). Then a further examination of some of the aerial photography derived DEM sub-blocks (with both

larger and smaller mean values) was carried out. Finally slopes in the aerial photography sub-blocks are extracted from 1:25,000 maps. These results are presented together in the following table (table 5.9):

DEM SUBBLOCK	MEAN (m)	SD (m)	SLOP.ES Range	SLOP.ES %	DEM SUBBLOCK	MEAN (m)	SD (m)	SLOP.ES Range	SLOP.ES %
012a	-8.18	10.65	10%	15	015	-1.07	14.66	10%	15
			10 - 50%	60				10 - 50%	27
			>50%	40				>50%	58
019	-12.45	10.46	10%	67	017	1.84	16.55	10%	22
			10 - 50%	23				10 - 50%	23
			>50%	10				>50%	45
020	-1426	11.51	10%	39	018	-2.32	20.65	10%	32
			10 - 50%	23				10 - 50%	28
			>50%	28				>50%	40

Table 5.9. Examination of the slope effect on the measurements.

From table 5.9 we can see that when the mean value is small a deterioration of SD occurs.

Comparing the mean and standard deviation values of the left DEM sub-blocks (with small systematic errors) with the right DEM sub-blocks (larger systematic errors which have a random appearance), we can see that slopes are not correlated with the systematic bias and shifted standard deviation. This happens because of the random distribution and magnitude of the systematic error which do not allow the further examination of the systematic error introduced by the slope.

5.2.4.2.7. The vegetation effect.

The "bald earth" problem is a significant problem in the photogrammetric

production of DEM's. The DEM should be representative of the land surface after removal of natural growth and manmade cultural features. Any such cover does not always allow the elevation of the ground to be measured. For example an elevation profiling scenario in an analytical plotter may well pass through an isolated tree, but will probably lose its ability to "see" the ground in a dense forest area, and the resultant DEM will probably have a portion of the tree height combined with the ground elevation. The inability to see the "bald earth" needs to be considered in all DEM accuracy estimates.

Leupin & Cherkaoui (1980) studied the vegetation effect (tree effect) in an automatically generated DEM. The DEM generated from a Gestalt Photomapper (GPM-2), which produces a dense grid - based DEM (a point every 7 m) on 1:40,000 photographs. A stereopair of the same area (in Canada) at scale 1:15,000 was set up on a WILD A7 and 400 points were plotted.

The frequency distribution of the estimated Δz values (for the 400 points) showed a systematic effect, due to a large overrepresentation of positive values. This was to be expected as all zones covered with forest must more or less show a Δz in the magnitude of the trees. Moreover an investigation of the three largest negative values found showed that all three points were on a topographical break-line and that a small difference in the planimetric position could easily lead to such differences.

Comparing the two DEMs in forest areas showed a regular Δz difference in the order of a mean tree height. It was as if the GPM-2 treated the tree-surface as ground level assuming a relatively dense and uniform tree population. In order to estimate the tree effect all the points in forested areas were picked out and underwent separate treatment. Moreover, different profiles were selected to help determine the z shift due to the trees. A "tree correction" was applied based on statistical data on mean tree heights.

The vegetation coverage is a very important factor in the accuracy of the elevations. DEMs produced on the GPM-2 at a 1:40,000 photo scale are for the sole use of the 1:50,000 topographical map in Canada. In forest areas where the

"tree correction" can be applied the resulting DEM can be used to produce maps for topographical use, at larger scales than 1:50,000 up to 1:20,000 (Leupin & Cherkaoui, 1980).

Again in the test of the vegetation effect the third DEM was chosen randomly (mean = -6.41 m, standard deviation = 14.43 m). Then a further examination of some of the contained aerial photography derived DEM sub-blocks (which show both the larger and the smaller mean values) was carried out. The ground vegetation coverage extraction is shown in table 5.10:

DEM SUBBLOCK	MEAN (m)	SD (m)	Vegetation Kind	Vegetation %	DEM SUBBLOCK	MEAN (m)	SD (m)	Vegetation Kind	Vegetation %
012a	-8.18	10.65	Tree Bush	87 13	015	-1.07	14.66	Tree Bush Uncult.	76 10 14
019	-12.45	10.46	Tree Bush Uncult.	27 10 63	017	1.84	16.55	Tree Bush Uncult.	77 1 22
020	-14.26	11.51	Tree Bush Uncult.	63 9 28	018	-2.32	20.65	Tree Bush Uncult.	80 2 18

Table 5.10. Examination of the vegetation effect on the measurements.

Comparing the left DEM sub-blocks mean and standard deviation values (with small systematic error effect) with the right DEM sub-blocks (larger systematic error effect which has a random appearance), we can see that vegetation coverage does not seem to affect the measurements. This happened because the reference elevation matrix measurements ("ground truth") were carried out on the top of tree canopy where it was present rather than attempting to estimate ground elevation. The SPOT elevation matrix measurements were carried out in the same way. So the only estimation from the results presented in

the table 5.10 is left only to the variation on the tree height. It is easy to see the tree-height variation on the aerial photography at 1:30,000, while in the SPOT images it is not possible. Trees appear on a SPOT image like a "cloud" covering the terrain surface. However, the random distribution of the significant systematic error does not allow the further examination of the systematic error introduced from the vegetation coverage.

So there is another stronger source(s) apart from slope and vegetation that affects the measurements accuracy, causes systematic error and shift the standard deviation value. Some of these sources could be the image physical quality and the illumination (shadowed parts due to object orientation and sun angle, or due to ground characteristics, ie steep-sided valleys).

5.2.4.2.8. Off-line correction to observations.

The off-line correction is a method of correcting systematic effects in the observations in photogrammetry. It can be done by correcting the observations and replacing them with a new set of values (correction to the observations). Observations , once made, should not on any account be changed and the expression is thus seen to be an invitation to carry out an illegitimate operation (Thompson, 1976).

The data captured from SPOT were found to have a systematic bias the magnitude of which is known after the application of the data checking procedure. The following table 5.11. shows the original statistical analysis results before applying the off-line correction:

DEM BLOCK	NUMBER OF COMPAR- POINTS	POINTS WITH LIMIT >= HEIGHT_DIF >= LIMIT	AREA MEAN HEIGHT (m)		STATISTICAL RESULTS OF ELEVATION DIF		OF ABSOLUTE ELEVATION DIF	
			FIRST SOURCE	SECOND SOURCE	MEAN(m)	SD(m)	MEAN(m)	SD(m)
2	640	128	299.29	294.22	4.80	16.18	10.48	22.47
6	664	52	523.45	519.27	4.35	18.95	11.79	25.50
7	648	116	557.33	539.57	16.03	23.16	21.24	45.48

Table 5.11. Statistical analysis results before applying off-line correction.

In order to apply the height limits an average categorisation of the terrain within the sub-blocks was applied as follows:

1. 2nd block. Gently rolling terrain σ = 4.80 m, 3σ = 14.40 m.
2. 6th block. Semirough terrain σ = 8.90 m, 3σ = 26.70 m.
3. 7th block Very rough and steep terrain σ = 14.00 m, 3σ = 42.00 m.

The elevation data were filtered from the systematic error, by adding the opposite sign to the mean height values, so the SPOT data mean height level becomes the same as the aerial photography data mean height level. A Pascal program is written to apply this procedure. The SPOT data were checked again in reference to the aerial photography data. Table 5.12. shows the statistical analysis result after the off-line correction to the data:

DEM BLOCK	NUMBER OF COMPAR- POINTS	POINTS WITH LIMIT >= HEIGHT_DIF >= LIMIT	AREA MEAN HEIGHT (m)		STATISTICAL RESULTS OF ELEVATION DIF		OF ABSOLUTE ELEVATION DIF	
			FIRST SOURCE	SECOND SOURCE	MEAN(m)	SD(m)	MEAN(m)	SD(m)
2	640	144	299.29	299.29	0.00	16.20	11.20	19.70
6	664	51	523.45	523.45	0.00	19.86	12.36	23.40
7	648	71	557.33	557.33	0.00	23.35	17.42	29.14

Table 5.12. Statistical analysis results after off-line correction.

The assumption of applying off-line correction equal to the estimated mean in each block (25 rows x 36 columns) did not work, as we can see from tables 5.11 and 5.12. This was expected because of the "random" appearance of the systematic error in the SPOT data, even in the same row of data.

Examining further the number of erroneous points, which appear before and after the off-line correction, we can see the effect of the off-line correction. The number of the erroneous points before and after the off-line correction is presented in table 5.13.

DEM BLOCK	ORIGINAL DATA		AFTER OFF-LINE CORREC.		SYSTEMATIC ERROR (AVERAGE) (m)
	POINTS WITH -LIMIT >= HEIGHT_DIF >= LIMIT	POINTS WITH -40m >= HEIGHT_DIF >= 40m	POINTS WITH -LIMIT >= HEIGHT_DIF >= LIMIT	POINTS WITH -40m >= HEIGHT_DIF >= 40m	
2	128	26	144	23	-4.80
6	52	23	51	18	-4.35
7	116	91	71	53	-16.03

Table 5.13. Number of erroneous points before and after off-line correction.

In the second and sixth block the number of erroneous points do not change. This happened because the applied correction is less than the actual measurement accuracy. In the seventh block the results became better because of the large correction.

It has been decided not to apply the off-line correction to the observations, or more specifically to the height values. There are two reasons for this assumption. The "random appearance" of the systematic error and the generality of the work, because in the production the mean height value of a set of data is not usually known.

5.2.4.2.9. Comparison of statistical results between the project and the experienced operator measured DEM blocks.

Blocks numbered 6, 7, and 11, which showed the stronger systematic errors and the greater standard deviations were remeasured again by the experienced operator. These blocks are located in the very rough and steep terrain area of the Montagne Sainte Victoire. Moreover illumination, atmospheric conditions and problems related to the terrain steepness make the measurements a difficult task.

The same comparison procedure was followed. The comparison of statistical results between the project operator and the experienced operator is shown in table 5.14.

DEM BLOCK	NUMBER OF COMPARED POINTS	PROJECT OPERATOR		EXPERIENCED OPER.	
		MEAN (m)	SD (m)	MEAN (m)	SD (m)
6	708	4.35	18.95	8.58	12.36
7	708	16.03	23.16	10.08	18.02
11	708	11.78	24.88	6.14	16.83
Overall values	2124	10.72	22.46	8.27	15.92

Table 5.14. Comparison of statistical results between the project and the experienced operator.

As we can see the standard deviation value is decreased (better measurements), while the mean value retained a systematic bias. If we substitute the new values recorded by the experienced operator, the overall data statistical values become:

mean= 2.18 m; standard deviation=13.13 m and absolute mean= 5.39 m.

The line scattering diagram of all the height differences of the 2056 compared points estimated from the experienced operator measurements is presented in figure 5.12. The class interval is every 4 m.

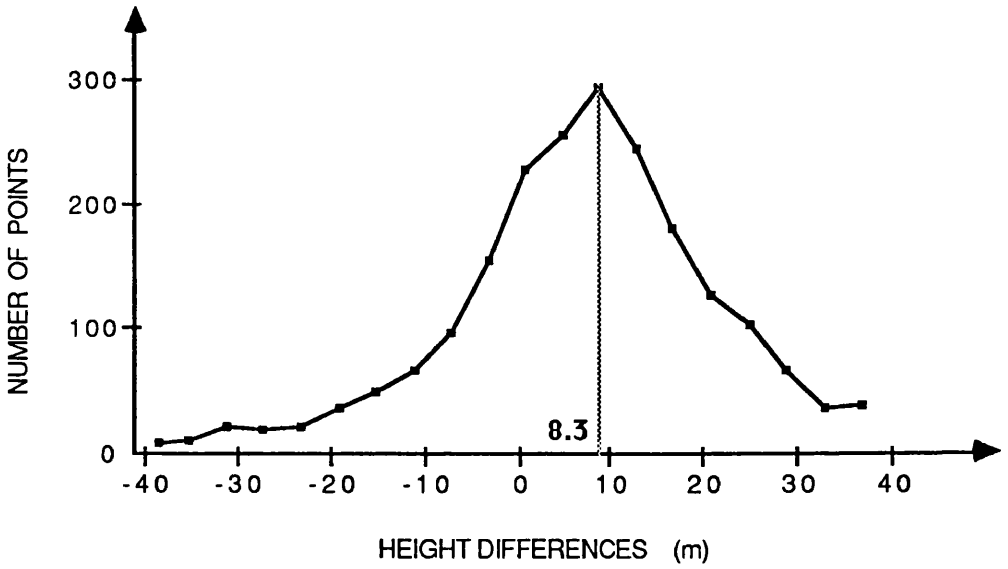

Fig. 5.12. Scattering diagram of height differences of the experienced operator measurements.

This diagram does not include the points in which the height differences were found to be greater than 2.7*(SD of height differences). The number of those

points is estimated to be 68 points in a total of 2124 points, or 3.20 %. In the above diagram we can see that the observations follow the normal distribution law. In these blocks, which cover a very rough and steep area, there is a strong positive shift of 8.27 m in the estimated height differences as we can see from the estimated mean value and the above diagram.

5.2.4.3. SPOT measurements on a second stereopair.

The second SPOT model was set up on a DSR1 analytical plotter. The 15 control points were used in order to define the orientations of the sensors. The exterior orientation R.M.S vector error on the ground control points was 7.80 m (accuracy of the model set up is described in more detail in § 4.2.2).

Six digital elevation matrix blocks were measured (5,400 points), in a normal grid with 100 m grid interval.

The SPOT elevation data were compared again with the independently measured dense grid elevation matrix derived from underflight photographs. The comparison was done with the use of the Pascal checking program (details of the program are given in the appendix B).

The derived statistical results from the compared heights, are given in the table 5.15.

DATA SET	NUMBER OF COMPARED POINTS	MEAN (m)	SD (m)	MINIMUM - MAXIMUM ELEVATION DIFFERENCES		AVERAGE SLOPE (%)
1	177	-3.76	6.90	-17.84	18.08	26.1
2	640	4.17	10.77	-26.65	58.53	35.5
3	650	4.88	10.67	-37.90	42.62	41.7
5	157	-6.25	7.49	-46.94	11.14	30.3
6	664	0.09	12.22	-95.64	55.98	43.3
7	648	9.75	18.12	-29.86	82.57	64.6

Table 5.15. Aerial photography and second SPOT pair elevation data comparison.

The overall statistical values of the new data sets (6 blocks) are:

mean= +3.60 m; standard deviation=12.75 m and absolute mean= 10.00 m, in the area with an average slope 40.3%.

The line scattering diagram of all the height differences of the 2886 compared points estimated from the first and second measurements is presented in figure 5.13. The class interval is every 4 m.

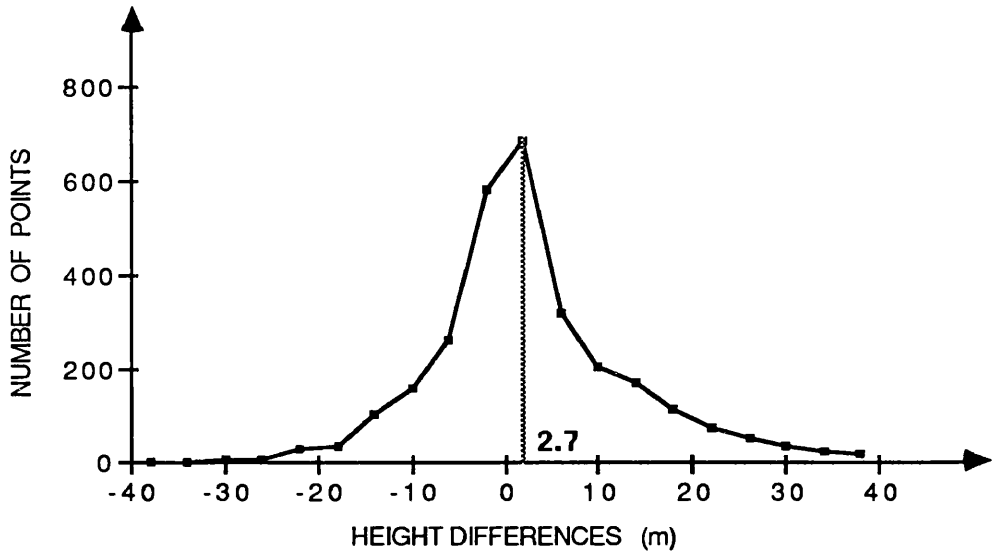

Fig. 5.13. Scattering diagram of height differences in the second SPOT hardcopy measurements.

This diagram does not include the points in which the height differences were found to be greater than 2.7*(standard deviation of height differences). The number of those points is estimated to be 50 points in a total of 2936 points, or 1.70 %. In the above diagram we can see that the observations follow the normal distribution law.

The mean and standard deviation of the height differences for the first and second SPOT stereopair, of the 6 data sets, are given together in table 5.16.

DATA SET	FIRST SPOT STEREOPAIR		SECOND SPOT STEREOPAIR	
	MEAN (m)	SD (m)	MEAN (m)	SD (m)
1	-3.88	10.52	-3.76	6.90
2	4.80	16.18	4.17	10.77
3	-6.41	14.43	4.88	10.67
5	-3.81	8.89	-6.25	7.49
6	4.35	18.85	0.09	12.22
7	16.03	28.17	9.75	18.12

Table 5.16. Statistical results of the first and second SPOT stereopair.

From table 5.16. we can see that the changes in the means are not so great. However, there is a correlation between the two data sets mean values. We calculate the correlation coefficient ρ_{12} which is defined as: Linear correlation $\rho_{12} = (\sigma_{12} / \sigma_1 * \sigma_2)$,where: σ_{12} is the covariance between the groups mean1 and mean2, σ_1 is the standard deviation of the group mean1 and σ_2 is the standard deviation of the group mean2. The ρ_{12} is calculated to be 0.67.

Because this value lies within the empirical limit $0.35 < | \rho_{12} | < 0.75$, (Nassar, 1985, page 23), we can say that the two different SPOT stereopair derived mean values are positively significantly correlated (Cooper, 1974, page 19).

Comparing the new 6 data sets derived values with the same original test (6 data sets) values (mean = 4.14 m, standard deviation= 17.83 m) we can see that the standard deviation value of the new measurements became much better (30% better). This happened because:

the quality of the second pair of SPOT images is better (no atmospheric effects, or strong shadowed parts) than the first.

the second SPOT stereopair was set up with better control (33% more GCPs) with one control point lying in the test area.

5.2.4.4. Error display.

The relative position of the aerial photography and SPOT captured digital

elevation blocks appear in figure 5.14. All the available data, were not statistically further processed because of the limited amount of the computer space that was available (disc quota) and because the processed results were sufficient in number and representative enough, to get the right results and conclusions. The aerial photography data were scattered in many files. So the overall data processing was problematic.

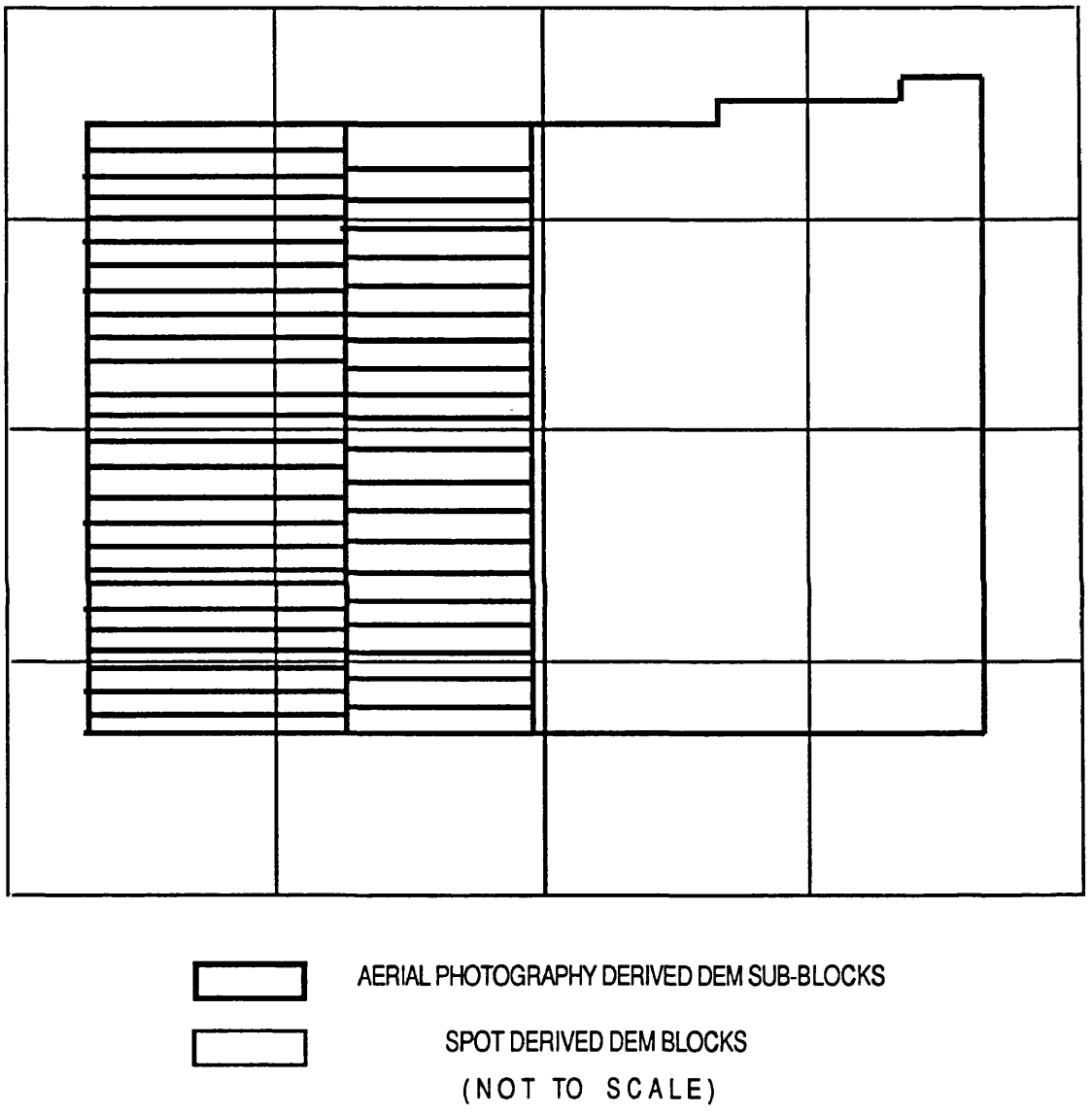

Figure 5.14. Relative position of the aerial photography and SPOT digital elevation data that were used in the further statistical analysis project.

A Pascal program (JOIN1.PAS) integrated the aerial photography derived DEM sub-blocks, approximately corresponding to the area of the SPOT derived DEM block, without destroying the normality of the data matrix. With the

application of the JOIN1.PAS program eight digital elevation blocks were created as shown in figure 5.15.

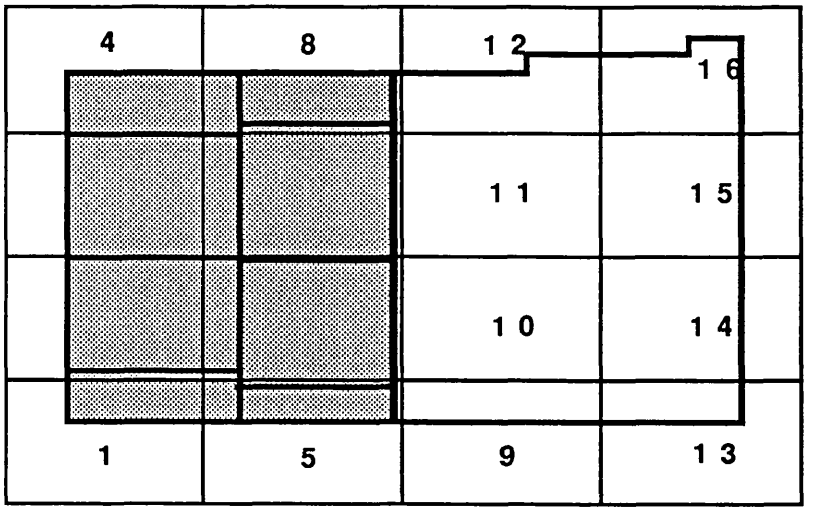

——— SPOT derived grid elevation blocks
——— Aerial photography derived grid elevation blocks.

(Not to scale)

Figure 5.15. Showing relative position of aerial photography derived blocks and SPOT derived blocks.

Each of these sets of data (from aerial photographs and from SPOT) were then regarded as one block of data as shown in figure 5.16.

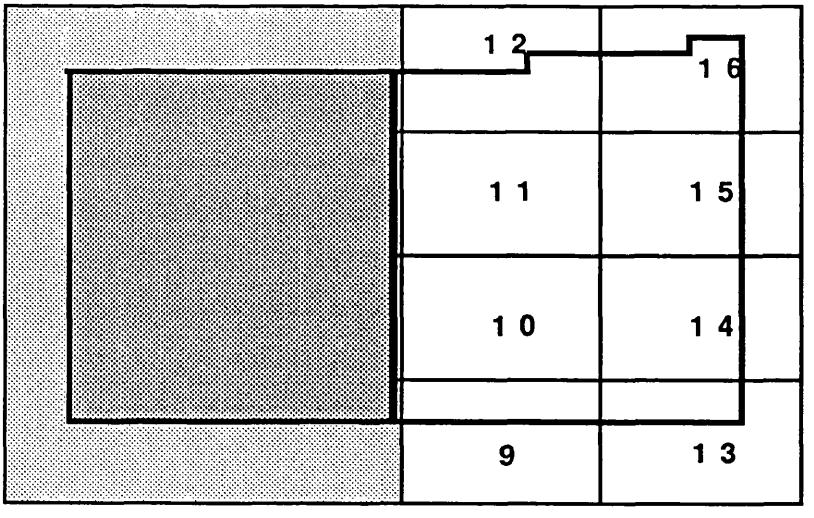

——— SPOT derived grid elevation blocks
——— Aerial photography derived grid elevation blocks.

(Not to scale)

Figure 5.16. Showing the 2 sets of integrated data.

This was useful because the CHECK.PAS program was applied directly on a large number of data derived from the two sources. The program except of pointing out the erroneous points, which have -limit >= height differences >= limit (where limit is the user specified limit 3 * standard deviation), gives all the calculated height differences values. The magnitude of the height differences indicate the amount of error included in the observations. These values are written to an output file in row, columns, height differences format.

This output file was created by the VAX the Fortran language EX1.FOR program, linked with the EX2.FOR, DEM_IO.FOR subroutines and the LSL$LIBRARY package which converted the digital elevation matrix from ASCII form to DTI (digital terrain image) form. Because the DTI files can be used as an input to the Laser-Scan ROVER module, and displayed as an image on the graphics screen, the resulting height differences (errors) (in DTI form) could be displayed.

The program offers the following facilities during the creation of the DTI file:

1. To categorise the above values (height differences) in up to 10 groups. In this work were used 5 groups or categories (same as the estimated height limits), as follows:

Group 1 :	Height differences	from	0	to	8.40	m
Group 2 :	Height differences	from	8.40	to	14.40	m
Group 3 :	Height differences	from	14.40	to	26.70	m
Group 4 :	Height differences	from	26.70	to	42.00	m
Group 5 :	Height differences	above	42.00	m		

The same routine gives also the total number of compared points and the number of points included in each category.

2. To convert the rows, columns, and the actual values of height differences from ASCII to DTI form.

The two DTI output files which are created can be displayed on the VAX/VMS graphical screen. A colour legend shows the grouped height differences according to their range, or the height differences according to their actual value.

The program was used for displaying the DEM individually and joined together. Figures 5.17 and 5.18, represent the height differences (errors) which correspond to the joined area shown in figure 5.16.

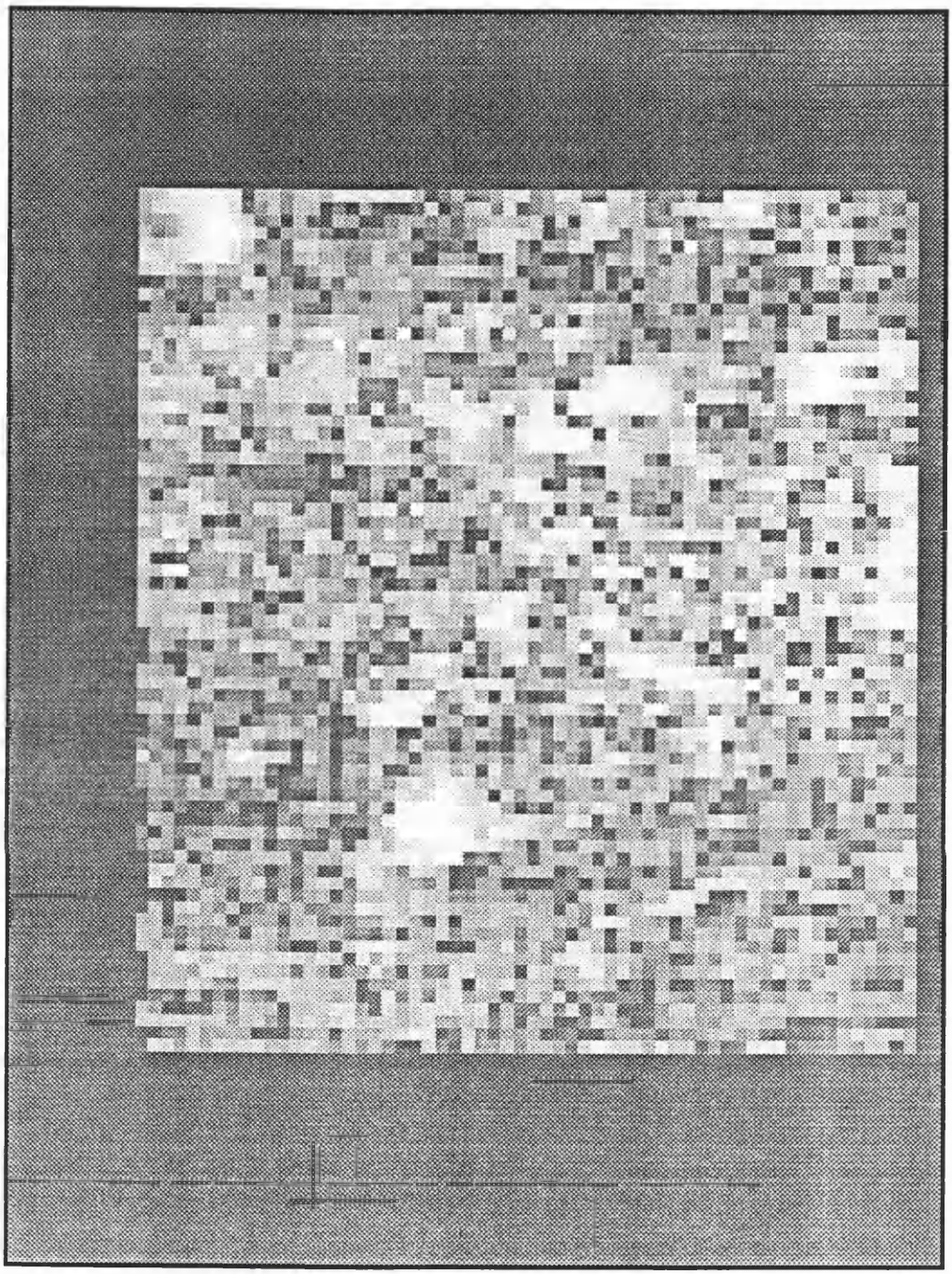

(Not to scale)

Aerial photography and SPOT data comparison of half of the area (4071 points).

White parts correspond to large errors, while the dark appearance in the compared area means height differences (errors) ≈ 0 (less than 0.50 m). The same dark appearance part at the three edges means that there are no aerial photography data for comparison.

Figure 5.17. Height differences (errors) from the comparison of the two sources elevation data. Errors ungrouped.

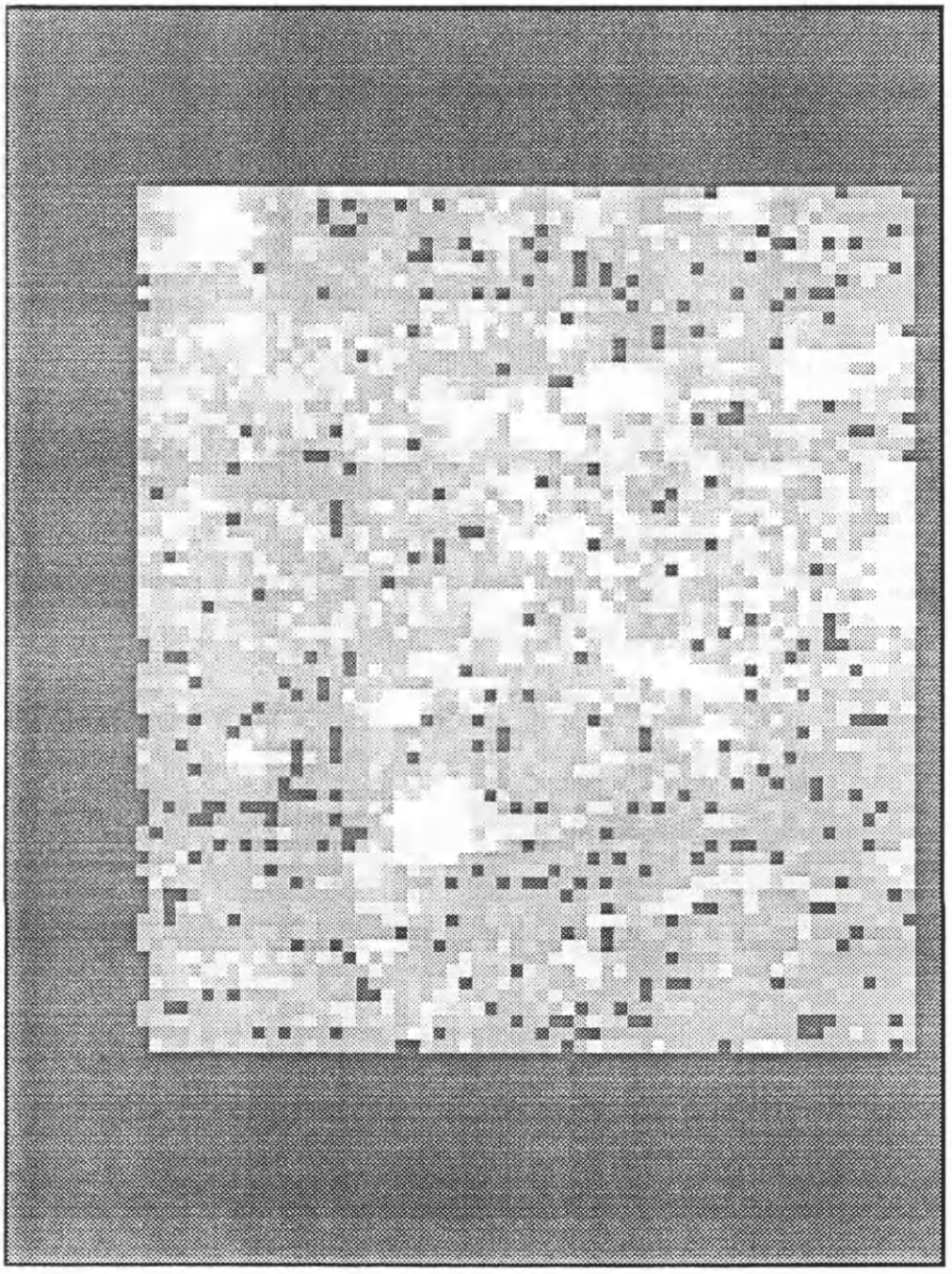

(Not to scale)

Aerial photography and SPOT data comparison of half of the area.
Height differences grouped in 5 groups for better visualisation.

Number of compared points			4071	
0.00 m	-	8.40 m	2069	points
8.40 m	-	14.40 m	850	points
14.40 m	-	26.70 m	715	points
26.70 m	-	42.00 m	267	points
above 42.00 m			170	points

White parts correspond to large errors, while the dark appearance in the compared area means height differences (errors) ≈ 0 (less than 0.50 m). The same dark appearance part at the three edges means that there are no aerial photography data for comparison.

Figure 5.18. Height differences (errors) from the comparison of the two sources elevation data. Errors grouped errors.

From this output the user can see the position of the problematic points or areas in relation with the map.

5.2.4.5. Discussion.

At the beginning of this section it is useful to present how Rosenholm (1986) described the systematic effect on the elevations. Systematic effect could well be caused mainly by the radiometric characteristics of SPOT images. Unlike normal photographs, the stereo SPOT images were not taken at the same moment. Therefore the same areas (especially hardwood and agricultural areas) could have different radiometric characteristics due to different observation angles and sun angles at these two times. This fact has caused peculiar radiometric effects on the grey levels of these areas. A piece of land which is totally black in the left image may give a very bright response in the right image. These factors could possibly have caused systematic mis-positioning of the measuring mark.

Sources of error involved during the image recording procedure are examined in § 3.4.1.2. In the following section the sources of error in the height measurements of the SPOT stereoimage are examined, using the statistical analysis program. The results of this analysis mainly concern the first SPOT hard copy pair which was more problematic. The results of this analysis are as follows:

1. *Image (physical) quality.*

Some parts of the image are not well illuminated. The possible reason is the sun angle (time that the images are recorded) and the satellite attitude with respect to the sun. SPOT images are convergent images, so the sun angle becomes more critical. This causes problems not only to the shadowed part of the mountains but also along valleys. It is a fact that the two DEM blocks (number 7 and 11) with the larger bias and standard deviation value are located in the shadow of the northern part of Montagne Sainte Victoire.

2. *Human operator error.*

The operator interprets problematical part of the model in different ways. From the further data statistical analysis it was found that the operator had

difficulty in the problematic parts of the model and only under certain circumstances. The project operator had difficulties in 'finding the ground' in several instances. Surfaces with a very dark appearance are difficult to height accurately. Steep-sided valleys often seem to be almost bottomless to the observer.

The operator had the tendency of setting the floating mark over the ground in the dark parts of gently sloping areas (particularly in areas of high vegetation cover and deep shadow, which have a very dark appearance), and also had the tendency of setting the floating mark deep in the ground in very steep areas with dense vegetation cover. In the strongly lit and rough areas the operator had the tendency of setting the floating mark deep below the 'ground' surface level. This becomes more critical in the measurements of the rough south part of Montagne Sainte Victoire which is over-illuminated.

The operator made use of the DSR 1 analytical plotter function of driving to a point when the spatial coordinates are given. The erroneous points and their differences in height - magnitude were known (pointed out from the two sources comparison procedure). So it was easy to revisit the exact position and to set the floating mark in the 'true' estimated position. With this procedure the operator revisited, remeasured and reexamined the height value and particularly the reasons which led him to make the mistake.

The experience of project operator was another factor which was examined during this project. In terms of interpretating the systematic error the overall mean value is misleading (§ 5.2.1). Statistics do not give good interpretation of the phenomenon because of the "random" appearance of the systematic error. This was proved with the further statistical analysis which followed (§ 5.2.4.2.5). It is also proved that the operator is not the source of the systematic error. This does mean of course that operator experience is not an important factor - because the operator does not usually measure at one instant with say a accuracy and the next time with $a/2$ accuracy - under the same conditions it follows that the "random" appearance of the systematic error cannot be attributed to the operator. The same can be assumed in regard to operator fatigue. Moreover the observer's ability test (§ 5.2.4.2.2), in which parts of four DEM blocks were measured gave very reasonable results (low mean differences and the standard deviation values

correlated with the terrain roughness). In addition the remeasurement of the DEM blocks with big systematic bias procedure (§ 5.2.4.2.3), gave the same statistical values in the one, while in the other appears a deterioration to the results. However, the entire procedure indicates that the operator appears to have more or less a constant performance.

Finally the experienced operator measured 3 DEM blocks (§ 5.2.4.2.8) and the comparison of statistical results between the project and the experienced operator showed that the standard deviation decreased (indicates better measurements), while a systematic bias remained in the mean value.

3. *Atmospheric conditions.*

Haze which is in evidence in one image caused problems. The project operator, after the two data set comparison, knows the coordinates of the erroneous points and the height difference values of those points (pointed out from the checking program). The Kern DSR1 has the facility to drive to a point if the coordinates of this point are input from the terminal. After this check it was found that the gross errors occurred in areas that were affected by the haze.

The project operator tried not to skip any point during the data capturing procedure. The idea proved not very good because the uncertainty in the SPOT observations gave totally wrong height measurements. This idea was followed in the parts which were covered by clouds (in one scene). In the cloud covered area it is difficult to have a good impression of relief not only for the observing point, but also for areas obscured by cloud shadow on one of the two images.

Comparing the derived values (6 data sets) using the second SPOT hardcopy (§ 5.2.4.3.) with the same original test values, we can see that the standard deviation value of the new measurements became improved by 30%. This was because the second SPOT image quality is better (no atmospheric effects - haze, clouds -, or strong shadowed parts) than the original one.

4. *Vegetation.*

Another source of error is in areas of high vegetation (forests). Tests with a helicopter - borne laser profiler indicated that in an area of trees varying from 10 m to 15 m tall the DEM surface was biased high by 2.4 metres with a standard

deviation about that mean of 1.8 metres (Toomey, 1986).

The vegetation coverage, in a model formed from aerial photography appeared and was interpreted in a different way than in a model derived from SPOT imagery. In the aerial photography derived model the operator can see the height variation of the trees. In SPOT images derived model the vegetation gives the impression of a 'cloud' covering the area.

The slope and vegetation effect test (§ 5.2.4.2.6) showed that slopes seem to have no effect on the systematic bias (because of the systematic error appearance). The same conclusion we can get from the examination of the ground coverage. This was because of the random distribution and magnitude of the systematic error, which do not allow the further examination of the systematic error introduced by the slope and vegetation coverage.

5. *Relief.*

The relief is a very important factor in the measurement accuracy. From table 5.1. we can see that some blocks contain very rough and steep areas. In the rough and steep parts very bad illumination conditions were found. The southern part of the Montagne Sainte Victoire is over - illuminated, while the northern part is badly illuminated with dense vegetation covers.

In the second SPOT hardcopy measurements on a second pair test, (the results are shown in tables 5.15 and 5.16) we can see that there is a significant correlation between the mean values of the two data sets. This leads to the conclusion that the relief is a possible factor in the systematic error appearance.

5.2.4.6. Conclusions.

These tests show that SPOT has, with relaxed and acceptable specifications, the potential for providing data for topographic mapping. The accuracy necessary for mapping at 1:50,000 scale with 20 m contours is attainable and if the image quality and ground control are very good then 1:25,000 scale plotting also is possible (DEM interpolation and interpolation contouring errors are not included into this assessment).

It has been shown that when observing a DEM there are significant systematic errors. An analysis showed that these errors are due to factors such as the difficulty of the operator in responding to the variable image quality caused by factors affecting processing, illumination condition, atmospheric condition and relief. Human operators interpret in different ways problematical parts of the model. In contrast a mathematical algorithm (ie a stereomatching algorithm), interprets always in the same way.

The variable systematic errors in the mean values derived from the further statistical analysis, leads to the consideration of the quality of image geometry as an added factor (camera model errors).

In any further mapping project using SPOT data it is desirable that attention is paid to the quality aspects of the data and that some form of the quality assessment is included in the output.

5.2.4.7. Recommendations and further research.

A SPOT image covers approximately a 60 x 60 km^2 of the ground surface. The test area represents a small part of a SPOT scene. Thus a further investigation is required with data samples in different parts of the image or different images with the same or different base/height ratio. The systematic error biases of the SPOT measurements need further investigation in order to determine whether this is caused by physical image conditions or due to errors in the SPOT camera model.

There are some problems still existing in the SPOT images which are pointed out in this work:

The quality of the original initial hard copy was not good and a new copy had to be prepared.

Data of many areas is difficult to obtain because of cloud cover and of poor atmospheric conditions (haze).

The sun angle affects the measurement accuracy.

The different date of the image acquisition causes some problems in relation to the vegetation and the sun angle.

Chapter 6.

Manipulation of DEM data.

6. Manipulation of DEM data.

6.1. General.

The elevation model can be stored as discrete values. A grid model is a common discrete representation and consists normally of a coarse regular grid which covers the DEM area. The data consists of coordinate triplets with associated codes, expressed in the ground coordinate system.

The data manipulation stage includes a large number of procedures depending on the source, the capturing method and technique. The data manipulation methods followed and developed in this project are:

Data transformations. To transform the data to the same projection (Lambert Conformal Conic zone III) in order to be directly comparable and/or to the projection that is adopted by the national mapping organisation.

Data checking for gross errors (blunders). A pointwise local self-checking blunder detection algorithm is developed for blunder detection and trapping particularly for the grid elevation data which was derived from the second source.

Data merging. A data merging algorithm is developed to merge the two different data sources bearing in mind a known and a uniform final product. The first data source was merged with the second set of data in dense form and sparse form in order to see the influence of the second (less reliable source) on the first.

Data structure. To structure the data by changing the format. Data structure nowadays is limited in that the data has to be adapted to the processing package to be used. In the project a data structure recommended by the Laser-Scan Laboratories Ltd for the commercially available package DTMCREATE (DEM creation and manipulation) is used. A Pascal program was written to change the string of coordinates (for both sources derived data) to the Laser-Scan Internal Feature Format (Text file) in order to be acceptable by the DTMCREATE package.

Some other data manipulation procedures which are not examined in this project are the data filtering-smoothing procedure (to remove the degradations and to improve the accuracy), and the data compression (which reduces superfluous data to a minimum necessary amount in accordance with criteria of economy and accuracy). Two data smoothing-filtering procedures are applied to the gradient and

aspect estimation program (see appendix A). One smooths the elevations in a 3 x 3 window, with weighting in inverse proportion to distance from the central cell, and the other by a low pass filtering in a convolution array 3 x 3.

The effect of the data smoothing-filtering procedure by applying a low pass filter (see A.2.2) on the SPOT elevation data can be seen on the gradient and aspect raster images (figures 2.5 and 2.6) in comparison with the gradient and aspect raster images derived from the SPOT elevation unfiltered data (figures 2.3 and 2.4).

These procedures are well documented and presented as the data filtering-smoothing procedure is applied in remote sensing and in automated techniques; and the data compression is applied to the data captured by the manual digitising, contouring and profiling method .

6.2. Map projections.

6.2.1. General.

A map projection is a device for reproducing all or part of a round body on a flat sheet. Since this cannot be done without distortion, the cartographer must choose the characteristic which is to be shown accurately at the expense of the others, or a compromise between several characteristics.

It can not be said that there is one "best" projection for mapping. It is even risky to claim a "best" projection for a given application, unless the parameters chosen are artificially constricting.

The characteristics normally considered in choosing a map projection are as follows:

1. Area. Many map projections are designed to be equal - area, so that an area on one part of the map represents exactly the same area of the actual Earth as the same area on any other part of the map. Shapes, angles and scale must be

distorted on most parts of such a map. Those projections are called Equal Area projections.

2. Shape. Most common projections are the conformal or orthomorphic projections. A large landmass must still be shown distorted in shape, even though its small features are shaped correctly. An important result of conformality is that angles at each point are correct, and the local scale in every direction around any one point is constant. Those projections are called Equidistant projections.

3. Scale. No map projection shows scale correctly throughout the map, but there are usually one or more lines on the map along which the map scale remains true.

4. Direction. Projections in which directions or azimuths of all points on the map are shown correctly with respect to the centre, are called azimuthal or zenithal projections.

5. Special characteristics. Several map projections provide special characteristics that no one projection provides. Some examples of such projections are: the Mercator, Gnomonic, Stereographic and some newer projections specially designed for satellite mapping.

In terms of the size and shape of the earth and positions on it, there are three surfaces to be considered:

1. The physical surface of the earth.
2. The geoid - the level (equipotential) surface (also a physical reality).
3. The ellipsoid - the mathematical surface or reference frame for computation.

6.2.2. The datum and the earth as an ellipsoid.

The shape of the earth is nearly an oblate ellipsoid of revolution, also called an oblate spheroid, because of gravitation. This is an ellipse rotated about its

shorter axis. The flattening of the ellipse for the earth is only about one part in three hundred, but it is sufficiently large to become a necessary part of calculations for plotting accurate maps of scale 1:100,000 or larger.

Historically, each map system has, as a basis, a model of the earth. These models range from a simple sphere, a symmetric ellipsoid, through to more accurate "pear-shaped" earth models and gravitationally-defined geoid. Euclidian geometries (spheres, ellipsoids) have undoubtedly been accepted as good models of the geometry of nature. However, their validity is only for the purpose of analytical simplification. For this reason the geodetic positions on the earth are computed on the reference ellipsoid, the mathematical surface or reference frame, rather than on the geoid which is mathematically very complicated. For map projections however, the problem has been confined to selecting constants for the ellipsoidal shape and size and not generally been extended to incorporating the much smaller deviations from this shape, except that different reference ellipsoids are used for the mapping of different regions of the earth. The significant element of an elevation model is leading us towards a more exacting question of " Height above what ? ". Spacecraft tracking technology is in at least one way leading the state of earth modelling. Perhaps with the advent of global positioning satellites, a world reference geoid and an update mechanism will be established to the accuracy of today's capabilities.

The ellipsoid used in this project is the Clarke 1880 (used in France), which has the following parameters:

1. Equatorial Radius a = 6,378,249.1 m
2. Polar radius b = 6,356,514.9 m
3. Flattening f = 0.003407550 or 1 / 293.46 .

In this work the test area (12.42 km by 6.9 km) occupies only a small part of the satellite image. For this reason the ellipsoid is used without any correction. For higher accuracy geoid undulation has to be taken into account. Also using space imagery the distortion of the projection to be applied and the earth curvature have to be taken into account (see § 6.2.3).

6.2.3. Project used projections, coordinate systems and transformations.

When setting up satellite imagery, such as SPOT - a single stereopair, or a block of them - a large ground area is covered. If a map projection is used we have to take the effects of earth curvature caused by flattening (mathematically) of the earth surface to the map projection. In order to avoid this a general earth-centred rectangular Cartesian coordinate system such as a geocentric coordinate system, is commonly used.

The DEM data capture software (DEM generation program) is installed on the PDP 11/73 microcomputer (Saksono, 1988), which supports the Kern DSR1 analytical plotter (§ 3.2.1.2). The main output of the data capture program is a file which contains the digital elevation data in string of coordinates format (Point identification number, X, Y, Z ground coordinates in UTM projection).

Each DEM block derived from SPOT contains 900 points in a normal grid with 100 m grid interval. The derived SPOT data are in Universal Transverse Mercator (UTM) projection. Each DEM block derived from aerial photography contains a variable number of points, but always less than 1000, which is the program limit. Those derived from aerial photography are in French Lambert Conformal Conic projection (zone III).

Two projection transformation programs are written in Pascal to transfer the SPOT derived data from UTM to Geographical (L, L, H) and to French Lambert Conformal Conic projection. Four other Pascal programs were written in order to check the complete procedure and to find out the errors which are caused by the transformations, eg. for the inverse and other transformations, such as from geographical to geocentric system.

Projection transformations have a great significance for mapping due to the planimetric error which is introduced in every transformation. There are two projections (UTM, French Lambert zone III); and two coordinate systems (geocentric, geographical) used in this project.

The sequence of transformations used in this project is the follows:

1. Control points stage.

These transformations were carried out in order to set up the SPOT model on the analytical plotter.

- Lambert zone III to geographical system.
- Geographical to geocentric system.

2. Output coordinates from the analytical plotter.
   - Geocentric to geographical system.
   - Geographical to Universal Transverse Mercator projection.

3. Further data transformations - Data manipulation stage.
   - Universal Transverse Mercator to geographical system.
   - Geographical coordinates to Lambert zone III projection.

6.2.3.1. Geographical coordinate system.

Latitude (ϕ) and longitude (λ) make a convenient coordinate system with which positions on the ellipsoid can be represented. Lines of equal latitude are called parallels and are small circles on the ellipsoid. Lines of equal longitude are called meridians and form the meridian ellipses on the surface of the ellipsoid.

The geographic or geodetic latitude ϕ of a point, is the angle between the ellipsoidal normal through the point and the equatorial plane. Latitude is zero on the equator and increases towards the poles to a maximum of $\phi = 90^{o}$ N at the North Pole and $\phi = 90^{o}$ S at the South Pole. Sometimes latitudes on the southern hemisphere are by convention with negative.

The geographic or geodetic longitude λ is the angle between the meridian ellipse which passes through Greenwich and the meridian ellipse containing the point in question. It is measured along the equator from the meridian of Greenwich $\lambda = 0^{o}$ either eastward and westward through 180^{o} E and 180^{o} W or eastward

through 360° (sometimes westward angles are indicated by negative angles).

To indicate positions on the physical earth surface, the ellipsoidal height h is added to the geographic coordinates ϕ and λ.

6.2.3.2. Geocentric Cartesian system.

Cartesian coordinates are a convenient method of defining position. The geocentric Cartesian system is a coordinate system with its origin approximately at the centre of the earth and with the X and Y axes in the plane of the equator. The X axis passes through the meridian of Greenwich, and the Z axis coincides with the earth's axis rotation, with its positive direction being through the north pole. The three axes are mutually orthogonal and form a right - handed system (see appendix C, figure C.1).

Geocentric Cartesian coordinates are usually used as the computational system when considering satellite positions. GCPs have to be transformed to geocentric coordinates. This avoids problems of map projection discontinuities over large areas and aids the integration of orbital parameters and auxiliary sources of data into the geometric model. In the DSR 1 analytical plotter software the ground-image transformation is actually computed in this earth-centered system and it is generally hidden from the user. Problems arise with the exact position of the centre of the earth, and the difference between geocentric and geodetic latitude. The geocentric system used in the software is considered as unique to the earth ellipsoid in use.

The major advantage is that height values are referenced to the earth ellipsoid required by the map projection, because the equations involve the a and e parameters (semi-major axis and eccentricity) of the earth ellipsoid (see appendix C).

6.2.3.3. Universal Transverse Mercator projection.

The Universal Transverse Mercator (UTM) projection is the ellipsoidal Transverse Mercator to which specific parameters such as central meridians, have been applied. The Earth between lats. 84° N. and 80° S., is divided into 60 zones each generally 6° wide in longitude. Bounding meridians are evenly divisible by 6°, and zones are numbered from 1 to 60 proceeding east from the 180th meridian from Greenwich with minor exceptions. So while the regular Mercator has constant scale along the Equator, the Transverse Mercator has constant scale along any chosen meridian. UTM projection is a conformal projection and is often used to show regions with greater north - south extent. For civilian mapping only the zone number and the x and y coordinates are used which are sufficient to define a point if the ellipsoid and the hemisphere (north or south) are known. In the northern hemisphere, the Equator at the central meridian is considered the origin (false origin), with an x coordinate of 500,000 m and y of 0. For the southern hemisphere, the same point is the origin, but, while x remains 500,000 m, y is 10,000,000 m. In each case, numbers increase toward the east and north.

6.2.3.4. Lambert Conformal Conic projection.

Lambert developed the regular Conformal Conic, with either one or two standard parallels of latitude, as the oblique aspect of a family containing the previously known polar stereographic and regular Mercator projections. The geometric interpretation is that of a cone either tangential or cutting the ellipsoid along one or two parallels or latitude. Standard parallels are applied to the Lambert Conformal Conic when an area the size of a country or smaller is considered.

Parallels project as circular arcs concave to the nearest pole, while meridians are straight lines converging toward the nearest pole. Meridians and parallels cross at right angles.

Standard parallels are usually chosen to divide the north - south extent of the projection area into three parts in the approximate ratio 1/6, 2/3, 1/6.

Scale is constant in the east - west direction but varies in the north - south

direction. It will be correct along the standard parallels, too large outside them and too small between them.

If the projection is extended toward either pole and the Equator, the differences become more obvious. Although meridians are equally spaced radii of the concentric circular arcs representing parallels of latitude, the parallels become further apart as the distance from the central parallels increases. Conformality fails at each pole. The pole in the same hemisphere as the standard parallels is shown on the Lambert Conformal Conic as a point. The other pole is at infinity. Two parallels may be made standard or true to scale, as well as conformal. It is also possible to have just one standard parallel. Since there is no angular distortion at any parallel (except at the poles), it is possible to change the standard parallels to just one, or to another pair, just by changing the scale applied to the existing map and calculating a pair of standard parallels fitting the new scale.

Lambert Conformal Conic zone II and III are adopted by IGN in France as the official projection.

6.2.4. Error caused by transformations. Estimation of the transformation error in this project.

In each country a map projection and an ellipsoid are adopted. This projection is called a national grid, such as the Lambert zone III for France. Selected points (triangulation network points, boundary points in cadastral, ground control points etc) are given their coordinates in that projection. Transferring coordinates from one projection or coordinate system to another causes an error to be accumulated because of the complexity of the calculations.

In this experiment the sequence of transformations (see also § 6.2.3) is as follows:

When setting up the SPOT models, the coordinates of the control points had to be transformed from Lambert projection via Geographical to the Geocentric coordinate system.

When measuring points on the model and getting the output coordinates from the analytical plotter, the coordinates have to be transformed from geocentric to

Universal Transverse Mercator via Geographical system.

Finally the output data from the analytical plotter in string of coordinates format have to be transformed again from Universal Transverse Mercator projection to Lambert zone III via Geographical system.

As we can see from the above procedure the output data from the analytical plotter are in UTM projection. That means that the data have to be transformed from Geocentric to UTM via Geographical system, through the Kern DSR1 software, then transformed from UTM to Geographical and finally to Lambert zone III. These multiple transformations cause propagation of errors.

A testing procedure of the transformation programs and a study of the errors caused by transformations was carried out. A sample of 20 points (the SPOT model check points) (see § 4.2.1.2) were used. The sequence of the applied transformations and errors introduced during the procedure are as follows:

1. Geographical to Geocentric and Geocentric to Geographical (1 complete loop).

Absolute differences in Geographical coords (Decimal Degrees or Degrees):

Longitude = 0.00000034 Decimal Degrees, or 0° 00' 00.00"

Latitude = 0.00000275 Decimal Degrees, or 0° 00' 00.01"

Height = 0.00 m.

1a. Geographical to Geocentric, Geocentric to Geographical and Geographical to Geocentric (1 1/2 loop).

Absolute differences in Geocentric coords (metres):

Dx = 0.21 m, Dy = 0.01 m, Dz = 0.22 m.

2. Geographical to UTM and UTM to Geographical (1 complete loop).

Absolute differences in Geographical coords (Decimal Degrees or Degrees):

Longitude = 0.000000341 Decimal Degrees, or 0° 00' 00.00"

Latitude = 0.000016858 Decimal Degrees, or 0° 00' 00.06"

Height = 0.00 m.

2a. Geographical to UTM, UTM to Geographical and Geographical to UTM
(1 1/2 loop).

Absolute differences in UTM coords (metres):

Dx = 0.03 m, Dy = 1.87 m, Dz = 0.00 m.

When the Geographical to UTM transformation is applied, the errors introduced are totally insignificant. However, when the UTM to Geographical transformation is applied the resulting errors are more significant. The calculation of the latitude and longitude in the program is carried out by application of the transformation formulas once, so there are errors introduced during the calculations (approximation errors).

The errors are not significant when the Geographical to UTM and UTM to Geographical transformations were applied (case 2), but the small errors occurring in case 2 were exaggerated when the application of Geographical to UTM transformation were applied for second time.

For the project requirements the results are acceptable. If we wanted to obtain better results an iteration loop should be used, in order to minimise the approximation errors in the calculations of latitude and longitude.

3. Lambert zone III to Geographical and Geographical to Lambert zone III
(1 complete loop).

Absolute differences in Lambert coords (metres):

Dx = 0.02 m, Dy = 0.31 m, Dz = 0.00 m.

A further test was carried out for all the project transformation procedure as follows:

- Lambert to Geographical, Geographical to Geocentric (control points transformation stage),
- Geocentric to Geographical, Geographical to UTM (DSR1 output coords stage),
- UTM to Geographical, Geographical to Lambert (data manipulation stage).

The results are as follows:

Absolute differences in metres:

Dx = 0.02 m, Dy = 2.48 m, Dz = 0.00 m.

Vector error Dxy = 2.48 m, variance = 0.30 m^2,

standard deviation = 0.55m.

The vector error resulting from all the project transformations is significant because of the UTM to geographical transformation stage. For most photogrammetric tasks this vector error is not acceptable. For the project requirements, however, it is acceptable, as it is much less than the SPOT sub-pixel accuracy (5 metres).

6.2.5. Coordinate projection used in this project for the output data.

As mentioned in 6.2.4 the output data from the analytical plotter are in UTM projection. So the coordinates have to be transformed from geocentric to UTM via geographical system, through the Kern DSR1 software. These have to be transformed from UTM to geographical and then to Lambert zone III.

In this transformation stage a question can arise. Why is data output from the analytical plotter chosen to be in UTM projection, rather in geographical system, which can be transformed directly to Lambert zone III.

The answer is that if the captured data has to be in a normal grid, then it should not use the geographical system because the grid interval in the X-direction (transformed from longitude) is not the same as the grid interval in the Y-direction (transformed from latitude). X increments (transformed from longitude) further from the equator becomes smaller in relation to Y increments (transformed from latitude) . This occurs because of the shape of the earth. It can be seen that in azimuthal or zenithal projections for small scale maps the shape of the map is trapezoidal with the parallel closer to the equator being longer than the parallel further from the equator.

In the Latitude 43° 30' ,in which the project test area lies, a Longitude of 0.01237 Decimal Degrees (0° 00' 44.53") is equivalent to X =99,992 m in Lambert zone III and a Latitude of 0.009001 Decimal Degrees (0° 00' 32.40") is equivalent to Y =100.007 m in the same projection.

The grid interval as input to the grid generation program should be in the format of decimal degrees * 10000. Therefore by averaging the longitude and latitude values : (123.7 + 90.01) / 2 = 106.85

A grid interval of 105 (0.0105 decimal degrees) gave:
84.88 m in X direction; 116.66 m in Y direction and diagonal 144.27 m.

The idea of getting output in Geographical system was abandoned in this project because:

1. The irregular grid interval specification (orthogonal grid).
2. To get a regular 100 metre grid interval an interpolation can cause further errors to be introduced (see § 7.5.2).
3. The geographical coordinates are not suitable for plotting, because of the different scale along the x and y axes as already described above.

6.2.6. Conclusions.

Projection transformations have a great significance for mapping due to the planimetric error which is introduced in every transformation. The sequence of transformations used in this project are:

1. Control points transformations stage, in order to take the effects of earth curvature caused by flattening, when setting up the SPOT model on the analytical plotter.
   - Lambert zone III to Geographical System and Geographical to Geocentric system.
2. Output coordinates from the DSR1 analytical plotter stage.
   - Geocentric to Geographical system and Geographical to Universal Transverse Mercator.
3. Data manipulation stage.
   - Universal Transverse Mercator to Geographical and Geographical to Lambert zone III.

The projection transformation error, found in the the whole procedure (control points, output data from analytical plotter and data manipulation stage) checking 20 points, is Dx=0.02 m Dy=2.48 m and Dz=0.00 m. So the vector error

is Dxy=2.48 m and standard deviation=0.55 m. For the project requirements the results are acceptable. If it is necessary to obtain better results an iteration loop should be used in the UTM to geographical transformation stage, in order to minimise the approximation errors in the calculations of latitude and longitude.

6.3. Blunder error detection and trapping.

6.3.1. General.

Gross errors (or blunders or mistakes) have the main characteristic that their magnitude is significantly very large in comparison to the measured value itself. In other words, any observation in a series of repeated measurements which contains gross errors can be obviously detected as an abnormal one among the series.

Blunder processing includes blunder location and blunder elimination (Molnar, 1980). In a statistical process (evaluation of least square models using reliability studies), the largest residuals occur at the location of the gross error, which gives hope that errors in observations can be detected by the analysis of the residuals.

However, in practice this detection cannot be achieved directly due to the following reasons.

1. Blunders may occur in more than one point.

2. Matrix Q_{vv} (variance-covariance matrix of the residuals) is singular; therefore it is not possible to compute the value of the gross error or its point of application (Hassan, 1988). Q_{vv} matrix plays a very important role in the study of reliability in photogrammetry . Its characteristics are given by Amer (1981).

In recent years much attention had been paid to the blunders involved in the aerial triangulation process in the international photogrammetric community, but less emphasis has been focussed on the blunders involved in the captured data for DEM purposes. The detection of blunder techniques can be classified in two categories: global and local techniques.

The detection and isolation of gross errors in gridded DEM observations, is obtained by fitting, via least squares a simultaneous patchwise polynomial (ie. bicubic spline) to a small set of observations and analysing the residuals, for the presence of outliers. Jancaitis & Junkins (1973) centred their work on the fitting of polynomials to the data. Bethel & Mikhail (1983) worked on the partial quadratic form algorithm. Johnson (1978) investigated filtering in both the spatial and frequency domains, and other global techniques.

The partial quadratic form algorithm (Bethel & Mikhail, 1983) was checked by introducing blunders with varying multiplicity and varying magnitudes (large magnitudes from 5σ to 10σ) . The location algorithm appears to be effective in the case of multiple blunders of large magnitude, while its capability diminishes for smaller magnitudes. Generally the presented results are not very good. Bethel mentioned that the algorithm locates blunders well when the a priori observational (reference) variance is known and suggested that the overall performance would be improved by having a better approximation of the maximum chi-squared ratio distribution function.

Hannah (1981) developed some local methods to detect and correct the errors introduced in the correlation-derived digital elevation models, when the stereo correspondence algorithm produces mismatches. This was done by focusing on the use of constraints on both the allowable slope and the allowable change in slope in local areas around each point. The methods were applied iteratively to achieve the desired results. Three sets of tests were performed on these slopes: a set of slope constraining tests, a set of local neighbour consistency tests, and a set of distant neighbour slope consistency tests. The correctness indicator had two components. The first used the change-in-slope constraints (analysis) to produce a slope consistency evaluation of the data. The second used the slope constraints forming an elevation consistency evaluation. These two indicators were combined into an overall evaluation of the correctness of each terrain data point. In the simple indicators of correctness the slope consistency evaluation is based on the application of constraints (or thresholds) to the differences in slopes involving both the local and the distant neighbours of a point , while in the weighted iteration of correctness indicators, it performed a simple averaging of the contributions

made by each confidence measure. Relaxation-like techniques were employed in the iteration of the detection and correction phases to obtain best results. These techniques were applied to digital terrain models for which no classification information was available, with good results. Hannah concluded that these techniques have a significant potential in the detection and correction of errors in digital elevation models.

Global techniques have the drawback that they give identical treatment to all areas of digital elevation model. Terrain is rarely uniform in roughness, so uniform application of a global technique can produce over-smoothing in rough areas while failing to correct errors in relatively flat areas. Local techniques, on the other hand, have the potential for coping with different terrain types within a model.

6.3.2. Blunder detection study. Some figures derived from the project.

The number of gross errors in photogrammetrically acquired DEM data is usually very small; 0.5% according to Torlegård et al (1984). This conclusion came out from a test which was carried out in six areas in which the DEM data were captured from aerial photography of different scales. Although blunders appear in small numbers in the aerial photography captured data, the situation appears different using SPOT as a source of data. This is pointed out with the blunder figures derived. The main reasons which introduce blunders are the image physical quality, the terrain roughness, the atmospheric effects and the operator mainly related with the measuring conditions, because of the difficulties in finding the "ground" (see § 5.2.4.5).

Some of the investigators accept that the gross errors are defined as having a value greater than 3 * (standard deviation of random error) + (systematic error).

In this study gross errors in elevation are considered to have a value greater than 2.7 * (standard deviation).

The choice of the σ value as basis for the threshold in the detection is ambiguous and questionable. An a priori known σ would be far better. But what is the true σ of a particular DEM? In this study not only one value for σ is adopted, but several values according to the terrain roughness.

The standard deviation (σ) or height limits is estimated in 5.2.4.2.2. The systematic error was not put into account as it is not known, because neither the value nor the sign is constant but changes frequently as it is pointed out from the partial statistical analysis within small sub-blocks of digital elevation data (§ 5.2.4.5).

The procedures of blunder snooping and DEM levelling can be examined in this project as we know the true elevations in the check points. In the following paragraphs a two stage test for filtering and removing blunders is carried out in order to estimate the number of blunders caused in the photogrammetrically captured from SPOT data and to understand the nature of errors which are involved during the data capture procedure. As the "true" elevations are known after the two sources checking procedure any point for which the height difference appeared to be larger than the 2.7σ value, is considered as a blunder and rejected.

Table 6.1 presents the initial statistical values for four DEM blocks according to the estimated height difference values. The check was carried out over the first SPOT hardcopy measurements, in respect to the first source data through the checking program (see appendix B). In order to assign height limits (σ) an average categorisation of the terrain was applied. The average terrain categories for each block are the follows:

Block 2. Gently rolling terrain σ = 4.80 m, 2.7σ = 12.96 m.
Block 3. Semirough terrain σ = 8.90 m, 2.7σ = 24.03 m.
Block 6. Semirough terrain σ = 8.90 m, 2.7σ = 24.03 m.
Block 7. Very rough and steep terrain σ = 14.00 m, 2.7σ = 37.80 m.

BLOCK NAME	NUMBER OF COMPARED POINTS	POINTS WITH -LIMIT >= HEIGHT_DIF >= LIMIT	POINTS WITH -40 >= HEIGHT_DIF >= 40	AREA MEAN HEIGHT (m)		STATISTICAL RESULTS OF ELEVETATION DIF		OF ABSOLUTE ELEVATION DIF.	
				FIRST SOURCE	SECOND SOURCE	MEAN(m)	SD (m)	MEAN(m)	SD (m)
2	640	128 (20.0%)	26 (2.9%)	299.29	294.22	5.07	16.20	10.48	17.08
3	650	47 (7.2%)	10 (1.5%)	384.31	390.23	-5.92	14.17	12.38	23.16
6	664	56 (8.4%)	23 (3.5%)	523.45	519.27	4.18	19.86	11.79	21.27
7	648	95 (10.6%)	102 (11.3%)	557.23	541.15	16.17	23.63	20.91	24.10

Table 6.1. Initial descriptive statistical results.

A first stage filtering is applied in which points with height differences larger than the 2.7σ are considered as blunders and rejected. The two sources data (after rejecting blunders) are checked again applying the same height limits. Table 6.2 gives the figures of the number of rejected points as blunders and the new statistical values.

BLOCK NAME	NUMBER OF COMPARED POINTS	POINTS WITH -LIMIT >= HEIGHT_DIF >= LIMIT	POINTS WITH -40 >= HEIGHT_DIF >= 40	AREA MEAN HEIGHT (m)		STATISTICAL RESULTS OF ELEVETATION DIF		OF ABSOLUTE ELEVATION DIF.	
				FIRST SOURCE	SECOND SOURCE	MEAN(m)	SD (m)	MEAN(m)	SD (m)
2	617	105 (17.0%)	3 (0.5%)	296.07	293.20	2.88	11.50	8.49	12.80
3	638	35 (5.5%)	0 (0.0%)	384.54	390.61	-6.06	13.01	11.82	22.12
6	645	37 (5.7%)	4 (0.6%)	519.90	518.08	1.82	12.73	9.65	14.95
7	617	64 (10.4%)	71 (11.5%)	554.42	541.31	13.11	19.49	18.08	20.12

Table 6.2. Descriptive statistical results after first stage filtering for removing blunders.

The statistical results obtained, shown in table 6.2, after the first stage filtering, are generally good, as there is a remarkable improvement in the standard deviation value.

Again after rejecting the possible blunders (points which were found to have height differences >= 2.7σ) shown in table 6.2 (first stage),the SPOT derived data were compared again with the aerial photography data. The assigned height limits remained the same. The comparison of the two sources derived data (second stage) is shown in table 6.3.

BLOCK NAME	NUMBER OF COMPARED POINTS	POINTS WITH -LIMIT >= HEIGHT_DIF >= LIMIT	POINTS WITH -40 >= HEIGHT_DIF >= 40	AREA MEAN HEIGHT(m)		STATISTICAL RESULTS OF ELEVETATION DIF		STATISTICAL RESULTS OF ABSOLUTE ELEVATION DIF.	
				FIRST SOURCE	SECOND SOURCE	MEAN(m)	SD (m)	MEAN(m)	SD (m)
2	598	86 (14.4%)	0 (0.0%)	294.28	292.48	1.80	9.93	7.60	11.50
3	629	26 (4.1%)	0 (0.0%)	384.68	390.66	-5.98	12.43	11.47	21.43
6	631	23 (3.6%)	0 (0.0%)	518.00	516.87	1.13	11.64	9.02	14.07
7	595	42 (7.1%)	49 (8.2%)	553.47	542.00	11.48	17.86	16.64	18.59

Table 6.3. Descriptive statistical results after second stage filtering for removing blunders.

If we extract the mean and standard deviation values from tables 6.1, 6.2 and 6.3 and put them together we have the following table (table 6.4):

BLOCK NUMBER	ORIGINAL RESULTS		1st STAGE FILTERING		2nd STAGE FILTERING	
	MEAN(m)	SD (m)	MEAN(m)	SD (m)	MEAN(m)	SD (m)
2	5.07	16.20	2.88	11.50	1.80	9.93
3	-5.92	14.17	-6.06	13.01	-5.98	12.43
6	4.18	19.86	1.82	12.73	1.13	11.64
7	16.17	23.63	13.11	19.49	11.48	17.86

Table 6.4. Summary of the initial statistical results and after 2 stage filtering.

The number of the possible blunders in the complete procedure after comparing the two sources data are shown in table 6.5.

DEM BLOCK	NUMBER OF POINTS	FIRST STAGE		SECOND STAGE		TOTAL BLUNDERS PERSENTAGE	AVERAGE SLOPE (%)
		2.7σ VALUE	BLUNDERS > 2.7σ	2.7σ VALUE	BLUNDERS > 2.7σ		
2	640	43.7	23	31.3	19	6.6%	35.5
3	650	38.3	12	35.1	9	3.2%	41.7
6	664	43.6	19	34.4	14	5.0%	43.3
7	648	63.8	31	52.6	22	8.2%	64.6

Table 6.5. Figures of possible blunders after the complete filtering procedure.

Except for the 2nd block results the blunders follow the terrain roughness (indicated by the slope). The reason that the number of blunders in the 2nd block do not follow the terrain roughness is that the applied height limit is smaller than the actual limit which has to be applied for this type of terrain. From the table we can estimate a total level of 5.7% blunders in measurements with an average slope of 46%.

From the comparison of the statistical results presented in table 6.4, we draw the following conclusions.

Blunders affect very much the quality of the data. After rejecting the blunders the results became better as is clearly evident in the case of the 2nd, 3rd and 6th blocks. The rejection of the blunders in the 7th block gave better results, but the biased mean and the large standard deviation remained. The 7th block data derived from a badly illuminated, partially cloudy, very rough and steep area (north oriented part of the Montagne Sainte Victoire). This area caused to the operator great uncertainty in his measurements. The statistical analysis showed that a strong positive systematic bias has the same effect as the operator setting the floating mark above the ground surface systematically.

Table 6.6 gives some figures of the possible blunders in two DEM blocks from the first SPOT hardcopy measurements by the experienced operator. The rules for considering a point as a blunder and the assigned height limits remained the same.

DEM BLOCK	NUMBER OF POINTS	FIRST STAGE		SECOND STAGE		TOTAL BLUNDERS PERSENTAGE	AVERAGE SLOPE (%)
		2.7 σ VALUE	BLUNDERS > 2.7 σ	2.7 σ VALUE	BLUNDERS > 2.7 σ		
6	664	34.4	29	24.8	31	9.0%	43.3
7	648	50.1	5	48.4	3	1.5%	64.6

Table 6.6. Figures of possible blunders after the two stage filtering procedure. (experienced operator measurements).

Comparing the results found from the filtering procedure of the project operator and the experienced operator measurements (table 6.5 and 6.6), we can see that the blunder percentage in the 6th DEM block is larger in the experienced operator measurements, but with 9.6 m better 2.7σ (3.6 m better standard deviation), which means that the experienced operator made more blunders but with much smaller magnitude. In the 7th DEM block, the results are much more clear with 6.7% less blunders in the experienced operator measurements and 1.4 m better standard deviation. From the above analysis it can be concluded that the blunders are related to operator experience.

Table 6.7. gives some figures of the possible blunders in four DEM blocks measured by the project operator on the second SPOT hardcopy. The rules for considering a point as a blunder and the applied height limits remained the same.

DEM BLOCK	NUMBER OF POINTS	FIRST STAGE		SECOND STAGE		TOTAL BLUNDERS PERSENTAGE	AVERAGE SLOPE (%)
		2.7 σ VALUE	BLUNDERS > 2.7 σ	2.7 σ VALUE	BLUNDERS > 2.7 σ		
2	640	29.1	12	25.8	7	3.0%	35.5
3	650	28.8	18	24.8	7	5.4%	41.7
6	664	33.0	10	28.6	5	2.3%	43.3
7	648	48.9	19	43.1	8	4.2%	64.6

Table 6.7. Figures of possible blunders after the two stage filtering procedure for removing blunders (second SPOT hardcopy measurements).

Comparing the figures derived from the second SPOT hardcopy measurements with that of the first, we can see that the figures derived from the second hardcopy are much better (35.2% less blunders). The results appear to be better in all the DEM measured blocks (2.0%, 2.8%, 0.9% and 2.4% respectively). From this

procedure it is obvious that the image quality is an important factor in avoiding blunders.

6.3.3. The blunder detection program.

6.3.3.1. Purpose.

SPOT stereoimages as a source of height information for DEM production opened new fields in the intensive procedure (manual, semi-automatic or automatic) of capturing elevations. However, the SPOT images present several problems, which make the task of the extraction of the height information difficult and uncertain. As result of this uncertainty blunders will involve not only because of the operator carelessness or fatigue, but mainly of the uncertainty or difficulty of the operator in finding the ground itself.

So it is necessary in the case of manual data capture procedure later in off line usually mode; or during the automated capturing procedure, if a correlator is used, to develop an algorithm, for the elevation data check, capable in detecting and removing the blunders. The blunder detection procedure which is developed is a local self-checking technique for identifying, pointing and labelling blunders.

6.3.3.2. Description of the algorithm.

Blunders may be detected if redundant observations exist. In the case of estimating values of unknown points from a sequence of data related mathematically, ie. in aerial triangulation, we attempt to have redundant observations in order to apply a statistical analysis such as least squares. Based upon the residuals, it is clearly difficult to recognise the blunders because they affect "innocent points". So different techniques were developed in order to increase the residuals derived from blunders, ie. Robust estimation. Moreover in the case of aerial triangulation the calculated points have both a strong relation and correlation so they can be processed statistically.

In the captured data as a digital elevation matrix form, there is no relation

or correlation, because each point has a unique set of values X,Y, and Z (coordinates) which represent this point and only this point in the space. However, in close neighbours (small patches within a few metres radius from the point) the ground behaviour appears as a continuous surface with smooth or relatively smooth changes, except in a very small number of cases (natural, or artificial terrain "accidents"). In addition even in the extreme case of break and cliff lines the feature is repeated in a smaller or bigger area. That means that any point has a relationship with the close neighbour points, if the distance from that point does not extend beyond a certain limit.

So if we have an area we can classify it according to the relief peculiarities or ground characteristics. This can be done by dividing the area into small patches with the same (pre-specified magnitude) slopes. Within the small patches the ground behaviour is assumed to be the same. The patch size (related with the grid interval in the program) should vary according to the terrain behaviour. For very flat areas we can have very large patches, for gently rolling areas large patches, for semi-rough terrain small patches and so on.

In the case of measuring data in a standard regular grid, the grid size remains the same and it does not follow the terrain roughness. The developed blunder detection program uses data captured in a regular grid. In case of rapid terrain changes (rough and steep terrain) the grid interval should not be greater than 100 metres because the algorithm is based on the comparison of neighbouring points. The grid interval has less effect for flat and gently rolling terrain so it seems to be unrestricted.

The constraints which the algorithm uses depending on the slope in the application of certain height limits during the checking elevation with the surrounding points procedure. The convolution array changes in size. Various cases are considered depending on the number of the examined points together (1,2 or 4 points) with their close neighbours. A close neighbour point is one which is distant no more than one grid interval in x or y.

The cases which have been developed for the comparison are:

1. Of the examination one point with the 3 closer points (4 cases), 5 closer points (2 cases), 8 closer points (1 case).

2. Of the examination of two points with , 6 closer points (2 cases) 10 closer points (2 combinations), and

3. Of the examination of four points with 12 closer points (1 case).

As the algorithm compares neighbouring points, in a digital elevation matrix of n rows by m columns, the points which lie on the edges of the DEM block are not going to be fully detected, because they do not have the full number of surrounding neighbours.

Each point is examined through three routines:

The first two routines test the point in relation with the close neighbours through one procedure and certain limits. If the checked elevation is out of the elevation limit range, this is pointed out as a possible blunder.

The third routine examines the surrounding close neighbours in relation to the point. The elevations are examined again to be within certain limits. If the points are not within the elevation limits, the routine points out the checked neighbour points as suspicious points (possible blunders).

The program asks the user:

1. Input the file name to be detected for blunders (data elevation matrix).
2. Output file names.
   - 2a. To write the detected blunders.
   - 2b. To write the suspicious heights
   - 2c. To write the height limits according to the slopes.
3. The data elevation matrix spacing.
4. The number of rows.
5. The number of columns.
6. The Height limits or standard deviation of random error (found height limits for SPOT images, as result of statistical analysis of the operator variance).

The terrain classification, slope categories and height limits are presented in table 6.8. The slope categories are estimated as overall and average slopes .

Terrain classification	Angles (Degrees)	Slopes (%)	Height Limits (σ) (m)
Flat areas	0 - 6	0 - 10	2.80
Gently rolling areas	6 - 14	10 - 25	4.80
Semi-rough terrain	14 - 26.5	25 - 50	8.90
Rough and steep terrain	above 26.5	above 50	14.00

Table 6.8. Terrain classification and height limits for the SPOT imagery derived data.

The program does not delete the located possible blunder or replace it with another calculated value ie. with the 'average' height of the 8 surrounding points lying within on grid interval. Instead it writes the possible blunder (point number, X, Y and Z coordinates) checked by the routines Check_Neighbourhoods1 and Check_Neighbourhoods2 in an output file, or writes the suspicious points (point number and case which detected the points) by the routine Heights_Check_and_test to another output file (see appendix D).

This is because blunders affect their neighbours. The program logic is that the points which are trapped as blunders and the suspicious points should be checked by the user. For this reason they are included in a separate file with some labels, indicators and information which are helpful to the user for interpretation and decision. Interpretation by the user is possible in the experimental stage provided the data set does not contain a large number of points. However, in production with an enormous amount of data user checking is not possible so an automated procedure should be applied.

The best solution is to reject the point if there is a high possibility of it being a blunder and not to insert an interpolated height value, unless the user likes to keep the grid normality.

When there is a lot of data to be checked, the work of interpreting suspicious points (based on the number which appear the suspicious point) is very tedious and boring. An auxiliary Pascal program is written to count how many times a

suspicious point appears to the output file. The program is applied independently and the user can choose the upper bound of number of times for a counted point to be written to a separate file. The maximum number of a point appearance as suspicious is 16. From my experience after 11 times there is a strong possibility of this point being a blunder.

One big advantage of this method is that is very fast. The calculation time depends on the dimensions of the data elevation matrix and it increases linearly.

6.4.3.3. Testing the detection blunder algorithm - results.

The most common, useful and final presentation of an algorithm is in a program form. Once the algorithm is applied as a program, the final step and the most important is to check its applicability and power. That means that it has to be checked if the predicted theoretical capability of doing certain job, is the same as the practical. Some algorithms are perfectly documented and established in mathematical way, but never work properly, because the mathematical model does not represent closely enough the physical (real) model which it attempts to describe or the mathematical parameters and limitations do not describe the phenomenon properly.

In addition some algorithms are built with a lot of restrictions which make them inflexible, expensive in computing time and generally not satisfactory. Others contain a poor range of restrictions, which lead to erroneous results in quality or in quantity (poor, superfluous, or wrong results). Keeping a balance in the number or the magnitude of the restrictions which are going to be used is a very hard procedure, which needs experience, full knowledge of the subject and a large number of tests.

The blunder detection procedure is peculiar because the blunder appearance is completely random (there are some times some reasons or circumstances leading to blunders). Moreover blunders involved in a formed mathematical model affect their surrounding neighbours. Although it may appear that much terrain is too complex (even if its behaviour is not entirely random) for mathematical treatment, all the algorithms for blunders location are based on the assumption

that it is possible to represent the ground surface by an analytical function. For this reason all the global blunder detection algorithms suffer from instability.

The most common way to check well the behaviour of a blunder detection algorithm is to construct an imaginary surface, with dummy data. This is done in this project with the creation of an 8 rows by 8 columns digital elevation matrix using dummy SPOT data.

At the beginning the algorithm was applied in the constructed terrain representation without introducing any blunders. Later some blunders with a known magnitude were introduced. The algorithm was applied to a slanting plane (a simple terrain) and to an irregular surface (terrain with variable changes).

When the algorithm is applied on the constructed hypothetical relief nothing happened, but when later small blunders were introduced, the routine Heights_Check_and_Test (see appendix D) pointed out the points as suspicious. When the blunder value increased the two other routines (Check_Neighbourhoods1 and Check_Neighbourhoods2) pointed out the points as blunders. The applied height limits are those estimated for the SPOT data (see table 6.8)

The algorithm is checked by applying thresholds or height limits equal to the 3σ value instead of 2.7σ as it was applied in the blunder detection study. The application of threshold values is a matter of consideration. Height limit values of 3σ were applied as it was considered that 99.7% of the measurements should fall within 3σ of the mean. 3σ or 4σ (99.7 and 100% respectively) are usually taken as the tolerance limit for random error. Errors greater than the chosen limit may be considered as blunders (Manual of Photogrammetry pp. 73).

The results of this test are shown in table 6.9.

RELIEF CATEGORY	HEIGHT LIMIT 3σ	NUMBER OF INTRODUCED BLUNDERS	BLUNDER MAGNITUDE (m)	NUMBER OF DETECTED BLUNDERS	NUMBER OF DETECTED AS SUSPICIOUS POINTS	COMMENTS ON INTRODUCED BLUNDERS
Regular Slanting Plane	8.40	0	-	0	0	-
Regular Slanting Plane	8.40	4	+/- 9	0	4	far from each other
Regular Slanting Plane	8.40	4	+/- 11	4	4	far from each other
Regular Slanding Plane	8.40	7	+/- 11	3	6	2 pairs of are close
Irregular surface	8.40 14.40	0	-	0	0	large variations from 10 to 25m
Irregular surface	8.40 14.40	4	+/- 10	2	1	3 close and one far (same column)
Irregular surface	8.40 14.40	3	+/- 10	0	2	close together

Far from each other: None of the close neighbours is blunder.

Close : The introduced blunder neighbouring with another blunder(s).

Table 6.9. Testing the blunder detection algorithm.

Further study of the algorithm behaviour showed that the program suffers when the relief function changes continuously.

Figure 6.1 shows a representation of the terrain changes which cause problems to the detection algorithm. The small slope magnitude is not a restricting factor, because the applied height limits in the checking procedure is small (ie. for SPOT images the applied height limits for slopes up to 10% is 3 * 2.80 = 8.40 m, from 10 to 25% 3 * 4.80 = 14.40 m etc.

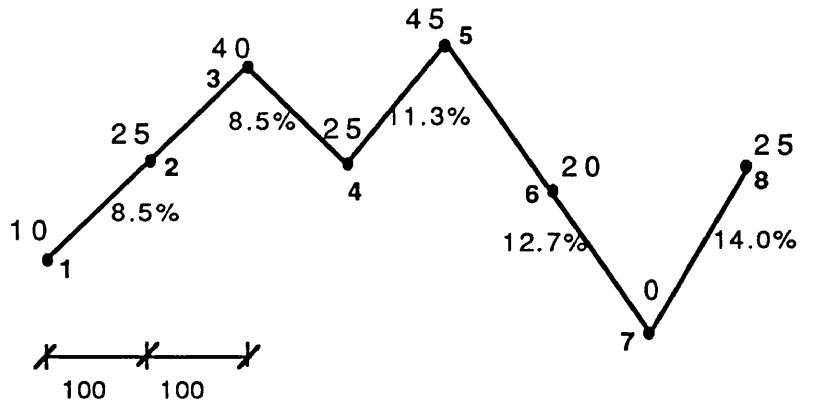

Elevations are in metres
Horizontal distances are in metres

Figure 6.1. Case of terrain changes which cause problems to the detection algorithm.

When the program applied to the situation shown in figure 6.1, the point 5 and 7 were pointed out as blunders, while the point 3 was not detected as a blunder.

Unfortunately although the algorithm gives very good results in blunder detection of dummy data (shown in table 6.9), when it was applied to the real SPOT data gave poor results (36% successful in blunders detection). Some points which were known to be non-blunders were nevertheless assigned by the program as blunders or suspicious points. On the other hand some points which were known to be blunders were not trapped. The independent determination of whether or not a point was a blunder was carried by the blunder detection study (see §6.3.2).

Further tests showed that the fault is not due to the algorithm, but to the SPOT data itself as there is the "random appearance" of the systematic error (similar behaviour as presented in figure 6.1), apart from the observation random error, involved during the collection procedure (for reasons presented in § 5.2.4.5).

The low percentage of the detected blunders, when the program is applied on the real data, implies that the applied height limits are not the correct ones under the current circumstances. Because these height limits had been obtained through extensive statistical analysis tests, it believed that these are the right figures

which have to be applied to this particular group of data.

Another way of suitable height limit application each time, can be done by estimation of the semivariance (along rows, along columns, or all over the tested block) . The attempt of using the semivariance (see § 7.3.1) in real time supplying height limits for this particular set of data was abandoned, because of the non representative value of the semivariance, which is estimated over a large set of data and the quality of the data. However, this assumption makes the algorithm independent from the user in supplying the height limits.

The applied procedure of applying different height limits according to the slope criterion is the right decision and the next probable step is that the height limits should be variable following the random systematic error magnitude. This is not easily applicable because the magnitude of the random systematic error is not known.

6.3.3.4. Conclusions derived from the blunder detection study.

SPOT images present several problems which make difficult and uncertain the extraction of height information. As result of this uncertainty blunders are involved. The main reasons which introduce blunders are the image physical quality, the terrain roughness, the atmospheric effects and the operator, not only because of his/her careless or fatigue, but because of the uncertainty or difficulty in finding the ground by itself. Therefore SPOT data contains a large number of blunders (5.7%). Thus blunders should be trapped and removed before any process starts (particularly before interpolation).

Global techniques for blunder detection have the drawback that they give identical treatment to all areas of a digital elevation model. A uniform application of a global technique can produce over-smoothing in rough areas while failing to correct errors in relatively flat areas. Local techniques (point to point within variable patches) have better behaviour but with the potential for coping with different terrain types within a model.

Blunder prediction and behaviour is a very difficult task and so far there is

not a complete remedy. All the applied techniques do not give fully satisfactory results.

The pointwise local self-checking blunder detection technique applied in this project did not give satisfactory results either. This occurred because of the nature of the SPOT data. The author believes that local techniques are more suitable in blunder detection and in particular the technique developed in this project is going to give far better results when used with different source or sets of data.

6.4. Data Merging.

6.4.1. General.

Merging implies a simple form of resampling. Data merging concerns closely related data sets. Two or more related data sets can be merged into a single set. The corresponding intensity values can be merged ie. by appending, averaging or applying more complicated mathematical expressions (as followed in this project).

Data linking is a more complicated technique. It is applied to different data sets, eg. attributes, to tie them with the image raster via a key. This implies gridding data, ie. distinct lines and surfaces of morphometric and/or artificial features into a raster. Key-features can be linked with different attributes by means of pointers or addresses. Example are classes of regions and networks (of chains and points). Such a classification can serve for specifying the parameter values for an autonomous data set and should therefore be preserved (in original form) for further uses.

The need to merge existing data from two or more different sources is a very common situation in the production line. Usually the most common sources of data are the existing maps. Nowadays these data are produced extensively, by massive digitising procedure from the existing maps and used as a background in the creation of the national data bases. The continuation of such projects could be later demanding, asking or directing the data capture from another source such as aerial photography in (different scales) or space imagery in order to extend or update the mapping area.

In this project two data sources are used: the aerial photography and the SPOT satellite imagery. The applications arising from this work could be as:

1. Collecting data from SPOT in a dense grid as a main frame (background). Suppose a SPOT DEM exists in a dense grid covering a large area as a main frame and then in a part of this large area we capture some additional data from aerial photography with a similar density of grid. This applies when we want to fill a gap; to improve the relief representation and the terrain features in order to map this part of the area with better accuracy keeping the SPOT information. This is possible when there exists a SPOT DEM created by automated techniques which provide a large amount of elevation information.

2. Collecting data from aerial photography in a dense grid as a main frame and then capturing additional data from SPOT imagery in a sparse grid to fill a gap, or to get the later relief changes for updating purposes. The case it is not very realistic, but it has some applications in countries with boundary problems, such as the Arabic Yemen Republic (Hartley, 1988).

Also it can happen in the experimental stages, such as this project, where the aerial photography elevation data was captured in 30 m regular grid (main frame), while the SPOT data in a 100 m grid.

6.4.2. The data merging program.

6.4.2.1. Purpose.

The Laser-Scan DTMCREATE package which exists in the Department of Photogrammetry and Surveying at UCL and used for DEM creation, accepts random, grid node data, gridded data with different grid spacing, or combination of random and gridded data. The software cannot properly deal with data of different reliability or data from different sources (assuming different accuracy) because the user can not supply weights to the input data according to their accuracy.

Therefore the data have to be merged during the manipulation stage. The

merged sets of data were derived from two different sources, the aerial photography and the SPOT satellite imagery. It is obvious that the derived data from aerial photography (more reliable source) are used as reference and the SPOT data (less reliable) were treated in respect to the aerial photography.

A Pascal program was written to merge the data before the use of the DTMCREATE package.

6.4.2.2. Description of the data merging algorithm.

This program merges the data captured from two different sources in two different ways (figure 6.2):

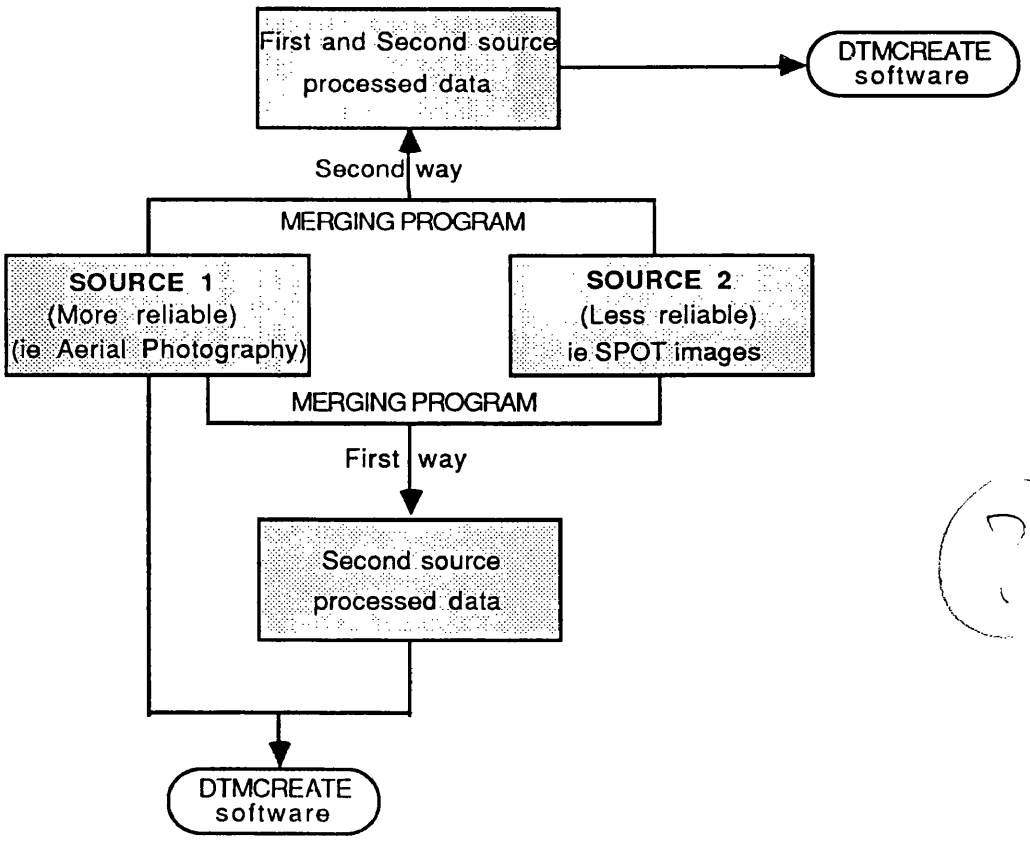

Figure 6.2. Two different ways of merging the two sources of data.

1. *First way of merging the two sources of data.*

The program reads the captured data of the first source (more reliable) from a file and the second source of data (less reliable) from another file. The first aim is to make the data of the second source equivalent in terms of reliability to the first data source. In this procedure the accuracy of the second data source is not going to be improved. However, the second source of data suitably weighted can be merged as being equivalent to the first source data.

This is carried out for each point of the second source lying in the first source defined cell as follows:

a. Estimation of the average height from the elevation of four first source neighbours. The simulated height (average) is assumed to be the elevation value of each of the four first source points.

b. Calculation of the planimetric coordinates of a simulated point lying in the centroid of this cell.

c. Estimation of the elevation value of the second source point taking into account the relative accuracy factors (RAF) for each source, the distance of the second source point to the centroid, and the distance of the centroid from the first source point (is constant equal to 21.21 m).

d. The simulated second source point has the planimetric coordinates of the centroid and the elevation value estimated in c.

The output files are:

a. The second source processed data.

b. The superfluous second source data which lie outside of the first source data defined DEM block.

2. *Second way of merging the two sources data.*

The program reads the second source captured data (less reliable) from a file and the data of the first source (more reliable) from another file. The second aim of the program is to merge the second source data and the first source data into one file, taking into account the data quality in relation to the source. This way of merging the two sources of data is followed in this project.

This is carried out for each of the four first source points surrounding a second source point as follows:

The elevation for each of the four first source elevation neighbour points surrounding a second source point is estimated by taking into account the relative accuracy factors (RAF) for each source and the distance of this point to the second source point. The situation it is not easy because some first source points can be affected by one, two, three or four second source points (see appendix E.6.1 and E.6.2).

The output files are:

a. One file which contains the processed first source data by taking into account the second source data (one output file which contains the processed data of the two input files).

b. The superfluous second source data which lie outside of the first source data defined block, as described above for the first way of merging the data.

Note:

The first file should contain data captured in a regular grid. It does not matter whether or not the data of the second file lie in a regular grid or if they are random points.

The program can also merge data from the same source ie. data in a regular grid and random data. These two sets of data can be merged into one output file. In this case the weights could be Weight1=1.0 and Weight2 = 1.0, because the data are coming from the same source, unless the user wants to give more reliability to the random data.

The program asks the user for:

1. The first source data file name.
2. The second source data file name.
3. The output processed second source data file name.
4. The output superfluous second source data file name.
5. The output processed first source data file name.
6. The output superfluous second source data file name.
7. The first source matrix number of rows.
8. The first source matrix number of columns.
9. The first DEM captured grid interval.
10. The second source total number of points.

11. The relative accuracy factor (RAF) or weight of the first source data.
12. The relative accuracy factor (RAF) or weight of the second source data.

The estimation of the relative accuracy factors is presented in § 6.4.3.

The program implements a local interpolation algorithm in order to merge the two sets of data (which can be grid and random points). It keeps the reference grid matrix, and it merges the values of the grid nodes and the random data, with the additional and very important option for the two data sets to be weighted.

6.4.3. Estimation of the relative accuracy factors.

The choice of the accuracy factor (relative or absolute) as the basis for the source categorisation is questionable. For some experiments this could be estimated empirically and in others after an extensive statistical analysis. The accuracy factor could be generally representative for the particular source of data. However, this is not possible because of the variable conditions under which each experiment is carried out. So a small variation in the accuracy factor should be expected.

In this work the relative accuracy factor (RAF) was estimated from the calculated standard deviation of random error for each source. It made a serious effort to ensure that the estimation of the RAF between the two sources is as representative as possible, so an extensive statistical analysis was followed. For the aerial photography the standard deviation of random error, for data captured in stationary mode, was estimated to be 1.3 m (see § 5.2.3.3). As the aerial photography in this experiment is the high resolution source the relative accuracy factor (RAF) is assumed to be 1.0.

For the SPOT data captured in stationary mode, the standard deviation of random error was found to be:

a. 15.82 m in the first used SPOT hard copy after statistical analysis of 6833 points.

b. 13.13 m in the first used SPOT hard copy after substituting the

measurements made subsequently by the experienced operator (2124 points).

c. 12.75 m in the second used hard copy after statistical analysis of 2936 points.

Taking into account the number of points (as weights) the SPOT accuracy factor is estimated to be 0.095 or ~ 0.10.

So in this work the RAF (weight) of the first source data (aerial photography to scale 1:30,000) was taken 1.0, whereas the RAF (weight) of the second source (SPOT imagery scale 1:400,000) was estimated to be 0.1.

6.4.4. The data merging experiment.

In the following experiment the program merges the first source data in 30 m grid interval with the second source data (described in § 6.4.2.2).

A modification of the elevation checking and statistical analysis program (see appendix B) allowed a point-to-point comparison by using the initial aerial photography data and the merged data.

The two data sources are merged twice and processed statistically in an independent procedure. The first merge used RAF of 1.0 for the aerial photography and 0.1 for the SPOT data and the second merge used 1.0 and 1.0 for the two RAFs respectively. That means that in the second merge the SPOT data are considered to have an equivalent accuracy as the aerial photography data.

The statistical results of merging the two different data sources in a 30 m grid interval appear in table 6.10.

In the third column of table 6.10 appear the number of aerial photography and the number of the SPOT points merged together. This number of points is the same for the two independent merging procedures (using RAF 0.1 and 1.0 for the SPOT data).

In the fourth column appear the number of merged points which have a

difference in elevations greater than +/- 20 m (20 m is an arbitrary chosen upper/lower limit).

In the seventh and eighth columns appear the points with the minimum and maximum elevation difference after the two sources merging procedure and the comparison with the initial aerial photography data.

In the last four columns are presented the statistical results of this comparison.

BLOCK NAME	SPOT DATA WEIGHT	NUMB OF COMPAR POINTS AER PHOT / SPOT	POINTS WITH -20 >= HEIGHT_DIF >= 20	AREA MEAN HEIGHT (m) FIRST SOURCE	AREA MEAN HEIGHT (m) SECOND SOURCE	ELEVATION DIFFERENCE MINIM (m)	ELEVATION DIFFERENCE MAX (m)	STATISTICAL RESULTS OF ELEVATION DIF. MEAN(m)	OF ELEVATION DIF. SD (m)	OF ABSOLUTE ELEVATION DIF. MEAN(m	OF ABSOLUTE ELEVATION DIF. SD (m)
1	0.1	3190	0	309.89	309.97	-2.50	2.93	-0.08	0.53	0.22	0.61
	1.0	202	0		310.34	-13.77	16.13	-0.45	2.91	1.22	3.36
2	0.1	9680	0	326.17	326.05	-2.77	8.52	0.12	0.80	0.27	0.89
	1.0	640	104		325.53	-15.24	46.86	0.64	4.43	1.49	4.91
3	0.1	8580	0	403.31	404.04	-4.99	6.60	-0.13	0.79	0.34	0.92
	1.0	598	55		404.65	-27.42	36.32	-0.74	4.32	1.85	5.04
4	0.1	3960	0	422.62	422.54	-3.34	5.96	0.08	0.81	0.33	0.85
	1.0	286	45		422.18	-18.40	32.78	0.44	4.47	1.81	4.68
5	0.1	1980	0	485.20	485.28	-3.78	3.55	-0.08	0.48	0.20	0.56
	1.0	157	2		485.65	-20.79	19.51	-0.46	2.65	1.08	3.06
6	0.1	8370	0	535.60	535.88	-8.88	8.34	-0.28	0.88	0.38	1.10
	1.0	664	114		537.15	-48.85	45.89	-1.55	4.82	2.08	6.03
7	0.1	7920	0	545.93	546.24	-8.61	5.67	-0.30	1.15	0.55	1.43
	1.0	648	195		547.61	-47.35	31.21	-1.67	6.31	3.04	7.87
8	0.1	2520	0	515.24	515.01	-5.03	6.15	0.22	0.79	0.37	0.80
	1.0	243	19		514.02	-27.69	33.83	1.22	4.32	2.06	4.40

Table 6.10. Statistical results of the merging of the two data sources in 30 m grid interval. Aerial Photography RAF (weight) = 1.0

As we can clearly see when the RAF for the SPOT data is 0.1 the effect of the SPOT data on aerial photography data is not significant. That means that the SPOT merged data do not affect seriously the aerial photography data. However, when the RAF used for the SPOT data is 1.0, the effect is significant.

From table 6.10 it is easy to verify that the SPOT data are less accurate than the aerial photography data by a factor 0.10 (as it was estimated before). The statistical figures shown in table 6.10 agree with the statistical figures shown in table 5.1. In particular the 6th and 7th SPOT DEMs have accuracy problems as was pointed out in the statistical analysis results shown in table 5.1. These blocks transfer the problem to the aerial photography merged data as it is clearly shown from the large number of the points with -20m >= Height difference >= 20m.

In conclusion when SPOT data have to be merged with aerial photography data to scale 1:30,000, the SPOT data are less accurate than the aerial photography data by a factor 0.1.

From table 6.10 the overall statistical results can be estimated. The two data sources are merged for a third time with an RAF of 1.0 for the aerial photography and 0.5 for the SPOT data. The statistical analysis results are not presented. However, those results were used in order to estimate the overall statistical values.

The overall statistical results for the SPOT data merged with RAF of 0.1, 0.5 and 1.0 respectively are as follows:

1. For the SPOT data with RAF = 0.1 (Aerial photography data RAF = 1.0)
mean = -0.10 m , standard deviation = 0.87m and absolute mean = 0.36m
2. For the SPOT data with RAF = 0.5 (Aerial photography data RAF = 1.0)
mean = -0.37 m , standard deviation = 3.17 m and absolute mean = 1.33m
3. For the SPOT data with RAF = 1.0 (Aerial photography data RAF = 1.0)
mean = -0.54 m , standard deviation = 4.74 m and absolute mean = 1.97m

From the overall statistical results (3 values) we can draw the following figure which summarises the effect of the second source on the first source:

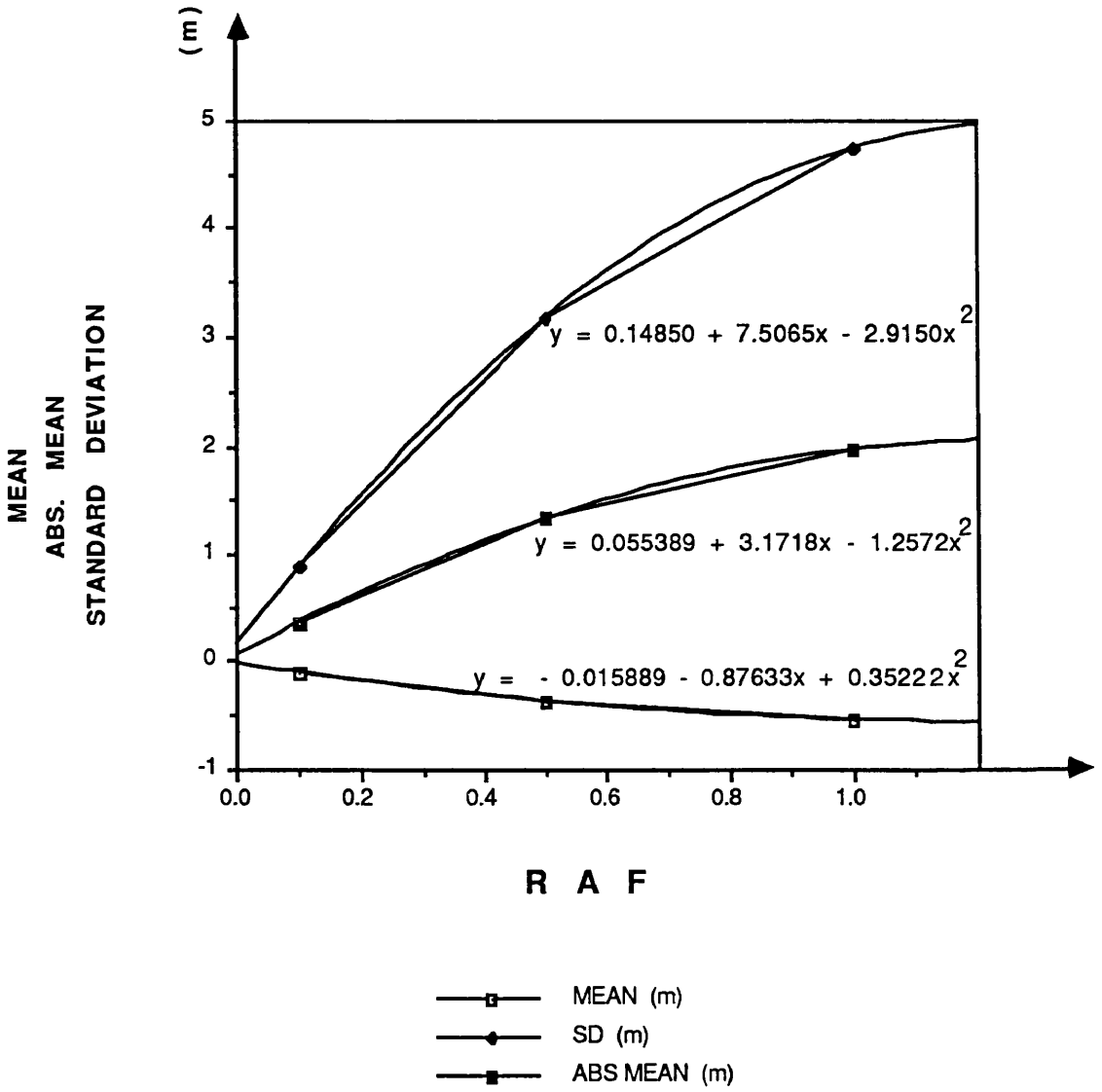

Figure 6.3. Overall statistical curves for different values of RAF.

By fitting a second degree polynomial to the known values (the equation for each statistical value is presented in figure 6.3), we can estimate the effect of the second source data on the first source data for any RAF (RAF <= 1.0).

6.4.5. Discussion and conclusions of the data merging procedure.

Elevation data from different sources exist in almost every application. Sometimes it is possible that two sets of data exist from the same source, but these

can be of different reliability due to the different scale (ie. data digitised from different scale maps or different scale aerial photography) or capture method. In addition, two sets of data can exist from the same source (ie. grid and random points) and the user wants to merge them into one set. Commonly one set of the elevation data (ie. produced by digitisation of contour maps or captured from aerial photography) is larger than the other.

As the data derived from the digitisation procedure are less accurate than from the same scale aerial photography captured data, when these two sets have to be merged the relative accuracy of the one source to the other has to be taken into account.

In this project SPOT and aerial photography data are merged. A merging algorithm was developed which merged the data from the two sources without destroying the grid normality. This presupposes that the data of the one source should be in a normal grid. This algorithm implements a local interpolation algorithm in order to merge two sets of data.

The relative accuracy factor RAF of the SPOT data is estimated to be 0.1, while the aerial photography data source (more reliable) was taken as 1.0.

From all the above we can see that the data merging procedure is a controlled procedure, as from figure 5.3. we can predict the effect on the accuracy of SPOT data to the aerial photography data for any RAF (RAF <= 1.0).

6.5. Variable density DEM grid data. The data skipping program.

6.5.1. Purpose.

The figures given by Forstner (1983), Ostman (1987), Kostli and Wild (1984) and Balce (1986 & 1987) are well presented and documented (see § 2.4.5.6).

The variable grid spacing study which is carried out in this project, is to find out the accuracy of a DEM using a variable number of measured points, which

means a variable grid interval, but it also is concerned with reducing the number of points of one source and then merging this data with the other source.

The aerial photography data are captured in 30 m grid interval, while the SPOT data are captured in 100 m grid interval. In order to produce a less dense digital elevation matrix of data, it is not necessary to repeat the measurements, with the desirable grid spacing, but to skip data from the already existing data, in order to get the desired grid spacing.

6.5.2. Algorithm description.

A Pascal program was written which produces data in different grid intervals, from a dense data file, by skipping the necessary grid points eg. if there is a file with data captured in 30 m grid interval (in this work from aerial photography), it is possible through this program to produce output data files with grid intervals of 60 m, 90 m, 120 m and 150 m, simply by skipping the necessary grid points in the column-direction, and skipping an equal number of lines (points) in the row-direction.

The program asks the user for:

1. The input file name.
2. The output file name.
3. The total points number of the input file.
4. The number of the lines which the user likes to skip.

One restriction of this simple algorithm is that it will work only when the output number of rows and number of columns is an integer multiple of the input number of rows, columns and the output grid interval is an integer multiple of the input grid interval. This is necessary in order to have resulting data in a normal grid.

6.5.3. The data skipping experiment.

In the following experiment the aerial photography data was produced in a sparse form (60 m grid interval) by the data skipping program. The sparse aerial photography data were used as input to the data merging program. The merging program takes as input the first data source (reformatted in a 60 m grid) and the second data source (see § 6.4.2.2).

These two sets of data are processed statistically by the modified elevation checking and statistical analysis program (see appendix B) which allowed a point to point comparison by using the initial aerial photography data and the merged data.

The two data sources are merged twice in an independent procedure. The first merge used RAF of 1.0 for the aerial photography and 0.1 for the SPOT data and the second merge used 1.0 and 1.0 for the two RAFs respectively. That means that in the second merge the SPOT data are considered to have an equivalent accuracy as the aerial photography data.

By doubling the grid interval, the number of rows and columns are each halved. Therefore the number of compared aerial photography points is reduced by a factor of 4, except in the first block (29 rows x 110 columns) and the sixth (93 rows x 90 columns) in which the last row was rejected in order the number of rows is even and therefore divisible by 2.

The statistical results of merging the two different sources data in a 60 m grid interval are shown in table 6.11.

BLOCK NAME	SPOT DATA WEIGHT	NUMB OF COMPAR POINTS AER PHOT / SPOT	POINTS WITH -20 >= HEIGHT_DIF >= 20	AREA MEAN HEIGHT (m) FIRST SOURCE	AREA MEAN HEIGHT (m) SECOND SOURCE	ELEVATION DIFFERENCE MINIM (m)	ELEVATION DIFFERENCE MAX (m)	STATISTICAL RESULTS OF ELEVATION DIF. MEAN(m)	OF ELEVATION DIF. SD (m)	OF ABSOLUTE ELEVATION DIF. MEAN(m)	OF ABSOLUTE ELEVATION DIF. SD (m)
1	0.1	770	0	306.99	307.22	-2.31	2.67	-0.22	0.77	0.53	1.08
	1.0	177	0		308.21	-12.72	14.69	-1.22	4.26	2.93	5.95
2	0.1	2420	0	325.28	324.95	-3.22	7.76	0.33	1.31	0.75	1.37
	1.0	640	80		323.46	-18.25	42.70	1.82	7.19	4.14	7.56
3	0.1	2145	0	403.35	403.66	-5.60	7.84	-0.32	1.25	0.87	1.73
	1.0	572	35		405.10	-30.81	43.09	-1.75	6.88	4.80	9.50
4	0.1	990	0	421.25	421.15	-4.05	5.84	0.10	1.30	0.83	1.49
	1.0	260	33		420.68	-22.27	32.15	0.58	7.13	4.56	8.17
5	0.1	495	0	482.92	483.26	-5.25	3.55	-0.35	1.03	0.67	1.45
	1.0	157	10		484.83	-28.89	19.50	-1.91	5.66	3.67	7.95
6	0.1	2070	0	529.24	530.08	-10.89	8.34	-0.83	1.44	1.10	2.41
	1.0	664	86		533.83	-59.92	45.88	-4.59	7.90	6.08	13.27
7	0.1	1980	0	547.98	548.83	-6.39	5.52	-0.86	1.85	1.59	3.07
	1.0	648	150		552.70	-35.13	30.35	-4.72	10.18	8.74	16.88
8	0.1	630	0	511.32	510.69	-4.23	5.85	0.62	1.25	0.97	1.30
	1.0	216	18		507.89	-23.25	32.17	3.43	6.87	5.35	7.13

Table 6.11. Statistical results of the merging of the two data sources in 60 m grid interval. Aerial Photography RAF (weight) = 1.0

The structure of table 6.11 is similar to that of table 6.10 (§ 6.4.4).

As we can clearly see when the RAF for the SPOT data is 0.1 the effect of the SPOT data on the aerial photography data is not significant compared with the case when an RAF for SPOT data of 1.0 is used.

Again the 6th and 7th SPOT DEM blocks transfer the problem to the aerial photography merged data as is clearly shown from the large number of points with -20m >= Height difference >= 20m.

From table 6.11 the overall statistical results can be estimated. The overall statistical results for the SPOT data merged with RAF of 0.1 and 1.0 respectively

are as follows:

1. For the SPOT data with RAF = 0.1 (Aerial photography data RAF = 1.0)
mean = -0.30 m , standard deviation = 1.41 m and absolute mean = 1.01m
2. For the SPOT data with RAF = 1.0 (Aerial photography data RAF = 1.0)
mean = -1.67 m , standard deviation = 7.75 m and absolute mean = 5.56m

The statistical overall figures given on the data skipping experiment with those estimated from the data merging experiment (§ 6.4.4) are shown in table 6.12:

		Statistics	Grid Spacing		Times of deterioration
			First source 30 m Second source 100 m	First source 60 m Second source 100 m	
Relative Accuracy Factor	Aerial Phot 1.0 SPOT 0.1	Mean (m)	-0.10	-0.30	3.00
		SD (m)	0.87	1.41	1.62
		Absolute Mean(m)	0.36	1.01	2.81
	Aerial Phot 1.0 SPOT 1.0	Mean (m)	-0.54	-1.67	3.09
		SD (m)	4.74	7.75	1.64
		Absolute Mean(m)	1.97	5.56	2.82

Table 6.12. The statistical overall figures of the data merging experiment with the data skipping experiment.

6.5.4. Discussion and conclusions of using variable dense DEM data.

The variable grid spacing study which is carried out in this project is concerned with reducing the number of points of the most reliable source (aerial photography) and then to merge this data with the SPOT data.

The grid interval is reduced from 30 m to 60 m by skipping the necessary grid points in the column-direction, and skipping an equal number of lines (points) in the row direction. By doubling the grid interval, the number of rows

and columns are each halved. Therefore the number of aerial photography points is reduced by a factor of 4.

The aerial photography data produced in the sparse form (60 m grid interval) were merged with the SPOT data (100 grid interval). The statistical analysis results of merging these two different sources showed that the mean value was made 3 times worse, the standard deviation 1.6 times worse and the absolute mean value 2.8 times worse.

The proportion between the weighted SPOT data with weight 0.1 and 1.0, merged with aerial photography data with 30 m grid spacing and with 60 m grid spacing remained the same.

6.6. Data structure.

6.6.1. General.

The design of a data structure is far too important to leave to chance or to pursue haphazardly. For almost all applications a poorly designed data structure can result in the failure of the application: the structure may be too inflexible to allow some data manipulations, the manipulations may be too costly in run time or in storage space, the data structure may not be transferable to an updated hardware system, or in the worst case the manipulation routines may never function correctly because of obscurity and unnecessary complexity in the data structure.

Data structure is the logical arrangement of data as used by a system for data management; a representation of data model in computer form.

Data model is an abstraction of the real world which incorporates only those properties thought to be relevant to the application or applications at hand. The data model would normally define specific groups of entities, and their attributes and the relationships between these entities. A data model is independent of a computer system and its associated data structures. A map is one example of an analogue data model (Committee on enquiry into the handling of geographic information, 1987).

A data structure in a vector file format has to be flexible and representative. The user should be able to generate and to manipulate the file structure and contents. Within this file the components should be built in a flexible hierarchical structure. Finally structure is essential for efficient cartographic production flowline planning and management.

6.6.2. Data format.

Two features are involved in mapping, the different geodetic parameters (projection, ellipsoid, datum) and the data format. A standard geoid may be one concern for standardisation (see § 6.2.2). Most distributed DEM data are distributed on Computer Compatible Tapes, stored as regularly sampled data on a fixed map grid. Those data are available to the users not only in national but very often on a worldwide scale. Therefore it is necessary to be able to handle the data without problems. Problems do not occur and data compatibility is one of the most serious problems in the application of computers because although the format standardisation problem seems to be very simple, it is not. In theory it is easy to define a worldwide unique data format, but in reality it is very difficult, because of the different user requirements and the different software available for data manipulation and processing.

6.6.3. Data storage format.

As elevation model accuracy increases, efficient storage, transmission, and indexing mechanisms become more important to the utilisation of the elevation data. There are several alternate storage methods for elevation data. Tessellation, the definition of polygons whose vertices are known feature heights, is one method that saves storage costs, the most popular being triangulation. Irregular sampling holds promise as well, a technique whereby there are more feature points near the areas of greatest terrain variation. Terrain modelling, in which a mathematical model of the terrain is derived, may also be an effective manner of storing elevation data as well as an efficient scheme for further numerical processing.

Digital elevation can be stored in a vector format obtained by digitisation of

map contours. Measures such as slope and visibility may be obtained from this data, but the algorithms required are often complex, and computation time high. A DEM that provides data in a raster or grid format, lends itself to the development of software that is able to efficiently exploit the elevation information, often using relatively simple operations repeatedly applied to the data, and achieving relatively high processing rates.

6.6.4. Data representation.

Data representation is of importance in the context of media storage capacity that has to be allocated for any particular application. By media is meant computer compatible technology eg. disc or tape.

Consider a regular 100 m grid at ground scale. This grid will be equivalent to approximately 100/400,000 = 0.00025 m = 0.25 mm at SPOT image scale.

Assuming a 150 X 150 mm^2 SPOT image. A single model (there is no overlap to the SPOT images) will yield 4 points in 1 mm.

4 points * 150 mm = 600 points. In two dimensions this is 600 points * 600 points = 360,000 points.

If X, Y, Z values are all recorded, there will be 360,000 points * 3 values = 1,080,000 data entries per SPOT model excluding identification numbers such as: point number and the headings such as : model number, scan line number etc. At 4 bytes per single precision word for computer storage this is equal to 4,320,000 bytes per SPOT model. If a word takes 32 bits for single precision there will be 138,240,000 bits required per model.

6.6.5. Data changing format.

In this work, all data was produced and manipulated only for the project purposes. That means that there are no data provided from other sources or organisations. Although the data was produced and manipulated only for the project purposes, the number of data formats used was quite significant. The different output formats were as follows:

1. The count number - string of coordinates, which is the output of the Kern DSR 1 through the DEM generation program (see § 3.2.1.2.1).

2. The Internal Feature Format (text form), which the count number - string of coordinates data have to be transferred (see § 6.6.6).

3. The Internal Feature Format (binary form). Is the Internal Feature Format (text form) transferred to binary form in order to be acceptable by the Laser-Scan DTMCREATE software. In IFF form can also be files created from DTICONTOUR module. These contain interpolated contours from points in a regular grid stored in a DTI format.

4. The Digital Terrain Image (DTI) format (binary form). It is used mainly for display purposes (word data) or as a stage for further processing (real data). Data in DTI format can be produced from the TRIGRID module of the DTMCREATE package, the NE1.FOR program (see § 2.4.3.2.2) and the SLOPE.FOR program which reads a DTI file and writes the calculated gradient and aspect in DTI form (see § 2.4.3.2.2 and appendix A).

5. The strings of elevations format (text file) output from DTI2TEXT module, after transferring a DTI file to a text file.

6. The rows, columns, heights format output from the DTITEXT.PAS program after transferring the strings of elevations in: rows, columns, elevations.

The above presentation includes only the creation of files in the primary stage It does not include created files in secondary procedures or processes.

6.6.6. The Internal Feature Format (IFF).

The data before the processing stage using the Laser- Scan software DTMCREATE should be in a special layout and the entries should have a pre-specified order. Internal Feature Format (IFF) in text form is a unique format used in digital cartography. It is adopted in order to adequately record not only elevation information, but digital map data.

A Pascal program is written to change the data format from string of coordinates, output from the Kern DSR1, and after the projection transformations, to the IFF format (text form). Text form IFF files (*.TXT) are still in ASCII form and it can be manipulated directly using a text editor. On the contrary in the later

stage the IFF files processed by the module IFROMTEXT (*.IFF) are in binary form and they can not be manipulated directly using a text editor.

The IFF file structure is broken down into Maps, Sections, Layers, Features and Entries.

The internal feature text file structure contains briefly the following information:

1. Entries at File Level.

File level represents the highest division of data within the hierarchic IFF structure. All data within an IFF file share a common range entry which describes the minima and maxima in X and Y. The data in the file are also considered to share a common production history.

2. Entries at Map Level.

In historical IFF files the map level was used when there is a need for holding different maps within the same file. The main reason for this was for edgematching of multiple maps in the (now obsolete) LITES cartographic editor. As the LITES2 cartographic editor can read multiple IFF files, this requirement in no longer valid. IFF files must contain at least one map within the hierarchic structure of the file.

3. Entries at Section Level.

Sections are used to separate the data resulting from different digitising sessions. Such data may all be part of the same map, but the coordinate system used in one section will not necessarily be the same as that of another (due to the map being repositioned between sessions).

4. Entries at Layer Level.

LITES2 editor enables IFF files containing many layers to be edited. Layers offer the user great flexibility in data classification and division within a single IFF file. The feature codes contained in all IFF features may be used to further subdivide the data within the layers.

5. Entries at Feature Level.

The precise content of features varies with the type of feature. IFF features can contain 2D or 3D strings and must contain at least one ST, ZS, or CB entry (see appendix G). Features may not contain a mixture of these entries.

The order in which IFF entries occur within each level is given in appendix G.

6.6.7. Conclusions on the data structure.

Nowadays the commercially available packages lead the way and the user simply has to follow the data structure which is recommended. In this work the data output from the analytical plotter (count number, string of coordinates) have to be transformed to the Laser-Scan Internal Feature Format (IFF) text form, then to IFF binary form in order to be acceptable input to the DTMPREPARE - DTMCREATE package.

6.7. Conclusions on the manipulation of the DEM data.

The data manipulation stage includes a large number of procedures. Data has to be transformed into a unique coordinate transformation system, having the minimum possible error, and suitably structured.

In the data manipulation stage the captured data has to be arranged, examined and processed with different methods Some of the data manipulation stages, methods and techniques which are examined are the follows:

Data smoothing -filtering procedure.

The effect of data smoothing-filtering procedure was showed by using a low pass filter. Filtered SPOT data was used only for displaying purposes.

Coordinate transformation stage.

Coordinate transformations have a great significance for mapping due to the planimetric error which is introduced. Three coordinate transformation stages have been used in this project (control points transformation stage, output of coordinates from the analytical plotter stage and data manipulation stage) with two transformations in each stage. The transformation error accumulated in all the transformations (6 transformations) is Dx=0.02 m ; Dy=2.48 m and Dz=0.00 m. For the project requirements the results are acceptable. If it is necessary to obtain better results an iteration loop should be used in the UTM to geographical stage in order to minimise the approximation errors in the calculations of latitude and longitude.

Blunder detection method and technique.

A data capture procedure involves gross, systematic and random errors.

Random errors were estimated in chapter 5 (Accuracy of captured data). In the same study significant systematic errors were found in the SPOT DEM data. An analysis of those errors showed some of the reasons.

In this chapter a blunder study showed that data captured manually from SPOT contain a large amount of blunders (5.7%. of the test data). A blunder analysis showed some of the causes of blunders. Blunder prediction and behaviour is a very difficult task and so far there is not a complete remedy. None of the applied techniques give fully satisfactory results.

A pointwise local self-checking blunder detection algorithm was developed. The algorithm was applied to the SPOT data but gave poor results (36% successful in blunder detection). This happened because of the "random appearance" of the systematic error as distinct from the observation random error. The author believes that local techniques are more suitable in blunder detection and the algorithm developed in this project could give much better results when used with a different source of data.

Data merging method and technique.

In the worldwide cartographic data bases, elevation data from different sources exists. Elevation data sets have sometimes to be merged into a single set, in order to produce a unique and of known accuracy contour map. A merging algorithm has been developed in this project. This algorithm merges data from two sources by implementing a local interpolation technique and the estimated relative accuracy factors of the one source to the other. Aerial photography (in 30 m grid interval) and SPOT data (in 100 m grid interval) merged. The whole merging procedure can be controlled and the final product can have accuracy which satisfies the requirements of project. Sparse aerial photography data (in 60 m grid interval) and SPOT data were merged and the accuracy effect of the SPOT data (less reliable source) on the aerial photography data (more reliable source) was estimated.

Data structure.

Data structure is very important for all the applications. Data structure for a particular situation should be : sophisticated, satisfactory in terms of memory requirements and processing speed. Nowadays the commercially available packages

lead the way and the user simply has to follow the data structure which is recommended. In this project the Laser-Scan DTMCREATE software leads the data to be transformed to the Internal Feature Format (IFF) form and then to IFF binary form in order to be ready for further processing.

Chapter 7.

Accuracy of the DEM.

7. Accuracy of the DEM.

7.1. General.

Accuracy standards are an inherent part of any mapping agency's production programme. Conventional cartographic relief models are assessed separately for vertical errors and for horizontal or planimetric inaccuracies of the cultural detail and are graded accordingly; it is assumed that the horizontal error of the relief portrayal is generally the same as that of the detail. These give insights into those parameters which govern accuracies of DEMs and enable proposals to be put forward for a series of consistent vertical and horizontal standards related to DEMs. The assessment of vertical accuracies is relatively straightforward but to assess the horizontal component separately is conceptually more difficult and far more time consuming. A number of different methods were advocated for both types of error, each processing advantages and disadvantages.

However, an alternative solution to accuracy assessment is to combine the vertical and planimetric errors and produce a measure of morphological fidelity. Initial work has shown that a comparative measure of mean slope combined with the vertical error of the DEM may provide a more comprehensive assessment of the model's quality; further work is required (Ley, 1986).

The term accuracy related to DEM's means many things to different people. It would be appropriate to define accuracy in terms of geomorphological quality, precision of information, positional accuracy, data commonality, data compatibility, and compression (representation). See Marshall and Faintish (1984).

Geomorphological quality of a DEM is the degree to which the DEM represents the actual landform. This concept is extremely difficult to define quantitatively. It considers all of the statistically measurable quantities of the DEM as well as the visually apparent anomalies, texture, and fit to the actual landform. Forstner (1983) presents a good discussion on the effect of sampling interval and form of data collected on the quality of a DEM. He presents evidence that demonstrates that slope and curvature information are extremely important in the quality of a DEM. However, it is remarkable that most DEM production systems do not collect this

information.

The precision of the data described by a DEM is a statistical representation of the primarily random error or noise in the model. Precision is generally determined by statistical comparison of related measurements and relates to the quality of the production process. It should be borne in mind, though, that the precision measure is not the accuracy measure.

The positional accuracy of a DEM is a measure of all errors with respect to a fixed (absolute) or relative (local) coordinate system. Such errors include horizontal and vertical displacement, rotation of axes, and non-linear differential scaling / warpage in any direction.

Data commonality is the degree of congruence between different DEM's (ie. the degree to which two DEM's have the same parameter values for the same geographical location).

Data compatibility is the degree of agreement between different DEM's (ie. the degree to which two DEM's have parameter values within the precision tolerances of each other for the same geographical location).

Compression (representation) error. Once the DEM information is compiled, further processing may add additional errors into the DEM when it is compressed or reformatted.

Photogrammetric DEMs have the advantage that the form relies upon rigorous mathematical computation based upon the geometry of the sensor and the terrain, but it relies upon an approximation model for representing the surface. Photogrammetric DEM's suffer from additional instrument and processing errors however, they could still be better mathematically modelled and controlled. Another significant problem in the photogrammetric production of DEM's is the "bald earth" problem. The inability of the photogrammetric measurements in measuring the "bald earth" needs to be considered in all DEM accuracy estimates (see §5.2.4.2.7).

The relative accuracies of elevation values as derived by various surveying

techniques, categorisation and the accuracy factors (AF) are presented in § 5.1. In paragraph 6.4.3. are presented the relative accuracy factors (RAF) for the aerial photography and the SPOT elevation data.

It is clear that the fidelity of the elevations derived by different techniques can vary substantially. For small scale visualisation applications (such as flight simulation), these inaccuracies in the absolute values in the database may be relatively unimportant provided that the dataset is free from gross errors and the relative heights of points are within an acceptable tolerance. As long as these limitations in accuracy are recognised by and are acceptable to users then lower quality data are tolerable.

In the following paragraphs the morphological fidelity (accuracy assessment of combined planimetric and vertical errors) of the DEM derived from SPOT data is examined. Data commonality and compatibility are also examined as two DEM data for the same area derived in an independent way from two different sources were merged together in one data set.

7.2. Accuracy considerations.

Some research (eg. Torlegård et al, 1984; Balce, 1986 & 1987) considers DEM accuracy as a subject for the whole production procedure because, as with any survey measurement, an accurate assessment of the accuracy of the observed data is vital. This assessment can be carried out theoretically by using the theory of error analysis and error propagation, or can be done experimentally. Whatever the situation, to assess DEM data, one must consider the required accuracy of the end product, and the method(s) of observing and of data processing. Accuracy of the end product here means the accuracy of the interpolated terrain elevation data. Accuracy of DEM data can be measured at two levels: data acquisition stage and data processing stage.

The accuracy consideration of the DEM, as a subject for the whole production procedure, depends on a series of parameters such as:

1. Terrain type
2. Surface structure of the terrain.

3. Type of measurement or measurement method (on the fly eg. contours, or static measurements eg. progressive, selective sampling, profiles, grids).
4. Density of measured points, if random points, or DEM grid width.
5. Quality of information source (eg. photographs, SPOT etc.).
6. Flying height and B/H ratio. The larger the B/H, the more precise the DEM can be.
7. Instrument and operator precision.
8. Number, location (distribution) and accuracy of control points.
9. Setting up procedure (interior and exterior orientation).
10. Interpolation method used to compute the terrain model between the measured points.

Some of these parameters should be varied in an experiment and others will be constant. Terrain type, type of measurement and point density are examined in chapter 2. Quality of information source and instrument precision are examined in chapter 3. Accuracy of control points and setting up procedure are examined in chapter 4, while the accuracy of the SPOT elevation data is estimated in chapter 5. In this chapter the surface structure of the terrain, the interpolation method used to compute the terrain model between the measured points and density of measured points are examined.

The relative accuracy of the data points in the data capturing procedure depends on:

a. The quality of the instrument.
b. The quality and the scale (flying height) of the image.
c. The terrain type (surface structure).
d. The human operator.
e. The selection and distribution of points on natural surface.

On the other hand some of the researchers (eg. Leberl, 1973; Jacobi, 1980; Ley, 1986 and Kubik, 1988) ignore the source, the implementation used and the operator. The problem of the DEM accuracy is separate from the accuracy problem of the set up of the model in the analytical plotter.

Jacobi (1980) and Ley (1986) give an accuracy consideration in which the

accuracy of a DEM depends on the following main factors:

1. The selection and distribution of points on the natural surface (sampling density and pattern) whose coordinates are measured.
2. The mean square error of measuring method (accuracy of the recorded heights).
3. The method of interpolation.
4. The terrain type and the surface structure of the terrain.

The influence of these factors on the performance of a DEM are shown in figure 7.1.

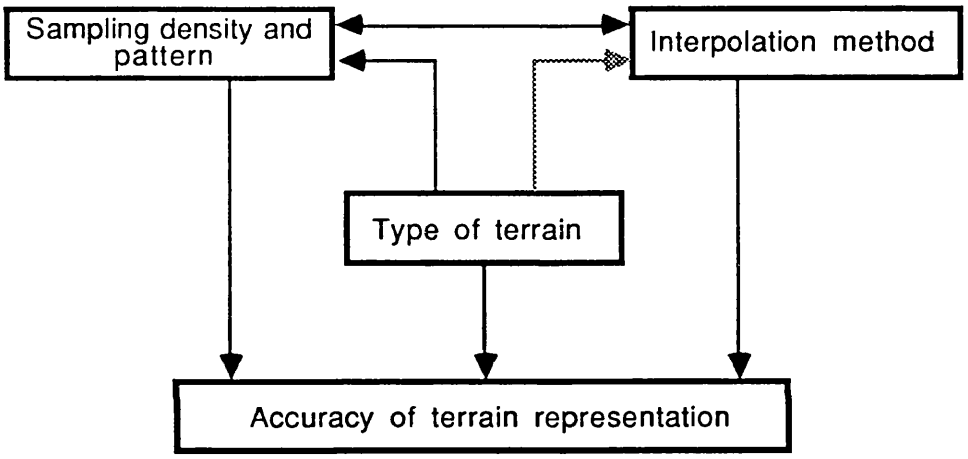

Figure 7.1. Factors influencing the performance of a DEM.

In this project the error introduced during the data capturing procedure is estimated and fully studied in the second, third, fourth and fifth chapters. Therefore in the following paragraphs it is assumed that DEM accuracy is separate from the accuracy problem of the model set up in the analytical plotter , as the accuracy of the 'raw' DEM data is known.

The methods of assessing the accuracy of a DEM are experimental and analytical.

The experimental methods are the direct survey, and the photogrammetric methods. These are classical methods of checking the vertical accuracy of a random sample of the area or of random selected points. Some of these methods are: differential levelling, trigonometric levelling, inertial surveying, global

positioning systems (GPS) or airborne laser profiling.

The analytical methods provide a check only on the accuracy of interpolation (σ_{int}), which depends primarily on the spacing of sampled elevations and to a lesser extent on the mathematical stochastic models used for interpolation. The analytical methods are, least squares, Fourier transforms, variograms and transfer functions. In fact these techniques, apart from least squares, may be used for determining the optimal sampling interval for grid DEM sampling (see § 7.5.1).

One final accuracy aspect is given by Ackermann (1979) who considered accuracy as being two independent problems:

1. The vertical accuracy of the original and derived DEM points proper, and
2. The problem of how well the points define or represent the ground surface.

7.3. Influence of the terrain structure.

The accuracy of a digital elevation model depends primarily on the properties of the terrain surface and on the spacing of the measured points. (Jacobi, 1980). Terrain type is a factor of great importance in determining the standard deviation of a digital elevation model.

7.3.1. The semivariogram.

Profiles and contours of the terrain may exhibit a very complicated geometry which is too complex to be analysed by standard deterministic methods. The variations of the terrain profiles or the contour lines may seem unpredictable for mathematical treatment, but the behaviour is not entirely random, so in analysing the data some systematic behaviour is usually revealed. A value at a terrain point is correlated, in a way dependent on the nature of the terrain, with the value at points nearby. By adopting a statistical approach we can produce useful numerical results from an analysis of these correlations.

The regionalized variable, has properties intermediate between a truly random variable and one that is completely deterministic. Regionalized variables are functions which describe natural phenomena that have geographic distributions, such as the elevation on the ground surface. Unlike random variables, regionalized variables have continuity from point to point, but the changes in the variable are so complex that they can not be easily represented as a deterministic function.

Even though a regionalized variable is spatially continuous, it is not usually possible to know its value everywhere. Instead its values are known only through samples, which are taken at specific locations.

The semivariance is used to express the rate of change of a regionalized variable along a specific orientation. It is a measure of the degree of spatial dependence between samples along a specific support. Estimating the semivariance involves procedures similar to those of time series analysis, hence the introduction of geostatistics at this point. The semivariance is a measure of the degree of spatial dependence between samples along a specific support.

The sample are point measurements of a property such as height to a subsurface horizon. The samples are uniformly spaced along straight lines (ie. in a profile or in a normal grid). If the spacing along a line is distance Δ, the semivariance can be estimated for distances that are multiples of Δ:

$$\gamma(h) = \sum_i^{n-h} \left(H_{(i)} - H_{(i+h)} \right)^2 / 2n \qquad (7.3.1.1)$$

Where i= 1, ... ,n and (H(i) - H(i+h)) are the he mean square of the differences which measures the relationship between sample values at distance h.

In this rotation H_i is a measurement of a regionalized variable taken at location i, and H_{i+h} is another measurement taken h intervals away. We are therefore finding the sum of the squared differences between pairs of points separated by the distance Δ_h. The number of points is n, so the number of

comparisons between pairs of points is n - h.

If we calculate the semivariances for different values of h, the easiest way to display these figures is in a graph. We can plot the results in the form of a semivariogram. That is, the distance between the pairs of samples is plotted along the horizontal axis and the value of the semivariogram along the vertical. By definition h starts at zero, since it is impossible to take two samples closer than no distance apart. The γ axis also starts at zero, since it is an average of squared values.

The semivariogram is one way of characterising variables which are partly stochastic and partly deterministic in their behaviour. The "semi" refers to the factor 1/2, but some authors sloppily call it a variogram. The variogram (since it varies with the distance and direction h), was introduced by Matheron (1971) and is now one of the basic statistical measure of geostatistics. It is used to express the rate of change of a regionalized variable along a specific orientation (to quantify the magnitude and extension of the various surface fluctuations). The terrain profiles should be sufficiently long to include the major surface fluctuation in their full extent. Terrain discontinuities have a significant influence on the variogram.

The variogram is related to the concept of self-similarity. Self-similarity means that for any curve or surface a portion of the curve or surface is geometrically similar to the whole. (Mandelbrot, 1967 & 1977). In other words variation in one is scale repeated at another.

The variogram for the terrain and the point spacing h of a self-similar curve are related by:

$$V(h) = k * h^{\beta} \quad (7.3.1.2)$$

where k : is the value of V(h) for the distance h = 1 unit (constant).

h : is the distance chosen to be the sample spacing used for the estimation of the variogram.

This has been proven from the theory as well as experiments to be of this form (Frederiksen et al, 1983 and 1986). On a log-log plot the variogram

appears as a straight line with slope β. The slope β tells about the roughness of the terrain.

The variogram of a rough surface has a slope close to zero, while a smooth terrain has a steep variogram. The parameters of the variogram are used to enter in formulae which relate sample spacing to accuracy of interpolation.

7.3.1.1. Interpretation of the semivariogram of the test area.

The semivariogram is a graph describing the expected difference in value between pairs of samples with a given relative orientation. If V(h) is zero, this implies that we expect no difference between grades a distance h apart. When the distance between sample points is zero, the value at each point is being compared with itself. Hence, all the differences are zero, and the semivariance for V_o is zero. If Δ_h is a small distance, the points being compared tend to be very similar, and the semivariance will be a small value. As the distance Δ_h is increased, the points being compared are less and less closely related to each other and their differences become larger, resulting in larger values of V(h). At some distance the points being compared are so far apart that they are not related to each other, and their square differences become equal in magnitude to the variance around the average value. The semivariance no longer increases and the semivariogram develops a flat region called a sill. The distance at which the semivariance approaches the variance is referred to as the range or span of the regionalized variable, and defines a neighbourhood within which all locations are related to one another.

The Aix En Provence (Montagne Sainte Victoire) grid elevation matrix, was measured manually from aerial photography at scale 1:30,000 . This is the basis of the experimental work in this project as it is considered as the "ground truth" in finding the SPOT heighting accuracy as a part of this project and the DEM accuracy as another. The aerial photography derived elevation measurements cover an area 87 km^2 in a 30 m regular grid. The area has not a canonical geometrical shape (see figure 5.4). The normal shape area is E-W size of 12420 m by N-S

size 6900 m (231 rows x 415 columns). The minimum elevation is 191.7 m and the maximum is 1011.0 m. For this area the calculated semivariance (experimental variogram) values are presented in appendix I.

The semivariance of elevations as a graph, representing all the Aix En Provence (Montagne Sainte Victoire) test area, is shown in figure 7.2 :

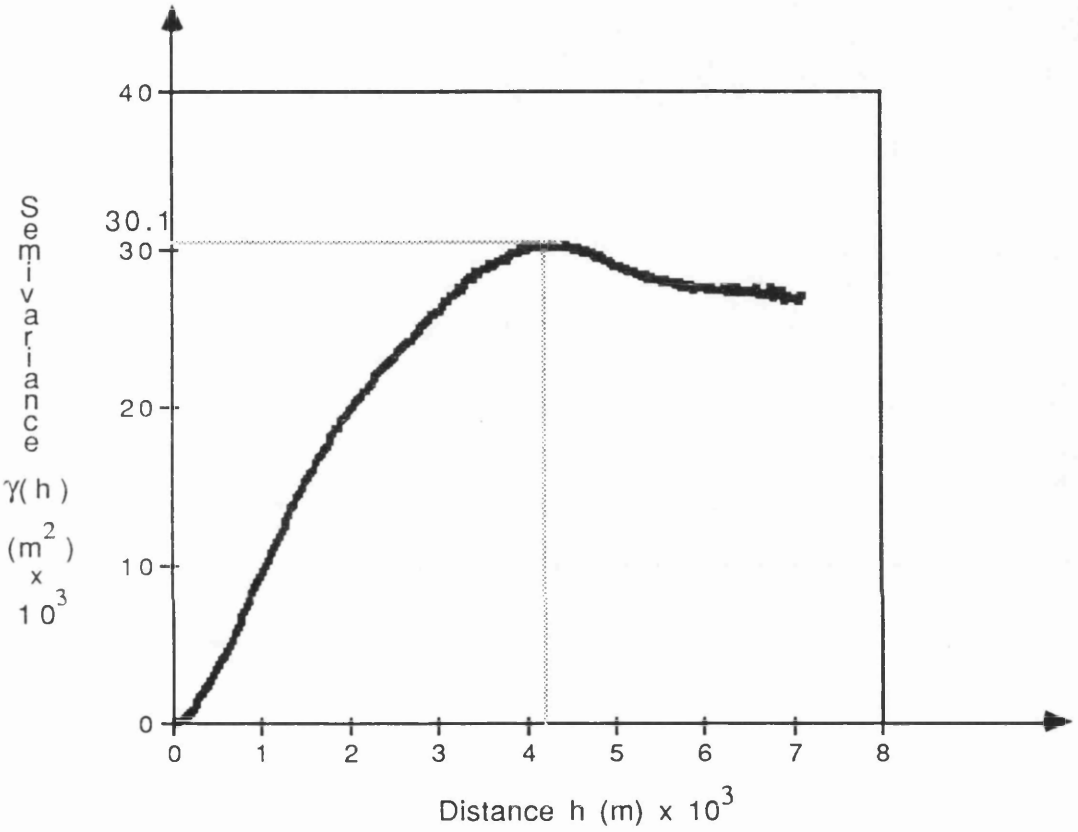

Figure 7.2. Semivariogram of elevations representing all the Aix En Provence test area.

The horizontal dotted line represents the sill, or variance of elevations, and is equal to 30,080 m^2. The range at the vertical dotted line is the distance beyond which difference between semivariance and sill is considered negligible and is equal to 4.15 Km

The variogram of elevations in a log-log plot, representing all the Aix En Provence (Montagne Sainte Victoire) test area, is shown in figure 7.3:

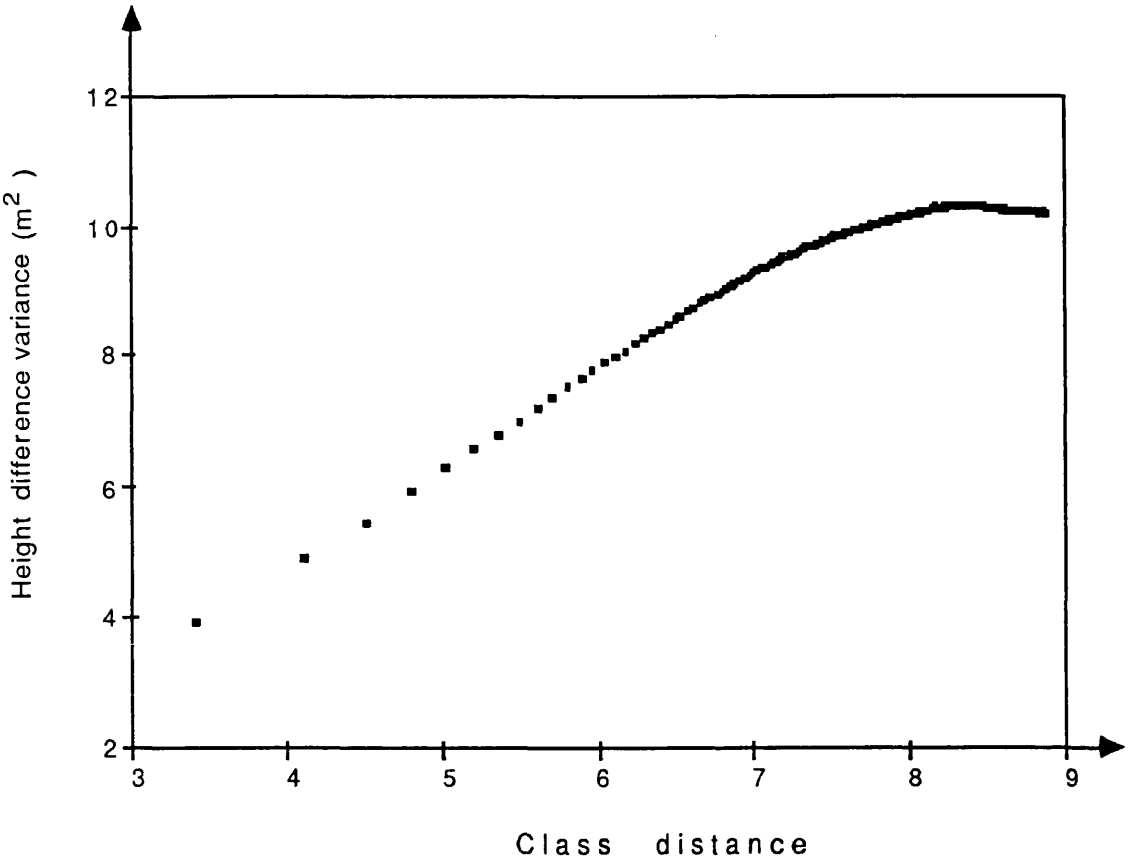

Figure 7.3. Variogram of elevations in a log-log plot,representing all the Aix En Provence test area.

As one can see for log class up to 7.5 the curve is almost linear (as expected from the theory). The turning point beyond this class is called a sill. From the slope β we can estimate the sample spacing including the discontinuities for a required accuracy of the elevation model σ_{mean} (Frederiksen & Jacobi, 1986).

When we compare the height of a stereomodel derived point (transformed to ground coordinates), with a DEM point some distance away, we are introducing an additional error because the terrain will vary increasingly with distance from the DEM point. We estimate the variance of this error from the variogram of the terrain (Frederiksen & Jacobi, 1986).

For the aerial photography 30 m DEM, by substituting the value of slope β (estimated from the variogram of figure 7.3) in equation 7.3.1.2, we can estimate

that the variance of the error variogram rises from 'zero' at zero planimetric distance to 74.5 m^2 at 21.2 m distance (the furthest a manually measured SPOT point can be from a DEM point on a 30 m grid). However, we do not observe this effect when we classify and test our manually measured SPOT points by distance from the point with which they were compared.

7.3.2. Fractals.

Fractal geometry is increasingly becoming accepted as a basis for the modelling of naturally occurring structures from the molecular to the astronomical such as landscapes, geographical coastlines and surfaces, clouds, turbulence in fluids, the growth of plants, the distribution of galaxies in the universe, and even fluctuations of price on the stock exchange (Falconer, 1985). The best known fractals arise from the geometric model of Brownian motion.

A fractal is defined as "a set of which the Hausdorff - Besicovitch dimension strictly exceeds the topological dimension" (Mandelbrot, 1977, p.15b) .

Hausdorff - Besicovitch dimension > topological dimension.

Fractal (Latin: *fractus* related to *frangere* = to break). This responds to the need for a term to denote a mathematical set or a concrete object whose form is extremely irregular and/or fragmented at all scales.

Hausdorff definition. If one knows ahead of time that S is two-dimensional, it suffices to evaluate the measure for $h(\rho)= \pi \rho^2$. If one knows nothing of a shape except that it is a standard one, one will evaluate the measure for all $h(\rho)= \gamma(d) \rho^d$ with d an integer. If one finds its length to be infinitive and its volume zero, the shape is surely two-dimensional.

Besicovitch has shown that the core of this last conclusion continues to be valid when d is not integer and/or when S is not a standard shape. For every set S, there exists a real value D such that the d measure is infinite for $d<D$ and vanishes for $d>D$. This D is called Hausdorff - Besicovitch dimension. So the approximate measure behaves reasonably if and only if $d=D$.

A set's D-dimensional Hausdorff measure may be either zero, or infinite, or positive and finite. Hausdorff had already considered this third and simplest category.

This concept has been proposed in an attempt to depict the irregularity of nature. Burrough (1984) suggested that geophysical phenomena are not strictly fractal for all scales, but exhibit fractal behaviour in a specific scale range that ought to be related to generating processes.

The fractal (line, surface etc) has two important characteristics. The first is the property of self-similarity (see concept of self-similarity in § 7.3.1). The second is that a fractal is defined when a mathematical parameter "D" (D need not be integer) known as the Hausdorff-Besicovitch dimension exceeds the topological dimension. Hausdorff-Besicovitch dimension is often called fractional dimension.

The D of terrain is an extremely useful parameter in geomorphological and geological studies, because it indicates the roughness of the surface, and more than that the D values can separate scales of variation that might be the result of particular natural processes (can be applied to all scales). The interesting aspect of the fractal dimensions is that they are deduced from the interrelationship of the three important characteristics of terrain form (relief, slope and wavelength); therefore, they reflect the presence of both higher and lower frequency in DEM data.

One general approach involves the "dividers" relationship between the number of steps and the step size . Mandelbrot (1977) and others used this method to estimate the dimensions of coastlines. The logarithm of the number of steps is plotted against the logarithm of step size, and the slope of this line is interpreted as - D. For surfaces, this same method can be applied to the contour derived from the surface; the surface dimension would then be the contour dimension plus 1. Fractal dimension may also be estimated from the number of grid cells above an elevation which adjoin those below the elevation, computed for a number of different grid cells sizes (Goodchild, 1982). Analysis of contour lines and coast lines has generally produced estimated fractal dimensions of around 1.2 to 1.3, indicating surface dimensions of 2.2 to 2.3 for most earth topography; furthermore these values usually produce visually realistic simulated terrains.

In this project, fractal dimension (D) is estimated from the important statistical property of fractional Brownian surfaces (Mandelbrot, pp. 229a), the semivariance.

Surface processes which are Gaussian, as well as self-similar, have a "texture" which is defined completely by the similarity parameter k. Such processes may be characterised by the fractal dimension. If the mean of the squared height differences (variance) is computed for different distances then fractal dimension can be estimates from the slope β, of a (log-log) plot of variance against the distance as follows :

$$D = 3 - k \qquad \text{and} \qquad k = \beta/2 \qquad (7.3.2.1)$$

where β is the slope of the line from the log-log regression of the mean squared elevation difference between points and the horizontal distance between points. This method was used by many scientists (Frederiksen, 1980 ; Jacobi, 1980; Goodchild, 1980; Mark and Aronson, 1984), in their effort to examine the degree in which a physical topographical terrain can be described by the fractal model.

If k --> 1, then D --> 2, which is the dimension intuitively to be expected of a surface (ie. a plane); samples of the process then are smooth. However, if k --> 0, then D --> 3; the samples then become rough and, from a fractal point of view, fill three dimensions. Thus for surfaces the D values range between 2 (completely smooth plane) and 3 (completely rough) ($2 < D < 3$).

Typical graphs of the process for a range of values k, showing the change in roughness as k ranges from 0.10 to 0.90, have been presented by Burrough (1984).

The fractal dimension is a simple expression in classifying the terrain type. It involves a complete description of the whole range of irregularities of the terrain such as relief, slope and wavelength (Frederiksen et al, 1985). However, there are still problems which come from the fact that the first property of the fractal Brownian surface (statistical selfsimilarity at all scales) is not practically

fulfilled in the real world. This has caused the fractal dimension to be variable over the whole range of "terrain scale". The problem is how to determine the significant part of the graph (ie. variogram) in order to compute the slope of the graph and the fractal dimension. It is a fact that for the computation of the slope only the first half of the variogram is significant for the computation of the slope of variogram. However, this is not always true in all conditions (Conradsen and Nielsen, 1987).

Fractal dimension can be used for classifying terrain type according to its degree of roughness, providing the significant part of the variogram can be selected appropriately. There are not any standards in defining the significant part, but only empirical rules.

A log-log graph for the Aix En Provence test area is presented in figure 7.3. A linear regression was applied to the graph. From the slope the regression line was computed as being 2H, or β, = 0.7389. Therefore the average fractal dimension of this area is then computed from equation (7.3.2.1):

$$D = 3 - (0.739/2) = 2.63$$

This average fractal dimension is larger than the topological dimension of a plane which is 2, and smaller than the topological dimension of space which is 3. As it is close to 3 the Aix En Provence (Montagne Sainte Victoire) test area, can be categorised as a rough area.

7.4. Relief representation - interpolation methods.

7.4.1. General.

Many photogrammetric techniques make use of grids to provide a basis for later contouring of the data. Registration to a regular grid is the ideal mode for basic DEMs, because a high density of measured points can be achieved economically. As the points are measured a priori, in a regular grid, there is no need for further interpolation. This mode of registration sometimes, however,

proves too rigid and, when a chosen constant grid interval is large in relation to the geomorphology of the terrain, certain characteristic features of the relief may be lost (see § 2.4). To overcome this the operator can manually digitise additional points. Alternatively, special software can be used (progressive sampling), or continuous registration of the scanned profile, so the density of the DEM can be adjusted to the varying character of terrain. This option, however, destroys the regularity of the grid and mathematical interpolation is needed before use of the DEM can be made. In order to estimate the value of the elevation points in places other than the reference points it is necessary to produce a model or an interpolation surface, capable of satisfactorily describing the relief form even for a very close area.

The problem of interpolation from discrete observations can be described as follows: On a number of points P_i in n-dimensional space, called "reference space", vectors of dimension m are defined. Interpolation consists of finding the unknown vectors to any number of other points P_k, using the known vector in points P_i . As an interpolation problem this is simple. The reference space is two dimensional (n = 2), because it consists of the XY coordinate plane. The dimension m of the vector to be found is 1, since the entities to be interpolated are the one-dimensional heights z.

Relief representation methods or techniques for surface fitting by computers are nowadays well presented and widespread. Almost all the existing software is essentially based on either:

the regular grid digital elevation model (normally containing a conversion procedure to transform from random to regular grid data) or

the triangular network of irregular randomly-located height data (Petrie and Kennie, 1986).

The whole interpolation procedure for gridded and non gridded data is shown in figure 7.4.

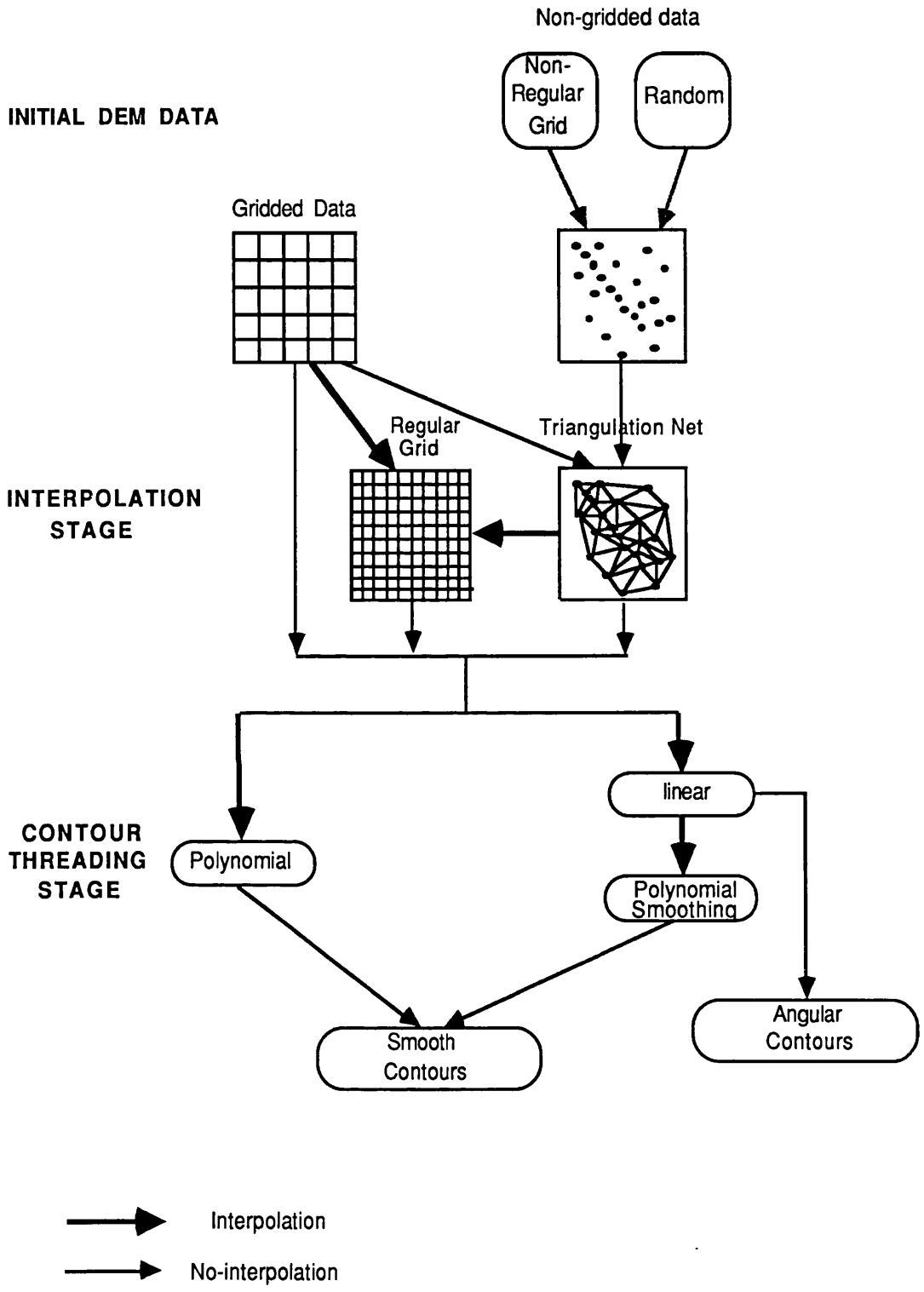

Figure 7.4. Interpolation procedure for different kind of data.
(from digital elevation models to contours)

A very large number of computer packages for integrated DEM production exist in the market. The rapid evolution of computers has affected analytical plotters which nowadays are completely independent cartographic units. Most of the photogrammetric manufacturers now provide, sometimes as standard, appropriate software with the new type "analytical plotters" for every step from the data capturing procedure to the last DEM creation stage.

In photogrammetry, the regularly spaced DEMs are preferable as they simplify data manipulation, data retrieval and so on. The spot height method is undoubtedly the most common and most beneficial mode of input to DEM. Most of the current software is written to support that method.

7.4.1.1. Grid-based interpolation models (random to grid interpolation).

The term grid implies a network of values arranged in a rectangular mesh and calculated in such a fashion that the values at the grid nodes are accurate samples from the surface that is being contoured. The interpolation which is carried out converts the measured data (specific but randomly located points), to a suitably dimensioned regular grid.

In order to honour the data points, the criterion used has to be half the gap between the closed data points in the area as a maximum. The consequences of this conclusion in terms of time can be horrifying because the standard grid interpolation process has a speed proportional to the number of the interpolations being performed and not to the number of data points being contoured. Thus grid based systems exhibit a geometric increase in computing time as grid size is enlarged.

There is a large number of random to grid interpolation procedures. The distinguishing feature between them is the range of the interpolation function which is employed in the interpolation. There are three major classes of interpolation methods. The pointwise, the global and the patchwise or piecewise (Leberl, 1973):

The pointwise methods (local interpolation functions) interpolate each intermediate point independently. Each intermediate point is interpolated from the neighbouring points lying within a specified window. The local surface follows some mathematical function which is constructed from the surrounding points within a local window. The parameters of the local surface model will normally vary from point to point. They produce a continuous surface because they assume that there is an autocorrelative effect present in the surface that decreases with distance away from the location where the interpolation is made. The advantage of a locally applied function is that it has only to consider local data points and can be computationally as small and simple as required. These methods are therefore fast.

The global methods fit some function to a large amount of the data set in such a way that all the data points exist on the function surface. All data points are honoured, but not necessarily on the grid sampling of the surface that will be used for contouring. The advantage is that once the function is constructed, any point within the surface model can be computed directly from the function. Another advantage comes from the fact that there will be no "crack" problems as with the patchwise methods. However, if the terrain surface is very irregular then performing a best fitting with a global function can lead to difficulties when high order polynomials are used and a large data set is required to form the model, requiring a large amount of computation time.

Hardy (1971) claimed the following multiquadratic equation as being more flexible:

$$z = \sum c_i \left[(x_i - x)^2 + (y_i - y)^2 + c_i \right]^{1/2}.$$

The most important disadvantage of the application of the above multiquadratic equation is that for n sample points, the inverse of an (n x n) square matrix is necessary because a least squares solution is employed.

The patchwise or piecewise methods lie in an intermediate position between the pointwise methods and the global methods. The whole area is divided into equal size patches (windows) of identical shape. The problem of solving large sizes of linear equation systems is therefore avoided. However, "cracks" may occur at the edge of each local window as a result of inconsistency among local functions. The

problem of "cracks" can be solved by choosing an appropriate function that has characteristics such that it has continuity of tangent and curvature (first and second derivatives) along the edge of the window. The B-spline function forms smooth joints and avoids discontinuity at edge points (Foley and Van Dam, 1982; Gerald, 1980). Another way of solving "crack" problems is by imposing conditional constraints in the adjustment system so that continuity can be maintained at edge points (Leberl, 1973). However, it is necessary to calculate the additional unknown parameters introduced by the functional constraints themselves. Therefore heavy computational problems occur. There are two distinct methods of patchwise interpolation: The exact fit patches and the overlapping patches. The patchwise method is the fastest and, with its efficient storage, makes it more suitable in a restricted computer environment.

General polynomial equations (polynomial functions or gradient analysis) are used in the global and patchwise methods of interpolation in order to represent the terrain surface. These estimate the height of each individual point by generating a low or high polynomial equation. Typical types of surface used to model patches are: The obvious ones to be applied in practice are linear interpolation, quadratic and quartic. However, the most popular (because of their simplicity) are: the 4-term bilinear, the still simpler 8-term biquadratic, the incomplete 12-term bicubic polynomial, and the most sophisticated full 16-term bicubic polynomial. The polynomial functions fall in the category of overprecise and computationally expensive methods.

Most interpolation techniques in existence and operational in practice today are essentially derived from the pointwise method, because it is fast, flexible and gives better accuracy than the global and patchwise functions.

7.4.1.1.1. Accuracy of the grid based interpolation methods.

In general the accuracy of the interpolated grid is greatly affected by the type of interpolation used. A test by Grassie (1982) derived the following results:

Pointwise methods give satisfactory results (in terms both of standard errors and number of extreme values) with the exceptions of input river and

breakline data, but vary marginally between methods.

Also Leberl (1973) mentioned that due to its flexibility, the numerical simplicity and local definition of pointwise interpolation should provide at least as accurate or even better results than piecewise or single functions.

Global methods give the poorest results. This emphasises the point that a single global function cannot fit the nuances of terrain. Patchwise methods are also not satisfactory and this is generally a result of poor data distribution creating areas of data voids; thus poorly fitting polynomials result in poor grid patterns of contours.

7.4.1.2. Triangulation-based interpolation models.

The most widely known alternative method is based on triangulation of the data set. In this method the reference points are used as the vertices of a net of triangles which cover the interpolation area without overlapping. Every measured data point is being used and honoured directly since they are used as the vertices of the triangles used to model the terrain, to determine the heights of additional points by interpolation and to carry out the construction of contours McCullagh (1983). Furthermore, the method is easily implemented and ideally suits the natural or artificial terrain features (cliff and breaklines).

Originally, the triangulation method suffered from several problems. However, these problems have been overcome and now the same network of triangles are generated from a single set of randomly located measured points no matter from which point in the data set the triangulation started, and for any given set of data it is now much faster to generate unsmoothed contours from any automatic triangulation procedure than from the use of a grid interpolation approach.

Any triangular based approach that is to be used for the basis of isarithmic map production should attempt to produce a unique set of triangles that are as equilateral as possible and with minimum side lengths, stability and non intersection. Two main algorithms are used to implement these requirements.

These are the Delaunay Triangulation method (Delaunay, 1934) and the Radial Sweep Algorithm.

In the following paragraphs a brief description of the Delaunay triangulation approach, the neighbour search algorithm and the point choice is carried out since this technique is applied to the Laser-Scan DTMCREATE software used in this project.

In the Delaunay triangulation the Thiessen polygon (figure 7.5) endeavours to define geometrically the region of influence of a point on a real basis. This is done by constructing a series of perpendicular bisectors on each of the triangles formed around that specific point. These intersect at the Thiessen vertices. The polygon so defined is the Thiessen polygon. The data points surrounding a specific data point are known as its Thiessen neighbours.

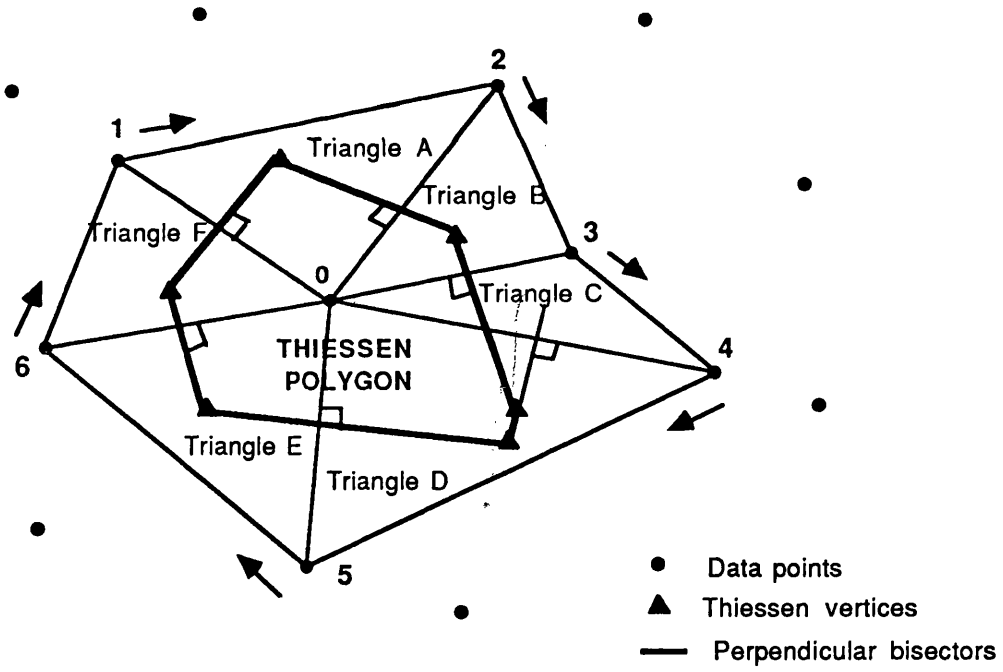

Figure 7.5. Rotational search for Thiessen neighbours to create Delaunay triangles and construction of the Thiessen polygon.

A step before the preliminary triangulation begins is to define a set of artificial boundary points (imaginary points) to form a perimeter around the edges of the data set area, just outside the data window to be polygonised. It is the

most efficient method to solve the boundary problem. This satisfies not only surveyors who prefer that contours stop when the data stops, but also other disciplines, particularly geology, which prefer to extrapolate to the edges of a map area between data areas within a map sheet. The boundary points usually have arbitrary values and are added to the data set. These are necessary to create a frame to the terrain model and a set of boundary triangles. These triangles allow the contours to be extrapolated outside the area of the data set itself. Then the whole area can be triangulated starting with a pair of the imaginary points located in the bottom left hand corner.

The search for the next neighbour is made by constructing a circle with the base of the two starting points as diameter and searching clockwise to find any point which falls within this circle. If no data point lies within the circle, it is increased to perhaps twice the size. The base of the two starting points is now a chord in the larger circle. Any data points lying within the new circle are tested to discover which one meets the criteria set for the nearest Thiessen neighbour (figure 7.6).

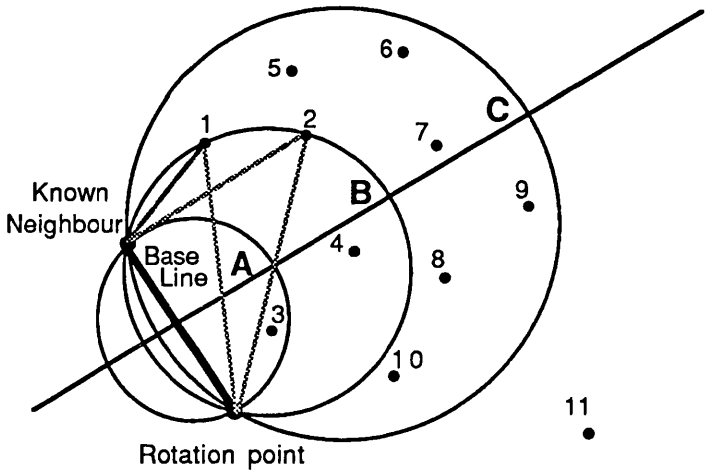

Figure 7.6. Expanding circle search using angular measurement to determine closest neighbour. After McCullagh (1983).

Once this has been achieved, the search for the next neighbour then continues clockwise. Then onto the next neighbour and so on, till the next imaginary point is reached. The formed triangles constitute the shell. The process of the triangulation continues with each point in the shell being used in turn as the starting point for the search until the next set of Thiessen neighbours. This continues in a systematic manner until the neighbours for all the points existing in the data set have been

found and the corresponding triangles formed.

The triangular based approach is very fast. For 7000 points in the data file the data structuring phase for the map took approximately 2 minutes CPU time on a VAX/780, and the generation of a 161 row by 161 column grid to cover the area another 1 minute CPU time. The grid creation option used involved the mapping of linear triangular facets onto the grid rather than smooth patches, as point data density was sufficiently great that no slope estimations were necessary (McCullagh, 1983).

When the GIS is used for technical maps it takes only a few minutes to compute the triangulated irregular network (TIN) and the contours. (1000 triangles are computed per minute on a PRIME 2350) (Sandgaard, 1988).

7.4.1.3. Comparison of grid-based and triangular-based methods.

The direct calculation of a regular grid is less valuable in situations where (McCullagh, 1986):

1. Considerable computer time is needed to interpolate a detailed regular grid to represent few data points.
2. Data densities vary considerably in different parts of a map making much of a fine regular rectangular grid redundant.
3. Exact surfacing of supplied data points is essential and can only be achieved by using a very fine grid mesh.
4. Discontinuities such as cliffs or geological faults must be shown on the map integrated correctly into the surface.

The number of newly created points to be interpolated by the grid methods is much larger than the number of sets of calculations in Delaunay. If the average Delaunay computations for one point are considered approximately equivalent to the amount of effort needed for a grid interpolation then it can be seen that the time saving through producing a triangular structure rather than a square grid can be great, particularly as the number of points rises (McCullagh, 1988).

In the triangular method the original data points are located exactly on the triangular network and on the surface on which they should be found.

The contour interpolation time and surface patch fitting in order to produce a final smooth contour map varies depending on the grid method, so it is difficult to draw a general conclusion.

The definition in the triangular case will be equal to the data density in all areas and thus accurately represent the information content at different points in the surface.

7.4.1.4. Directing factors in choosing an interpolation method.

The mode of interpolation depends on the character of the digital elevation matrix initially measured. The choice of interpolation function is critical whatever system is chosen for modelling the terrain. Most functions are not related to the geometry of the terrain they are trying to represent. It is therefore important to consider very carefully the type of function used in any given model.

Each conversion algorithm uses a mathematical model which fits onto the measured object. The mathematical model is the base of the interpolation. Many of the surface fitting techniques have a smoothing effect. The interpolation method is important for the cartographic quality of the digital model, but it has only a minor effect on the standard deviation (Jacobi, 1980).

An interpolation function is required that:

1. Will provide a continuous surface (at least visually smooth in the first derivative) from a scattered and possibly linear data set;

2. Will be easy to calculate, because in order to create the grid for N data points, at least N^2 interpolations have to be calculated; and

3. Will have the mathematical properties of interest to the application.

Leberl (1973) in his study of the interpolation in a regular grid DEM used the following interpolation algorithms:

For the cases of more than the 4 closest reference points, four effective point/patchwise interpolation algorithms were selected:

a) Weighted arithmetic mean σ_n (AM): "Normalised" standard deviation of terrain relief.

b) Weighted moving averages (MA): RMS interpolation errors in three planimmetric locations.

c) Linear prediction (LP): least squares interpolation.

d) Minimum sized polynomial patches (PMA): Polynomial interpolation with minimum sized patches.

For the cases of 4 reference points the obtained interpolation was in a grid mesh by using the four corner points. Five algorithms were studied:

a) Weighted arithmetic mean (AM).

b) Linear prediction (LP).

c) Bilinear polynomial (POL) : Variance of the relief σ_t^2 .

d) Two linear interpolation (LI): one linear interpolation and one double linear interpolation.

Also 2 alternative patchwise polynomials (PMA1,PMA2) were studied.

The interpolation algorithms were applied in 6 test areas with variable relief. The interpolation methods were studied in three respects: weighting, accuracy, and computation time. Linear prediction and patchwise polynomial interpolation were found to be the most effective interpolation methods for the specific case of square grid DEMs. The method of moving averages is of the same accuracy as the two aforementioned algorithms, but somewhat more expensive. However, weighting deserves utmost attention when applying moving averages, or linear prediction. Incorrect weight might even have a detrimental effect on the performance of the methods.

For certain applications, the use of a patchwise polynomial surface rather than the pointwise interpolation algorithms might have a significant advantage. It was found that for such cases, the bilinear polynomial through 4 reference points, and the more sophisticated patchwise third degree polynomial do represent

valuable alternatives to linear prediction, with almost the same performance.

7.5. Accuracy predicted for DEMs - Interpolation error.

The geometric quality of a set of elevation data can be expressed in many ways, for example by its mean error, standard error and maximum error (Ostman, 1987). Functions of the elevations, such as the slope or the curvature, may be of interest in addition to the elevation themselves. The standard error (σ_0) of the elevations is a commonly used quantity to describe the accuracy of an elevation data set. It can, for a given area, be obtained from the expression:

$$\sigma^2 A = \int\int_A (\hat{z}(x,y) - z(x,y))^2 dxdy$$

where A is the area, z(x,y) are the true elevations and z(x,y) are the elevations of the DEM.

Ackermann (1979), expressed the accuracy of digital elevation models to a first approximation by the following formulae:

$m_h^2 = (a*d)^2 + b^2$

Where :

m_h : Standard vertical error of interpolated arbitrary points in DEM.

d : Mean (representative) point interval of terrestrial or photogrammetric survey.

a : Proportionality factor depending on the type and category of terrain (empirical proportionality factors between the vertical DEM accuracy and representative height interval). The a factor shows a very clear linear relationship between vertical DEM accuracy and the point interval. In the difficult terrain a = (2.2 to 2.3) * 10^2, in the rolling terrain a = 1.0 *10^2 and in simple terrain a = (0.4 to 0.5) * 10^2.

b : Measured error (accuracy of determination) of ground survey or photogrammetry, including the effect of, ie. vegetation.

For photogrammetric data acquisition factor b may be assumed to be

composed as follows:

b = 0.1 °/oo h + dynamic component , where h is the flying height.

Frederiksen (1981) and Frederiksen et al (1984), presented a practical method for predicting the accuracy of a DEM. In this method an accuracy estimate for a DEM in the area is considered, when a fixed sample spacing and the precision of the DEM data points are given. In this method the statistical properties of the terrain surface are described by an 'energy spectrum' compiled from the measurements of profiles. The spectral estimate is defined as the discrete Fourier transform of the autocorrelation function estimate. The raw spectral estimate can be calculated from the data (Schwartz & Shaw, 1975):

$$S_N(f) = L * C^2_f = L * (A^2_f + B^2_f) \qquad (7.5.1)$$

where

$$A_f = 2/N * \sum z_i \cos\left((2\pi / L) * \Delta x * i * f\right) \qquad (7.5.2)$$

$$B_f = 2/N * \sum z_i \sin\left((2\pi / L) * \Delta x * i * f\right). \qquad (7.5.3)$$

L : is the length of the profile.

z_i : is the sample value at the position i * Δx.

f : is the frequency corresponding to the wave length λ = 1/f and

N : the number of samples per profile (harmonic number or the number of cycles per basic interval).

Direct use of (7.5.2) causes a rather fluctuating estimate which is difficult to interpret. For practical applications the following filter is used which causes an averaging in the frequency domain:

$$S_N(f) = (1/4 * S_N * (f-1)) + (1/2 * S_N * f) + (1/4 * S_N * (f+1)). \qquad (7.5.4)$$

On the log-log graph of frequency of the power of spectrum (S_N^2) against wavelength, the power of frequency spectrum of the terrain is approximated to a

straight line (Jacobi, 1980, Frederiksen 1981). This straight line could be represented by the equation of the line:

$$\log (S^2) = \log E + a * \log \lambda \qquad (7.5.5)$$

where

a : is the slope of the spectrum

E : is the spectral value (" energy ") for the wavelength at λ= 1 m.

If we know the spectrum of the terrain surface and in particular the high frequencies, we can estimate the standard deviation between a digital terrain model and the terrain surface (Frederiksen et al, 1978; Frederiksen and Jacobi, 1982):

$$\sigma_o^2 = m_z^2 + \sum C_f^2 \qquad (7.5.6)$$

The sum is calculated from the frequency 1/ (2* Δx) to infinity. Δx is the point spacing in the grid where the DEM data are to be measured (valid only in the case of equally spaced samples in the x and y directions).

The term m_z^2 is the a-priori variance of the data points on which the DEM calculations are based (the accuracy of the DEM data sampling).

C_f^2 is the average terrain variation in terms of the spectrum.

Jacobi (1980) has given a spectral estimate for a moraine landscape. The spectrum is approximated by a straight line, so the formulae becomes:

$$\sigma_o^2 = m_z^2 + \left(E^* (2^* \Delta x)^{a-1}\right) / (a -1) \qquad (7.5.7)$$

Ackermann (1979) investigated the vertical accuracy in relation with the ground slope, and the survey points density. In his study he used various types of data acquisition and represented the DEM accuracy as a function of ground slope and of the mean point spacings used in the survey. The test area was in the Swabian Alb mountains, about 1.7 x 0.9 km in size with ground slopes up to 50% (about 30°). He used wide angle aerial photography at 1:10,000 scale. Profiles spaced 15 m and 30 m apart were acquired as well as direct contours. Profiling resulted in approx. 8,000 and 2,000 profile points with 1,200 additional points on break or feature lines. The photogrammetric plots were used to compute DEMs of regular 5 m grids

and to derive contours from them. Twenty two representative or specially placed check points with a total of 485 check points measured on the ground were used for directly checking the vertical accuracy of the DEM.

The DEM accuracy represented as a function of ground slope for the photogrammetric profiling is given by the following formulas:

For mean point interval 15 m, m_h = (0.21 + 0.72 * tan a) in metres. The mean vertical DEM error for the test area was found to be 40 cm.

For mean point interval 30 m, m_h = (0.21 + 1.50 * tan a) in metres. The mean vertical DEM error for the test area was found to be 59 cm.

The DEM accuracy for photogrammetric contouring represented as a function of ground slope is given by:

m_h = (0.32 + 0.21 * tan a) in metres. The mean vertical DEM error for the test area was found to be 37 cm.

It is interesting to note that direct photogrammetric contouring reveals practically no sensitivity to ground slope.

Comparing the accuracy of DEMs we can see that those derived from contours are more accurate than those from profiling, which is contradictory to the consideration that on the fly measurements are more accurate than static measurements. This happened because the photogrammetric plots were used to compute DEMs and to derive contours from them.

7.5.1. Estimation of the required accuracy of the interpolation.

There are constraints on the accuracy of the final contour map: the size of grid itself and the accuracy of interpolations at the grid nodes. It is therefore necessary to consider the likely requirements for grid size related to the number of data points in the area of concern. Information theory would lead to the conclusion that the number of grid interpolations should be roughly equivalent to the number of data points.

In spite of the several shortcomings or disadvantages of grid-based models, they are still widely used because photogrammetrically captured data are mainly based on grids. Many research projects have been carried out concerning them. Forstner (1983), and Ostman (1987) studied the point density in relation to the ground forms (slope and curvature) and the standard error of the elevations. Balce (1986 & 1987) experimented with data sampled at various grid sampling intervals, from large and small scale aerial photography, in order to find out the optimum grid sampling (see § 2.4.5.6).

The required interpolation accuracy is a key factor in planning the sample spacing, for a required accuracy DEM. The parameter σ (mean square error or standard deviation) either denotes the average standard deviation σ_{mean} of elevations extracted from the model or it may refer to the maximum standard deviation σ_{max}.

The interpolation accuracy or the evaluation of the interpolation method is usually attempted on a basis of interpolation error. So what is this error and how can it be obtained?

In a controlled experiment, the interpolation error can be found by using checkpoints in which the interpolation and the known values are compared. In this case if the measuring error is not known a propagation of the measuring error into the interpolated value will occur. This assumption is made in § 7.5.2 when the interpolated height values are compared with the initial values.

In the actual applications, the interpolation error can be estimated by interpolating the value at data points, without using the information of the data point except for comparison with the interpolated value. In the case of regular sampling this method might produce an error estimate which is too large, since the distance between any non-data point to the closest reference value is at least half as small as the distance from such check points to the closest data point (Leberl, 1975).

Balce (1987) considers the whole procedure (photogrammetric and data capture) while Jacobi (1980) and Kubik (1988) consider that the final accuracy

of the DEM is composed of data acquisition and the accuracy of interpolation.

For the Balce (1987) assumption, the error components of overall accuracy are:

1. Aerial triangulation.
2. Model set up
3. Sampling error.
4. Interpolation error.
5. Contouring error.

Estimating the required accuracy for interpolation σ_{int} by applying the law of propagation of variances we can get the following approach:

$$\sigma_{int} \approx (\sigma^2_{req} - \sigma^2_{AT} - \sigma^2_{setup} - \sigma^2_{samp})^{1/2} \qquad (7.5.1.1)$$

Where

σ_{req} : the project required accuracy.

σ_{spec} : the specification accuracy (from the mapping standards).

σ_{AT} : the aerial triangulation accuracy

σ_{setup} : the model set up accuracy

σ_{samp} : the sampling process error

σ_{int} : the interpolation error.

The required accuracy σ_{req} may be estimated as follows:

$$\sigma_{req} \approx CI/ (2 * 1.64) \qquad (7.5.1.2)$$

The aerial triangulation accuracy σ_{AT} may be estimated as follows:

$$\sigma^2_{AT} \approx RMS^2_{CP} + RMS^2_{TP} \qquad (7.5.1.3)$$

Where

RMS_{CP} : RMS of vertical control point residuals of block adjustment.

RMS_{TP} : RMS of vertical tie point residuals of block adjustment.

If no aerotriangulation has been done such as in the case of full model control or levelling points transferred from other triangulated photography, then the appropriate standard deviation for these points can be used instead.

The model set up accuracy σ_{setup} may be estimated as follows:

$\sigma_{setup} \approx CI/ (2 * 1.64)$ and C-factor $\approx H / CI$

Thus $\sigma_{setup} \approx H / (\text{C-factor} * 2 * 1.64)$ (7.5.1.4)

Where

CI : smallest contour interval possible with a given combination of photography, instrumentation and operator;

1.64 : the χ^2 distribution factor, one dimensional at 90% confidence level;

H : the ground height above mean ground elevation.

C-factor : All the analytical plotters have a C-factor (commercial) = 3,000 (Thorpe, 1984) or C-factor = 2,500 (U.S Federal Agencies).

The sampling accuracy σ_{samp} may be estimated to be in the same order as σ_{setup}.

$\sigma_{samp} \approx \sigma_{setup}$ (7.5.1.5)

Jacobi (1980) and Kubik (1988) considered that the final accuracy of the DEM is composed of data acquisition and the accuracy of interpolation as follows:

$\sigma^2 = \sigma^2_{int} + \sigma^2_{sample\ points}$

and thus $\sigma^2_{sample\ points} = \sigma^2 - \sigma^2_{int}$

If the required accuracy of the DEM is given or it can be predicted, by relating the sample spacing to σ_{int} we can predict the accuracy of interpolated heights for the terrain using the variogram (see §7.3.1.1). The required accuracy for interpolation is the key factor in determining the optimum sampling interval.

The specification accuracy for aerial photography at scale 1:30,000 is $\sigma_{spec} \approx 1.45$ m. From this aerial photography scale we can plot contours with 5 - 10 m interval. The specification in compiling maps at scale 1:25,000 at 5

contour interval is 7.5 m standard error in position and 1.5 m in elevation (Manual of photogrammetry p. 900). For the project requirements using 1:30,000 aerial photography (Flying height = 4,800 m) contours were produced at scale 1:25,000 in a 20 m contour interval (CI) in order to be able to compare with the SPOT derived contours at 20 m (same CI). In the following an estimation of the required interpolation and contour accuracies is carried out:

1. Substitute in (7.5.1.2) the required accuracy σ_{req} is :

$\sigma_{req} \approx$ CI/ (2 * 1.64) $\approx$ 20 / (2*1.64) $\approx$ 6.098 m

2. The σ_{AT} was estimated (§ 4.1.2) σ_{AT} = 1.436 m. As mentioned in § 4.1.2 the aerial triangulation accuracy is three times worse.The aerial triangulation accuracy is adequate for the present requirements for comparing SPOT data, but not under normal mapping project conditions. Aerial triangulation error should be less than 1/3 of the specification accuracy: $\sigma_{AT} < (1/3)\ \sigma_{spec}$

3. Substitute in (7.5.1.4) the σ_{setup} accuracy is:

$\sigma_{setup} \approx$ H / (C-factor * 2 * 1.64) $\approx$ 4800 / 2,500*1.64*2 $\approx$ 0.585 m

The σ_{setup} procedure (§ 4.1.3.) gave RMS Vector error = 0.467 m. If we compare those two values we can see that they are very close.

4. Because of (7.5.1.5) the $\sigma_{samp} \approx \sigma_{setup} \approx$ 0.585. The estimated sample σ_{samp} accuracy (see §5.2.3.2) was 1.3m. The estimated sampling accuracy is 2.2. times worse, probably because of the aerial triangulation results.

If we substitute these values in (7.5.1.1) we have:

$\sigma_{int} \approx (6.098^2 - 1.436^2 - 0.467^2 - 0.467^2)^{1/2}$

thus for 20 m contour interval the required accuracy for interpolation

$\sigma_{int} \approx$ 5.89m.

For 10 m contour interval the required accuracy for interpolation is

$\sigma_{int} \approx$ 2.61m.

By specifying the interpolation accuracy σ_{int} we can estimate the sample interval from the sampling accuracy σ_{samp} and vice-versa.

For the contour interpolation the accuracy of the discrepancies of contour lines may be estimated as follows:

$$\sigma_{disc} \approx (\sigma_{req}^2 + \sigma_{AT}^2 + \sigma_{setup}^2 + \sigma_{samp}^2)^{1/2} \qquad (7.5.1.6)$$

If we substitute these values we have:

$$\sigma_{disc} \approx (6.098^2 + 1.436^2 + 0.467^2 + 0.467^2)^{1/2}$$

Thus the required accuracy for the contour map is $\sigma_{disc} \approx 6.30$ m

So for the project requirements using 1:30,000 aerial photography mapping at scale 1:25,000 at a 20 m contour interval (CI) the required interpolation accuracy σ_{int} is 5.89 m, while the contour accuracy σ_{disc} is 6.30 m. These required values are sufficient to compare the contours derived from the SPOT measurements.

7.5.2. Accuracy of the interpolation method of the DTMCREATE software.

The DTMCREATE package is a triangular to grid form interpolation package. It has no details of the interpolation method for input definition, input parameters and quality control and as with all the commercial packages it contains some smoothing parameters, which should be set with utmost care to get a proper representation of the terrain.

There is no numerical check of the DTMCREATE package. The only operational example (McCullagh, 1983) was carried out in a part of the Cairngorm region of Scotland 16 x 12 km^2. The extreme relief of the area with associated crags, lochs, and river valleys made it a suitable test area. The digitisation was done manually from the Ordnance Survey map. Therefore only contours were available. In addition

the rivers, lochs, ridge lines and spot heights were marked with appropriate height information. There were about 7,000 points in the data file.

The check was done through the isometric displays. No surface "glitches" were visible on the displays indicating that the input data were accurate and that the system has been able to create a suitable terrain model without the benefit of smooth patch fitting. Careful observation on the lochs show that they are horizontal without any unfortunate hills or valleys in the loch surface. Providing the edge of a lake or sea is represented as a discontinuous data type this will always be the case, even when using a smooth patch function as the surface continuity is broken at the lake edge. Similarly crags and other features that necessarily create edges can be represented as breaklines.

DTMCREATE software offers four different interpolation options for estimation of the height of imaginary points which are created in the edges of the DEM area. It also offers two types of interpolation from the triangular form to DEM grid; the linear and the smooth 'patch' interpolation (see appendix H). It is questionable whether smoothing should be used on the SPOT data or not. It is preferable for smoothing not to be done when the measuring errors are small compared to the possible terrain undulations. The SPOT data however, contain errors whose magnitude is significant in comparison to the terrain undulations, so it was decided to use the smoothing function.

In this project the interpolation option BOX is applied which interpolates heights on the basis of known heights using an expanding box search and the function QUARTIC. The QUARTIC interpolation is the highest degree interpolation function existing in the DTMCREATE software. Thus this is the the most flexible of those functions provided by the software; suitable for the terrain roughness and low resolution data of the project test area. The triangular to grid point transformation was done by applying a smooth patches interpolation.

One of the most serious problems using a commercially available interpolation package, is that the height of interpolated values are not known, so the estimation of the accuracy of the interpolation procedure which is used in the package is not possible.

Facing this problem in this study it was obvious that the only way of solving it, was that the interpolated height values should be kept in a file in a readable form, in order to be able to compare them with the initial (before interpolation) values and to analyse statistically. The direct comparison and statistical analysis was possible because the initial data were in a regular grid. So the problem was to produce the interpolated values in the same regular grid, in order to be able to compare them.

The interpolated height values created by the DTMCREATE software are kept in a DTI file. The contents of a DTI file is in binary form. It only keeps the interpolated height values in an integer form in order to be able to display them through the DTIVIEW module (display data should be in word format). It was likely to be a command in the TRIGRID module which allowed for asking the height values to be in a real format.

The module DTI2TEXT is used in order to be able to transfer the interpolated height values from binary form to a readable form. The output file contained strings of the interpolated height values in a sequence, without any other information.

A Pascal program (DTI2TEXT.PAS) was written in order to transfer the continuous strings of height values into a sequential file in row, column, height value format. A further modification of the checking program (see appendix B), allowed the comparison of interpolated height values with the initial values and the estimation of statistical analysis results.

Firstly the aerial photography data were interpolated using a 30 m sidelength (the same as the grid interval used in capturing the initial data). The interpolated values were compared with the initial height values.

The statistical analysis results of this comparison are shown in table 7.1.

BLOCK NAME	NUMBER OF COMPARED POINTS	1m >= POINTS >= 1m	ELEVATION DIFFERENCE		STATISTICAL RESULTS OF ELEVETATION DIF		OF ABSOLUTE ELEVATION DIF.	
			MINIM (m)	MAXIM (m)	MEAN(m)	SD (m)	MEAN(m)	SD (m)
1	3190	48	-10.68	1.37	0.10	0.60	0.22	0.69
2	9680	40	-10.68	2.57	0.05	0.34	0.19	0.42
3	8580	77	-3.36	6.95	0.04	0.38	0.27	0.49
4	3960	10	-1.94	3.15	0.09	0.25	0.17	0.36
5	1980	37	-0.75	4.97	0.17	0.30	0.20	0.46
6	8370	61	-2.79	3.58	0.17	0.49	0.33	0.70
7	7920	119	-2.16	5.64	-0.13	0.43	0.35	0.48
8	2520	70	-0.77	1.92	0.26	0.33	0.31	0.66

Table 7.1. Comparison of the aerial photography initial and interpolated height values.

Secondly the merged aerial photography data and SPOT data with RAFs (weights) 1.0 and 0.1 respectively, were interpolated using a 30 m sidelength (the same as the grid interval used in capturing the aerial photography data). The interpolated values were compared with the initial aerial photography height values. The statistical analysis results of this comparison are shown in table 7.2.

BLOCK NAME	NUMBER OF COMPARED POINTS	4m >= POINTS >= 4m	ELEVATION DIFFERENCE		STATISTICAL RESULTS OF ELEVETATION DIF		OF ABSOLUTE ELEVATION DIF.	
			MINIM (m)	MAXIM (m)	MEAN(m)	SD (m)	MEAN(m)	SD (m)
1	3190	19	-10.68	3.35	0.02	0.83	0.41	0.93
2	9680	102	-10.69	8.43	0.17	0.87	0.43	1.05
3	8580	40	-5.28	7.10	-0.09	0.88	0.54	1.08
4	3960	22	-3.71	6.19	0.17	0.85	0.47	0.90
5	1980	5	-2.98	4.97	0.08	0.59	0.34	0.64
6	8370	74	-7.93	10.92	-0.11	0.97	0.59	1.20
7	7920	200	-9.94	6.06	-0.44	1.30	0.85	1.82
8	2520	20	-4.09	7.21	0.48	0.86	0.62	0.87

Table 7.2. Comparison of the aerial photography and SPOT merged initial and interpolated height values (using SPOT data weight 0.1).

Finally the merged aerial photography data and SPOT data with RAFs 1.0 and 1.0 respectively, were interpolated using a 30 m sidelength (the same as the grid interval used in capturing the aerial photography data). The interpolated values were compared with the initial aerial photography height values. The statistical analysis results of this comparison are shown in table 7.3.

BLOCK NAME	NUMBER OF COMPARED POINTS	20m >= POINTS >= 20m	ELEVATION DIFFERENCE		STATISTICAL RESULTS OF ELEVETATION DIF		OF ABSOLUTE ELEVATION DIF.	
			MINIM (m)	MAXIM (m)	MEAN(m)	SD (m)	MEAN(m)	SD (m)
1	3190	0	-13.54	16.54	-0.35	3.01	1.41	3.19
2	9680	103	-14.74	46.73	0.70	4.42	1.64	5.00
3	8580	66	-27.73	36.27	-0.70	4.34	2.05	5.14
4	3960	46	-18.68	33.75	0.53	4.47	1.95	4.69
5	1980	3	-20.10	20.52	-0.26	2.74	1.25	3.13
6	8370	101	-47.21	47.99	-1.38	4.80	2.28	6.04
7	7920	204	-49.76	31.20	-1.81	6.39	3.32	8.19
8	2520	21	-27.24	35.60	1.48	4.33	2.29	4.41

Table 7.3. Comparison of the aerial photography and SPOT merged initial and interpolated height values (using SPOT data weight 1.0).

The overall statistical values from tables 7.1, 7.2, and 7.3 are shown in table 7.4.

Kind of interpolated data	STATISTICAL RESULTS			
	OF ELEVATION DIF.		OF ABS. ELEV. DIF	
	Mean (m)	SD (m)	Mean (m)	SD (m)
Initial aerial photography data	0.06	0.41	0.27	0.54
Aerial photography and SPOT merged data (RAFs 1.0 and 0.1)	-0.03	0.96	0.56	1.21
Aerial photography and SPOT merged data (RAFs 1.0 and 1.0)	-0.45	4.74	2.15	5.69

Table 7.4. Overall statistical values of the initial and the interpolated height values.

From table 7.4 we can see that when the lower resolution source data were involved the interpolated height values became worse. Seeing the initial aerial photography interpolated values as well as comparing the interpolated values of merged data with the same of table 6.12, we can see that the smoothing procedure did not affect the accuracy of the elevation data.

Note.

In all the above procedures the 30 m grid data were interpolated again to a 30 m sidelength. So actually no proper interpolation was involved, but the height discrepancies were due to the applied smoothing procedure and the effect of the imaginary points .

An effort was made for the imaginary points to be as close as possible to the interpolated data. This was done by specifying the maximum extent of the data in the IFF file coordinate RAnge (RA) to be slightly larger than the data coordinates. The imaginary points are created at the edges of the interpolated area by the TRIANG module . TRIDER module provides the z value for the imaginary points. As the imaginary points lie close to the interpolated data the a z values are almost the same as the nearest neighbour data points. With this procedure the errors due to imaginary points are minimised.

An attempt was made to interpolate the SPOT data from 100 m to a 30 m sidelength, the same as the high resolution source, to compare directly the SPOT interpolated height values with the high resolution source elevation data (aerial photography data). This was carried out in order to estimate the actual interpolation accuracy, particularly for the interpolated height values in the intermediate points, this was not possible because of the structure of the TRIGRID module which gives only the interpolated height values and keeps the planimetric coordinates in the header as IFF units. An attempt to retrieve these planimetric coordinates was not a success and so the procedure was abandoned.

7.6 Contouring from DEMs.

7.6.1. General.

Line maps and DEMs attempt to serve two fundamental purposes: to portray an accurate, continuous model of terrain related to some stated datum by including a sample of elevations at stated locations, and to make it possible to calculate (interpolate) the height of any intermediate point from this sample.

The vertical accuracy is reflected in line map assessment by incorporating a varying standard related to terrain and scale. Specifically, the vertical standard states that 90% of points should fall within x metres vertically of their correct elevation. The value x is half the contour interval for first class mapping (Singels, 1968). The contour interval of a map is selected on the basis of map scale and terrain type (Richardus, 1973). Specifically, in considering line maps contour interval increases as scale decreases. Consequently, although the standard for line maps is universally consistent (eg. half contour interval), it is not universally constant.

Horizontal standards for line maps are directly related to the map scale. Generally, first class mapping is that in which the locations of 90% of well - defined points (not subject to generalisation or symbolisation) are within 0.5 mm at map scale of their true position. However, contour lines are not included as they are not well - defined points. Thus they are not horizontal standards related to relief portrayal specifically for line maps; it is assumed that the horizontal error of the relief portrayal is usually the same as that of the detail.

From the computation point of view, contours are of two basic forms: open contours which start at one border of the sheet and continue to another border, and closed contours which form a loop.

Since 1970's an enormous number of packages have been developed and made commercially available. The criteria which make a contouring package efficient are mainly to give an optimum fit to original data, and to use the computer time efficiently.

There are two common contouring methods and techniques of creating a contour map, as follows:

7.6.1.1. Contour creation from grid and

7.6.1.2. Contour creation from triangulated data.

Moreover for each of the above methods there are two main options for the contour threading : simple linear interpolation and the generation of curved smoothed contours using some type of function. A simple procedure for obtaining smooth contours consists of using polynomials in two steps. First at each of two successive discreet points the direction of the contour line is determined, using polynomials of even degree. Then, a curve is fitted between each two discreet points, using polynomials of odd degree.

The increased quality of smooth contours exacts a price in terms of computation. Whereas a linear contour interpolation is cheap to compute, the smoothed surface represents an investment in computer time at least proportional to the level of smoothness required.

7.6.1.1. Contour creation from grids.

A tremendous number of alternative grid construction schemes are available in commercial contouring packages.

In the grid based contouring methods a simple linear interpolation is carried out along each of the four sides in turn based on the values of the nodes. The densification of the grid needs to be efficient to allow linear interpolation of the contour points. The positions of all the contour values are determined for each side. Then they are connected up by straight lines or vectors, since for each entry point there must also be an exit point. Ambiguities can arise with alternative (possible) solutions and impossible situations during linear contour interpolation, in the step of contour threading, in a single cell (from the possibility of four entry points for a given contour). The solution to the problem is contour interpolation by function fitting, usually using a local bilinear polynomial.

For smoothed contours a sub-grid is formed within each generated cell and

then the contours are interpolated linearly and threaded between the points on the grid sub-cell.

The objections to the grid based methods are :

1. Developing faulted structures.
   - Cliff recognition from the basic contour and spot height data.
   - The problem of making the contours run up to a cliff and no further, without the need for elaborate masking techniques.
   - Lack of flexibility in responding to variable data densities in different part of a map.

2. The considerable computer time needed to interpolate a detailed regular grid to represent a few data points. There are some methods which are usually particularly quantity sensitive. For instance the multi-quadratic approach used by Hardy (1971) requires the inversion of an N by N matrix which quickly becomes a prohibitively expensive exercise.

3. The non-honouring of data points caused by insufficiently fine a grid in order to keep computer time down to reasonable levels.

7.6.1.2. Contour creation from triangulated data.

The procedure for contouring from a triangular mesh follows three basic steps:

1. The extraction of points on each contour line. The linear interpolation method is very common when the terrain is based on triangulated data, because this gives a simple and robust solution. It relies on the development of a network of triangles based on the data points to subdivide the area. Ambiguity problems regarding the direction that the contour might take do not exist.

2. The joining of points in a logical order. Two cases arise in the contour creation stage. The open contours, which start at the border of the sheet and continue to another border, and the closed contours in which the arbitrary starting point is remembered and duplicated at the end of the closed contour. This technique has a problem with node levels equal to contour value.

3. Fitting of a curve through them to form a contour line, as a spline fitting of a curve. For smoothed contours the area of an individual triangle can be sub-divided into smaller triangles. A series of cubic splines, polynomials, or a fit

of some type of curved three-dimensional surface patch to each triangle ensure a smooth transition from one triangle to the next.

7.6.1.3. Conclusions for contouring from grids and triangulated data.

Contouring utilising a triangulated net consistently produces good results. Similarly random-to-grid interpolations usually produce quite accurate results, except the global and patchwise methods which often produce poor results (Grassie, 1982).

7.6.2. Accuracy of the contour map derived from SPOT data.

Data from each of the two sources data are captured in a normal grid . The aerial photography derived data are captured in 30 m grid interval, while SPOT data in 100 m. Therefore the data already exist in a regular grid so it was not necessary to interpolate.

DTICONTOUR module is a Laser-Scan software (see appendix H.2.3) for producing smooth contours from the interpolated heights, or heights lying in a regular grid via a triangular or rectangular grid, by curve fitting using linear interpolation techniques. An optional smoothing may be applied using a least squares filter.

DTICONTOUR accepts input files in DTI format created through the TRIGRID module of the DTMCREATE software. Using the DTMCREATE software additional errors occur, (ie. errors in the edges as shown in 7.5.2). Because the data from the two sources were already in a regular grid it was not necessary to interpolate them. Therefore a way was found for the data to be transferred in DTI format without passing through the DTMCREATE software . This was carried out through the NE1.FOR program in order to convert the string of coordinates (Point_Number, X, Y, Z) from ASCII form, to DTI form (see §2.4.3.2.2).

Three DTI format files were created: one from the aerial photography data

(46,200 points in 30 m grid interval, 231 rows x 200 columns), one from the SPOT hardcopy measurements (14,400 points in 100 m grid interval, 100 rows x 144 columns) and one from a second set of SPOT hardcopy measurements (5,400 points in a 100 m grid interval, 75 rows x 72 columns). Those three DTI files were used as input in the DTICONTOUR module (see appendix H.2.3 and H.3) and contours in 20 m interval were interpolated from the spot heights.

There is a problem when more than one smoothing parameter is used. The smoothing effects are usually cumulative, resulting in a very smooth surface between the main terrain features such as break-lines. When smoothing parameters are used there is no warning message. The results after contouring look better, but are erroneous. In this project the contour smoothing option provided from the software was not used as the contour maps were required to be realistic rather than well presented.

Three contour maps were plotted in two scales 1:25,000 and 1:50,000 on the Kern GP1 plotting table with the assistance of the Laser- scan FPP (Fast Plotting Package) which transfers the IFF format files to Kern CAM format (see appendix H.2.3). These maps were the aerial photography derived contour map, and two SPOT derived contour maps (first and second hardcopy data).

In addition two 1:25,000 superimposed contour maps were produced from the same contour data: one by overlaying aerial photography and first SPOT hardcopy derived contours; and one by overlaying aerial photography and second SPOT hardcopy derived contours. The overlay contours were plotted with different colours, red for the aerial photography and black for the SPOT derived contours while the grid in the overlapping area was drawn in blue. This was carried out for easy interpretation and comparison of the two sources contours. The superimposed maps are presented in the following pages (maps 7.1 and 7.2).

The differences between these two data sets were determined from the superimposition by comparing graphically the two contour sets. Those differences can provide important information because are the accumulated errors of the orientation of the SPOT scene, the measurements in it and the interpolation of grid points from the SPOT stereomeasurements.

SCALE 1: 25000

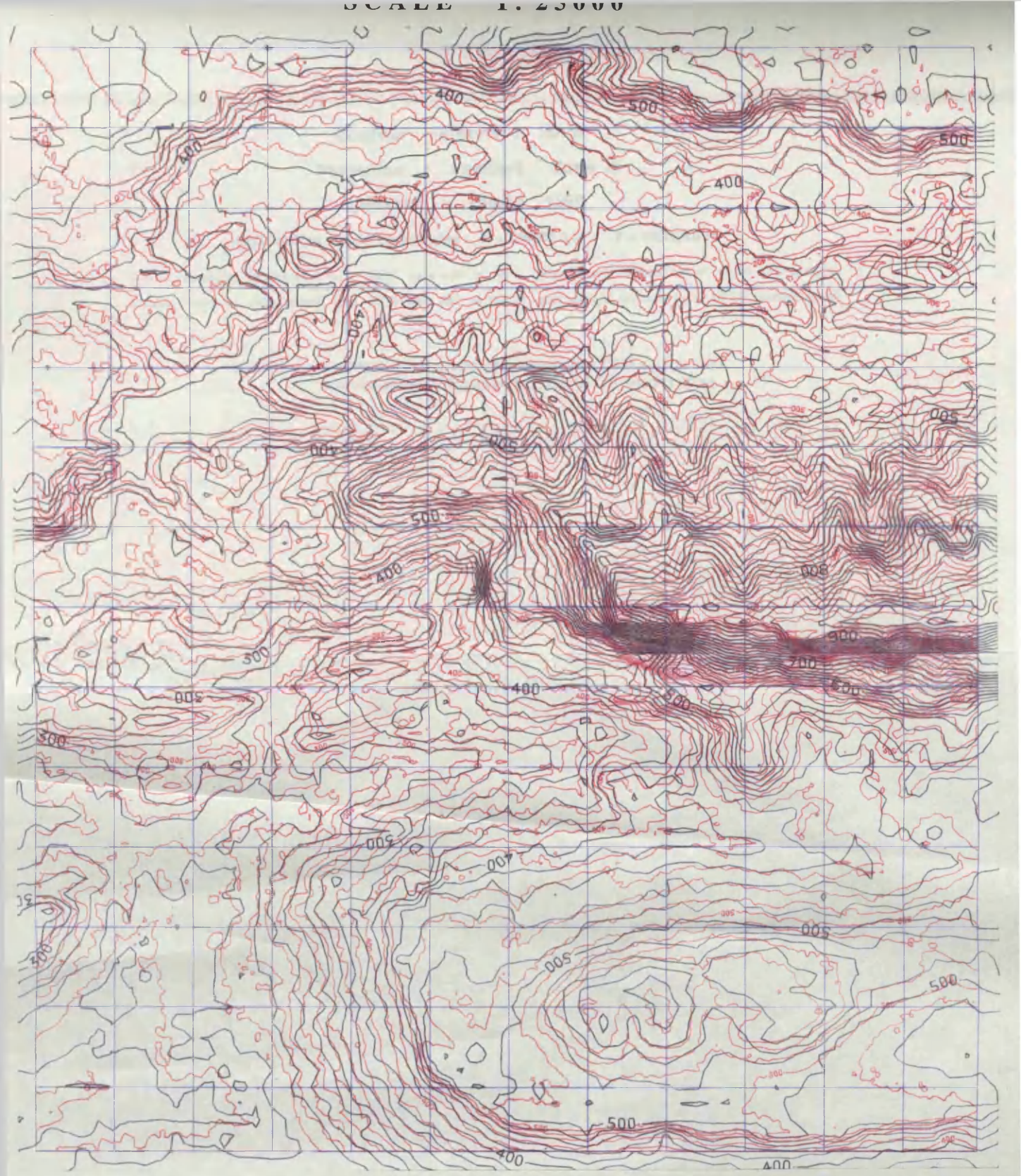

Overlay of contour map derived from two sources

Contour interval : 20 m

Projection : Lambert Zone III

Ellipsoid : Clarke 1880

Left bottom origin coordinates : X = 858000.0 m , Y = 138600.0 m

——— Contours interpolated from DEM data with a 30 m grid interval derived from aerial photography.

——— Contours interpolated from DEM data with a 100 m grid interval derived from SPOT (first copy).

Map 7.1. Overlay of contour map interpolated from DEM data derived from the aerial photography and from SPOT (first copy).

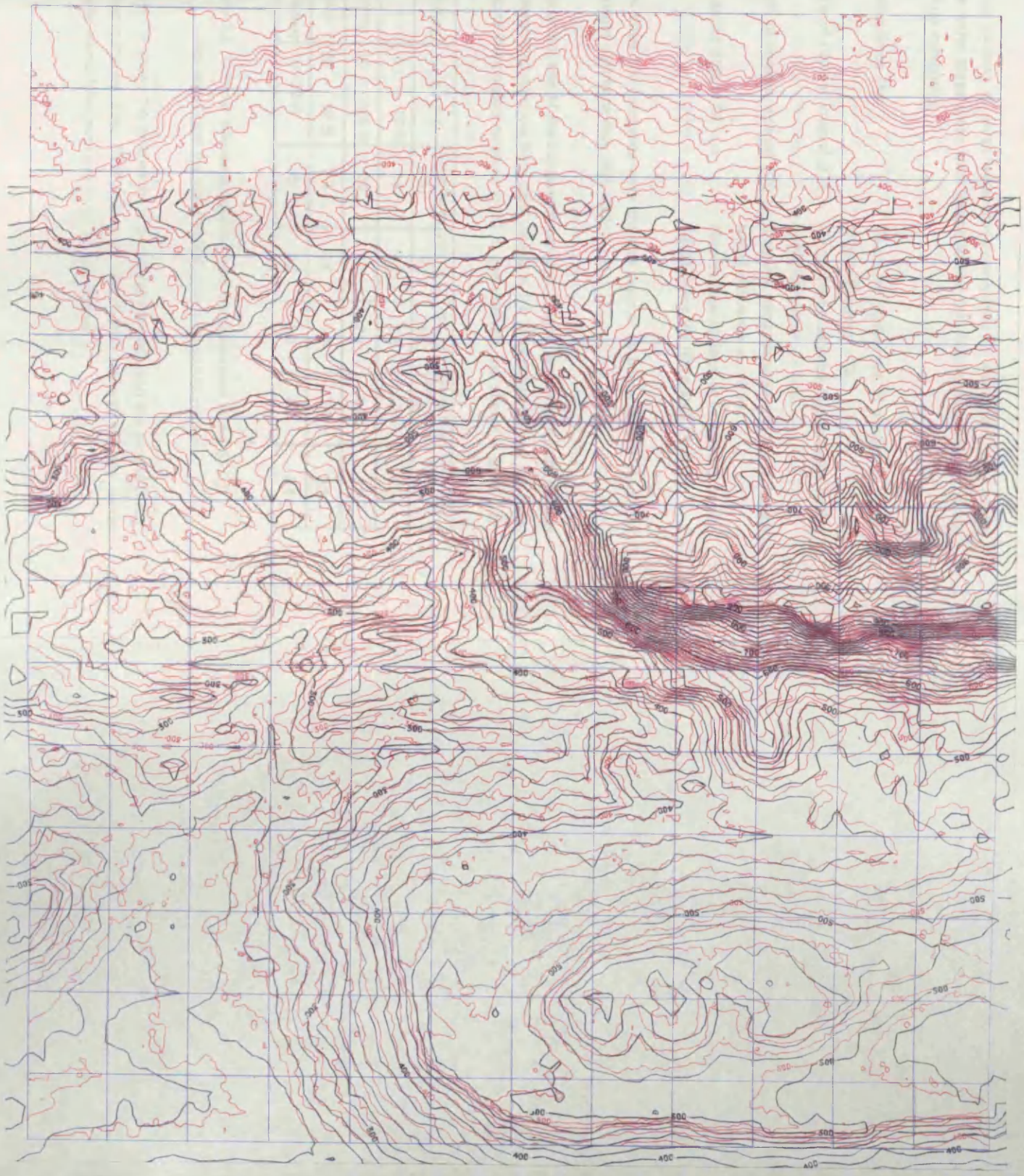

Overlay of contour map derived from two sources

Contour interval : 20 m

Projection : Lambert Zone III

Ellipsoid : Clarke 1880

Left bottom origin coordinates : X = 858000.0 m , Y = 138600.0 m

——— Contours interpolated from DEM data with a 30 m grid interval derived from aerial *photography.*

——— Contours interpolated from DEM data with a 100 m grid interval derived from SPOT (second copy).

Map 7.2. Overlay of contour map interpolated from DEM data derived from the aerial photography and from SPOT (second copy).

Four samples of areas were chosen according to the terrain type. All the contours within these areas were examined and the differences were grouped as (%) in four categories:

Coincidence (%)	:	Gives the percentage of elevations having height difference ≈ 0.
20% of contour interval (CI)	:	Gives the percentage of elevations having height difference <= 4 m.
50% of contour interval (CI)	:	Give the percentage of elevations having height difference <= 10 m.
More the 50% of CI	:	Give the percentage of elevations having height difference more than 10 m.

The three first categories were grouped together as percentage of elevations having height difference less than CI/2 (10 m).

The differences of the comparison between these two contour sets (the first SPOT interpolated contours from DEM values in 100 m grid interval and the aerial photography interpolated contours in 30 m grid interval), are shown in table 7.5:

TERRAIN TYPE	SLOPES	Coincidence (%)	20% of CI (%)	50% of CI (%)	More than 50% of CI (%)	Error less than CI/2 (%)
Flat	0 - 10 %	28	40	30	2	98
Gently rolling	10 - 25 %	20	37	28	15	85
Semi-rough	25 - 50 %	23	25	35	17	83
Rough and steep	> 50 %	5	20	30	45	55

Table 7.5. Contour differences derived from the comparison of the SPOT (first copy) and the aerial photography interpolated contours.

Table 7.6 shows the differences of the comparison between the second SPOT interpolated contours from DEM values in 100 m grid interval and the aerial photography interpolated contours in 30 m grid interval :

TERRAIN TYPE	SLOPES	Coincidence (%)	20% of CI (%)	50% of CI (%)	More than 50% of CI (%)	Error less than CI/2 (%)
Flat	0 - 10 %	40	35	25	0	100
Gently rolling	10 - 25 %	30	40	20	10	90
Semi-rough	25 - 50 %	40	20	25	15	85
Rough and steep	> 50 %	7	30	28	35	65

Table 7.6. Contour differences derived from the comparison of the SPOT (second copy) and the aerial photography interpolated contours.

The background contours were derived from interpolation of heights in a 30 m regular grid. The elevation data are captured from aerial photography at scale 1:30,000.

The first SPOT hardcopy images were not good quality. The images were set up with the assistance of 10 GCPs. On the other hand the second SPOT hardcopy images were better quality and were set up with the assistance of 15 GCPs (see chapter 4).

The required accuracy for the contour map for this project is estimated (see § 7.5.1) as $\sigma_{disc} \approx 6.30$ m. The committee for specifications and standards (1985) for mapping at CI of 20 m, gives the following specifications:

Standard error (σ) = 6.08 m

VMAS = 10 m

and Maximum error (3σ) = 18.24 m.

Actually those values are interpolated from the table of Class 1 . Accuracy Standards in Terms of Elevation and the values referring to the 10 m CI.

Note:

VMAS : Vertical Map Accuracy corresponding to the definition that 90 percent of well-defined points are not in error by more than one-half the contour interval.

From tables 7.5 and 7.6 and the above specifications we can conclude that the compiled contour map at 1:25,000 scale at 20 m interval derived from

interpolated SPOT DEM data meets the specification accuracies for flat and gently rolling areas, while for semi-rough and rough terrain it does not satisfy the accuracy specifications.

Chapter 8.

Automated techniques of capturing data for DEM production.

8. Automated techniques of capturing data for DEM production.

8.1. General.

Automated techniques for the production of three-dimensional data via stereo compilation are receiving increased interest for a variety of applications, including cartography (Panton, 1978). Automated techniques were initially developed on photogrammetric instruments, and nowadays on digital plotters or computers using digital data as a source.

The automation of stereoscopic plotting instruments requires a means for the rapid and accurate sensing of parallax between stereoscopic images. This is generally achieved by the automatic scanning and matching (correlating) of conjugate imagery.

The automatic measuring process is carried out in stereoscopic plotting instruments using the so-called correlator. A scanning system is used to scan a small area on each of the aerial photographs comprising the stereopair, converting the photographic images into a matrix of intensity (or brightness) values. These values are then compared in the correlator to give measurements of parallax (disparity) which in turn can be converted to height values. The scanning may again be carried out systematically in a raster-scan pattern till the whole stereomodel has been converted, once again resulting in a 3D terrain model of the area covered by the stereopair. In the later developments the approach was almost entirely digital, with the photographic image converted to a raster of finely-spaced intensity values, and the correlation between the respective photographs of the stereopair being carried out digitally in the machine's on-line computer system.

Different techniques were used for the scanning of the stereoscopic pair such as:

Electronic scanners (cathode-ray-tube (C.R.T) devices, vidicon - type devices, or image-dissector tubes).

Solid-state scanners (self-scanned photodiode devices, charge-coupled devices, charge-injection devices, or charge-coupled photodiode devices)

Electro - optical scanners (lasers, light-emitting diodes, or conventional lamps).

The photogrammetric instruments have the same limitations as the analogue plotters, with the additional problems deriving from the film printing procedure, of using hard copy.

This problem is overcome by using digital correlation techniques which use soft copy (CCT) as data source instead of film, and the same image setting up algorithm. The current methods involve application of automated techniques to the digital image. These techniques primarily use area-based measures, such as correlation between image patches , or edge-based methods that match linear features in images, but also include the use of feature extractors to match single points in the images, as well as global optimisation techniques that simultaneously match all points in the two images.

The first and most difficult step in recovering the 3-D information from a pair of stereoimages is that of matching points from one digital image of a pair with the corresponding points in the second image. Each image point to be matched is in fact the centre of a small window of points in the first or reference image, and this window is statistically compared with similarly sized windows of points in the second or target image of the stereopair. The measure of match is either a difference metric that is minimised, such as RMS difference, or more commonly a correlation measure that is maximised, such as mean - and variance - normalised cross correlation.

At the time being the better known stereomatching algorithms are as follows:

CC : Cross correlation coefficient.

LSM : Least squares matching.

VLL : Vertical line locus method. Cross correlation coefficient with geometric constraints.

ALSM : Adapting least squares method . Least squares method with geometric constraints.

MPM : Multi point method. Extended LSM for multiple point solution.

FBM : Feature based method.

In practice combinations of the above methods are used in order to get the beneficial effects of one method to compensate for the drawbacks of another. These

combined methods are as follows:

FBM + LSM.
FBM + ALSM
FBM + MPM.
DP (dynamic programming) + LSM
FAST : Facet matching.

It is hard to say which method gives the best results, because of the large number of different cases (eg. satellite imagery, aerial photography, urban area, rural area etc) and the large number of factors which involved in the procedure. From the above methods the most successful methods appear to be the FBM+LSM and FBM+ALSM methods.

8.2. DEM production by stereomatching SPOT-image pairs.

8.2.1. General.

An algorithm for digital matching of image densities was described by Panton (1978). The algorithm includes an image matching procedure in which parallax components are determined by automatically correlating corresponding images. The basic idea behind the method is to set up a regularly spaced grid of points on one image and to find its conjugate of point on the other image. The algorithm is implemented on a distributive parallel network of digital processors.

Most of the automated procedures for height extraction are currently being investigated and developed. SPOT scenes give the opportunity (because of the large amount of information contained in each scene) for a massive extraction of the height information.

Although automated techniques are at a good stage of investigation, manual techniques remain an important production method for capturing the height information for DEM construction at the moment.

8.2.2. Description of algorithms and methods used in UCL.

Alvey MMI-137 project on "Real time 2.5D vision systems", is concerned with producing fast and accurate DEMs from sources such as level 1A ("Raw") SPOT stereopairs (whole images 6,000 by 6,000 pixel data). One of the collaborating partners is the Department of Photogrammetry and Surveying at UCL.

Three stereomatching algorithms were used and an empirical comparison of their performance is presented (Day & Muller, 1989).

The three stereomatching algorithms which are used in the Alvey MMI-137 project are:

1. Barnard and Thompson.
2. PMF method.
3. Otto and Chau.

Brief descriptions of the stereomatching algorithms are presented in the following paragraphs.

1. Barnard and Thompson.

This is a non - epipolar operator based matcher. The method finds multiple likely matches for each point, then uses a relaxation process to disambiguate the results (Barnard & Thompson, 1980). It produces relatively sparse output using the Moravec operator as a feature extractor (use of image hierarchies) (Moravec, 1977) . A match network is constructed using disparity limits, then iteratively refined using similarity between raw grey levels in a 5 x 5 pixel window centred on the feature. The Moravec operator does not locate features to sub-pixel accuracies, so it is unable to resolve elevations in steps smaller than the height change due to one pixel disparity.

The algorithm is being implemented on transputers without virtual storage by the Royal Signals and Radar Establishment (RSRE) at Malvern and a Kilostream-networked 120 miles to the UCL SUN network. Because it does not produce sub-pixel disparities or sufficient density for DEM generation the

algorithm is primarily used as a source of seed points for the sheet-growing Otto & Chau algorithm.

2. PMF (Pollard, Mayhew and Frisby) method.

PMF is an edge - based algorithm developed at Sheffield University. It is a stereo correspondence algorithm using a disparity gradient limit (Pollard et al, 1985). It operates only along scan lines so it requires epipolar images as an input (epipolar based).

SPOT images of the same area are generally rotated with respect to each other (different orientation angles) so we can use an affine transformation to wrap the images to near epipolar. In practice it appears we cannot resample to true epipolar without iterative adjustment (Otto, 1988). Software to produce eppipolar images when supplied with a DEM has recently been written (O'Neill & Dowman, 1988).

3. Otto & Chau.

This quasi - epipolar algorithm is basically an extension of Gruen's Adaptive Least Squares Correlation algorithm ALSM (Gruen, 1982; Gruen & Baltsavias, 1986). The algorithm is claimed to be of extremely high accuracy, approximately 0.05 pixels, based on figures reported for aerial photography. With this algorithm the whole images can be automatically matched, instead of just selected patches.

The basic idea is to minimise the sum-of-the-square-of-the-differences between two image patches, with the minimisation being over a set of parameters specifying how the patches (and their grey levels) are allowed to be distorted between images (Otto, 1988). The correlator can only correct an initial estimate of disparity at a point and it has a limited pull in range (of the order of two pixels) so it must be given some approximately matching starting points. However, it also produces shaping information which can be used to estimate the disparity locally and thus the matcher can sheet grow out from these initial seed points (Chau, 1987).

8.2.2.1. The UCL experiment.

The SPOT images (three images) cover the same Aix En Provence area in the South of France (scene number 50-252).The images are in digital form (soft copy). These images were used as test data. The image characteristics are as follows:

1. Vertical image (free from atmospheric effects).
2. Left image (angle of incidence -17.5°) (affected by haze).
3. Right image (angle of incidence +22.6°) (several opaque clouds).

Note:

From the above SPOT images only the Left image and the right image are available in the Department in positive films (as hard copy).

The test area is the same as described in 4.2.1.1. Height information derived from the stereomatching algorithms is directly compared with the manually derived DEM (from 1:30,000 aerial photographs), which is assumed to be accurate ("true background").

8.2.2.1.1. Quality Assessment.

Two of the stereomatching algorithm methods are examined. The stereomatched points (SPOT elevations) are simply compared with the nearest more accurate reference point derived from aerial photographs, provided one exists, within a user specified distance. The distance is chosen with the criteria for minimising the additional error due to the variation of the terrain height (see § 5.2.4.2.1).

The Gruen errors (full 30 m DEM area) are shown in table 8.1 (Day & Muller, 1988).

Elevation error statistics	
Number of points	27835
Mean (m)	10.84
SD (m)	18.19
RMS (m)	21.18

Table 8.1. Gruen errors (full 30m DEM area).

The stereomatcher (PMF method and Gruen) output elevation errors are shown in table 8.2. (Day & Muller, 1989):

	PMF Method	OTTO & CHAU			
		21 pixel patch		9 pixel patch	
Image Pair	Left-Vert.	Left-Vert.	Vert.-Right	Left-Vert.	Vert.-Right
Points matched within DEM area	8380	25014	28053	23285	26759
Points compared with reference point	2903	8662	9794	8079	9302
Mean (m)	3.80	-6.92	-0.09	-6.54	-0.07
S.D (m)	45.19	12.67	11.24	12.09	12.71
R.M.S (m)	45.35	14.43	11.24	12.74	12.71
Max. (m)	548.70	138.66	126.42	162.80	547.81
Min (m)	-669.77	-106.62	-115.05	-109.06	-347.94
$\lvert \text{error} - \mu \rvert > 3\sigma$	1.24%	1.76%	1.54%	1.68%	3.03%

Table 8.2. Stereomatcher output elevation errors . After Day & Muller (1989).

The Error statistics of grid-point interpolated stereomatcher derived DEMs (95,865 points) are shown in the table 8.3. (Day & Muller, 1989):

	PMF Method	OTTO & CHAU		
		21 pixel patch		9 pixel patch
Image Pair	Left-Vert.	Left-Vert.	Vert.-Right	Vert.-Right
Mean (m)	-2.26	-7.32	-3.49	-3.19
S.D (m)	63.26	18.75	25.14	27.19
R.M.S (m)	63.30	20.31	25.39	27.37
Max. (m)	549.14	203.06	138.01	500.03
Min (m)	-684.86	-206.34	-268.56	-330.58
$\lvert$ error - $\mu \rvert > 3\sigma$	2.20%		2.67%	3.03%

Table 8.3. Error statistics of grid-point interpolated stereomatcher derived DEMs (95,865 points) . After Day & Muller (1989).

8.2.3. Other experiments.

8.2.3.1. The MacDonald Dettwiler (MDA) system (Hawkins and Westewell-Roper, 1987).

Stereoimages are matched using techniques originally developed in the field of computational vision. Image correspondence includes three steps:

1. Application of edge operator. The edge operator locates those lines in an image where there is a sharp change in image intensity. These lines are assumed to represent the edges of features on the earth's surface.

2. Boundary extraction. Boundary extraction builds feature descriptions from the detected edges. It locates and links together edges to form boundaries and gauges the shapes of the boundaries to determine the features represented in the images. The linked boundaries are then screened to separate those due to image noise from those due to actual image features.

3. Boundary matching. As a final step, a boundary matcher determines for each boundary in one image the corresponding boundary in the other image (if any). Once it has determined the correspondence, it calculates the disparity or parallax between the corresponding boundaries. Boundary elevations are calculated from the boundary correspondence using geometric modelling algorithms.

Geometric modelling relates the stereo imaging geometry and the parallax measured by the boundary matcher to the desired elevations. Spacecraft models derived in the image correction phase and the GCPs information are used in the geometric model.

Parallax is measured to subpixel precision to obtain sufficient accuracy in the DEM. To obtain high precision, several models must be used to compensate for earth, image and satellite effects.

Recent rigorous tests with SPOT imagery over a wide range of terrain types in both Europe and North America have demonstrated elevation accuracies better than 6m RMS, which will allow contour mapping with a 20 m contour interval at full accuracy.

8.2.3.2. The French - Canadian experiment (Begin et al, 1988).

The test area is between Sherbrooke and Coaticook (Quebec) where 5 digital elevation models were measured. A level 1A SPOT stereopair was used. Details of the SPOT images are given below:

Date	Angle of incidence
25 Oct. 86	-2.96
20 Jun. 87	29.29

The base/height ration = 0.6.

The images were problematic, with difficulties arising for the following reasons:

1. Different acquisition time . The images are acquired with one year and four months difference and different season (Summer and Autumn). This has resulted in a different land use.
2. The contrast was not good in the autumn image.
3. Small height/base ratio.

Six hundred (600) points to control the 5 digital elevation blocks were measured by aerotriangulation with an accuracy of 1 to 2 m.

In the first test the implementation which was used was a GESTALT Photo Mapper (GPM II) and a MDA system running the Meridian software. Five digital elevation blocks were measured. Each block covers a 5 x 5 km^2 area in a 50 m grid spacing (10,000 points). The digital elevation models were produced from the GPM II from 1:50,000 aerial photographs. The precision of a Gestalt Photo Mapper was estimated as 3 m. Those points are compared with the MDA elevation data captured from SPOT. The elevation data were measured on the top of the trees. In the MDA system ephemeris data were used. The statistical analysis of the results for three test areas are shown in table 8.4.

BLOCK	NUMBER OF POINTS	MEAN (m)	RMS (m)
1	10000	+7.5	14.2
2	10000	+5.9	9.9
3	10000	+12.4	9.2
Total	30000	+8.6	11.7

Table 8.4. Statistical results between the Gestalt Photo Mapper and MERIDIAN.

From table 8.4 we can see that the RMS elevation errors vary from 9 to 14 metres. This happened because of: the vegetation coverage, the difference in density particularly for the autumn image, the error ephemeris results.

Because of these factors a different analysis approach was applied using known elevation points. The statistical results using the known elevation points are shown in table 8.5.

BLOCK	NUMBER OF POINTS	MEAN (m)	RMS (m)
1	5	-1.0	2.4
2	15	+2.5	5.0
3	21	+9.6	9.9
Total	41	+5.7	8.7

Table 8.5. Statistical analysis results between the MERIDIAN and the known elevation points.

These results were affected by two factors: the error ephemeris data and the subtraction of one point with the other within a 50 x 50 m^2 area.

Moreover, the elevation values from the MERIDIAN were compared with the (600) reference points. Only 40% of those points were well defined in the autumn image. The statistical analysis results between the MERIDIAN and the reference points are shown in table 8.6.

Coords	NUMBER OF POINTS	MEAN (m)	RMS (68%) (m)
X	230	1.18	6.2
Y	230	-1.35	5.2
Z	230	-3.48	13.1

Table 8.6. Statistical analysis results between the MERIDIAN and the reference points.

In another experiment the elevation values from the Anaplot analytical plotter were compared with the (600) reference points. Again only 40% of those points were well defined in the autumn image. In this experiment ephemeris data are not used. The statistical analysis results between the Anaplot and the reference points are shown in the table 8.7.

Coords	NUMBER OF POINTS	MEAN (m)	RMS (68%) (m)
X	230	-1.26	6.1
Y	230	0.33	5.2
Z	230	0.98	8.0

Table 8.7. Statistical analysis results between the Anaplot and the reference points.

8.2.3.3. The Taiwan experiment (Chen et al, 1988).

The test area covered 3 x 3 Km^2 near Miao-Li area (central Taiwan). A DEM was created automatically from digital SPOT images with a 30.1° convergence angle and a base/height ratio of 0.57. The elevations range from 4 m to 175 m. The data were compared with grid of 2,500 check points produced from a base map (2.5 x 2.5 Km^2).

The mathematical model included four parts: a) a bundle adjustment for SPOT imagery of CSRSR at Central University, b) epipolar image transformation, c) image matching and d) DEM computation. The target window size was 7 x 15 and the matching is a 1-D operation. The generated DEM comprises 90,000 (300 x 300) points and each point represents 10 x 10 m^2 area. The average of the differences between the two DEMs is +7.3 m. This shows that the DEM produced from SPOT is systematically higher than the DEM base. Through the investigation it was found that there were some peaks where matching failed. Accordingly, using linear interpolation for the parallax difference cannot describe the terrain properly. The RMS for the differences was 13 m.

8.2.3.4. The near mount Fuji experiment (Fukushima, 1988a & 1988b).

Three digital image correlation methods were used:

1. Simply using stereopair.
2. Eliminating mismatches using two stereopairs.
3. Using the condition that three bundles have the same intersection point.

DEM were generated by image correlation for three test areas each of 2 x 4 km^2. The ground features of the test areas are as follows:

Test area 1: Mountainous with steep slopes. Some areas covered with a little snow.

Test area 2: The centre of this area is flat and each side of this area is mountainous.

Test area 3: This area covered with coniferous forest. The slope is gradually

changing.

To evaluate the accuracies of DEM generated by image correlation, the base DEMs were acquired from 1:25,000 topographic maps.

In this study, the following three image correlation methods were applied:

Case 1 - 1 : Stereomatching. Centre and left image pair was used (B/H =0.20).

Case 1-2 : Stereomatching. Centre and right image pair was used (B/H=0.52).

Method 2-1 : Triplet matching. Eliminate mismatching using two stereopairs.

Method 2-2 : Triplet matching. Using the condition of the same intersection point.

In this experiment the standard deviation means the root mean square error of the discrepancy after removing bias.

From the above experiments we can summarise as follows (Fukushima, 1988a):

1. Preliminary tests:

The highest accuracy was given by method 2-2 with 5 x 5 window size and using median filter (3 x 3). The standard deviation was 12.26. The biases in this test area were -22 to -24.

Case 1-1 (B/H=0.2) was more accurate than case 1-2 (B/H=0.52). The reason may be that the quality of the right image is worse than the other images.

2. Image correlation of test areas:

Window size 7 x 7 was used as it was found to give better accuracy.

The condition of same intersection point method gave the best results. The standard deviation was from 11 to 14. In the flat area the accuracy is about 10 m.

The area of large error using triplet matching is smaller than that using stereo matching. However, both method 1 and 2-1 using the right image wandered near steep slopes.

In the snow covered area, the distributions of snow were different for each image, but a large error was not detected.

The biases depend on the test area and the method. The reason for this may be systematic errors of orientation or some other factors.

In another experiment (Fukushima, 1988b) a flat area and a mountainous area were measured. Two SPOT stereopairs were used with B/H= 0.52 and

B/H=0.72. The DEM were again compared with those from 1:25,000 maps. The DEMs in the flat test area had better accuracy than those in mountainous areas. One reason is that the planimetric displacement has more influence on height discrepancy in a mountainous area. There is not much difference in accuracy between the DEMs from SPOT with higher B/H ratio and those with lower B/H ratio. The height discrepancy of DEMs is shown in table 8.8.

AREA	B/H	RMSE (m)		MAX (m)	
		100m Mesh	50m Mesh	100m Mesh	50m Mesh
Flat	0.52	16.8	13.7	72	42
Flat	0.72	15.1	11.7	99	68
Mountainuous	0.52	17.9	16.7	-75	45
Mountainuous	0.72	25.1	33.5	-102	113

Table 8.8. Height discrepancies of DEMs from SPOT in the Mt Fuji experiment.

From this result, a 40 to 50 m contour interval can be drawn using SPOT (Fukushima, 1988b).

8.3. Relation between two UCL experiments (manually captured DEM data and by stereomatching techniques).

8.3.1. General.

In the following section a quality assessment between automated and manual methods of extracting elevation data is carried out.

The SPOT images used in both experiments are the same. The hardcopy prints used in this project were derived from the digital tapes (softcopy data) using a McDonald Dettwiler Fire 340 film writer. The aerial photography data used as the ground "true" are the same (see § 5.2.3).

In both experiments the SPOT elevation data were compared directly with those derived from aerial photography utilising the nearest reference point, if this

exists within a specified distance. The distance is chosen with the criteria for minimising the additional error due to the variation of the terrain height (see § 5.2.4.2.1). The compared heights were checked within radii of 15 and 5 m. The statistical analysis results are similar. The program used for comparison of the two data sets utilising the nearest reference point also gives satisfactory results.

The statistical analysis results were compared with those found through the check program written for the project requirements (see appendix B) in which the four neighbouring points from the aerial photography are compared with the SPOT point weighted over the square distance. The two comparison programs agree with the statistical analysis results.

8.3.2. Quality assessment of the stereomatched elevation data.

The Gruen stereomatcher (Otto & Chau, 1989) statistics (see table 8.1) for 27,835 points in the test area are :

mean = 10.84 m and standard deviation = 18.19 m.

In another experiment the stereomatcher output errors derived from:

the vertical image (free from atmospheric effects) with the right image (several opaque clouds) and

the vertical image (free from atmospheric effects) and the left image (affected by haze).

Quality assessment of the Gruen algorithm is carried out in this study as it gives the best results of the stereomatching algorithms in use at UCL.

The Gruen partial and overall statistical results are shown in table 8.9 derived from table 8.2.

	21 pixel patch		9 pixel patch		21 and 9 pixel patch overall statistical values
Image pair	Left-Vert.	Vert.-Right	Left-Vert.	Vert.-Right	
Points compared with refer. point	8662	9794	8079	9302	
Mean (m)	-6.92	-0.09	-6.54	-0.07	-3.19
SD (m)	12.67	11.24	12.09	12.71	12.17

Table 8.9. Gruen stereomatcher output partial and overall statistical results.

8.3.3. Quality assessment of the manually measured elevation data.

The statistical results derived from the manual measurements are shown in table 5.1.

The overall statistical values after comparing 6,833 points are:

mean 2.94 m and standard deviation = 15.82 m

The statistical results derived from the data recorded by the experienced operator (2,124 points or 31.1%) are shown in table 5.14.

The overall statistical values are:

mean = 2.18 m and standard deviation = 13.13 m.

The statistical values from the second SPOT hardcopy measurements (2,936 points) are shown in table 5.15.

The overall statistical values are:

mean = 3.60 m and standard deviation = 12.75 m.

Thus the overall statistical values from the three sets are:

mean = 2.97 m and standard deviation = 14.65 m

8.3.4. Quality assessment of manually captured DEM data and by stereomatching technique.

By comparing the overall statistical values for the automated technique (mean= 10.84 m and SD = 18.19 m) with the overall statistical values for the manual measurements (mean = 2.97 m and SD = 14.65 m) we can see that although the mean statistical value of the elevation data derived using the automated techniques shows a systematic error larger than the mean value of the data derived by manual measurements, the standard deviation value is not very different .

In the second experiment with the automated technique, the statistical values (mean = -3.19 m and SD = 12.17 m) are better than the statistical values derived from the data measured manually (mean = 2.97 m and SD = 14.65 m).

The above comparison between the two techniques gives the impression that automated techniques can provide elevation data equally good, or better than, elevation data captured manually with operator assistance.

8.4. Manual data capturing techniques versus automated techniques.

Automated algorithms produce fast DEMs, depending on the implementation and the software (number of constraints included), but in any case much faster than the human operator.

The project operator estimated the time needed to measure one block (900 points) as 45 minutes (3 seconds per sample) in the overall area with an average slope of 36.5%, while for the same number of points in the overall area with an average slope of 58.1%, 49 minutes were needed (1 point in 3.3 seconds). The procedure of setting up the model and the preparation time is not included in these times. Ackermann (1978) and Dowman and Muller (1986) show some figures for scanning a stereomodel ranging from 2.3 sec to 6.1 sec per point.

Toomey (1988) estimates the average measurement time for aerial photography to be 1.5 second per mass (in a grid node) point. The time varies

according to the clarity of the aerial photography and the vegetation cover.

The Otto & Chau algorithm was applied to two SPOT panchromatic scenes taken 6 days apart. One view was from nadir; the other from 22.6° to the right. One pixel disparity between the images corresponds to approximately 30 m in elevation (Day et al, 1988b). For 98000 points this needs two and half days as a background program on a SUN 3/160 workstation. This represented an area of 20 x 30 km^2. Compare this to an experienced operator on an analytical plotter with automatic drive to each 50 m grid point, where 3 seconds per point (1,200 per hour) would result with between 7,200 (6 hours) to 9,600 points (8 hours) per working day; not accounting for breaks, model orientation, or operator fatigue. So one requires between 10 and 13 days to produce the same quantity of data. Using 30 T800 transputers, Otto & Chau (1988) claim a quality, dense disparity map from a pair of SPOT images (60 x 60 km^2), in about two hours. Compare this to the operator who realistically could produce about 7,000 points per working day, a 50 m grid (1,440,000 points) would require 205 working days, while a 100 m grid interval (360,000 points) would require 51 working days.

The whole CPU time on a VAX 8650 computer for the Taiwan experiment see § 8.2.3.3 (90,000 points), including the DEM interpolation was 43 minutes. That means it can produce 2,100 points per minute (Chen et al, 1988).

Some studies showed that the type of parallelism for the algorithm mapping on a transputer array will change the speed-up factor dramatically.

A theoretical study (Muller et al, 1988a) has suggested that an array of 32 floating-point transputers of T800-4MB RAM should be able to process a complete SPOT pair in around two hours (from raw image to DEM). With grid spacing 50 m, this timing is equivalent to a window 64 x 64 pixels processed in one second.

Automated algorithms produce accurate DEMs. Some of them work within a sub-pixel accuracy eg. adaptive least squares correlation technique.

Some researchers state that the digitally correlated Gestalt data are generally less accurate than manually digitised data because of limitations of image correlation. Generally, automated techniques appear to some people to be somewhat

worse than results obtained by setting the floating mark visually. However others, such as Ackerman and Schneider (1986), think that digital image correlation is capable of very high accuracy, as good as or better than human stereoscopic vision.

Human operators interpret problematic parts of images in different ways. In contrast, a mathematical algorithm (ie. a stereomatching algorithm) interprets in the same way (if the starting point is the same). One disadvantage of the automated procedure is that it can not interpret the ground level through the tree canopy.

The Otto-Chau stereomatcher algorithm has been applied to several complete SPOT satellite images with a variety of time differences between images ranging from 3 days to 8 months; land cover types; geographical areas (arable, tundra, snow, scrubland, urban, woodland, desert, sea); base to height ratios; atmospheric conditions (from light haze, contrails to dense clouds and their shadows) and intrinsic image qualities. In most cases, more than two-thirds of the maximum possible number of grid-points were matched. This includes the effect of atmospheric conditions. Preliminary results indicate that human operators could not set the floating mark for the majority of the points the matcher rejected. In addition, it appears that automated matching can produce more accurate estimates than trained photogrammetric operators (probably owing to the small-scale of the imagery). Above all, the stereo matcher produces millions of reliable estimates in the same time as a human operator would produce a few thousands (Muller, 1989).

8.5. Conclusions.

DEM generation by automatic and digital correlation is now starting to be applied in production on a wider scale. Large cartographic organisations in some countries produce large scale maps with these techniques. However, the main objective is to develop a system for generating accurate, dense DEMs of different application areas from satellite stereoimages (currently principally from SPOT). The DEM derivation will them be used in the rectification of the satellite images for orthophoto production and thus dense range-maps in "real-time" will be possible.

Some of the investigators claim a 10 m RMS vector accuracy by using

sophisticated stereomatching algorithms and a few seed-points from a SPOT stereopair. These results appear better than from those derived from the manual measurements carried out in this project. Therefore it is possible in the future that a further development of the stereomatching algorithms will be the way to extract the height information for production of digital elevation models.

Speed assessment shows that with the use of transputer arrays two SPOT images (36 MB each) can be matched in 6 to 7 hours (compared with 6 days on a single SUN 4 workstation). In the near future it will be possible to match two images in less than 2 hours, compared with the human operator who, for a scene with a 50 grid interval, needs 150 working days (8 hours per working day).

All the above shows that automated methods lead the way for the future in DEM generation, but with the drawback of the 'bald earth' problem and the additional manual measurements in the areas where the algorithm fails for various reasons (ie. in areas with different radiometric properties), or produces erroneous results (ie. in shining areas).

Chapter 9.

DEM applications.

9. DEM applications.

9.1. General.

Considerable developments have taken place in terrain modelling during the past 30 years, particularly in methods of data acquisition, data storage and speed of data processing. With the ever increasing capabilities of modern computing hardware it seems likely that this trend will continue.

DEMs are essential to many Geographic Information Systems (GIS). In such systems the elevation data, other information derived from this, gain increased importance when they are combined with other geographic information on surface and sub-surface characteristics. Many GIS now exist that exploit DEMs, particularly in disciplines concerned with the natural environment, and examples of GISs concerned with forestry management, hydrographic modelling and land-use analysis may be found in the literature.

The widespread use of DEMs and the importance they have assumed in many situations, derives from the basic elevation data they hold. Nowadays the techniques of terrain modelling are in widespread use and have been applied widely in physical and earth sciences.

A number of DEM products that form part of the output from the majority of terrain modelling and exploitation systems may be identified.

1. Gradient and aspect.

Information on slope (gradient and aspect) may be computed from the DEM, particularly if the elevation information is stored on a regular grid. Faced with this arrangement, slope values may be computed by applying a local operator. A 3 by 3 matrix is generally used. The local gradient in both the x and y directions are calculated and subsequently combined to provide an estimate for the slope of the central matrix point.

Gradient and aspect estimation are useful in many disciplines. Road/traffic engineering, geomorphology, geophysical exploration and environmental studies

use the gradient and aspect as a useful tool. Gradient and aspect estimation in raster form are presented in figures 2.3, 2.4,2.5, 2.6,2.7 and 2.8.

2. Surface visualisation.

The most advantageous and sophisticated form of terrain modelling is in the field of visualisation. Many people like to see a perspective view or an isometric view of the original terrain from a point of view chosen arbitrarily.

Terrain visualisation can be used in quality control. Quality control is used to counter the difficulty, associated with the production of large terrain data bases, of identifying gross errors at the data acquisition phase. Displaying techniques give a handy check for a generated DEM.

The main problem of surface visualisation is the projection of the 3D model on to 2D screen. Display techniques are based on computer graphics raster representation.

a) Vector techniques (3-Dimensional views - orthographic and perspective views).

For 3-Dimensional views either a parallel projection to produce an isometric (orthographic) model, or a perspective projection may be employed. Most viewing programs use a simple profiling technique, which involves sampling the DEM on a line or column basis, and enhancing the model by hidden line removal, the overlay of a grid, or the use of colour. More sophisticated viewing programs employ either surface or solid modelling techniques, and achieve a degree of realism by shading the terrain surfaces according to aspect, colouring according to depth, or by modelling shadows and surface texture.

Isometric projection gives an easily perceived 3-Dimensional view of the terrain. It is the best suited for its perception in the human brain and needs little computational effort.

Laser-Scan DTIVIEW module (see appendix H) produces perspective or isometric views of a DEM for validation or display purposes. The quality of the

isometric or perspective view on the laserwriter output is very poor. Therefore it was decided to present the isometric and perspective views from the SPOT measured elevation data for the area 14300 x 9900 m^2 (14400 points at 100 m grid interval) as photographs. Plate 9.1 shows a perspective view of the area from the South-West direction while plate 9.2 shows the perspective view from the South-East direction (height of view 250 m above sea level). Plate 9.3 shows an isometric view of the area from the South-West direction while plate 9.4 shows an isometric view from the South-East direction (for the explanation of the view elements see appendix H.3).

b) Raster representation.

Variation in elevations are normally represented symbolically by contours on topographic maps. Occasionally hill or relief shading is added manually by the cartographer in order to enhance the topography. The slope and aspect information may be combined to model the effect of illuminating the surface. Using this information, a conceptual light source, and a model that describes the reflectivity of the terrain surface, a shaded overlay may be produced. Conventionally the light source is placed in the northwest at a zenith angle of 45 degrees, although the user is usually free to vary both the azimuth and zenith angles. The degree of illumination received by a point on the surface, and therefore the grey value used to represent the point on the shaded overlay, is related to the angle of incidence. Slopes normal to the light source appear brighter than slopes facing away from the source of illumination.

Terrain display techniques by raster representation are developed at the Department of Photogrammetry and Surveying UCL on SUN computer graphics work station. The techniques already developed are as follows:

1. Intensity range image (digital terrain image).
2. Shadowed image.
3. Colour-coded isometric projection.

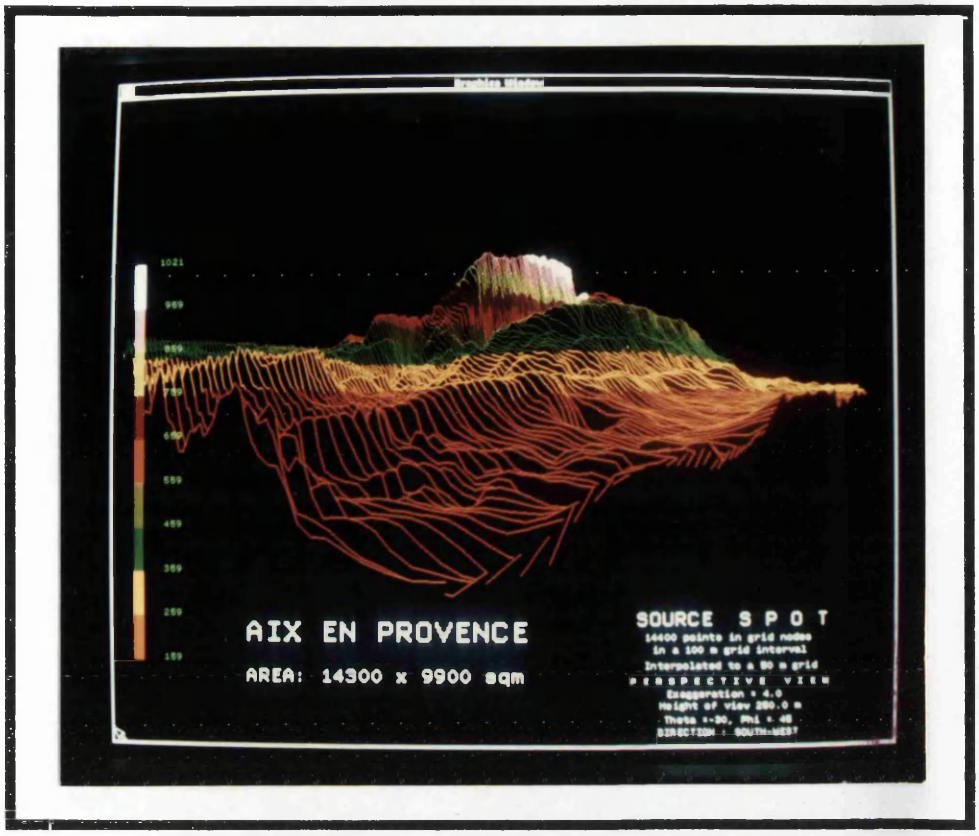

Plate 9.1. Perspective view of the SPOT DEM from South-West direction (height of view 250 m above sea level)

Plate 9.2. Perspective view of the SPOT DEM from South-East direction (height of view 250 m above sea level)

Plate 9.3. Isometric view of the SPOT DEM from South-West direction

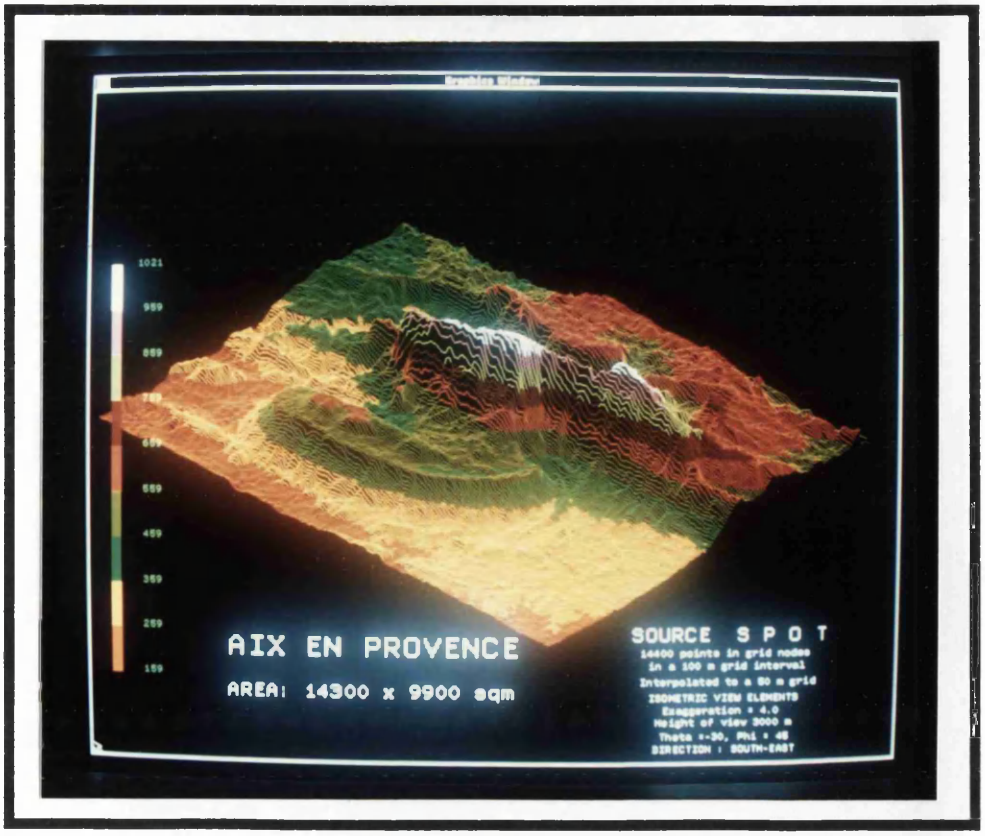

Plate 9.4. Isometric view of the SPOT DEM from South-East direction

Also Laser-Scan ROVER module (see appendix H) displays both grid based and vector geographic data (combined raster and vector data). In this thesis the term digital terrain image (raster form) is followed as more specific rather than intensity range image as the images produced dealing with the terrain.

Only the intensity ranges and shaded relief images are included in this section. The principle of the intensity range image technique is simple. Each planimetric position of a pixel is assigned with a particular grey value which ranges in proportion to the height of the point from the DEM data available. Since the DEM spacing may be larger than the pixel size of the computer graphics screen, subsampling techniques are obviously involved in this case.

The shaded relief image technique is more complicated. First of all, the reflectance properties of a surface cover are determined by the bidirectional reflectance distribution function (BRDF). For the sake of simplicity, the BRDF is assumed to behave like a Lambertian reflector. Therefore, the terrain looks equally bright from all directions (Pearson, 1987). The shaded relief image synthesis is then modelled through a simple Lambertian surface, ie. the radiance is only a function of the incident sun angle which is expressed as a surface gradient computed from the DEM data.

Raster techniques of terrain representation on computer graphics work station is superior to the vector technique. Terrain reliability, such as break lines and drainage patterns are better represented.

The positive and negative digital terrain images (intensity range images) derived from the aerial photography measurements (46200 points) of half of the area (6900 x 6000 m^2) are shown in figures 5.3 and 5.3a, while the positive and negative digital terrain images derived from the SPOT measurements (14400 points) of the whole 16 measured blocks (14300 x 9900 m^2) are shown in figures 5.5 and 5.5a. Laserwriter outputs have the drawback of not including the key to the elevations represented by the grey levels. Plate 9.5 shows the digital terrain image of the same area as figures 5.5 and 5.5a but with all the information that appears on the screen and the key of the elevation range

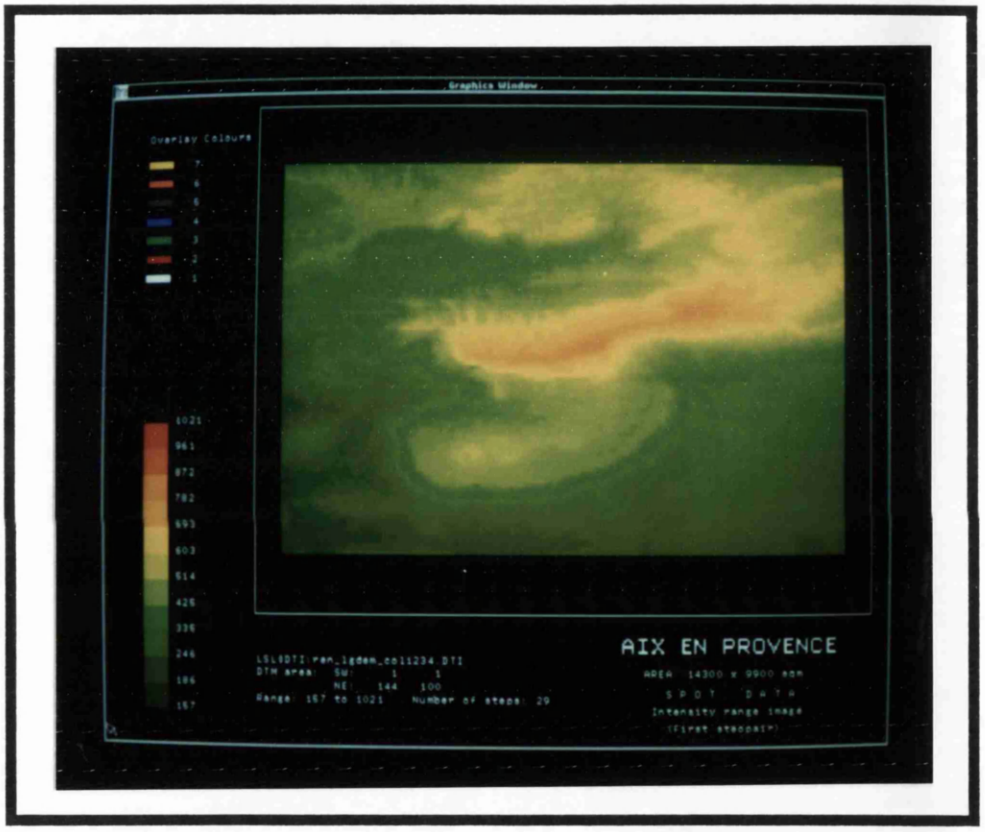

Plate 9.5. Digital terrain image derived from the SPOT elevation measurements

The Lambertian shaded nadir view of the DEM produced from the aerial photography measurements (95220 points) of all of the test area (12420 x 6900 m^2) is shown in figure 5.2.

c) Visibility.

Visibility may be computed from the DEM, particularly if the elevation information is stored on a regular grid. The visibility status of a point on the surface with respect to another point either on or above the surface may be determined by a consideration of the elevation values that lie between these two points. A large number of line of sight algorithms now exist. Some of them take into account factors such as: the curvature of the earth, atmospheric refraction, or in the case of radio propagation studies, the characteristics of the transmitter.

Visibility applications can be simple or complicated (eg radar, radio transmission, and observer positioning) where a large number of lines of sight calculations need to be performed in order that visibility within a particular cone or circle of vision may be determined.

9.2. The application of the DEMs.

This review of DEM utilisation is far from exhaustive. In this section it is not proposed to describe in detail all the applications to which DEMs are currently being put. Rather a number of brief descriptions which emphasise their multi-disciplinary and varied use in some fields are presented .

1. Cartography - topographic mapping.

Digital storage of elevation data for digital topographic maps in national databases for representations of the terrain is often one of the main elements of the mapping process. Digital elevation models have many uses in cartography and topographic mapping such as:

a. Contour production.
b. Relief shading (insolation) maps.
c. Production of orthophotos and vice versa.

d. Drawing of profiles along defined lines , estimation of volumes and cross - sections.
e. Regular grid comparison.
f. Single point and grid error comparison.
g. Intervisibility - view maps showing hidden areas from designated viewpoints.
h. Slope and slope orientation maps. Usually a morphological map superimposed on a contour base map and shaded according to slope steepness.
i. Difference models (ie. statistical analysis and comparison of different kinds of terrain).
j. Miscellaneous maps. (ie. as a background for displaying thematic information or for combining relief data with thematic data such as soils, land-use or vegetation.

All the above, the use of DEMs in contouring, relief shading, production of orthophotos and slope maps are further examined below.

a. Contour production.

This is one of the oldest terrain displaying techniques, but still remains the most useful for engineering applications. The representation of the terrain is based on isolines connecting the same heights in an area. Isolines is another name for contour lines produced after interpolation (in conjunction with terrain relief in topographic mapping, the isolines are contour lines). A large number of contouring algorithms have been developed which offer considerable flexibility in terms of contour smoothing and generalisation. However, sometimes it is difficult to identify which algorithm gives better results and consequently is the most suitable for a specific use.

b. Relief shading (insolation) maps.

On small scale maps hypsometric layering and hill-shading provide either an alternative to contour lines, or function as an additional aid to the perception of relief. The shaded overlay is particularly difficult to produce by manual cartographic means, requiring considerable artistic and geographic skill on the part of the cartographer. DEMs now enable shaded images to be produced rapidly, according to a wide range of cartographic design specifications. Calculation takes

into account not only terrain slope and orientation, and the cast shadows produced by the surrounding relief, but also absorption factors according to the elevation of the sun and to the altitude of the point.

c. Production of orthophotos and vice versa.

The process of producing an orthophotograph depends on the systematic scanning (in continuous parallel profiles) and measurement of terrain height over the whole of a stereomodel. Thus the technique produces a complete record of the height variations in the landscape as a by-product of the orthophotograph production process.

If DEM data are available the height information can be supplied to the computer which drives the instrument. The elevation data are already combined into a complete terrain height model.The resultant part of the photograph is exposed simultaneously, thus building up the orthophotograph.

h. Slope and slope orientation maps.

Slope form can be mapped by determining the position of breaks and changes of slope. A break slope occurs where there is a sharp junction line between two slope, or morphological units, of differing steepness. A change of slope occurs where the junction is more gradual and occupies a zone on the ground. When morphological maps are superimposed on a contour map, the resulting map gives much more detailed information and a more precise statement of surface form than is possible from contours alone. They provide a statement of the area distribution of morphological units, their steepness, and the space which they occupy. Thus for any hillside it is possible to obtain a complete assessment of the range of slope steepnesses, the area of the slopes at each slope angle or in each slope category, and the relative positions of the slopes at each slope angle. This type of data is highly amenable to numerical analysis.

The relationship between aspect and slope steepness has often been examined. In the higher latitudes of the northern hemisphere the south-facing slopes will receive a greater amount of sunshine and warmth, which especially under glacial and periglacial conditions may have a considerable effect on slope processes and the development of meltwater channels down the hillside (Doornkamp & King, 1971 pp. 175).

Slope and slope orientation maps are helpful for solving problems linked with planning and agriculture.

2. Hydrographic/Bathymetric mapping.

Once the depth information from echo sounder techniques is obtained, models of the seabed can be obtained. The mapping procedure (identification, location and measuring of the distinct lines such as ridges, valleys and breaklines) is difficult.

3. Road / traffic Engineering.

Initially DEMs were used almost exclusively for planning routes (highway and railway design) and the determination of earth work cut and fill volumes for highway engineering projects. A free choice of route location given to the designer is decreasing due to the environmental problems such as: forest destruction, noise and pollution.

Prescriptions on slope may be prescribed depending on the road category. A certain limit must not be exceeded, or if the slope value is close to the specified bounds, should not be exceeded for greater than a certain length of the road. Often slope calculations may be restricted to a particular area of interest or a particular direction (eg along the line of a proposed road).

Landscape analysis and visualisation has found a number of interesting applications in the field of road design. Many road engineering design systems now offer visualisation capabilities. These form an integral part of the design process and allow the design to be subjectively assessed and refined for safety and visual intrusion in the context of its environment. Some additional applications are: The road lighting scheme design, road safety and the street furniture design and placement.

4. Civil Engineering.

Nowadays DEMs are applied in projects with a large area of extent such as landscaping, estate modelling, digital design models of proposed structures (landscape design and urban planning), locations of dams and realistic visual impressions to illustrate the environmental impact of the civil engineering project.

5. Geomorphology.

DEM data sets captured in different time periods can help geomorphologists to study the changes of the ground surface, such as snow, to in relation time, undergo continuous metamorphic changes in response to wind, sunshine, temperature, rain, additional snowfall, and other factors such as erosion and run-off. Relevant

algorithms have been developed to extract form lines (ridges, valleys, drainage basins, stream networks etc.) from the DEMs. These are used for computing slope maps, aspect maps, and slope profiles that can be used to prepare shaded relief maps. DEMs also offer the opportunity to produce 3-D models of the surface allowing a investigator to visualise surfaces under different viewing conditions.

6. Geology and energy exploration.

Geological information can be derived from sparse or scattered data obtained during drilling. The data is usually highly clustered, and poorly distributed. The graphic representation of seismic and geological information as 3-D displays enables complex structures to be rapidly understood for planning decisions.

With that information, models of underground surfaces defining specific geological strata can be created. Depending on the geological problems (special features) a special technique can be applied in order to supply the data for modelling.

Geology has most benefited from space imagery since satellite data were made routinely available in 1973. The synoptic view of the earth surface brought by Landsat has been a milestone in geological knowledge as large portions of the globe could be visualised at a glance and regional trends or inter-regional relationships directly analysed. The most obvious contribution was firstly in structural analysis and regional interpretation with the discovery of large linear or sub-linear features (lineamends) generally linked to surface or deep seated faulting. Interpretation improved for rock discrimination with the use of multispectral analysis, best performed by the Landsat TM multispectral scanner. However, many photogeologists were still disappointed by satellite data that was found to have too coarse a ground resolution to resolve local problems, and more significantly by the lack of stereoscopic capacity for terrain interpretation. Landscape morphology is directly controlled by geology through differential erosion and weathering processes acting according to physical rock properties and structural organisation. Therefore, a large part of the surface geology information is deduced from morphology and landform study, which is in turn only fully grasped with relief perception.

7. Hydrology.

Terrain data might also be useful in fields such as management of water resources and understanding of the hydrology of high elevation ecosystems.

8. Geophysical exploration and mapping.

The DEM contributes to the development of basic theories and techniques by geophysicists in mapping and exploration, such as ground resistance, ground gravity field etc.

9. Mining Engineering.

This is a closely related field to that of geology and geophysics. Modelling of coal stocks or any other minerals to give the estimated volume is a common application.

10. Meteorology and air quality modelling.

Physical and chemical atmospheric processes that affect air quality, visibility, precipitation, and other weather phenomena has indicated a need to characterise more explicitly the topographical, geological, and vegetative features of the underlying terrain. Digitised terrain data for regions of complex topography have been used in modelling wind flow patterns, for predicting the wind fields, and the visibility in remote and scenic areas. DEMs are also useful in precipitation enhancement and mountain hydrometeorology.

11. Environmental and Forest studies.

DEM are used to evaluate impacts of a range of land management problems and planning applications. Depicting contours, slope and aspect, seen areas and perspective views provides a general overview for land management decisions such as alternative uses of forest lands etc.

12. Remote Sensing.

DEM data have several possible applications in remote sensing, particularly when regional data are available. For example they have been used to improve the geometric quality of satellite imagery, or to improve the accuracy of the supervised classification techniques which are currently being used. The correction of the radiometric and geometric effects in the image due to terrain variation over the terrain image is particularly important when dealing with non-vertical imagery.

The use of ancillary data for both image rectification and to built additional control and knowledge into image analysis operations is becoming increasingly important. Most image analysis systems are now designed to accommodate both

remotely sensed data and digital geographic data such as elevation and derived data in the form of a matrix (Catlow, 1986).

13. Navigation.

Airborne vehicles can carry a navigation checkpoint system to compare (correlate) the terrain data obtained by an on-board sensor with stored terrain data to find a data match and thus determine aircraft position. The data can be obtained using a range-limited horizon (Carlson, 1978) which is the maximum elevation to the terrain as a function of azimuth angle in front of the aircraft for terrain within a given range limit.

14. Radio communication.

The determination of areas of hidden or 'dead ground' is vital in estimation of the optimal position of communication equipments such as radio antennas and transmitters in order to minimise the number. This can be carried out by estimating the field-strength level for a land mobile radio communication system and the nature of the transmitter (the refraction of the propagating waves etc).

15. Film production (stochastic fractal models).

Realistic or unrealistic terrain modelling can be used. A further approach for texturing terrain models involves the use of fractals, a class of irregular shapes that are defined according to the laws of probability. Fractals can be used to create views of artificially created surfaces and is of particular relevance in the field of computer graphics and animation. Landscapes generated with fractal dimensions (see § 7.3.2) between 2.2 and 2.3 have been found to produce realistic looking images in several animated sequences for science fiction films and advertising (Kennie and McLaren, 1988). Fractals can accurately model the natural terrain (Mandelbrot, 1982) so the applications are wider than merely in film production.

16. Military.

Flight and radar simulation is an advanced and sophisticated form of terrain modelling. Realistic representation of the earth surface derived from terrain models, is combined with the requirements for real time constantly changing simulations of the pilots view of the ground. Static simulations can be applied in battlefield planning. In military Engineering terrain models may be used to derive the visibility from a specific point on the terrain and for missile guidance.

Information about slope may be used to plan suitable routes for tracked and untracked vehicles.

As digital terrain modelling is an application of surface modelling which describes the process of representing a physical, or artificially created, surface by means of a mathematical expression, some additional applications arise from using surface modelling in other disciplines such as:

a. Medicine (representation of the human body).

b. Architectural Engineering (building representations).

c. Archaeology (ruin representations).

d. Industry. In many fields such as mechanical, shipbuilding and aeronautical applications (ships hull, car, aircraft surfaces).

9.3. SPOT derived DEMs and their applications.

Mapping from satellite imagery offers advantages over conventional techniques in terms of large area of coverage, with substantially lower cost. In particular SPOT imagery possesses the following key advantages in topographic mapping:

1. Data acquisition flexibility.
2. Large ground coverage.
3. Improved spatial resolution.
4. Good geometric performance.

The large area of coverage and the small image scale offers the advantage of employing automated techniques for extracting the height information. There is a great tendency to develop automated techniques for extracting information from SPOT imagery which is adequate for :

a. Image map production (controlled mosaics, orthophotographs).

b. Digital elevation models, landscape 3D, perspective, flight simulation.

c. Topographic maps (compatible with standards currently in use).

As a SPOT scene covers a large area, SPOT images are adequate for large projects such as the creation of DEMs of not only a nationwide but also of a

continental scale, ie a few hundred SPOT images are sufficient for a DEM production over all Europe, in a reasonable time. Accuracy of the SPOT derived DEMs is obviously a restriction for most of the applications referred to in § 9.2, but they can be used in many disciplines that carry out projects with global goals or general purposes.

9.4. Conclusions.

DEM is an important part of most GIS. Their importance derives from the basic elevation information they hold. The elevation data form a separate overlay layer, which is combined with other information in many disciplines. For this reason DEM utilisation appears to be far from exhaustive.

Techniques of terrain modelling are in widespread use in physical and earth sciences and in engineering, while many other disciplines use terrain modelling as one of the most important factors when planning, producing and developing their systems.

Terrain visualisation is one advantageous and sophisticated form of terrain modelling. Apart from a handy quick check for DEM quality, terrain visualisation can also give a representative and easily understandable image for planning and immediate action, while the real-time visualisation techniques facilitate and improve the quality of decisions.

Satellite images facilitate the automated extraction of the height information. Height information can be used in image rectification for mapping production, while by overlaying the image over the DEM it is possible to produce simulated models of the earth which are useful in many applications.

Chapter 10.

Conclusions.

Discussion and recommendations.

10.1. Conclusions.

10.1.1. Mapping from SPOT data.

Mapping from satellite imagery offers advantages over conventional techniques, in terms of large area of coverage and substantial cost savings, compared with conventional aerial photography for providing the height information. Data acquisition and ground control costs are substantially less than for equivalent aerial photography, due partly to a decreased need for ground control. However a mapping project using polar orbiting satellite data introduces different considerations from those using traditional aerial photo based methods because more rigorous testing is required, especially in conjunction with the need for effective ground control points and the effect of the earth curvature.

SPOT satellite is, at the present time, the most suitable system for topographic purposes. Mapping from SPOT possesses the following advantages over other current satellites : data availability, constant global coverage which can be programmed, and the formation of stereopairs with good geometry, B/H ratio, spatial resolution and radiometric properties.

SPOT satellite imagery compared with aerial photography is more sensitive as regards the geometric quality, the radiometric quality and the operator comfort . Some of these factors affect both the geometric and radiometric quality while all of them affect the quality of the measurements made by the operator. For manual measurements and mapping the geometric accuracy is more important than the radiometric quality which only causes difficulties and uncertainties to the operator.

The accuracy (quality) of ground control points is of major significance in the procedure for setting up the SPOT model. GCPs must be well distributed and identifiable in the satellite image. The control is better when chosen (if possible) in the valleys (lower level) rather than on the top of hills or mountains (upper level). The location of the GCPs is also very important. It has been found found that the best GCPs are on road junctions (main and secondary roads) particularly if the roads are joined at an angle of about 90 degrees, as these are easy to detect, to locate and to observe. They should be avoided in the crossing centre (centre of

gravity) as this is difficult to define in planimetry.

Recent tests carried out by OEEPE on the aerial triangulation of SPOT imagery showed that SPOT models can provide appropriate and satisfactory ground control for later use in the exterior orientation procedure. This is very useful for large mapping projects, because the SPOT imagery is going to be less dependent on the ground control. Moreover, using the SPOT orbital parameters and ephemeris data the number of control points could be reduced dramatically, even as far as zero. With the use of orbital parameters and zero control points an RMSE vector error of 50 to 100 m on the check points is possible. Also with the use of two control points and the orbital parameters the results obtained are generally satisfactory.

In large area mapping projects, it is necessary to make sure that the cartographic specifications of the earth's geoid are accurate, and to begin to address standard methods of storing and accessing the huge quantities of data. One major shortcoming of using satellite imagery is the difficulty in deriving accurate object space positions of geographic features from the imagery. This problem is usually not significant for small geographic areas (3,600 km^2 or less), where one monoscopic image or one stereomodel is all that is required; it is often easily solved by using an abundance of accurate photo identifiable ground control points. For large cartographic projects (particularly in areas of sparse control) the problem is much more significant. The derived object space positions between image boundaries will contain discontinuities, and a multiplicity of ground control points will be required. This can limit the use of SPOT data in large mapping projects over sparsely controlled terrain, unless special measurements are taken.

Unlike normal photographs the stereo SPOT images are not taken at the same moment. It is impossible to have a stereopair of SPOT images taken 'at the same moment' . Therefore in terms of data acquisition the mapping agency has to schedule a "look" from SPOT well in advance. In some cases, captured SPOT data could be useless if the target was obscured by clouds. Meanwhile, waiting for SPOT to be in the appropriate position for another "look" may result in changes of ground spectral data.

Off-nadir viewing often results in differences in the same ground areas between the two views. This occurs primarily when, in one view, the ground is between the satellite and the sun, while the other, both the satellite and the sun are the same side of the ground area. In forming a stereopair with base/height ratio close to 1 convergent images should be used, so the sun angle becomes more critical. Off-nadir viewing in combination with sun angle at the different acquiring instances of the images can even have the peculiar radiometric effect on the grey levels of these areas of making areas (especially hardwood and agricultural areas) that are light-coloured (bright response) in one image dark in the other. Even worse, if the images are acquired in different seasons in agricultural areas, the different radiometric characteristics could be accompanied by different patterns due to the different land use. These problems are most serious in the automated procedures, but they could even possibly cause a mis-positioning of the measuring mark in the manual tasks. Better radiometric characteristics will probably be achieved when the time delay between the left and the right image is reduced. In the higher latitudes this is possible, but the sun angle will be worse. The pair of images required for DEM extraction should ideally be acquired within 2 weeks of each other.

Furthermore, SPOT's sun-synchronous orbit is referenced to the nadir track of the satellite. With high off-nadir viewing , the satellite can be up to one-half a time zone away from the sun-time of the other pass. Shadows visible in the imagery will then have different orientations.

Quality and scale of an image are the most crucial factors which influence the accuracy of the observation. This is because the error in image coordinate location will be enlarged by approximately the scale factor of the image for the corresponding position on the object. The quality of the original copy was not good and a new copy had to be prepared from the original CCP data. The MDA fire 340 printer gave possibly the best results for a hardcopy production for cartographic purposes, but still did not contain as much information as the digital data. Comparison of digital data displayed on a SUN 3/260 with three photographic products showed considerable variation in the quality of the hardcopy product. The digital data was significantly better for image interpretation.

Film writers have been found to be extremely variable in the quality of their photographic output. Bjerkes (Satimage, Sweden) used Scitex to produce an excellent hard copy result for printing originals. RMS errors of 6 m in plan and 5 m to 15 m in height have been achieved for experimental products. Therefore until methods have been developed to obtain film products with the minimum of image degradation, all digital stereoplotters will remain superior to the analytical plotter. Maybe the new 1AP product (see § 3.4.1.1) with a much more rigorous specification will solve some of these problems.

The atmospheric effects affecting the image quality are examined by comparison with measurements from a second better quality SPOT hardcopy. The panoramic effect is examined (the second SPOT stereopair is corrected from the panoramic effect, while the first copy is not).

10.1.2. Tests to examine the systematic error found in SPOT elevation measurements.

It has been shown that when observing digital elevation data from SPOT there are significant systematic errors. An analysis of these showed some of the reasons such as the difficulty of the operator in responding to the variable image quality caused by processing, contrast illumination factors, atmospheric condition and relief (in relation to the operator measurements). Poor illumination on the images has caused errors in DEM observations to be formed. The errors in the observations are still normally distributed but the mean has been shifted from zero. It has been proved that although the operator had difficulties in the problematic parts of the model under certain circumstances, this is not the only source of the systematic error. The systematic error has a random appearance as shown after a further statistical analysis within small areas ($\sim$1 km^2) where an average of 50 - 70 points were compared. The variable systematic errors in the mean values derived from further statistical analysis creates the suspicion that another reason is the geometric fidelity of the image.

The comparison of the statistical results of the digital elevation measurements of the stronger systematic bias and the larger standard deviations

blocks between the project and the experienced operator, showed that in the measurements from the experienced operator the value of standard deviation is decreased (better measurements), but a systematic bias remained in the mean value. These DEM blocks were located in the very rough and steep area. Moreover the illumination and atmospheric conditions related to the terrain steepness made the measurements a difficult task. The statistical analysis results indicated that the experience of the photogrammetric operator is an important factor. However the large systematic bias and large standard deviation values still remained.

The comparison of the statistical results between the first (problematic) and the second (better quality) SPOT hardcopy measurements showed that the changes in the mean values are not so great. However the two data set mean values are significantly correlated. The standard deviation of the second hardcopy measurements are better (30% better). This possibly happened because the number of control points used in setting up the second SPOT image were greater (33% more GCPs) and the image quality is better (no atmospheric effects, or strongly shadowed parts) than the original one.

The variable values of the mean and the similar results found in the statistical analysis of the second SPOT stereopair are indications that there is no significant deformation of either models on exterior orientation. After further statistical analysis tests, the statistical analysis of the experienced operator measurements and the statistical analysis of the second SPOT hardcopy measurements leads to the consideration of the quality of image geometry (camera model errors).

10.1.3. Digital elevation models.

The relief has another great influence on the accuracy of the height measurements related to the planimetric error in rough areas. There is no expression relating planimetric positioning of the measuring mark and the height accuracy. However, a planimetric mis-positioning of the measuring mark will definitely cause error in the height information obtained.

It is a fact that the photogrammetric operator sets the floating mark on the ground more accurately on flat or gently rolling areas than on rough and steep terrain, where the uncertainty is a dominant factor accompanying the measurements. The terrain type is described according to the slopes and grouped in 4 categories. The slope categories were considered as a source of error in the SPOT elevation measurements and they are used in the estimation and the classification of the caused error in the applied statistical analysis. They are grouped into 4 categories to facilitate the statistical study, without losing the significance of the terrain roughness and its influence on the photogrammetric observations. They are also used as the main criterion in applying the height limits during the blunder detection procedure.

The categorisation of the land use in this work was done according to the difficulties, or uncertainties that vegetation creates in the operator when setting the floating mark on the ground. The main aim was for generalisation and simplicity by having as few categories as possible. The vegetation information was grouped into 3 categories. The land categories were used in the study of the vegetation effect on the SPOT elevation measurements

The digital elevation measurements were carried out in a regular (square) pattern. A regular grid is the simplest approach and it is usually followed for normal production because it is not as time consuming as ie. selective sampling of "random data" and does not require special software. These special techniques do not however offer the best solution (ie. progressive sampling). Depending on the specification accuracies a smaller grid interval is preferable to maintain accuracy.

10.1.4. Data manipulation.

10.1.4.1. Coordinate transformations.

Projection transformations have significance for mapping due to the planimetric error which is introduced in every transformation. The sequence of transformations used in that project are: control points transformation (in order to take account of the effects of earth curvature caused by flattening, when setting up the SPOT model on the analytical plotter); output of coordinates from

the DSR1 analytical plotter; and the data manipulation stage.

The projection transformation error, found in the the whole procedure (6 transformations) testing the 20 check points is: Dx=0.02 m Dy=2.48 m and Dz=0.00 m. So the Vector error Dxy=2.48 m and standard deviation=0.55 m. For the project requirements the results are acceptable. If it is necessary to obtain better results an iteration loop should be used in the UTM to geographical transformation, in order to minimise the approximation errors in the calculations of Latitude and Longitude.

10.1.4.2. Blunder detection.

As SPOT data contain a large amount (5.7% of the test data) of blunders, manual measurements should be checked for blunders. The blunders should be trapped and removed before any further processing (eg. interpolation) starts. A blunder study showed that the causes of blunders are the image quality, the terrain roughness, the operator and the measuring conditions.

A pointwise local self-checking blunder detection algorithm was developed. In this study not only one value for blunder detection threshold is adopted but several values according to the terrain roughness. The points were checked in relation to their neighbours in a variable size window from 1 x 1 (1 point checked in relation with the 3 neighbours) to 4 x 4 (4 central points checked in relation with their 12 neighbours). The algorithm was applied to the SPOT data but gave poor results (36% successful in blunder detection). This happened because of the "random appearance" of the systematic error. The author believes that the algorithm developed in this project could give much better results when used with data from other sources.

Blunder prediction and behaviour is a very difficult task and so far there is no complete remedy. None of the off-line applied techniques give fully satisfactory results. Local techniques within a window of size 4 x 4 (ie. 16 observations in the window) are more suitable than global techniques which apply the detection procedure over a large area.

A data smoothing and filtering procedure in a 3 x 3 window using a low pass filter was applied to the low resolution source. The gradient and aspect was estimated from the filtered data and presented as an image in raster form (intensity range image). Although this leads to the loss of the finest detail the presented results can be used as a quick check for blunders, if the images produced from the filtered data are compared with the gradient and aspect images produced from the original data. Terrain visualisation can be used in quality control (quick check) and identifying of blunders ie. representation of the relief in a vector form (isometric views etc).

10.1.4.3. Data merging.

In the worldwide cartographic databases and in almost every application, elevation data exists from different sources. Elevation data sets have sometimes to be merged into a single set, in order to produce a unique contour map of known accuracy. Data captured from different sources in a different scale and/or by different techniques (ie. implementation, data capturing procedure etc) always have different reliability, so the reliability factor has to be taken into account.

This was carried out in this project by estimating the relative accuracy factor (RAF) of the one source to the other. RAFs should be as representative as possible so it is recommended they be estimated after an extensive statistical analysis procedure. In this project the relative accuracy factor (RAF) of the 1:30,000 derived aerial photography data in a 30 m grid interval (high resolution source) is assumed to be 1.0, while for the SPOT derived data in a 100 m grid interval (low resolution source) it is estimated to be 0.1.

A merging algorithm was developed which merged the data from the two sources without destroying the grid normality. This algorithm implements a local interpolation procedure in order to merge the two data sets.

The effect of the low resolution to the high resolution source data was studied and it was found that when the data are merged with the estimated RAFs (1.0 and 0.1 respectively) the effect of the low resolution source is not significant (an error of 0.9 m in height is introduced), when they are merged with RAFs 1.0 for

the high resolution and 0.5 for the low resolution the low resolution source introduces an error of 3.2 m in elevation, while when RAFs 1.0 for the high resolution and 1.0 for the low resolution are used the effect of low resolution source is a 4.7 m error. From the statistical analysis results the curves for different values of RAF were drawn. From this curve the affect for any RAF of the low resolution to the high resolution source can be estimated.

The data merging method which was developed in this project showed that the merging of elevation data from different sources, or from the same source but existing as grid data and random data, is an achievable and controlled procedure. The final product can be of a known and unique accuracy if an estimation of the relative accuracy of the one source to the other is known.

From the high resolution source with 30 m grid interval, data were skipped so a 60 m grid interval was achieved. By doubling the grid interval, the number of rows and columns are each halved. The merging procedure with the low resolution source was applied again. When the data are merged with the estimated RAFs (1.0 and 0.1 respectively) the low resolution source introduces an error of 1.4 m in height, while when they are merged with RAFs 1.0 for the high resolution and 1.0 for the low resolution the low resolution source introduces an error of 7.8 m in elevation. Therefore when sparse data of the high resolution source (25% of the initial points) are used in the merging procedure the introduced error in elevations is deteriorated by a factor of 1.6.

10.1.4.4. Data structure.

The data structure is very important for all the applications. Nowadays the commercially available packages lead the way in this difficult and complicated problem and the user simply has to follow the data structure which is recommended. Some of the serious problems are that sometimes the recommended data structure could be far from ideal for a specific application, and the inflexibility and difficulties which modification of the standard structure presents.

10.1.5. Interpolation.

The interpolation package is of great importance, particularly the order of the curve to be fitted in the interpolation process (data smoothing procedure). The DTMCREATE software provides four interpolation options. Two of those were suitable for the current experiment, from which one was selected: the interpolation of heights on the basis of known heights found using an expanding hollow box search. Four interpolation techniques are provided: the unweighted, linear, quadratic or quartic, from which the quartic option was selected. The software also enables grid point estimation by smooth patches and linear facet interpolation in which grid heights are instead estimated using linear interpolation across the triangle facet planes. The smooth patches interpolation option was applied for the interpolation of SPOT data.

The terrain of the test area is rough with an average slope of 41% (average fractal dimension = 2.63). Therefore the higher degree interpolation functions which are provided (the quartic or quadratic functions) are more suitable. However all the curve fitting techniques have the drawback of terrain smoothing. The quality of SPOT data due to the random appearance of the systematic error and the number of blunders have a great impact in the interpolation procedure. When raw SPOT measured data are used then the interpolation package creates additional errors, because of the non normal terrain behaviour.

Firstly the aerial photography data were interpolated using a 30 m sidelength (the same as the grid interval used in capturing the initial data). The interpolated values were compared with the initial height values. The overall statistical values showed that an error of 0.41 m was introduced.

Secondly the aerial photography data were merged with the SPOT data (with 1.0 and 0.1 RAF). The merged data was interpolated using a 30 m sidelength (the same as the grid interval used in capturing the initial data). The interpolated values were compared with the initial height values. The overall statistical values showed an error of 0.96 m was introduced.

Finally the aerial photography data were merged with the SPOT data (with RAF 1.0 and 1.0 respectively) The merged data was interpolated using a 30 m

sidelength (the same as the grid interval used in capturing the initial data). The interpolated values were compared with the initial height values. The overall statistical values showed an error of 4.74 m was introduced.

The above procedure leads to the conclusion that the more the lower resolution source data is involved, the worse the interpolated height values become.

10.1.6. Feasibility of SPOT for providing data for mapping purposes.

Some of the previous tests on SPOT accuracy was regarding the results achieved. Therefore it was decided to refer to them as they are rather than averaging them. The results from previous tests are as follows:

SPOT claim a 3-5 m RMS error in height for models with a base/height ratio of 1.0 when plenty of excellent control is available (Hartley, 1988). Denis and Baudoin (1988) claimed that a 10m contour interval in flat areas is possible, but this seemed not consistent with the heighting accuracies.

Photogrammetric tests have yielded consistent results with RMS plan accuracy of 6 m and height accuracy of 3 to 14 m being achieved. Practical trials have produced 12 m plan accuracies and 10 m height accuracies. OS tests showed that adequate 1:100,000 scale maps with a contour interval of 40 m can be produced.

There is a definite trend to support the belief that SPOT can provide an accuracy of 8 m to 10 m in plan and 4 m in height, given adequate control. USGS clearly believes that a 1:24,000 scale product is of interest to some users (Hartley, 1988).

Mapping and Charting establishment has assessed the ground modelling capabilities of the DSR1, I^2R and MacDonald Dettwiler and Associates systems with heighting accuracies of 12 m, 12 m and 10 m respectively.

Accuracies of 6.2 m in plan and 3.1 m in height resulted from a nine parameter solution and 27 control points. Using only 4 control points presented no significant loss of accuracy Priebbenow and Clerici (1987).

Jones (Nigel Press Associates) using Geospectra's DEM package with eight ground control and a full grey scale correlation on a 10m grid succeeded in producing results on withheld GCPs of 18.4 m R.M.S.E elevation accuracy and 21 m in plan.

UCL (Day and Muller, 1988 & 1989) using a Gruen adaptive least squares correlation stereomatcher succeeded in producing accuracies in elevation of 18.19 m in one experiment and 12.17 m in another.

The quality assessment for the manual measurements carried out in this project showed that:

For the first SPOT hardcopy measurements in a problematic stereopair (haze, partly clouded and some model parts badly illuminated) by the project operator after checking 6,833 points the elevation accuracy is 15.82 m.

For the first SPOT hardcopy measurements by the experienced operator after checking 2,124 points the elevation accuracy is 13.13 m.

For the second SPOT hardcopy measurements in a better quality stereopair by the project operator after checking 2,936 points the elevation accuracy is 12.75.

All the above three tests lead to the overall elevation accuracy of 14.65 m.

Direct contouring is better than producing contours from DEMs. Because the elevation data were already in a regular grid it was not necessary to interpolate them, so contours were interpolated directly from the "raw" data.

All the above tests performed in this thesis and particularly from the differences of the comparison between the two interpolated contour sets derived from :

the first SPOT stereomodel (not good quality images, with illumination and haze problems, with a base/height ratio close to 1, controlled by 10 good and well distributed GCPs) DEM values at 100 m grid interval,

the second SPOT stereoimages (better quality the images which were set up with the assistance of 15 GCPs) DEM values at 100 m grid interval,

and the aerial photography contours interpolated from DEM at 30 m grid interval,

have shown that SPOT has, with relaxed and acceptable specifications, the potential for providing elevation data for the creation of DEMs for contouring in topographic mapping of areas not covered by high vegetation in the following cases:

1:25,000 with 10 m contour interval, for flat or gently rolling areas (slopes up to 25% or average fractal dimension = 2.3), when the image quality, control quality and number of GCPs are good .

1:50,000 with 25 m contour interval in rough areas (slopes up to 50% average fractal dimension 2.7). The author found that from the first SPOT stereopair, using 10 GCPs capturing data in a regular grid with 100 m grid interval in a rough area (average slope 41% average fractal dimension = 2.63) a contour map with 25 m grid interval fulfils the accuracy specifications for a 1:50,000 map.

1:100,000 with 50 m contour interval in very rough and steep areas (slopes more than 50%).

Moreover, SPOT images can be used not only for extracting the height but also the planimetric information. A number of tests were carried out to see the amount of planimetric detail we can get. The presented results have shown that for 1:50,000 basic details can be mapped from SPOT images, but finer details could be omitted or erroneously created. SPOT images can be used to give accurate positioning but that information will not be complete and, without ground details, may be subject to misinterpretation. The use of multispectral data and increased experience in using the data would probably improve the amount of information extracted. The extent of ground completion and ground verification is likely to be greater than that expected when aerial photographs are used (given the same specification) and therefore has a clear bearing on the cost of a mapping project (Dowman et al, 1989).

10.1.7. Summary of main conclusions.

It has been demonstrated that SPOT stereoimages are a useful source of accurate height information for DEM production .

SPOT elevation measurements were found to have significant systematic errors. An analysis of these showed some of the reasons to be difficulty for the operator to respond to variable image quality, contrast illumination factors, atmospheric conditions and relief. However, extensive statistical analysis and tests lead to the consideration that another reason for these systematic errors is the geometric fidelity of the image.

The physical image quality, atmospheric conditions, vegetation and terrain type have a great influence on the accuracy of the height measurements.

All the parts of the image are not well illuminated. One possible reason is the sun angle. The east facing image will always appear in more shadow than the west facing.

Haze, clouds (and their shadows) and areas in strong shadow cause problems.

The vegetation coverage, in a model formed from aerial photography appears and is interpreted in a different way than in a model derived from SPOT imagery. In the aerial photograph the operator can see the height variation of the trees. In SPOT images stereomodel the vegetation gives the impression of a "cloud" covering the area.

Rough and steep areas usually have illumination problems. They could be either over-illuminated or badly illuminated.

Manual elevation measurements from SPOT contain a large number (5.7% of the test data) of blunders. Therefore blunders should be trapped and removed before any further processing (eg. interpolation) starts. An off-line pointwise local self-checking blunder detection algorithm which was developed was found to suffer because of the "random appearance" of the systematic error of SPOT data. The best way of detecting blunders is probably either in the on-line procedure, or in the off-line adjustment process.

Elevation data sets can be merged into a single set, in order to produce a unique contour map of known accuracy. A merging algorithm was developed which

merged the data from the two sources without destroying the grid normality by implementing a local interpolation procedure and the relative accuracy factor of the two sources. The effect of the low resolution on the high resolution source (for full and sparse data) was studied and some figures for different values of RAF were drawn.

The error introduced due to interpolation was estimated. This error is not significant when the initial high resolution source elevation data were interpolated, but when the low resolution source were merged with the high resolution source this error became significant.

From the comparison of the high and the low resolution contour sets, it has been shown that a good SPOT stereopair with good quality and distribution of GCPs has, with relaxed and acceptable specifications, the potential for providing elevation data for the creation of DEMs for contouring in topographic mapping of areas not covered by high vegetation in the cases 1:25,000 with 10 m contour interval for flat and gently rolling areas; 1:50,000 with 25 m contour interval in rough areas; and 1:100,000 with 50 m contour interval in very rough and steep areas.

10.2. Discussion and recommendations for further research.

In this study one of the most commercial of the operating satellites which can currently be used for cartographic purposes is examined as a second source of providing elevation data. The most interesting Soviet high resolution system KFA-1000 has been proved to be a lower accuracy source with residual error of 7 m in plan and 25 to 35 m in height (Jacobsen, 1988) and commercially it is not well established.

A SPOT image covers approximately a 60 x 60 km^2 of the ground surface in a vertical view. In this study measurements were carried out in two different SPOT pairs of the same area with a base/height ratio close to 1. The terrain type of the test area is rough with an average slope 41.3% (average fractal dimension 2.63). The quality of the first SPOT model used was bad, so the experiment was carried out

under unfavourable rather than ideal conditions. Therefore the results represent a real case. However the test area represents only a small part of a SPOT scene. Thus a further investigation is required with different data samples spread all over the image or different images covering the same test areas with the same or different base/height ratio.

In space photogrammetry, the existing problems in classical photogrammetry become sharper because many more factors and error sources are involved. The same happened for mapping from space imagery where a large number of factors are involved. The most important problems which are involved in space photogrammetry and mapping from space imagery procedures are the following:

1. obtaining the raw data due to the information registration method and technique.
2. reliability of the information recording device (camera or sensor).
3. image quality (geometric and radiometric quality).
4. image quality related with the film processing procedure which transfers the problems to the analytical plotter.
5. nature of the earth surface such as the earth curvature and the relief surface.
6. data capture method and technique.
7. accuracy due to the human capabilities for the manual task, or the algorithm sophistication on automated procedures.
8. instrument limitations.
9. means, method and technique of data processing.

Some of the problems which affect the operator measurements are:

Data is difficult to obtain in many areas because of cloud cover and poor atmospheric conditions (haze).

The sun angle affects the measurement accuracy.

The different date of the image acquisition causes some problems in relation to the vegetation and the sun angle.

The level of operator experience.

The big problem is identification of the actual sources causing the error(s) or deciding which have to be considered. The only way to overcome this problem is

to keep some of them under consideration in an experiment and some others constant.

Further investigation with the existing 1A level and the new release 1AP are required. Film level 1AP is going to be improved in geometric accuracy and photointerpretation quality. The systematic biases of the SPOT measurements need further investigation in order to determine whether this is caused by physical image conditions or due to SPOT camera model errors. It is remarkable that while a SPOT scene may require only three to six GCPs for correction to subpixel accuracy, 20 to 40 GCPs would be required to obtain the same accuracy using image warping (Hawkins and Westewell-Roper, 1987).

The procedure for SPOT setting up on the analytical plotter is now well established and documented. However a further and extensive study of SPOT's capability for mapping remains. In practice it may be that no evenly distributed ground control coverage over the model can be realised. Therefore, the way planimetric and height precision behave in the less controlled areas should be investigated. The second SPOT stereopair with 15 GCPs (33% more GCPs) with one ground control point lying in the test area gave 30% better accuracy in elevation than the first image where 10 GCPs were used. As onboard satellite orbital parameters are not used in the orientation procedure it remains to investigate how those parameters improve the image geometry, maybe not within a single pair but within a strip.

Map projection problems have been confined to selecting constants for the ellipsoidal shape and size, and not generally been extended to incorporating the much smaller deviations from this shape, except that different reference ellipsoids are used for the mapping of different regions of the earth. The significant element of an elevation in the digital elevation model leads to the establishment of a reference surface, particularly when large projects create digital elevation models over very large areas (a DEM over several countries). The problem was pointed out before and several attempts were carried out for the adoption of an international ellipsoid. However, those ellipsoids have problems in global applications. Spacecraft tracking technology is in at least one way leading the state of earth modelling. Perhaps with the advent of global positioning satellites, world reference geoid and an update mechanism will be established to the accuracy of

today's capabilities. Satellites can provide the data for estimation of the ellipsoid parameters, derived by a worldwide least squares fitting process to the geoid. Ellipsoids determined that way are the WGS 72, WGS 84 ellipsoids (World Geodetic System) and the GRS 80 ellipsoid (Geodetic Reference System).

The number of blunders which are involved in the data captured from SPOT images is large, because of the image quality . The blunder percentage of the manual measurements was found to be 5.7% (>2.7 σ) in a terrain with an average slope 46%. In the automated procedures the amount of blunders is estimated to be the same, or larger, depending on the correlation technique. Therefore a further study is necessary for each individual case, and development and testing of better algorithms for blunder detection and trapping.

The best way of detecting blunders is probably either in the on-line procedure ie. in a real-time satellite system where the detection and localisation of a blunder will be possible if the mathematical model used in the adjustment process has the correct assumptions functionally and stochastically, or else in a development of the interpolation software would include a procedure for checking for blunders. It will not be long before measurements made in the analytical plotter will be checked for blunders in an on-line procedure, giving a signal to remeasure any erroneous point.

This merging data from two different sources is possible with the application of the relative accuracy factor. The relative accuracy factor is the data accuracy estimation of one source relative to the other. In the developed algorithm the user can only specify one RAF value for each source. However an easy modification can allow the specification of more than one value (eg different values of RAF related to the terrain roughness), which the algorithm can choose and apply as appropriate during the execution of the program.

It is possible to produce digital elevation models from digital SPOT image data by automatic and digital correlation. Automation is a favourite topic in modern research and development in photogrammetry and remote sensing. The increased use of high altitude aircraft and space vehicles for the acquisition of information, the rapid increased use of sensors which collect the information in digital or image

form, lead the way in the development of integrated, automated cartographic systems in which photogrammetry and remote sensing techniques are the core of a continuously automated mapping process. However, those systems will be complicated (and expensive) because a large number of procedures will be involved from the preprocessing stage such as improvement of geometric and radiometric properties of the image, enhancement operations (noise removal, blur removal, contrast enhancement and grey level calibration) up to the complicated processing stages such as image matching, correlation and pattern recognition.

Computer processing reduces the labour intensity and consequently the speed and the costs of map compilation. Soon the use of ephemeris data for satellite positioning, orbital tracking data combined with the laser altimeter, and stellar camera observations will allow the computation of the exterior orientation using a minimum number of GCPs with very good results.

Human operators interpret difficult parts of the model in different ways while the stereomatching algorithm always interprets them in the same way. The comparative study between the quality assessment of the manually captured elevations and those using the stereomatching technique applied at UCL, gives the impression that automated techniques can provide elevation data equally as good as, or better than, elevation data captured manually with operator assistance. Generally, automated techniques appear to some people to be somewhat worse than results obtained by setting the floating mark visually. However, as the published results have shown, a further development of the stereomatching algorithms could lead to them being the future way of extracting the height information for production of digital elevation models. In addition, automated techniques produce fast DEMs, depending on the implementation and the software (number and nature of constraints included, but in any case much faster than the human operator).

If production of the digital elevation model by automated procedures is possible, then rectification of the SPOT images is an easy task for orthophoto production. It can also be used to produce videos of perspective views on panchromatic SPOT images (simulation of aerial movement around a SPOT model).

When considering whether the use of satellite data is appropriate for use in a mapping project it is necessary to consider the purpose of the map, the time

available, the scale in which the map is required and the availability of existing data. For conventional specification, and adequately funded long duration nationwide projects the use of satellite is inappropriate. Map specifications should depend on the product utility rather than just what is conventional. However, reduced specifications create problems of educating the user. For quick mapping projects, with a limited budget and tolerant accuracy specifications there is a good case for the use of satellite imagery. SPOT imagery can aid mapping projects at the economically important scales of 1:50,000 - 1:100,000 for effective strategic planning and development in the unmapped areas of the world. It can help in mapping of areas with poor control and bad weather conditions.

A new generation of integrated cartographic tools is being developed in the fields of high technology, where the digital stereoscopic images are stored into a memory and processed to yield a digital elevation model by automatic correlation, then corrected geometrically and radiometrically by a drawback procedure.

Digital techniques for extracting terrain height from stereosatellite images have been developed that match or better the accuracy and throughput of traditional photogrammetric techniques. While digital methods gain their followers, there are still issues to be resolved. These involve making sure that the cartographic specifications of the earth's geoid are accurate, and beginning to address standard methods of storing and accessing the huge quantities of data we are now in a position to produce about the shape of our world.

10.2.1. Summary of main recommendations for future work.

In this study measurements were carried out using two different SPOT pairs of the same area with a base/height ratio close to 1. The test area represents only a small part of a SPOT scene. Thus further investigation is required with different data samples spread all over the image or different images covering the same test area with the same or different base/height ratio.

In space photogrammetry for mapping production a large number of factors are involved which affect the accuracy of the final product. As the problem of identification of the actual sources which contribute to the error(s) is difficult,

some of these sources of error can be investigated while keeping the other sources constant.

The systematic biases appearing on the SPOT elevation measurements need further investigation in order to determine whether this is caused by physical image conditions or by the quality of the image geometry (camera model errors).

There is a tendency for reducing the ground control in setting the SPOT image procedure. However, ground control has a great impact on the model deformation. Therefore the behaviour of planimetric and height precision in the less controlled areas should be investigated.

Blunders have a large effect on the accuracy of the final product. The number of blunders in manual measurements and in automated procedures is large. Therefore a further study is required and more sophisticated algorithms have to be developed in the on-line or off-line procedure.

The merging data from two different sources in this project was carried out with the application of one relative accuracy factor per source. However, an easy addition option to the algorithm can allow the specification of more than one value of RAF related to the terrain roughness to be applied during the merging procedure.

Manual elevation measurements is a difficult and time consuming task. The statistical analysis of the results and the comparison with the measurements carried out by automated procedures does not show better accuracy results. Satellite images offer the opportunity for automated techniques to be applied. Therefore a further development and commercialisation of the automated algorithms is required in order to persuade the user of their reliability and capability of extracting fast and accurate height information.

References.

References.

Ackermann, F. and Schneider, W., 1986. Empirical investigation into the precision of digital image correlation. Presented paper, *ISPRS Synposium*, Commission III, Rovaniemi 1986: 11 pages.

Ackermann, F., 1978. Experimental investigation into the accuracy of contouring. *Proceedings of the digital terrain models (DTM) Symposium. American Society of Photogrammetry* : 165-192.

Ackermann, F., 1979. The accuracy of digital height models. *Proceedings of the 37th Photogrammetric week at Stuttgart University* : 133-144.

Amer, F., A., A., 1981. Theoretical reliability of elementary photogrammetric procedures - Part 1. *ITC journal*, Vol. 3, pp. 278-307.

Ayeni, O., O., 1976. Considerations for automated digital terrain models with applications in digital photomapping. *Ph.D. thesis*, Ohio State University, Columbus, Ohio.

Ayeni, O., O., 1978. Automated digital terrain models. *Digital terrain models (DTM) Symposium* : 275-306.

Ayeni, O., O., 1982. Optimum sampling for Digital models: a trend towards automation, *Photogrammetric Engineering and Remote sensing*, 48(11): 1687-1694.

Bahr, H., P., 1976. Geometrical analysis and rectification of Landsat MSS imagery: Comparison of different methods. *Nachrichten aus dem Karten und Vermessungeswesen* , 36: 25-46.

Balse, A., E., 1986. Determination of optimum sampling interval in grid sampling of digital elevation models for large-scale application. *International Archives of Photogrammetry and Remote Sensing*, 26(1/3) : 40 - 54.

Balce, A., E., 1986. Determination of optimum sampling interval in grid digital elevation models (DEM) .Data acquisition. *Anual ACSM-SPRS Convention.* Volume 4, March 16-21. Washington DC, page 201.

Balce, A., E., 1987a. Determination of optimum sampling interval in grid digital elevation models (DEM). Data acquisition. *Photogrammetric Engineering and Remote Sensing*, Vol. 53, No 3, pp 323-330.

Balce, A., E., 1987b, Quality control of height accuracy of digital elevation models. *ITC Journal*, 1987-4: 327-332.

Barnard, S., T. and Thompson, W., B., 1980. Disparity analysis of images, *IEEE Transactions on Pattern analysis and Machine Inteligence*, Vol. PAMI-2, No. 4: 333-340.

Beckett, P., H., T., and Webster, R., 1969. A review of studies on terrain evaluation by the Oxford-MEXE-Cambridge group, 1960-1969, *MEXE report* , No. 1123.

Begni, G. 1982. Selection of the optimum spectral bands for the SPOT satellite. *Photogrammetric Engineering and Remote Sensing*, 48(10):1613-1620.

Begni, G., Leger, D., and Dinguirard, M., 1984. An in-flight refocussing method for the SPOT HRV cameras. *Photogrammetric Engineering and Remote Sensing*, 50(12):1697-1705.

Begni, G., Boissin, B., and Leroy, M., 1986. SPOT image Quality. *ISPRS, ESA SP-252*, Stuttgart, Sep. 1-5 : 551-556.

Begni, G., 1988. SPOT image quality. Twenty months of experience. *International Journal Remote Sensing*, Vol. 9, No. 9: 1409-1414.

Bégin, D., Boucher, Y., Brodeur, J., Girard, C., Lapierre, D., Lemieux, J-P., Gauthier, J., R., R., 1988. Expériences Franco-Canadiennes. Précision Géométrique des données SPOT. *Proceedings of the International Symposium on topographic applications of SPOT data.* Quebec, Canada 1988 : 169-180.

Bethel, J., S., and Mikhail, E., M., 1983. On-line quality assessment in DTM. *Technical papers of ACSM-ASP fall convention*: 576-584.

Blaschke, W., 1968. Problems in obtaining and processing of photogrammetric data for digital terrain models. *XI International Congress of Photogrammetry*, Lussanne, Inter-Commission Working Group V/IV, Volume XVII-1969, Invited papers 2, 04: 7 pages.

Bomford, G., 1984. *Geodesy*. Clarendon press. Oxford. 4th edition. 855 pages.

Burrough, P., A., 1984, The application of fractal ideas to geophysical phenomena. *Inst. Mathematics and its applications Bull.*, Vol. 20, No. 3-4, 36-42.

Burrough, P., A., 1987. *Principles of geographical information systems for land resources assessment* . Oxford University press, Oxford- New York- Toronto, 194 pages.

Carlson, G., E., 1978. Application of digital terrain elevation data to range-limited horizon navigation checkpointing. *Digital Terrain Models (DTM) Symposium* : 541-555.

Catlow, D., R., 1986. The multi-disciplinary applications of DEMs. *International conference on the acquisition, management and presentation of spatial data*. Proceedings Auto Carto London. Vol. 1: 447-454.

Chaw, T., K., W., 1987. Specification and implementation of the PMF stereoranging algorithm. MMI-137 (UCL-CS) working paper 10, *University College London, Department of Computer Science*, February 1987, 7 pages.

Chen, L., -C., Lee, L., -H., and Lee, S., -S., 1988. DTM generation using SPOT digital data. *International Society for Photogrammetry and Remote Sensing.* Commission III, Vol. 27(B3): 100 -109.

Clark, I., 1984. *Practical geostatistics*. Elsevier applied science publishers Ltd. First edition, 129 pages.

Chevrel, M., Courtois, M., and Weill, G., 1981. The SPOT satellite remote sensing mission. *Photogrammetric Engineering and Remote Sensing*, 47(8): 1163-1171.

Cogan, L., and Hunter, D., 1986. Design concepts of software systems- Kern photogrammetric software. Technical papers 1986, *ACSM-ASPRS Anual Convention*, Volume 4, March 16-21, Washington DC: 74-82.

Committee of enquiry into the handling of geographic information, 1987. Handling geographical information. *Report to the secretary of state for the environment of the committee of enquiry into the handling of geographic information.* London - Her Majesty's Stationery Office. 208 pages.

Conradsen, K., Nielsen A., A., 1987. Interpolation of height data by means of a deterministic versus a statistically determined method. *ISPRS Working Group III/3 - Proceedings of the international colloquim on progress in terrain modelling.* Copenhagen. 20-22 May 1987 : 55-74.

Cooper, M., A., R., 1974. *Aspects of modern land surveying. Fundamentals of survey measurement analysis.* Crosby Lockwood Staples. London, 107 pages.

Curran, P., 1985. *Principles of remote sensing.* Longman Group Ltd. London and New York, 282 pages.

Day, T., & Muller, J-P, 1988. Quality assessment of digital elevation models produced by automatic stereo matchers from SPOT image pairs. *International Archives of Photogrammetry and Remote Sensing.* Commission III, 27(B3):148-159.

Day, T., Muller, J-P, Richards, S., 1988b. Spot the image. *Computer Graphics Conference* (CG88). London 11-13 Oct 1988. 10 pages.

Day, T., & Muller, J-P, 1989. Digital elevation model production by stereo-matching SPOT image-pairs: A comparison of algorithms. *Image & Vision Computing.* Vol. 7, No. 2 , 95 - 101.

Davis, J., C., & McCullagh, M., J., 1975. *Display and analysis of spatial data.* Nato Advanced Study Institute. John Wiley & Sons : 378 pages.

Davis, J.,C., 1986. *Statistics and data analysis in geology* . John Wiley & Sons, Inc. Second edition, 646 pages.

Davis, R., E., Foote, F., Anderson, J., M., and Mikhail, E., M., 1981. *Surveying theory and practice* . McGraw-Hill, Inc., 6th edition, 992 pages.

Delaunay, B., 1934. Sur la sphere vide, *Bulletin of the academy of sciences of the USSR*, Classe Sci Mat Nat, 793-800.

Denis, P., Baudoin, A., 1988. Applications topographiques de SPOT a l' IGN - France. *International Archives of Photogrammetry*, Commission IV, 27(B4): 106-115.

Doornkamp, J., C., & King, C., A., M., 1971. Numerical analysis in geomorphology an introduction. *Edward Arnold Ltd.* London. 372 pages.

Dowman,I., J., 1984. Instrumentation for topographic mapping from satellite data. *International Archives of Photogrammetry and Remote Sensing*, 25(A2):155-163.

Dowman, I., J., and Muller, J-P, 1986. Real-time photogrammetric input versus digitised maps. *Proceedings Auto Carto London*, Volume 1, Sep. 14-19: 538-543.

Dowman, I., J., Gugan, D.,J., Muller J-P., Peacegood, G., 1987. The use of SPOT data for mapping and DEM production. *In Prospects Int. conference on " SPOT1: Image utilisation, assessment, results"*, Paris, France, November 1987. 1213 - 1220.

Dowman, I., J., 1987. The prospects for topographic mapping using SPOT data. *SPOT 1 Image Utilisation, assessment, results.* Paris. France. November 1987: 1163-1172.

Dowman, I., J., 1988. The prospects for topographic mapping using SPOT data . *In Proceedings Int. conference on " SPOT1 Image utilisation, assessment, results"* , Paris, France, November 1987 : 13 pages.

Dowman, I., J., and Peacegood, G., 1989. Information content of high resolution satellite imagery. *Photogrammetria* (PRS), 43(1989): 295-310.

Doyle, F.,J., 1978. Digital terrain models : An overview. *Photogrammetric Engineering and Remote Sensing.* 11, (12) 1481-1485.

Doyle, F., 1984. The economics of mapping with space data. I*TC Journal* 1: 1-9.

DTMCREATE, 1989. DTMCREATE reference manual. *Laser-Scan laboratories Ltd.* Volume I and II. Issue 1.6, 8 February 1989, 627 pages.

Ducher, C., 1989. The current involvement of IGN in photogrammetry. *Photogrammetric Record*, 13(73): 111-126.

Evans, I., S., 1972. *General geomorphometry, derivatives of altitude, and descriptive statistics.* In: Chorley, R., J., (ed.), Spatial analysis in geomorphology, Methuen and Co. Ltd, London: 17-90.

Falconer, K., J., 1985. *The geometry of fractal sets.* Cambridge University press. Cambridge, 162 pages.

Foley, J., D., & Van Dam, A., 1982. Fundamentals of interactive computer graphics. *Addison - Wesley publishing company*, 664 pages. (page 521).

Forrest, R. & Deroughie, W., 1974. Refraction compensation. *Photogrammetric Engineering and Remote Sensing*, 40():577-582.

Forstner, W., 1983. On the morphological quality of digital elevation models. *Paper presented at International Colloquium on mathematical aspects of digital elevation models.* Stockholm 18 pages.

Franklin, S., E., 1987. Geomorphometric processing of digital elevation models. *Computers & Geosciences*. Vol.13, No 6, 603-609.

Frederiksen, P., Jacobi, O. and Justesen, 1978. Fouriertransformationen von Hobenbeobachtungen, *Zeitschrift fur Vermessungwesen 103*, Heft 2 : 64-79.

Frederiksen, P., 1980. Terrain analysis and accuracy prediction by means of the Fourier transformation. *14th Congress of the International Society of Photogrammetry*, Commission IV, Hamburg: 284-293.

Frederiksen, P., 1981. Terrain analysis and accuracy prediction by means of the Fourier transformation. *Photogrammetria*, 36(1981),145-157.

Frederiksen P., Jacobi, O., 1982. Terrain spectra. *International Society for Photogrammetry and Remote Sensing. Supplement to the proceedings of the Symposium "Mathematical models, Accuracy aspects and quality control"*. Helsinki. Commission III: 123-130.

Frederiksen, P., Jacobi, O., Kubik, K., 1983. Measuring terrain roughness by topological dimension. *International colloquium on mathematical aspects of digital elevation models*. Stockholm : 5 : 1-5 : 12.

Frederiksen, P., Jacobi, O., Kubik, K., 1984. Modelling and classifying terrain. *International Archives of Photogrammetry and Remote Sensing* , 25(A3a):256-267.

Frederiksen, P., Jacobi, O., Kubik, K., 1985. A review of current trends in terrain modelling. *ITC Journal*, Vol. 2 : 101-106.

Frederiksen, P., and Jacobi O., 1986. Optimal sample spacing in digital elevation models. *International Archives of Photogrammetry and Remote Sensing* , 26(3/1):252-259.

Frederiksen, P., 1987. A digital elevation model for radio communication. *Progress in Terrain Modelling Technical University of Denmark* : 127-133.

Fritsch, D., & Dusedau, G., 1987. On the use of curvature measures in digital terrain modelling. *Progress in terrain modelling. Technical University of Denmark* : 137-149.

Fukushima., Y., 1988a. Generation of DTM using SPOT image near Mt. Fuji by digital image correlation. *International Society for Photogrammetry and Remote Sensing*. Commission III, Vol. 27(B3): 225 -234.

Fukushima, Y., 1988b. Medium scale mapping possibility using LFC data and SPOT image near Mt. Fuji. *International Society for Photogrammetry and Remote Sensing*. Commission III Vol. 27(B3): 235 -244.

Gerald, C., F., 1980. Applied numerical analysis. *Addison - Wesley publishing company*, 2nd edition, 518 pages.

Goodchild, M., F., 1980. Fractals and the accuracy of geographic measures. *Mathematical Geology*, Vol. 5, No. 12 : 85-98.

Goodchild, M., F., 1982, The fractional Brownian process as a terrain simulation model: *Proceedings, thirteenth annual Pittsburgh conference on modelling and simulation*, Vol. 13, 1133-1137.

Grabmaier, K., Tuladhar, A., & Verstappen, H., 1988. Stereomapping with SPOT. *ITC Journal* ,1988-2:149-154.

Grassie, D.,N.,D., 1982. Contouring by computer: Some observations, *BCS Special Publication* , No 2, 93-116.

Grist, W., M., 1972. Digital ground models: an account of resent research. *Photogrammetric Record*, 7(40) : 424-441.

Gruen, A., W., 1982. Adaptive least squares correlation: a powerful image matching technique. *S. Afr. J. of Photogrammetry, Remote Sensing and Cartography*, 14(3): 175-187.

Gruen, A., W., and Baltsavias, E., P., 1986. High precision image matching for digital terrain model generation. *International Archives of Photogrammetry and Remote Sensing,* 26(3/1): 284-296.

Gugan, D., J., 1987a. Topographic mapping from SPOT imagery. PhD Thesis. *University of London* , 253 pages.

Gugan, D., J., 1987b. Practical aspects of topographic mapping from SPOT imagery. *Photogrammetric Record*, 12(69):349-355.

Gugan, D., J., 1988. Satellite imagery as an integrated GIS component. *Third annual International Conference GIS/LIS'88. Proceedings accessing the world.* San Antonio : 174-180.

Gugan, D., J., and Dowman I., J., 1988a. Accuracy and completeness of topographic mapping from SPOT imagery. *Photogrammetric Record*, 12(72):787-796.

Gugan, D., J., and Dowman, I., J., 1988b. Topographic mapping from SPOT imagery. *Photogrammetric Engineering and Remote Sensing*, 54(10) : 1409-1414.

Gugan, D., and Dowman, I., J., 1988c. Accuracy and completeness of topographic mapping from SPOT imagery. *CERCO seminar program on "The SPOT system and its cartographic applications"* . Saint-Mandé, 6-16 June 1988: 64-75.

Hannah, M., J., 1981. Error detection and correction in digital terrain models. *Photogrammetric Engineering and Remote Sensing.* Vol. 47(1): 63-99.

Hannah, M., J., 1988. Digital stereo image matching techniques. *International Society for Photogrammetry and Remote Sensing.* Commission III Vol. 27(B3): 280 -293.

Hardy, R., L., 1971. Multiquadratic equations of topography and other irregular surfaces. *Journal Geophysical Res*, Vol 76, No 8: 1905-1915.

Hartley, W., S., 1988. SPOT1 image utilisation assessment and results. *Photogrammetric Record.* 71: 673-677.

Hassan, M., M., 1986. A spectral analysis method for estimating the sampling density of digital elevation models. *International Archives of Photogrammetry and Remote Sensing*, 26(3/1): 306-316.

Hassan, M., M., 1988. Least squares surface fitting techniques for digital elevation models. *International Archives of Photogrammetry and Remote Sensing.* Commission III, Vol. 27(B3): 304-315.

Hawkins, D., & Westewell-Roper, A., 1987. Automated mapping from digital satellite imagery. *Paper presented at the India National Cartographic Association Conference on satellite cartography*, Ahmedabad, November 24-26: 9 pages.

Huang, Y., D., 1986. Posteriori reliability in both cases adopting data-snooping and robust methods. *International Society for Photogrammetry and Remote Sensing.* Commission III. Vol. 26-3/2: 367-373.

Jacobi, O., 1980. Digital terrain model, point density, accuracy of measurements, type of terrain, and surveying expenses. *International Archives of Photogrammetry and Remote Sensing*, 23(B4): 361-366.

Jacobsen, K., 1988. SPOT image evaluations for cartographic purposes. *Proceedings of the International Symposium on Topographic application of SPOT data.* Sherbrooke, Quebec, Canada: 19-26.

Jankaitis, J., R., and Junkins, J., L., 1973. Modelling irregular surfaces. *Photogrammetric Engineering and Remote Sensing*, Vol. 39, pp. 413-420.

Johnson, C., N., 1978. Processing of terrain elevation data for improced contouring. *Institute for advanced computation technical memo 5646*, Sunnyvale, California.

Kager, H., 1984. DTM - Displayed perspectively. *International Archives of Photogrammetry and Remote Sensing.* Commission III : A3a :513-522.

Kauffman, D., S., and Haja, S., R., 1988. Extraction of dense digital elevation models from SPOT stereo imagery. *Proceedings of IGARSS ' 88 Symposium.*, Edimbrug, 13-16 Sep. 1988 : 477 - 478.

Kennie, T., M., & McLaren, R., A.,1988. Modelling for digital terrain and landscape visualisation. *Photogrammetric Record*, 12(72): 711-745.

Konecny, G., Kruck, E., and Lohmann, P., 1986. Ein Universeller Ansaltz fur die Geometrische Auswertung von CCD-Zielenabtasteraufnahmen. *Bildmessung und Luftbildwesen*, 54(4) : 139-146.

Konecny, G., Lohmann, P., Engel, H., & Picht, G.,1987. The use of SPOT imagery on analytical photogrammetric instruments."*SPOT 1 Image utilisation, assessment, results* " , Paris, France, November 1987. 1173-1187.

Kostli, A., and Wild, E., 1984. A digital elevation model featuring varying grid size. *International Archives of Photogrammetry and Remote Sensing.* Commission III, 25(A3b): 1130-1138.

Krathy, V., 1973. Cartographic accuracy of ERTS. *Photogrammetric Engineering and Remote Sensing*, 40(2): 203-212.

Kratky, V., !987, Rigorous stereophotogrammetric treatment of SPOT images. *SPOT 1 Image Utilisation, assessment, results.* Paris. France. November 1987: 1281-1288.

Kratky, V., 1988. Rigorous photogrammetric processing of SPOT images t CCM Canada. *Invited paper to the International Symposium on topographic Application of SPOT data.* Sherbrooke, Oct. 13-14 : 15 pages.

Krige, D., G., 1951, A statistical approach to some basic mine valuation problems on the Witwatersrand, *J. Chem. Metall and Min. Soc. South Africa*, Vol. 52, No. 6: 119-139.

Kubik, K., 1988. Digital elevation models review and outlook. *International Archives of Photogrammetry and Remote Sensing*, 27(B3): 415-426.

Leberl, F., 1973, Interpolation in square grid DTM. *ITC Journal*. No. 5: 756-807.

Leberl, F., 1975. Photogrammetric interpolation. *ITC Journal*, No. 2: 173-302.

Lemeunier, H., 1988. An appraisal of results and a review of selected applications. *Survey Ireland* : 24-34.

Leupin, M., M., and Cherkaoui, M., 1980. The use of automatically generated DTM for mapping at different scales. *International Archives of Photogrammetry and Remote Sensing*, Commission IV, 23(B4):458-467.

Ley, R., G., 1986. Accuracy assessment of digital terrain models. *International conference on the acquisition, management and presentation of spatial data* . Proceedings Auto Carto London 14 - 19 September 1986, 455 - 464.

Ley, R., G., 1988. Some aspects of height extraction from SPOT imagery. *Photogrammetric Record*, 12(72): 823-832.

Logan, L., T., & Ritter, N., D., 1988. Real time georeferencing with stereo imagery: Ruled surface and neural network approaches. *GIS/LIS'88 Proceedings accessing the world. International conference*. San Antonio, Texas , Volume 1 : 122-131.

Makarovic, B., 1972. Information transfer in reconstruction of data from sampled points, *Photogrammetria*, 1972, No. 4: 111-130.

Makarovic, B., 1973. Progressive sampling for digital terrain models. *ITC Journal*, Vol. 3, 397-416.

Makarovic, B., 1975. Amended strategy for progressive sampling. *ITC journal* , 1975-1 : 117-128.

Makarovic, B., 1977. Composite sampling for DTMs, *ITC Journal*, 1977-3: 406-433.

Mandelbrot, B., B., 1967. How long is the coast of Britain? Statistical selfisimilarity and fractional dimension: Science, Vol. 156: 636-638.

Mandelbrot, B., B., 1968. Les constantes chiffrées du discours. *Encyclopédie de la pléiade*: Linguistique, Paris: Gallimard: 46-56.

Mandelbrot, B., B., 1977. *Fractals: form, chance and dimension*: W. H. Freeman and Company, San Francisco, 366 pages.

Mandelbrot, B., B., 1982. *The fractal geometry of nature*. W. H. Freeman, San Francisco. 468 pages.

Manual of Photogrammetry, 1980. *American Society of Photogrammetry*. Fourth Edition: pages 1056.

Mapping package. 1987. *Laser- Scan Laboratories Ltd*. Reference Manual, 288 pages.

Mark, D., M., 1975. Geomorphometric Parameters: A review and evaluation. *Geographiska Annaler* . 57A:165-177.

Mark, D., M., 1979. Phenomenon-based data-structuring and digital terrain modelling. *Geo-Processing* , 1(1979):27-36

Mark, D., M., and Aronson, P., B., 1984. Scale dependent fractal dimensions of topographic surfaces: An empirical investigation, with applications in geomorphology and computer mapping. *Mathematical Geology*, Vol. 16, No. 7, pp. 671-683.

Marshall, B., F., and Faintish, B., 1984. State-of-the-art and future needs for development of digital terrain models. *International Society of Photogrammetry and Remote Sensing*. Commission III, A3a, page 180-196.

Mather, P., 1987. *Computer processing of remotely sensed images (an introduction)*. John Wiley & Sons : 352 pages.

Matheron, G., 1963. Principles of geostatistics, *Economic Geology,* Vol. 58: 1246-1266.

Matheron, G. 1971. The theory of regionalized variables and its applications: *Les Cahiers du Centre de Morphologie Mathématique de Fontainebleau*, v.5, 211 pages.

McCullagh, M., J., 1983. Transformation of contour strings to a rectangular grid based digital elevation model. *Presented paper. Euro-Carto II*, 18 pages.

McCullagh, M., J., 1986. High accuracy Digital terrain models - the Panacea system. *British Computer Society.* 11 pages.

McCullagh, M., J., 1988. Terrain and surface modelling systems: Theory and practice. *Photogrammetric Record* .12(72) : 747-779.

Melton, M., A., 1960. Intravally variation in slope angles related to microclimate and erosional environment. *Bull. Geological Society* Am. 71, 134-144.

Meneguette, A., A., C., 1985. Evaluation of metric camera phoptography for mapping and coordinate determination. *Photogrammetric Record*, 11(66): 699-709.

Michaelis, M., A geometrical analysis of SPOT data. *SPOT 1 Image Utilisation, assessment, results.* Paris. France. November 1987: 1235-1243.

Mikhail, E., M., and Ackermann, F., 1976. Observations and least squares. *University press of America.* 497 pages.

Miller, C., & LaFlamme, R., A., 1958. The digital terrain model - theory and applications. *Photogrammetric Engineering*, 24, 3, 433-442.

Mitchell C., W., 1973. *Terrain evaluation* . Longman Group Limited . London: 221 pages.

Molnar, L., 1980. An extended blunder estimation procedure. *International Archives of Photogrammetry*. Commission III, Volume XXII, Part B3: 525-535.

Moravec, H., P., 1977. Towards automatic visual obstacle avoidance. *Proceedings of the 5th International joint Conference on Artificial intelligence*, Cambridge, Mass: 584.

Muller, J-P., and Saksono, T., 1986. An evaluation of the potential role of fractals for digital elevation model generation from spaceborne imagery. *International Archives of Photogrammetry and Remote Sensing*, 26(4), page 63.

Muller, J., P., Otto, G., P., Chau, T., K., W., Collins, K., A., Dalton, N., Day, T., Dowman, I., J., Jakson, M., J., O'Neill, M., Paramananda, V., Roberts, J., B., G., Stevens, A., Upton, M., 1988. Real-time stereomatching SPOT using transputer arrays. *Proceedings of IGARSS '88 Symposium*, Edinburgh, Scotland, 13-16 Sep. 1988, 2 pages.

Muller, J-P., 1989. Real-Time Stereomatching and its Role in future mapping systems. *Surveying and mapping 89*, University of Warwick, 17-21/4/1989: 15 pages.

Munier, P., 1989. Map production and map updating using SPOT data. Presented paper on OEEPE workshop of the triangulation of SPOT data. *University College London* . 27-28/9/89: 10 pages.

Nassar, M., M., 1985. *Matrix treatment of adjustment computations in surveying* . Ain Shams University, Egypt, 395 pages.

OEEPE workshop, 1989. OEEPE test on triangulation of SPOT data. *University College London.* 27-28 Sept. 1989.

Olsen, R., W., 1987. Standards and specifications for USGS Digital Terrain Data. *Progress in Terrain Modelling. Technical University of Denmark* : 239-247.

O'Neill, M., A., and Dowman, I., J., 1988. The generation of epipolar synthetic stere mates for SPOT images using a DEM. *International Archives of Photogrammetry and Remote Sensing*, Vol. 27(B3): 587-598.

Ostman, A., 1984. Sequential data processing for photogrammetric acqiusition of DEM. *International Archives of Photogrammetry and Remote Sensing.* Commission IV, Vol XXV, Part A4: 334-344.

Ostman A., 1986. Terrain analysis by Karhumen - Loeve expansion. *International Archives of Photogrammetry and Remote Sensing* , 26(3/2): 682-690.

Ostman, A., 1987. Quality control of photogrammetrically sampled digital elevation models. *Photogrammetric Record*, 12(69): 333-341.

Otto, G., P. 1988. Rectification of SPOT data for stereo image matching. I*nternational Archives of Photogrammetry and Remote Sensing.* Commission III, 27(B3): 635-645.

Otto, G., P., and Chau, T., K., 1989. A " Region-Growing" algorithm for matching of terrain images. *Image Vision Computing.* Vol. 7, No. 2(May 1989): 83-94.

Panton, D., J., 1978. A flexible approach to digital stereo mapping. *Photogrammetric Engineering and Remote Sensing*, Vol. 44, No 12, pp 1499-1512.

Pearson, J., 1987. Analysis of the relationship between solar illumination, terrain geometry, surface cover and shading effects. Internal report, *Department of Photogrammetry and Surveying, University College London*, 13 pages.

Pentland, A., P., 1984. Fractal - based description of natural scenes. *IEEE Trans. Pattern analysis and machine intelligence*, Vol. 6, No. 6, 661-674.

Petrie, G., & Kennie,T., J., M., 1986. Terrain modelling in surveying and civil engineering. *Conference of British Computer Society* : 32 pages.

Petrie, G., & Kennie, T., J., M., 1987. An introduction to terrain modelling: Applications and terminology. Short course on terrain modelling in Surveying and Civil Engineering. *University of Glasgow* : 3 pages.

Petrie, G., 1987. Data interpolation and contouring methods. Short course on terrain modelling in Surveying and Civil engineering. University of Glasgow. September 1987. 15 pages.

Petrie, G., & Kennie, T., J., M., 1988. *Digital terrain modelling* . Chapter 10 in Engineering Surveying technology. (Editors T., J., M., Kennie and G., Petrie) Blackie Publishing Co. In press.

Pitkin, M., 1988. Report on observation of MS Alvey grid DEM. Internal report, *Department of Photogrammetry and Surveying, University College London*, 8 pages.

Pollard, S., B., Mayhew, J., E., W., and Frisby, J., P., 1985. PMF: a stereo correspondance algortithm using a disparity gradient limit. *Perception*, 14: 449-470.

Priebbenow, R., J., and Clerici, E., 1987. Cartographic applications of SPOT imagery. *Porceedings of SPOT 1 Image Utilisation, assessment, results* , Paris. France. November 23-27: 1189-1194.

Priebbenow, R., J., 1989. Triangulation of SPOT imagery at DGI, Queensland. *Paper presented at the OEEPE workshop on the triangulation of SPOT data*, University College London, Sept 27-28 : 18 pages.

Rafferty, J., Norling, R., Tamaru, R., McMath, C., and Morganstein, D., 1985. *StatWorks - Statistics with graphics for the Macintosh.* Heyden and Sons Ltd, 98 pages.

Rafferty, J., and Norling, R., 1985. *Cricket-Graph - Presentation graphics for science and business.* Cricket Software Inc, 228 pages.

Richardus, P., 1973. The precision of contour lines and contour interval of large - and medium - scale maps. *Photogrammetria*, 29(1973), 81-107.

Rivereau, J., C., Pousse, M., 1987. SPOT: An appraisal of results and a review of selected applications. *In prospects Int. Conference on "SPOT1: Image utilisation, assessment, results"* , Paris, France, November 1987.

Rodriguez, V., Gigord, P., De Gaujac, A., C., and Munier, P., 1988. Evaluation of the stereoscopic accuracy of the SPOT satellite. *Photogrammetric Engineering and Remote Sensing*, 54(2):217-221.

Rosenholm, D., 1986. Numerical accuracy of automatic parallax measurements of simulated SPOT images. *Canadian Journal of Remote Sensing*, Vol. 12, No. 2, December : 103-113.

Rosenholm, D., 1988. Usefulness of automatically generated height information for topographic mapping and land information purposes - with emphasis on data extracted from SPOT-, *International Archives of Photogrammetry and Remote Sensing*. 27(B9): IV-176-182.

Rudenauer, H., 1978. Problemanalyse und untersuchungen zur zweckmassigsten photogrammetrichen datenarfassung, fur die digitale verabeitung zu strassenbaulichen zwecken. *Institut fur Photogrammetrie und Ingenieurvermessungen, Technishe Universitat Hannover*, 131 pages.

Saastamoinen, J., 1972. Refraction. *Photogrammetric Engineering and Remote Sensing*, 38(8):800-810.

Saastamoinen, J., 1974. Local variation of photogrammetric refraction. *Photogrammetric Engineering and Remote Sensing*, 40(3):295-301.

Saksono, T. 1988. Stochastic properties of the terrain: A study of reliability and precision of DEM interpolation with geometrical constrains, PhD Thesis, *University of London* (unpublished).

Sandgaard, J., 1988. Integration of a GIS and a DTM. *International Archives of Photogrammetry and Remote Sensing*. Commission III, 27(B3): 716 - 725.

Schut, G., 1969. Photogrammetric refraction. *Photogrammetric Engineering and Remote Sensing*, 35(1):79-86.

Schut, G., H., 1976. Review of interpolation methods for digital terrain models. *XIIIth congress of the International Society for Photogrammetry*. Commission III, 07 08, 22 pages.

Schwartz, M., and Shaw, L., 1975. *Signal processing*. McGraw-Hill Kogakusha, New York, 396 pages.

Segu, W., P., 1985. Terrain approximation by fixed grid polynomial. *Photogrammetric Record*, 11(65): 581-591.

Sigle, M., 1984, A digital elevation model for the state of Baden-Wurttemberg. *Contribution to the XVth ISPRS Congress*. Rio de Janeiro. Schriftenreihe, Institute of Photogrammetry, *University of Stuttgart* 10, 105-115. Also in *International Archives of Photogrammetry*, 25(A3b), 1016-1026.

Silar, F., 1969. Die interpolation der hohen auf dem DGM in Beziehung fur klassification der gelandeflachen und zur dichte and zerlegung der knotenpunkte. *ISP-Working Group IV/1*, Bratislava, 1969.

Silfer, A., T., 1988. Generating GIS coverage from satellite imagery. *International conference, GIS/LIS'88 .Proceedings accessing the world*. Volume 1 : 52-57.

Simard, R., Toutin, T., Leclerc., A., Haja, S., Allam, M., Boudreau, R., Slaney, R., 1987. Digital terrain modelling with SPOT data and geological applications."*SPOT 1 Image utilisation, assessment, results* " , Paris, France, November 1987. 1205 -1212.

Singels, C., 1968. Accuracy specifications in mapping. *South African Svy Journal*, 68, 11(4), 19-26.

Snyder, J. P. 1982. *Map Projections used by the Geological Survey*. United States government printing office. 313 pages.

(SPOTUK87) 1987, Joint meeting of the Photogrammetric Society and the Remote Sensing Society. London, November 1987.

SPOT USER'S HANDBOOK. 1988. Reference manual, *SPOT Image*. Toulouse Cedex: Volume 1 and 2, 465 pages.

Stamp, L., D., and Willatts, E., C., 1935. The land utilization survey of Britain. *London School of Economics*. 76 pages.

Swann, R., Kauffman, D., and Sharpe, B., 1988. Results of automated digital elevation model generation from SPOT satellite data. *International Archives of Photogrammetry and Remote Sensing*. 27(2):434-440.

Tadrowski, T., 1988. Use of SPOT images and CCD cameras on DSR-11 for stereo.matching aerial photography. *Dept. of Photogrammetry and surveying UCL*. MSc desertation. 51 pages.

Teillet, P., M., Guindon, B., & Goodenough, D., G., 1980. Integration of remote sensing data sets by rectification to UTM coordinates with the use of digital terrain models. *International Archives of Photogrammetry*, 23(B3):726-733.

Tempfli, K., and Makarovic, B., 1979. Transfer functions of interpolation methods, *Geo-processing*, 1(1979): 1-26.

Tempfli, K., 1980. Spectral analysis of terrain relief for accuracy estimation of digital terrain models. *ITC Journal*, 1980-3, 478-510.

Tempfli, K., 1982. Genauigkeitschatzung digitaler Hohenmodelle mittels Spekralanalyse. *Geowissenschaftliche Mitteilungen*, T.U. Wien, Heft 22.

Tesche, T., W., & Bergstrom, R., W., 1978. Use of digital terrain data in meteorological and air quality Modelling. *Digital Terrain Model (DTM) Symposium* : 125-140.

The Commitee for specifications and Standards (1985). Accuracy specification for large scale line maps. *Photogrammetric Engineering and Remote Sensing*. Vol. 51, No 2. pp.195-199.

Theodossiou, E., I., & Dowman, I., J., 1989. Heighting accuracy of SPOT. Unpublished paper, 22 pages.

Thompson, E., H., 1976. Some remarks on the calculation of aerial triangulation. *Photogrammetric Record*, 8(48): 708-725.

Torlegård, K., Ostman, A., Lindgren, R., 1984. A comparative test of photogrammetrically sampled digital elevation models. *International Archives for Photogrammetry and Remote Sensing*, Commission III. 25(A3b):1065-1082.

Toomey, M., A., G., 1986. Digital elevation models in Alberta. *A S P convention*. Washington DC, 9 pages.

Toomey M., A., G., 1988. Land information services division. *International Archives of Photogrammetry and Remote Sensing*. Commission III, 27(B3): 775 - 783.

Veillet, I., 1989a. Triangulation of SPOT data. Report from participant IGN. *Paper presented at the OEEPE workshop on the triangulation of SPOT data*, University College London, Sept. 27-28 : 20 pages.

Veillet, I., 1989b. Triangiulation test data. *Paper presented at the OEEPE workshop on the triangulation of SPOT data*, University College London, Sept. 27-28 : 6 pages.

Vertella, S., & Moccia, A., 1982. Analysis of linear array taking into account satellite-sensor performances and a digital terrain model. *International Archives of Photogrammetry and Remote Sensing*. Commission VII : 23-32.

APPENDIX A.

The Gradient and Aspect estimation program.

A. The gradient and aspect estimation program. Algorithm description.

The main program SLOPE.FOR calls 3 basic routines, MENU.FOR, SET1.FOR and DEM_IO.FOR. The DEM_IO.FOR subroutine calls routines from the LSL$LIBRARY package.

A.1. SUBROUTINE MENU.FOR.

The purpose of the MENU.FOR routine is to prompt to the user. It includes the following secondary subroutines:

A.1.1. The subroutine MENU. This includes the main menu asking the user to select an option (see § 2.4.3.2.2).

A.1.2. The subroutine ES_MENU. This includes the global elevation smoothing submenu.

A.1.3. The subroutine Namein, which asks the user to specify the input filename (in DTI format).

A.1.4. The subroutine Spacing_of_DEM, which asks the user to specify the DEM spacing.

A.1.5. The subroutine Flat_Terrain, in order to input the user the limiting gradient under which a terrain will be considered as flat and

A.1.6. The subroutine Save_Menu, for saving the matrices of the estimated gradient and aspect in two separate files (in DTI format).

A.2. SUBROUTINE EX1.FOR.

Calls the following routines:

A.2.1. ES_Distance.

A.2.2. ES_LowPass.

A.2.3. Slope.

A.2.1. SUBROUTINE ES_Distance.

Carries out elevation smoothing based on a 3 x 3 window with weighting in inverse proportion to distance from central cell.

```
Declarations:  x,y      : Array dimension.
               m,n      : Input/output rows and columns.
               i,j      : Loop indexes
               A(x,y)   : Input DEM.
               Sum      : Summation variable.

m=m-1,     n= n-1
Do j=2,m
      Do i=2,n
      Sum =  0.25    * FLOAT(A(i,j) +
             0.125   * (FLOAT(A(i-1,j) + FLOAT(A(i+1,j) +
                        FLOAT(A(i,j-1) + FLOAT(A(i,j+1))  +
             0.0625* (FLOAT(A(i-1,j-1) + FLOAT(A(i-1,j+1)) +
                        FLOAT(A(i+1,j-1) + FLOAT(A(i+1,j+1)))
      A(i,j) = IFIX(Sum)
```

A.2.2. SUBROUTINE ES_Low_Pass.

The elevation smoothing is based on a low pass filtering, in a convolution array 3 x 3.

```
Declarations:  Sum      : Summation variable.
               x,y      : Array dimensions.
               m,n      : Rows, columns.
               l, k, i, j : Loop index.
               A(x,y)   : Input/Output DEM.
               S        : Dummy variable.

m=m-1,     n= n-1
Do j=2,m
    Do i=2,n
       Sum = 0
          Do l=-1,1,1
             Do k=-1,1,1
                Sum = Sum+A(i+1,j+k)
    S= FLOAT(Sum) / 9
    A(i,j)=IFIX(S)
```

A.2.3. SUBROUTINE Slope.

Determines the slope vector for each point of a DEM. By definition the gradient is the magnitude of the slope and the aspect is the direction of maximum change.

Declarations:

x,y	: Array size.
In_N, In_M	: Input rows, columns.
N,M	: Output rows, columns.
Label	: Dummy variable.
Index	: Aspect points (ridges=2, rivers =1)
A(x,y)	: Input DEM matrix
Gra(x,y)	: Input gradient matrix.
Asp(x,y)	: Output aspect matrix.
i,j,k,l	: Loop index.
Flat	: Threshold for flat terrain (gradient)
Gr, As	: Dummy variables.
dx,dy	: Partial derivatives (dx=E-W, dy=N-S).
pi, p18	: pi=3.14152926, p18=180/pi.
spacing	: Spacing of the DEM.

Partial derivative computation E-W, N-S.

```
Do j=2,M
     Do i=2,N
     dx =  (a(i-1,j+1)  +  (2*a(i,j+1))  +  a(i+1,j+1))  -
           (a(i-1,j-1)  +  (2*a(i,j-1))  +  a(i+1,j-1))
     dy = -(a(i-1,j-1)  +  (2*a(i-1,j))  +  a(i-1,j+1))  +
           (a(i+1,j-1)  +  (2*a(i+1,j))  +  a(i+1,j+1))
     gr =  ((dx/(8*spacing))**2  +  ((dx/(8*spacing))**2)
     gr =  ATAN(SQRT(gr))*p18
```

Gradient and aspect extreme cases threshold for flat terrain divisions.

```
IF (gr LE Flat) THEN  as=200  ELSE
  IF (dx EQ 0 AND dy GT 0) THEN  as=90  ELSE
     IF (dy EQ 0 AND dx GT 0) THEN  as=-90  ELSE
       IF (dy EQ 0 AND dx LT 0) THEN  as=180  ELSE
            as = ATAN(-dy/dx)*p18    (normal case)
```

Ridge direction assignment.

```
  IF (dx LT 0 AND dy GT 0)  as=-180+as
    IF (dx LT 0 AND dy LT 0)  as=180+as
```

Pointing direction with respect to neighbours (figure A.1).

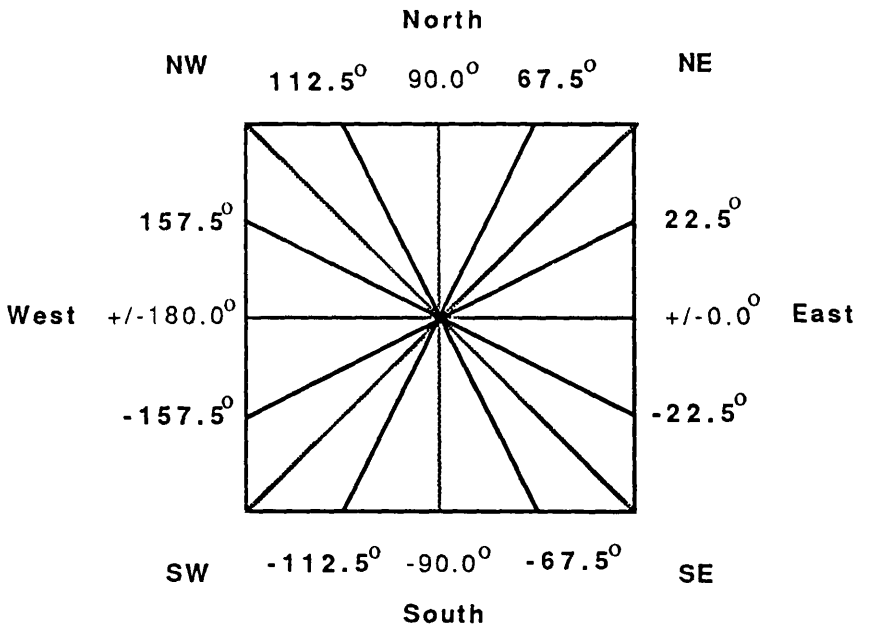

Figure A.1. Pointing direction with respect to neighbours.

```
      IF (as EQ 200) THEN                                Label = 0   (Undefined).
 ELSE IF (-22.5 LT as AND as LE 22.5) THEN               Label = 1   (East).
 ELSE IF (22.5 LT as AND as LE 67.5) THEN                Label = 2   (NE).
 ELSE IF (67.5 LT as AND as LE 112.5) THEN               Label = 3   (North).
 ELSE IF (112.5 LT as AND as LE 157.5) THEN              Label = 4   (NW).
 ELSE IF (157.5 LT as AND as LE 180) THEN                Label = 5   (West).
 ELSE IF (-180 LT as AND as LE -157.5) THEN              Label = 5   (West).
 ELSE IF (-157.5 LT as AND as LE -112.5) THEN            Label = 6   (SW).
 ELSE IF (-112.5 LT as AND as LE -67.5) THEN             Label = 7   (South).
 ELSE IF (-67.5 LT as AND as LE -22.5) THEN              Label = 8   (SE).

asp(i,j) = Label
IF (gr GT Flat)    THEN      gra(i,j)= IFIX(gr)  ELSE   gra(i,j) = 0
```

A.3. PROGRAM SLOPE.FOR.

Is the main program which calls the 3 other main routines and the secondary routines which are contained in the main routines, according to the user selection option. This user selection option can be in the range 1 to 4.

A.3.1. If the option is 1, the main program calls the secondary subroutines:

a. Namein (to input the input filename) and

b. DTI_in, in order to read the input DTI file.

A.3.2. If the option is 2, it calls the secondary routine Save_Menu ,to ask the output filenames for saving image (raster) form data (DTI files).

A.3.3. If option 3 is selected , it calls the secondary subroutines :

a. ES_Menu, which contains the global elevation smoothing submenu.

b. according to the user selection it calls the ES_distance (smoothing based on the distance) or the ES_LowPass (smoothing based on a low pass filter).

A.3.4. If the option is 4, it calls the secondary subroutines:

a. Spacing_of_DEM (to define the DEM spacing).

b. Flat_Terrain (gradient magnitude below which a terrain will be considered as flat).

c. Slope (gradient and aspect calculations).

APPENDIX B.

Elevation data checking and statistical analysis program using data from two sources.

B. Elevation checking and statistical analysis program using data from the two sources - aerial photography and SPOT imagery. Algorithm description.

A Pascal program was written in order to carry out the statistical analysis. The program compares the SPOT elevation data with the aerial photograph four neighbour elevations.

The program estimates the simulated height (calculated height value) of the aerial photograph from the four nearest neighbours and compares it with the less accurately known height of the corresponding position in the SPOT image.

The program takes the elevation data of the first source (aerial photography) from a file and the second source (SPOT) data from another file. The first source data should lie in a regular grid (in order to form the data elevation matrix). The second source data can be either lie on a grid or be random points.

The program asks the user for:

1. The first source data file name.
2. The second source data file name.
3. The output Height_differences file name . The output is in matrix form (row, columns, Height_Differences).
4. The output statistical analysis file name.
5. The first source elevation matrix number of rows.
6. The first source elevation matrix number of columns.
7. The first source elevation matrix grid interval.
8. The second source total number of points.

B.1. PROCEDURE Give_Prompts.

Prompts to the user to specify the input, output filenames and the other mentioned input values.

B.2. PROCEDURE Read_Rewrite_First_Source_File.

The aim of this procedure is to read the first source data from a sequential file and rearrange the data in rows, columns as they were during the collection procedure. The procedure also reads the DEM origin (bottom left) (X_Origin, Y_Origin).

B.3. PROCEDURE Calculate_the_Azimuths.

The purpose of the procedure is to estimate the azimuth and to define in which quadrant the data block lies, according to the azimuth.

Declarations: x1, y1 : First source point coords.

STEPS:

1. Find the Differences in Coordinates:
   Dx[m,n] = x1[m+1,n+1] - x1[m,n]
   Dy[m,n] = y1[m+1,n+1] - y1[m,n]

2. Find the Azimuth $\alpha((m,n),(m+1,n+1))$
   Azim[m,n] = ARCTAN(Dx[m,n] / Dy[m,n])

3. Find the differences in coordinates
   Dx1[m,n] = x1[m,n+1] - x1[m,n]
   Dy1[m,n] = y1[m,n+1] - y1[m,n]

4. Restrictions for the quadrant definition.

```
IF (Dx1[m,n] > 0 AND dy1[m,n] >= 0) THEN
        IF (Dx[m,n] > 0 AND dy[m,n] > 0) THEN        Quadrant = 1
IF (Dx1[m,n] < 0 AND dy1[m,n] >= 0) THEN
        IF (Dx[m,n] < 0 AND dy[m,n] > 0) THEN        Quadrant = 2
IF (Dx1[m,n] < 0 AND dy1[m,n] <= 0) THEN
        IF (Dx[m,n] < 0 AND dy[m,n] < 0) THEN        Quadrant = 3
IF (Dx1[m,n] > 0 AND dy1[m,n] <= 0) THEN
        IF (Dx[m,n] > 0 AND dy[m,n] < 0) THEN        Quadrant = 4
```

B.4. PROCEDURE Read_Data_Second_Source.

It reads the data from the input second source data file.

From an experiment carried out it found that the 4th and the 6th function give the best for this particular case results. Therefore it decided to be used the W = 1 / Distance^2 weight function.

1. Calculation of the distances of the four first source neighbour points:

```
Distance[m,n] = SQRT(SQR(x2[q]- x1[m,n]) + SQR(y2[q] - y1[m,n]))
```

2. Calculation of the four weights:

```
Weight[m,n] = 1/ SQR(Distance[m,n])
```

3. Calculation of the Simulated_Heights:

```
Simulated_Height[p] = ( z1[m,n]*Weight[m,n] + z2[m,n+1]*Weight[m,n+1]
                      + z3*[m+1,n+1] * Weight[m+1,n+1]
                      + z4[m+1,n]*Weight[m+1,n])
                      / (Weight[m,n] + Weight[m,n+1] + Weight[m+1,n+1]
                      + Weight[m+1,n])
```

4. Calculation of the difference between the simulated_height and the second source point.

```
Height_Difference[p] = z2[q] - Simulated_Height[p].
```

B.6.2. PROCEDURE Case_Quadrants.

This procedure defines the digital elevation matrix quadrant. It is also checks if any second source point lies in any cell of the first source elevation matrix.

STEPS:

1. Calls the PROCEDURE Calculate_Height_Differences.
2. Defines and allocates the first source elevation matrix through a CASE statement
3. Checks which of the second source points lie in the first source defined elevation matrix and in which cell.

IF the second source point lies in the first source defined matrix THEN

WRITE to the output file : Number_of_Row, Number_of_Column, Height_Difference

ELSE WRITE to Superfluous_Points_File: Point_Number2[q]

B.5. PROCEDURE Estimate_Origin_Source2_length.

The aim of this procedure is to find in which cell of the first source defined elevation matrix lies the second source point.

Declarations:

x2, y2	:	Second source point coords.
X_Origin,Y_Origin	:	First source DEM left bottom corner origin.
Grid_Interval	:	First source DEM grid interval.

```
Row_Cell[q]    = TRUNC(( |y2[q] - Y_Origin| ) / Grid_Interval ) + 1
Column_Cell[q] = TRUNC(( |x2[q] - X_Origin| ) / Grid_Interval ) + 1
```

B.6. PROCEDURE Sec_Pnt_Lie_Cell_Simul_Heights.

The aim of this procedure is to calculate the height differences between the second source heights and the four first source elevation neighbours in respect to the defined digital elevation matrix quadrant.

This procedure includes two other procedures.

B.6.1. PROCEDURE Calculate_Height_Differences.

B.6.2. PROCEDURE Case_Quadrants.

B.6.1. PROCEDURE Calculate_Height_Differences.

The aim of the procedure is to estimate the height differences. In this procedure is applied a weight function in order to estimate the simulated heights. The Simulated_Height is calculated from the first source 4 nearest neighbour points.

The application of the weight as a function depending on the distance can have one of the following forms:

1. $W = (1\text{-Distance})^3 * (1\text{-Distance})^2) \ / \ \text{Distance}^2$
2. $W = (1\text{-Distance})^2 \ / \ \text{Distance}^2$
3. $W = 1 \ / \ \text{Distance}^4$
4. $W = 1 \ / \ \text{Distance}^2$
5. $W = 1 - 0.9 * \text{Distance}^2$
6. $W = 1 \ / \ \text{Distance}$

NOTE:

The row, column, Height_Difference of all the compared points file is used for display purposes. With the display the user can have a visual representation of the erroneous points, so it is easy to identify their position and distribution.

The ELSE part is controlled by the user in order to save disc space (storage space).

B.7. PROCEDURE First_Source_Area_Mean_Height and PROCEDURE Second_Source_Area_Mean_Height.

The purpose of these two PROCEDURES is to estimate the reference surface (mean DEM height value) for each source.

B.8. PROCEDURE Find_Height_Differences_Range.

The aim of this PROCEDURE is to estimate some useful statistical parameters (range and extremes) as follows:

1. The groups of the Height_Differences in 4 metre bands (from -40m to +40m).
2. The more than +40m and less than -40m Height_Differences.
3. The larger and the smaller Height_Difference.
4. The user can to specify a Height_Limit. With that limit the program works out the more than +(Height_Limit) and the less than the -(Height_Limit), found in the second source (Count_Number, x, y, z and Height_Difference), which are possibly blunders.

The grouped Height_Differences can be used in forming the error histogram.

B.9. PROCEDURE Statistics.

The goal of this PROCEDURE is to calculate some descriptive statistical

results as follows:

1. The mean, variance and standard deviation of the found Height_Differences.

2. The mean, variance and standard deviation of the absolute found Height_Differences.

All the results of B.7, B.8 and B.9 above are all written to an output file (Stat.dat).

APPENDIX C.

Transformations used in the project.

C. Transformations used in the project.

C.1. Geocentric coordinate System.

The geocentric Cartesian system is a coordinate system with its origin approximately at the centre of the earth and with the X and Y axes in the plane of the equator The X axis passes through the meridian of Greenwich, and the Z axis coincides with the earth's rotation. The relationship between geocentric and geographical systems, assuming the earth is an ellipsoid is shown in figure C.1.

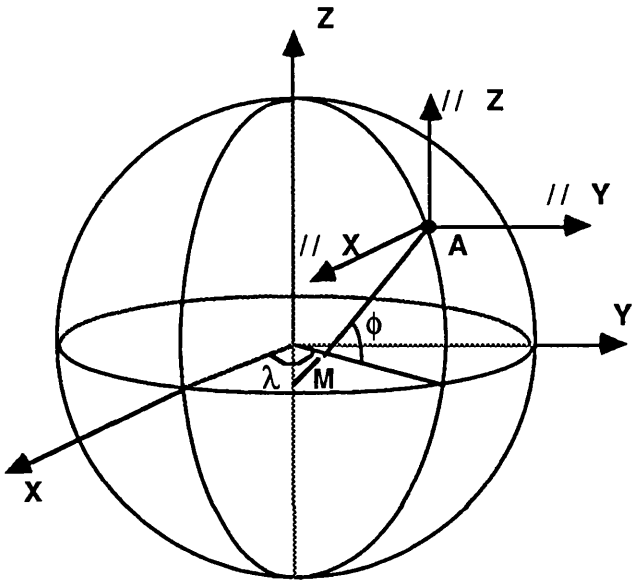

Figure C.1. The geocentric and geographical systems.

C.1.1. Geographical to Geocentric transformation.

The geodetic latitude ϕ of a point A on the surface of the ellipsoid is defined as the angle in the meridional plane at which the normal to the ellipsoid at A intersects the plane of the equator. The geocentric latitude is the angle ϕ at the centre of the ellipse.

The length AM is needed in any computations involving the ellipsoid. This is given by:

$$AM = N = a * \sqrt{1 - e^2 * \sin^2\phi} \qquad (1.1.1).$$

In practice we wish to consider a point lying a distance h from the ellipsoid and to relate the geodetic latitude and longitude to the three dimensional Cartesian geocentric coordinate system X, Y, Z.

$$X = (N + h) * \cos\phi * \cos\lambda \qquad (1.1.2).$$

$$Y = (N + h) * \cos\phi * \sin\lambda \qquad (1.1.3).$$

$$Z = (N * (1 - e^2) + h) * \sin\phi \qquad (1.1.4).$$

C.1.2. Geocentric to Geographical transformation.

The inverse computation Geocentric to Geographical cannot be carried out directly because the Latitude is needed to find N. An iterative method can be used assuming that the difference between ϕ and ϕ_1 is small. The number of iterations could be defined until the difference between ϕ and ϕ_1 becomes less than a specified limit:

Divide (1.1.3) by (1.1.2) $\qquad \lambda = \tan^{-1}\left(\frac{X}{Y}\right) \qquad (1.2.1).$

$$D = \sqrt{X^2 + Y^2} \qquad (1.2.2).$$

$$\phi_1 = \tan^{-1}\left(\frac{Z}{D}\right) \qquad (1.2.3).$$

$$N = \frac{a}{\sqrt{1 - e^2 * \sin^2\phi_1}} \qquad (1.2.4).$$

$$\phi = \frac{\tan^{-1} * (Z + N * e^2 * \sin\phi)}{D} \qquad (1.2.5).$$

$$h = \frac{D}{\cos\phi - N} \qquad (1.2.6).$$

C.2. Universal Transverse Mercator Projection.

The formulas for the consideration of the earth as an ellipsoid follows:

C.2.1. Geographical to UTM projection.

For the ellipsoidal form, the most practical form of the equations is a set of series approximations which coverage rapidly in a zone extending 3° to 4° of the longitude from the central meridian. Beyond this, the series have insufficient terms for the accuracy required.

$$e' = \frac{e^2}{(1-e^2)} \qquad (2.1.1).$$

$$N = \sqrt{\frac{a}{1 - e^2 * \sin^2\phi}} \qquad (2.1.2).$$

$$T = \tan^2\phi \qquad (2.1.3).$$

$$C = e'^2 * \cos^2\phi \qquad (2.1.4).$$

$$A = \cos\phi * (\lambda - \lambda o) \qquad (2.1.5).$$

$$M = a*\left[(1 - \frac{e^2}{4} - \frac{3*e^4}{64} - \frac{5*e^6}{256} - .....)*\phi - (\frac{3*e^2}{8} + \frac{3*e^4}{32} + \frac{45*e^6}{1024} + ...)*\sin 2\phi + (\frac{15*e^4}{256} + \frac{45*e^6}{1024} + ...)*\sin 4\phi - (\frac{35*e^6}{3072} + ...)*\sin 6 + ...\right] \qquad (2.1.6).$$

$$Mo = a*\left[(1 - \frac{e^2}{4} - \frac{3*e^4}{64} - \frac{5*e^6}{256} - .....)*\phi o - (\frac{3*e^2}{8} + \frac{3*e^4}{32} + \frac{45*e^6}{1024} + ...)*\sin 2\phi o + (\frac{15*e^4}{256} + \frac{45*e^6}{1024} + ...)*\sin 4\phi o - (\frac{35*e^6}{3072} + ...)*\sin 6\phi o + ...\right] \qquad (2.1.7).$$

$$x = ko*N*\left(A + (1 - T + C)*\frac{A^3}{6} + (5 - 18*T + T^2 + 72*C - 58*e'^2)*\frac{A^5}{120}\right) \qquad (2.1.8).$$

$$y = ko*\left[M - Mo + N*\tan\phi*(\frac{A^2}{2} + (5 - T + 9*C + 4*C^2)*\frac{A^4}{24} + (61 - 58*T + T^2 + 600*C - 330*e^2)*\frac{A^6}{720})\right] \qquad (2.1.9).$$

$$k = ko*\left[1 + (1 + C)*\backslash F(A\backslash S(2),2) + (5 - 4*T + 42*C + 13*C^2 + 28*e'^2)*\frac{A^4}{24} + (61 - 148*T + 16*T^2)*\frac{A^6}{720}\right] \qquad (2.1.10) \text{ or}$$

$$k = ko*(1 + \frac{(1 + e'^2*\cos^2\phi)*x^2}{2*ko^2*N^2}) \qquad (2.1.11).$$

Where ko : the scale of the central meridian 0.9996, for the UTM projection.

λ, λo, ϕ : angles (in radians).

M : the true distance along the central meridian from the Equator to ϕ.

C.2.2. UTM to Geographical projection.

The inverse computation UTM to Geographical can not be carried out directly. An iterative method can be used assuming that the difference between ϕ and ϕ_1 is small. The number of iterations could be defined until the difference between ϕ and ϕ_1 becomes less than a specified limit:

Calculating Mo from the (2.1.7) and e' from the (2.1.1)

$$M = \frac{M_o + y}{k_o} \qquad (2.2.1).$$

$$e_1 = \frac{1 - \sqrt{1 - e^2}}{1 + \sqrt{1 - e^2}} \qquad (2.2.2).$$

$$\mu = \frac{M}{a*(1 - \frac{e^2}{4} - \frac{3*e^4}{64} - \frac{5*e^6}{256} - .....)} \qquad (2.2.3).$$

$$\phi_1 = \mu + (\frac{3*e_1}{2} - \frac{27*e_1^3}{32} + ...)*\sin 2\mu + (\frac{21*e_1^2}{16} - \frac{55*e_1^4}{32} - ....)*\sin 4\mu + (\frac{151*e_1^3}{96} + ...)*\sin 6\mu + ... \qquad (2.2.4).$$

$$C_1 = e'^2 * \cos^2\phi_1 \qquad (2.2.5).$$

$$T_1 = \tan^2\phi_1 \qquad (2.2.6).$$

$$N_1 = \frac{a}{\sqrt{1 - e^2 * \sin^2\phi_1}} \qquad (2.2.7).$$

$$R_1 = \frac{a*(1 - e^2)}{\sqrt{(1 - e^2 * \sin^2\phi_1)^3}} \qquad (2.2.8).$$

$$D = \frac{x}{N_1 * k_o} \qquad (2.2.9).$$

$$\phi = \phi_1 - \left(\frac{N_1 * \tan\phi_1}{R_1}\right) * [(\frac{D^2}{2} - (5 + 3*T_1 + 10*C_1 - 4*C_1^2 - 9*e'^2)*\frac{D^4}{24} + (61 + 90*T_1 + 298*C_1 + 45*T_1^2 - 252*e'^2 - 3*C_1^2)*\frac{D^6}{720}] \qquad (2.2.10).$$

$$\lambda = \lambda_0 + [D - (1 + 2*T_1 + C_1)*\frac{D^3}{6} + (5 - 2*C_1 + 28*T_1 - 3*C_1^2 + 8*e'^2 + 24*T_1^2)*\frac{D^5}{120}] / \cos\phi_1 \qquad (2.2.11).$$

C.3. Lambert Zone III projecton.

The formulae for the consideration of the earth as an ellipsoid follows:

C.3.1. Geographical to Lambert projection.

Given a, e, ϕ_1, ϕ_2, ϕ_o, λ_o, ϕ, and λ.

Find ρ, θ, χ, ψ, κ.

$$m_1 = \frac{\cos\phi_1}{\sqrt{1 - e^2 * \sin^2\phi_1}} \qquad (3.1.1).$$

$$m_2 = \frac{\cos\phi_2}{\sqrt{1 - e^2 * \sin^2\phi_2}} \qquad (3.1.2).$$

$$t_1 = \frac{\tan\left(\frac{\pi}{4} - \frac{\phi_1}{2}\right)}{\sqrt{\frac{(1 - e * \sin\phi_1)^e}{(1 + e * \sin\phi_1)^e}}} \qquad (3.1.3).$$

$$t_2 = \frac{\tan\left(\frac{\pi}{4} - \frac{\phi_2}{2}\right)}{\sqrt{\frac{(1 - e * \sin\phi_2)^e}{(1 + e * \sin\phi_2)^e}}} \qquad (3.1.4).$$

$$t_o = \frac{\tan\left(\frac{\pi}{4} - \frac{\phi_o}{2}\right)}{\sqrt{\frac{(1 - e * \sin\phi_o)^e}{(1 + e * \sin\phi_o)^e}}} \qquad (3.1.5).$$

Find the map constants n, F, and ρ_o

$$n = \frac{\ln(m_1) - \ln(m_2)}{\ln(t_1) - \ln(t_2)} \qquad (3.1.6). \quad \text{or}$$

$$n = \sin\phi_1 \qquad (3.1.6a).$$

$$F = \frac{m_1}{n * t_1^{\,n}} \qquad (3.1.7).$$

$$\rho_o = a * F * t_o^{\,n} \qquad (3.1.8).$$

$$t = \frac{\tan\left(\frac{\pi}{4} - \frac{\phi}{2}\right)}{\sqrt{\frac{(1 - e * \sin\phi)^e}{(1 + e * \sin\phi)^e}}} \qquad (3.1.9).$$

$$\rho = a * F * t^n \qquad (3.1.10).$$

$$\theta = n * (\lambda - \lambda_o) \qquad (3.1.11).$$

$$\chi = \rho * \sin\theta \qquad (3.1.12).$$

$$\psi = \rho_o - \rho * \cos\theta \qquad (3.1.13).$$

Find the scale:

$$m = \frac{\cos\phi}{\sqrt{1 - e^2 * \sin^2\phi}} \qquad (3.1.14).$$

$$\kappa = \frac{\rho * n}{a * m} = \frac{m_1 * t^n}{m * t_1^n} \qquad (3.1.15).$$

Note :

In the application, because the Latitude of the first standard parallel, the Latitude of the second parallel, and the Latitude of the central meridian is the same, the formulaes (3.1.2) and (3.1.4) of estimating m_2 and t_2 are not active in the program. The estimation of n is carried out by applying the (3.1.6a) instead of (3.1.6).

The scale factor estimated by applying (3.1.15). From the Geographical to Lambert transformation the scale factor is estimated to be less than 1.0. The scale factor should be applied to all the calculated point coordinates (x and y coordinates myltiplied by scale factor).

If a unique scale factor is applied and provided, in the case of Lambert to Geographical transformation, x and y coordinates should be multiplied with the scale factor. Unique scale factor can also be applied to the ellipsoid parameters.

C.3.2. Lambert to Geographical.

Given a, e, ϕ_1, ϕ_2, ϕ_o, λ_o, χ, and ψ.

Find ρ, θ, κ, ϕ, λ.

Calculate m_1, m_2, t_1 ,t_2 and to from (3.1.1, 3.1.2, 3.1.3, 3.1.4, 3.1.5). In the application the formulaes (3.1.2 and 3.14) are not active.

Calculate the map constants n, F, and ρ_o, from the formulaes (3.1.6 or 3.1.6a, 3.1.7. and 3.1.8).

For the given Latitude and Longitude :

$$\rho = \sqrt{\chi^2 - (\rho_o - \psi)^2} \quad , \text{ where } \rho \text{ takes the sign of } n \qquad (3.2.1).$$

$$\theta = \tan^{-1} * \left(\frac{\chi}{\rho_o - \psi}\right) \qquad (3.2.2).$$

$$t = \sqrt[n]{\frac{\rho}{a * F}} \qquad (3.2.3).$$

Find the initial trial ϕg value :

$$\phi g = \frac{\pi}{2} - 2*\tan^{-1}(t) \qquad (3.2.4).$$

Inserting ϕg into the following formulae we can estimate ϕ:

$$\phi = \frac{\pi}{2} - 2 * \tan^{-1}\left(t*\sqrt{\frac{(1 - e*\sin\phi)^e}{(1 + e*\sin\phi)^e}}\right) \qquad (3.2.5).$$

Replacing the ϕ in the right hand side of (3.2.5), we recalculate the new ϕ on the left side. This could be done iterratively until ϕ does not change to 7 decimals.

$$\lambda = \left(\frac{\theta}{n + \lambda_o}\right) \qquad (3.2.6).$$

Find the scale from (3.1.15)

Note :

The scale factor estimated by applying (3.1.15). For the Lambert to Geographical transformation the scale factor is estimated to be greater than 1.0. The scale factor should be applied to all the calculated point coordinates.

If a unique scale factor is applied and provided, in the case of Lambert to Geographical transformation, x and y coordinates should be divided by the scale factor.

APPENDIX D.

The blunder detection of DEM data program.

D. Blunder detection of DEM data program. Algorithm description.

D.1. Basic calculations and estimations.

The blunder detection algorithm is a local self-checking pointwise technique (see § 6.3.3), based on the comparison of the tested point (elevation value) with its neighbouring points, as shown in figure (D.1). The constraints which the algorithm used depending on the slope in the application of certain height limits (see table 6.8) during the checking procedure.

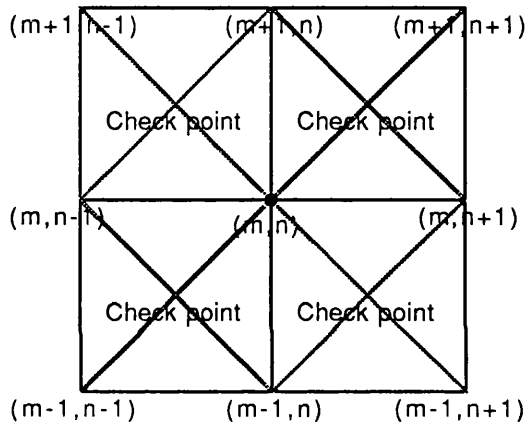

Figure D.1. Tested point (m,n) with its 7 surrounding neighbours.

In order to do the certain comparison between the tested point and the surrounding neighbours the algorithm is carries out the following basic calculations:

D.1.1. Find the absolute differences in heights.

|DZ[m-1,n-1]|	|DZ[m-1,n]|
|DZ[m-1,n+1]|	|DZ[m,n+1]|
|DZ[m+1,n+1]|	|DZ[m+1,n]|
|DZ[m+1,n-1]|	|DZ[m,n-1]|

D.1.2. Slope estimation from the height differences, grid interval and the hypotenuse.

Hypotenuse = $(2*(\text{Grid\_Interval})^2)^{1/2}$

Slope[m-1,n-1]	Slope[m-1,n]
Slope[m-1,n+1]	Slope[m,n+1]
Slope[m+1,n+1]	Slope[m+1,n]
Slope[m+1,n-1]	Slope[m,n-1]

D.1.3. Calculation of the slope differences.

|Slope[m-1,n] - Slope[m+1,n]
|Slope[m,n+1] - Slope[m,n-1]
|Slope[m-1,n-1] - Slope[m+1,n+1]
|Slope[m-1,n+1] - Slope[m+1,n-1]

D.1.4. Find the Height_Differences.

DifZ[m-1,n-1]	DifZ[m-1,n]
DifZ[m-1,n+1]	DifZ[m,n+1]
DifZ[m+1,n+1]	DifZ[m+1,n]
DifZ[m+1,n-1]	DifZ[m,n-1]

D.1.5. Estimate the Height_Differences average.

DifZ[m-1,n-1]/2	DifZ[m-1,n]/2
DifZ[m-1,n+1]/2	DifZ[m,n+1]/2
DifZ[m+1,n+1]/2	DifZ[m+1,n]/2
DifZ[m+1,n-1]/2	DifZ[m,n-1]/2

D.1.6. Find the height in the check points.

Ch_Height[m-1,n-1]	Ch_Height1[m-1,n-1]
Ch_Height[m-1,n]	Ch_Height1[m-1,n]
Ch_Height[m,n]	Ch_Height1[m,n]
Ch_Height[m,n-1]	Ch_Height1[m,n-1]

D.1.7. Calculation of the Check_Height_Differences.

Ch_Height[m-1,n-1]= |Ch_Height1[m-1,n-1] - Ch_Height1[m-1,n-1]|
Ch_Height[m-1,n] = |Ch_Height1[m-1,n] - Ch_Height1[m-1,n]|
Ch_Height[m,n] = |Ch_Height1[m,n] - Ch_Height[m,n]|
Ch_Height[m,n-1] = |Ch_Height1[m,n-1] - Ch_Height[m,n-1]|

The blunder detection algorithm described in flow-chart form is shown in the figure D.2.

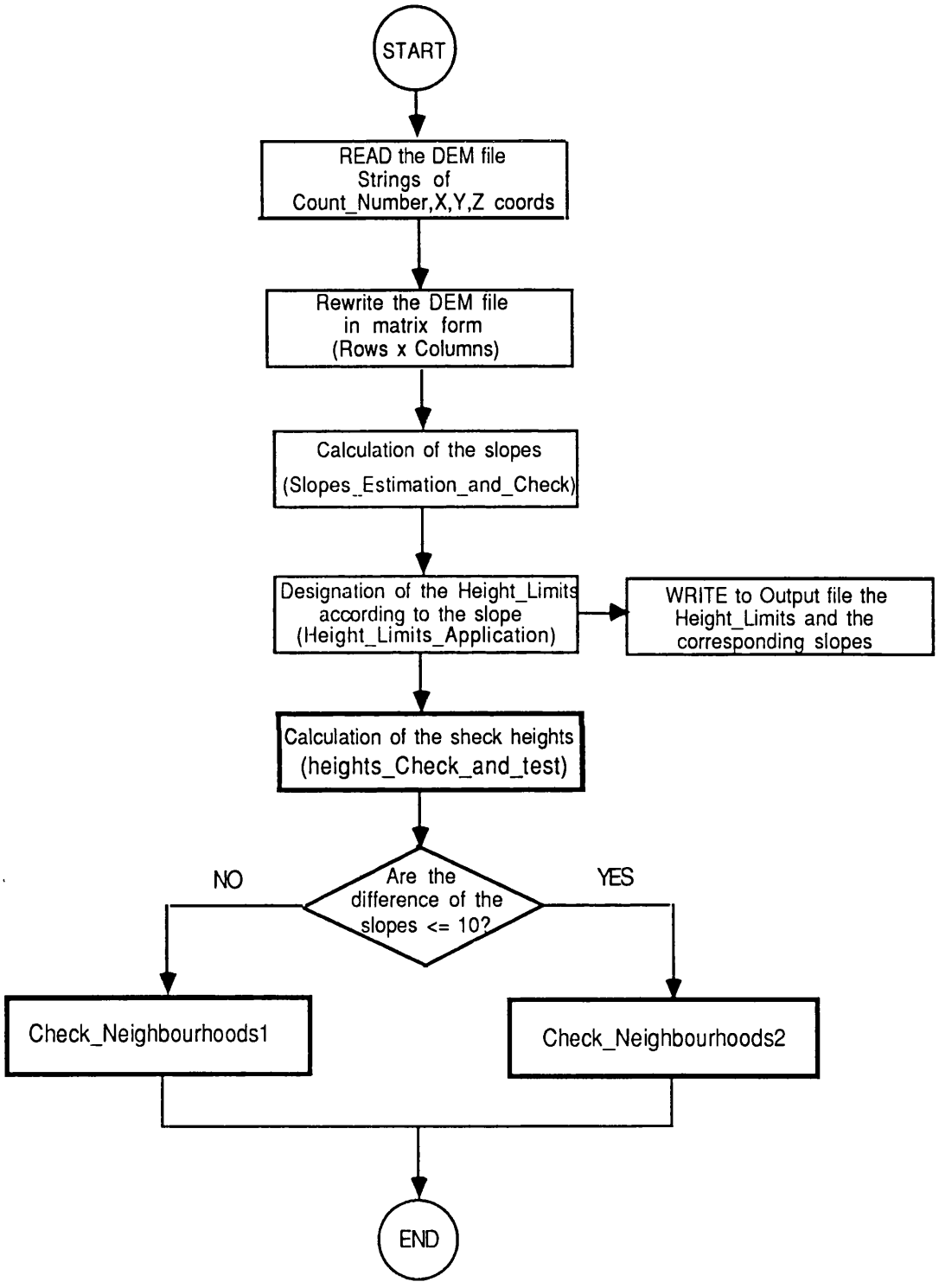

Figure D.2. The blunder detection algorithm flow-chart.

Each point is examined through three routines. The checking procedure is described in § 6.3.3.2.

D.2. PROCEDURE Read_Rewrite.

Reading of the sequential data file and rewriting it as rows-columns digital elevation matrix procedure. It is the same as in the CHECK.PAS program (described in appendix B).

D.3. PROCEDURE Slope_Estimation_and_Checks.

This routine calculates the slopes and decides according to the slope whether to apply the single or the multiple check during the test operations (Check_Neighbourhoods1 or Check_Neighbourhoods2 routine).

D.4. PROCEDURE Check_Neighbourhoods1.

The routine is applied in flat and gently rolling areas (slopes <= 10%). In this routine the tested point is examined in relation to its neighbours. The checking procedure steps are as follows:

D.4.1. Estimation of the Calculated_Height for each check point. This is the elevations average of the 8 surrounding nearest neighbour points.

```
Calculated_Height[m,n] = (Z[m-1,n-1] + Z[m,n-1] + Z[m+1,n-1] +
                          Z[m+1,n] +   Z[m+1,n+1] + Z[m,n+1] +
                          Z[m-1,n+1] + Z[m-1,n]) / 8
```

D.4.2. Add in the Calculated_Height[m,n] the quantity (2.7 * Height_Limit), (3σ). The Height_Limit has various values depending on the slopes.

```
Calculated_Height1[m,n] = Calculated_Height[m,n] + (2.7 * Height_Limit)
Calculated_Height2[m,n] = Calculated_Height[m,n] - (2.7 * Height_Limit)
```

D.4.3. Comparison of the Calculated_Height1 and Calculated_Height2 with the initial Z coordinate of the testing point.

```
IF NOT (Z[m,n] <= Calculated_Height1[m,n] AND Z[m,n] >=
                    Calculated_Height2[m,n])
                    THEN WRITE the point as blunder in (Blun_File).
```

The Height_Limit is chosen to be (2.7σ) in order to detect the medium and large blunders.

The procedure Check_Neighbourhoods1 described in flow-chart form is shown in the figure D.3.

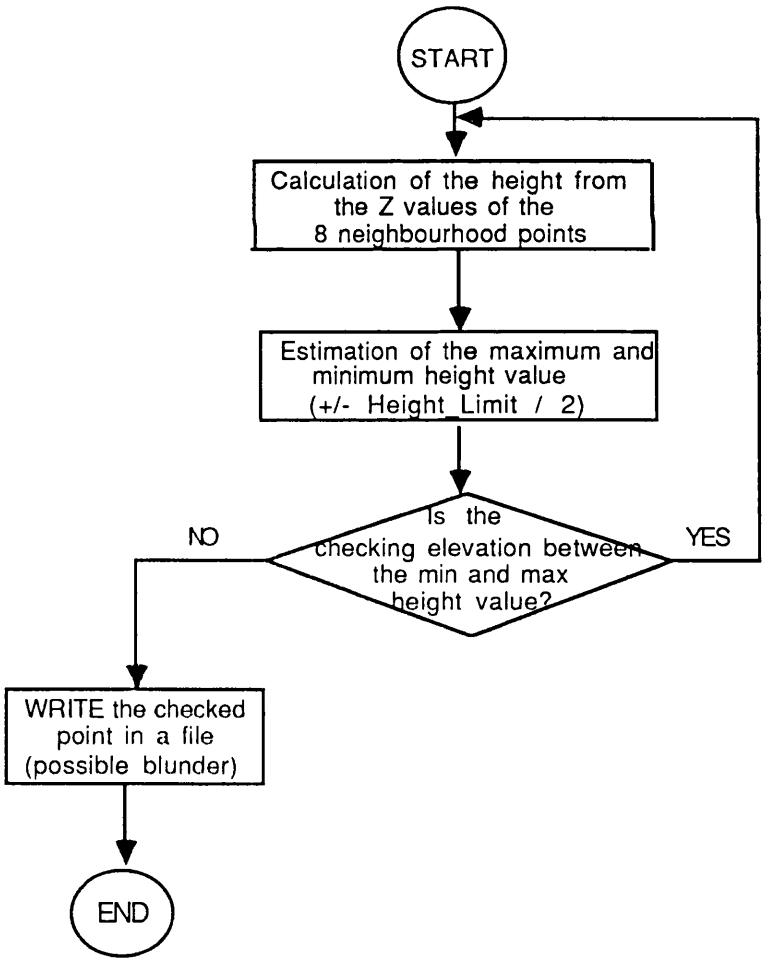

Figure D.3. PROCEDURE Check_Neighbourhoods1 flow-chart.

D.5. PROCEDURE Check_Neighbourhoods2.

The routine is applied to all the other slope categories (>10%). In this routine the point is tested again in relation to its neighbours. The checking procedure is the follows:

D.5.1. Estimation of the Calculated_Height_A and Calculated_Height_B which are the average of the 8 surrounding points, 4 directly and 4 calculated (see basic calculations in Ch_Heights estimation), for each point. This is the elevation average of the 8 surrounding closest neighbour points.

```
Calculated_Height_A[m,n] = (Check_Height[m-1,n-1] + Z[m-1,n] +
Check_Height[m-1,n+1] + Z[m,n+1] + Check_Height[m+1,n+1] + Z[m+1,n] +
Check_Height[m+1,n-1] + Z[m,n-1] )/ 8

Calculated_Height_B[m,n] = (Check_Height1[m-1,n-1] + Z[m-1,n] +
Check_Height1[m-1,n+1] + Z[m,n+1] + Check_Height1[m+1,n+1] + Z[m+1,n]
+ Check_Height1[m+1,n-1] + Z[m,n-1] )/ 8
```

D.5.2. Add in the Calculated_Height_A[m,n] and Calculated_Height_B[m,n] the quantity (2.7 * Height_Limit), (3σ). The Height_Limit has various values depending on the slopes.

```
Calculated_Height1_A[m,n] = Calculated_Height_A[m,n] + (2.7  * Height_Limit)
Calculated_Height1_A[m,n] = Calculated_Height_A[m,n] -  (2.7  * Height_Limit)
Calculated_Height1_B[m,n] = Calculated_Height_B[m,n] + (2.7  * Height_Limit)
Calculated_Height1_B[m,n] = Calculated_Height_B[m,n] - (2.7  * Height_Limit)
```

D.5.3. Comparison of the (Calculated_Height1_A and Calculated_Height2 _A) and the (Calculated_Height1_B and Calculated_Height2 _B) with the testing Z coordinate.

```
IF NOT (Z[m,n] <= Calculated_Height1_A[m,n] AND Z[m,n] >=
        Calculated_Height2_A[m,n]) THEN
IF NOT (Z[m,n] <= Calculated_Height1_B[m,n] AND Z[m,n] >=
        Calculated_Height2_B[m,n]) THEN
                WRITE the point as blunder in (Blun_File).
```

The Height_Limit again is chosen to be (2.7σ) in order to detect the medium and large blunders.

The Check_Neighbourhoods1 routine is applied in slopes up to 10%, because it requires less computing time. On the other hand it is less sensitive than the routine Check_Neighbourhoods2. If the relief is smooth the blunder detection procedure is easier and could be done through simple calculations as those applied in Check_Neighbourhoods1 routine.

The procedure Check_Neighbourhoods2 described in flow-chart form is shown in the figure D.4.

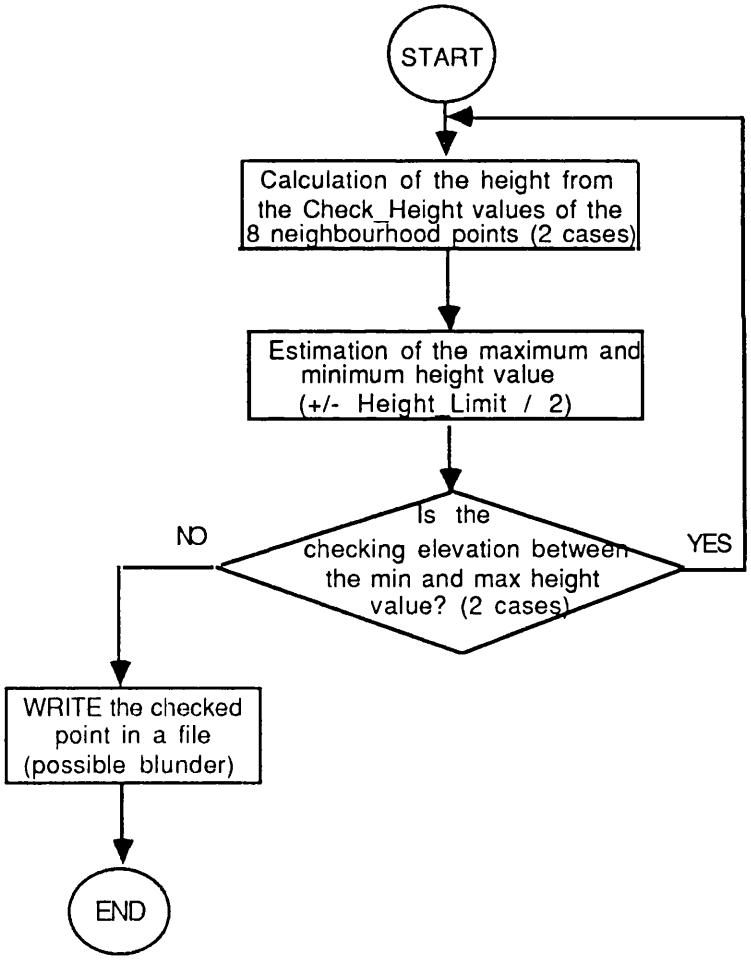

Figure D.4. PROCEDURE Check_Neighbourhoods2 flow-chart.

D.6. ROUTINE Heights_Check_and_test.

This routine examines the surrounding points (closer or distant neighbours) in relation to the point. If the examined point elevation is within certain limits the tested point is correct, otherwise the point with the suspicious elevation value and the surrounding neighbours are written to an output file as "suspicious" elevations for further examination.

The checks which take place are multiple and the tested point is examined with its neighbours in many combinations. The logic is that the erroneous tested point affects its neighbours by being involved in the local convolution (patch) calculations. On the other hand if the point is correct and the blunder is a surrounding point (one or more) it again involves calculations of the local convolution. The larger the number of combinations used the smaller is the effect of blunders in the calculation procedure.

The combinations which are used are the follows:

D.6.1. One tested point with 3 surrounding neighbours (4 cases).

D.6.2. One tested point with 5 surrounding neighbours (2 cases).

D.6.3. Two tested points with 6 surrounding neighbours (2 combinations).

D.6.4. One tested point with 8 surrounding neighbours.

D.6.5. Two tested points with 10 surrounding neighbours (2 combinations).

D.6.6. Four tested points with 12 surrounding neighbours.

The algorithm uses at the same time all the above combinations in order to trap the erroneous point(s).

The procedure Height_Check_and_Test described in flow-chart form is shown in the figure D.5.

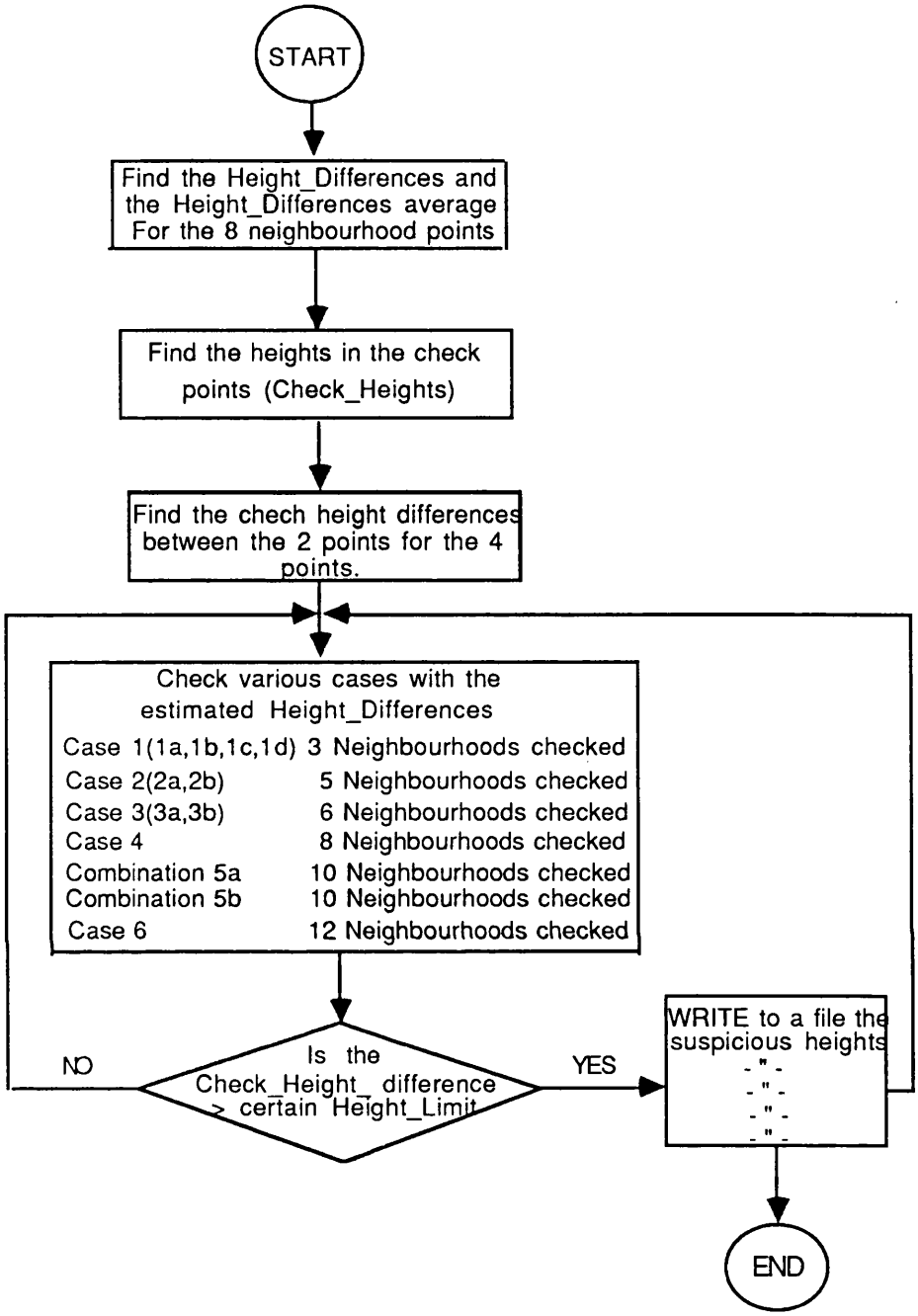

Figure D.5. Procedure Heights_Check_and_Test flow-chart.

The full description of the above operations and combinations is the following:

D.6.1. One tested point with 3 surrounding neighbours -4 cases - (figure D.6).

NOTE : Height_Limit = 2.7 * Height_Limit

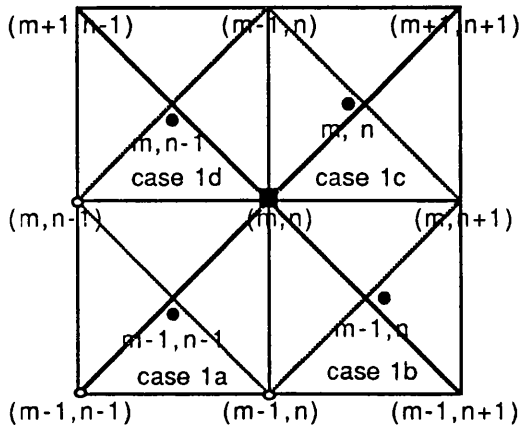

Figure D.6. One tested point with 3 surrounding neighbours (4 cases).

```
Case 1a.  IF (Check_Height_Dif[m-1,n-1] > Height_Limit*2) THEN WRITE(Sus_File Z1[m,n])
Case 1b.  IF (Check_Height_Dif[m-1,n]   > Height_Limit*2) THEN WRITE(Sus_File Z1[m,n])
Case 1c.  IF (Check_Height_Dif[m,n-1]   > Height_Limit*2) THEN WRITE(Sus_File Z1[m,n])
Case 1d.  IF (Check_Height_Dif[m,n]     > Height_Limit*2) THEN WRITE(Sus_File Z1[m,n])
```

D.6.2. One tested point with 5 surrounding neighbours -2 cases- (figure D.7).

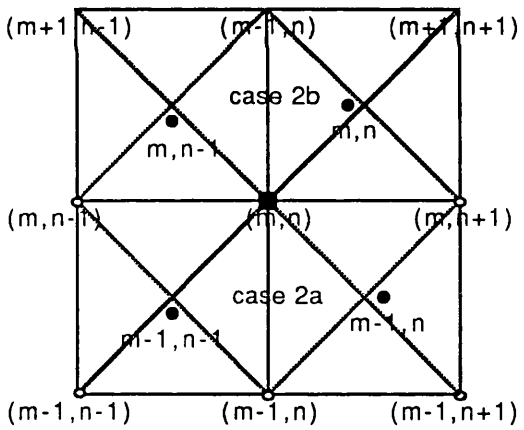

Figure D.7. One tested point with 5 surrounding neighbours (2 cases).

```
Case 2a. IF (((Check_Height_Dif[m-1,n-1] > Height_Limit ) AND
             (Check_height_Dif[m-1,n] > Height_Limit ))  THEN WRITE(Sus_File Z1[m,n])

Case 2b. IF (((Check_Height_Dif[m,n-1] > Height_Limit ) AND
             (Check_height_Dif[m,n] > Height_Limit ))  THEN WRITE(Sus_File Z1[m,n])
```

D.6.3. Two tested points with 6 surrounding neighbours -2 combinations - (figure D.8).

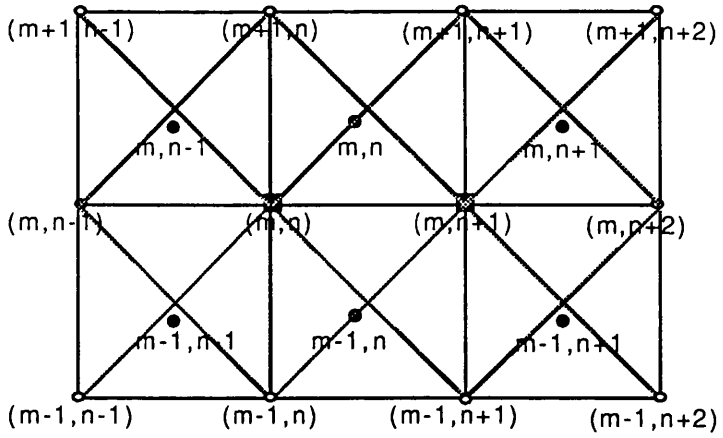

Figure D.8. Two tested points with 6 surrounding neighbours (2 combinations).

1st combination.

```
IF (((Check_Height_Dif[m-1,n-1]  > Height_Limit )AND
     (Check_Height_Dif[m-1,n] > Height_Limit )) OR
    ((Check_height_Dif[m-1,n]  > Height_Limit) AND
     (Check_Height_Dif[m-1,n+1] > Height_Limit))) THEN
       WRITE(Sus_File Z1[m,n], Z1[m,n+1])
```

2nd combination.

```
IF (((Check_Height_Dif[m,n-1]  > Height_Limit )AND
     (Check_Height_Dif[m,n] > Height_Limit )) OR
    ((Check_height_Dif[m,n]  > Height_Limit) AND
     (Check_Height_Dif[m,n+1] > Height_Limit))) THEN
       WRITE(Sus_File Z1[m,n], Z1[m,n+1])
```

D.6.4. One tested point with 8 surrounding neighbours (figure D.9).

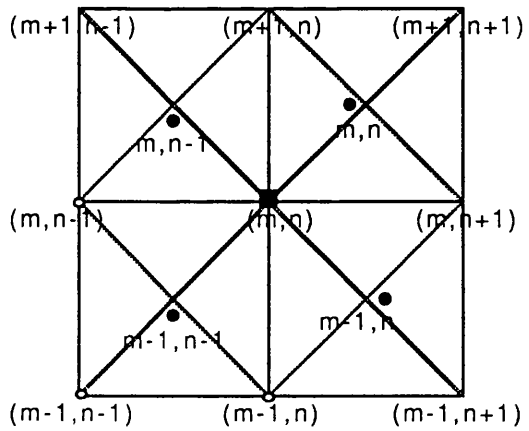

Figure D.9. One tested point with 8 surrounding neighbours.

```
IF (((Check_Height_Dif[m-1,n-1]  > Height_Limit / 2) AND
 (Check_height_Dif[m-1,n]   > Height_Limit / 2)) AND
 ((Check_Height_Dif[m,n+1]   > Height_Limit / 2) AND
    (Check_height_Dif[m,n]  > Height_Limit / 2))) THEN WRITE(Sus_File Z1[m,n])
```

D.6.5. Two tested points with 10 surrounding neighbours - 2 combinations - (figure D.10).

1st combination.

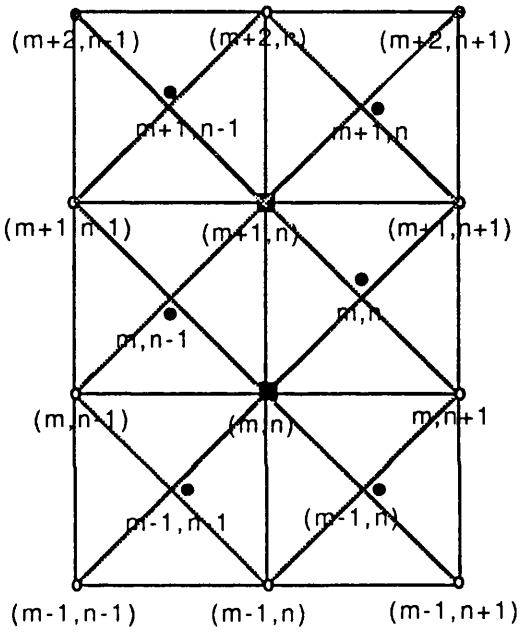

Figure D.10. Two tested points with 10 surrounding neighbours (first combination).

```
IF ((((Check_Height_Dif[m-1,n-1] > Height_Limit / 2) AND
    (Check_height_Dif[m-1,n] > Height_Limit / 2)) AND
     ((Check_Height_Dif[m,n-1] > Height_Limit / 2) AND
      (Check_height_Dif[m,n] > Height_Limit / 2))) OR
  (((Check_Height_Dif[m,n-1] > Height_Limit / 2) AND
    (Check_height_Dif[m,n] > Height_Limit / 2)) AND
     ((Check_Height_Dif[m+1,n-1] > Height_Limit / 2) AND
    (Check_height_Dif[m+1,n] > Height_Limit / 2)))) THEN
                    WRITE(Sus_File Z1[m,n], Z1[m+1,n])
```

2nd combination (figure D.11).

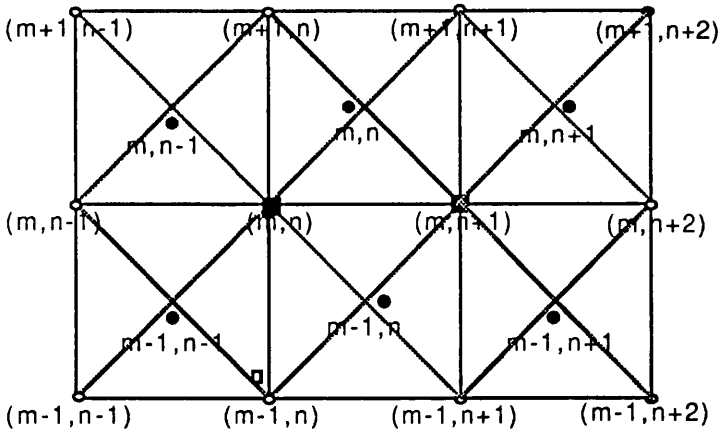

Figure D.11. Two tested points with 10 surrounding neighbours (second combination).

```
IF ( (((Check_Height_Dif[m-1,n-1] > Height_Limit / 2) AND
      (Check_height_Dif[m-1,n] > Height_Limit / 2)) AND
      ((Check_Height_Dif[m,n-1] > Height_Limit / 2) AND
      (Check_height_Dif[m,n] > Height_Limit / 2))) OR
    (((Check_Height_Dif[m-1,n] > Height_Limit / 2) AND
      (Check_height_Dif[m-1,n+1] > Height_Limit / 2)) AND
      ((Check_Height_Dif[m,n] > Height_Limit / 2) AND
      (Check_height_Dif[m,n+1] > Height_Limit / 2)))) THEN
                        WRITE(Sus_File Z1[m,n], Z1[m,n+1])
```

D.6.6. Four tested points with 12 surrounding neighbours (figure D.12).

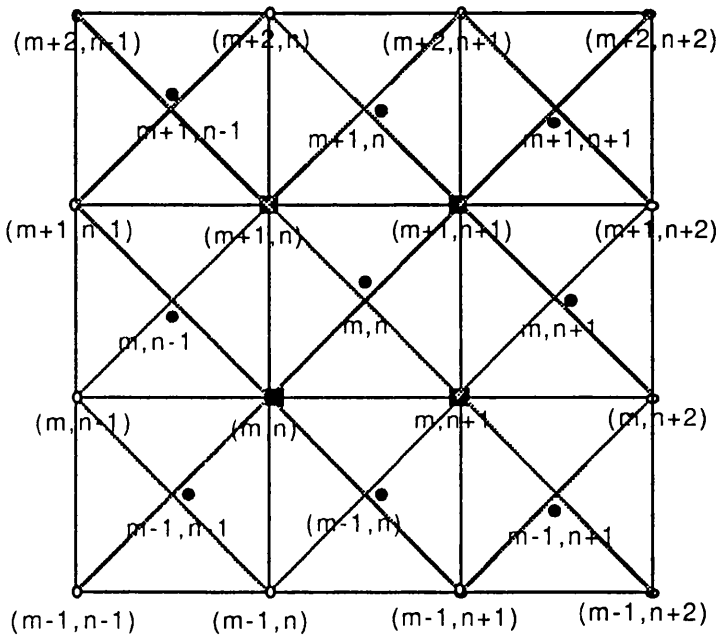

Figure D.12. Four tested points with 12 surrounding neighbours.

```
IF  ( (((Check_Height_Dif[m-1,n-1] > Height_Limit / 2) AND
          (Check_height_Dif[m-1,n] > Height_Limit / 2)) AND
        ((Check_Height_Dif[m,n-1] > Height_Limit / 2) AND
         (Check_height_Dif[m,n] > Height_Limit / 2))) OR
          (((Check_Height_Dif[m-1,n] > Height_Limit / 2) AND
            (Check_height_Dif[m-1,n+1] > Height_Limit / 2)) AND
        ((Check_Height_Dif[m,n] > Height_Limit / 2) AND
         (Check_height_Dif[m,n+1] > Height_Limit / 2))) AND
          (((Check_Height_Dif[m,n-1] > Height_Limit / 2) AND
            (Check_height_Dif[m,n] > Height_Limit / 2)) AND
         ((Check_Height_Dif[m+1,n-1] > Height_Limit / 2) AND
          (Check_height_Dif[m+1,n] > Height_Limit / 2))) OR
          (((Check_Height_Dif[m,n] > Height_Limit / 2) AND
            (Check_height_Dif[m,n+1] > Height_Limit / 2)) AND
        ((Check_Height_Dif[m+1,n] > Height_Limit / 2) AND
       (Check_height_Dif[m+1,n+1] > Height_Limit / 2))))  THEN
              WRITE(Sus_File Z1[m,n], Z1[m,n+1],Z1[m+1,n],Z1[m+1,n+1])
```

D.7. PROCEDURE Height_Limits_Application.

This routine allocates the appropriate Height_Limits according to the slopes.

The changing of the slope as a criterion in applying the height limits is crucial in terms that when a blunder involves it affects the changing of the slope. That means that if the slope becomes larger a larger height limit is going to be applied. This becomes against (contradictory) the blunder detection procedure and it is one disadvantage of using the slopes in applying the Height_Limits. On the other hand it is well known that the standard deviation in heights becomes larger with the steep and rough terrain. Therefore the slope factor in the application of the Height_Limit should be applied.

In this case it is decided in the Height_Limits application, instead of using the single slope, estimated from the elevation difference and the distance apart between two points, to use the average of the summation between the two estimated slopes (defined by 3 points, in which the tested point lies between the two others).

The Height_Limits are introduced by the user. These Height_Limit values would have depended on image source, scale, terrain roughness, operator ability as well as base/height ratio. The Height_Limits are estimated for a SPOT image as follows:

During the data capture procedure samples from four blocks were remeasured. This reobservation of the same data, was carried out to test the observer's ability to consistently measure height at the same planimetric position. From the two measured sets the height differences were estimated. Statistical analysis of the 1958 duplicated points are given in table 5.2. The estimated values were used to draw the diagram of standard deviation against slope (figure 5.7). From this diagram the height limits for the SPOT images according to the terrain classification were estimated (Table 5.3).

The routine finally writes the applied Height_Limit and the corresponding estimated slope between the examined point and its neighbours in a separate output file (Limits_File).

APPENDIX E.

The data merging program.

(Program to merge data from two sources).

E. Program to merge data from two sources. Algorithm description.

A Pascal program was written in order to merge the data captured from different sources such as aerial photography and SPOT (see § 6.4.2).

The program gives as output (see § 6.4.2.2) the following output files in two different ways of processing:

1. First way of merging of the two sources of data :

1.a. The second source (SPOT) processed data output file in which the second source data are equivalent in terms of reliability to the first source data. The first source (aerial photography) initial data file and the resulting second source data file can be used as input in the DTMCREATE software.

1.b. The superfluous second source data which lie outside the DEM block defined by the first source.

2. Second way of merging of the two sources of data :

2.a. The processed first source data output file by taking into account the second source data (one output file produced from the two input files).

2.b. The superfluous second source data, which lie outside the first source defined block, as in 1.b above.

Note : The output superfluous second source data file (§ 2.b) is not active in the program because it is a repetition.

E.1. PROCEDURE Read_Rewrite.

The aim of this procedure is to read the first source data from a sequential file and rearrange the data in rows, columns as they were during the collection procedure, as Digital Elevation Matrix data rows by columns (see appendix B).

E.2. PROCEDURE Calculate_the_Azimuths.

The purpose of the procedure is to estimate the azimuth and so define in which quadrant the data block (see appendix B).

E.3. PROCEDURE Estimate_Source2_Cell.

The aim of this procedure is to find in which cell of the first source defined elevation matrix defined by the first source lies the point from the second source.

Declarations:

x2, y2	:	Second source point coords.
X_Origin, Y_Origin	:	First source DEM left bottom corner origin.
Grid_Interval	:	First source DEM grid interval.

```
Row_Cell[q]    = TRUNC(( |y2[q] - Y_Origin| ) / Grid_Interval ) + 1
Column_Cell[q] = TRUNC(( |x2[q] - X_Origin| ) / Grid_Interval ) + 1
```

E.4. PROCEDURE Centroids_Calculation.

The purpose of the procedure is to estimate the centroid coordinates of each by the elevation matrix defined cells.

Declarations:

x1, y1	:	First source point coords.
x2, y2	:	Second source point coordinates.
x3, y3	:	Centroid coordinates.

E.4.1. Calculation of the length.

$$Length = \left[(2 * (Grid\_Interval / 2))^2 \right]^{1/2}$$

E.4.2. Calculation of the Centroid coordinates.

```
x3[m,n] = x1[m,n[ + ( Length/2 * SIN(Azim[m,n]))
y3[m,n] = y1[m,n[ + ( Length/2 * COS(Azim[m,n]))
```

E.5. PROCEDURE Read_Data_Second_Source.

It reads the data from the input second source data file.

E.6. PROCEDURE Sec_Pnt_Lie_Cell_Simul_Height.

The aim of this procedure is to calculate the height differences between the second source heights and the four first source elevation neighbours in respect to the defined digital elevation matrix quadrant.

This procedure includes two other procedures.

E.6.1. PROCEDURE Height_Calculations.

E.6.2. PROCEDURE Case_Quadrants.

Declarations:

x1, y1, z1	:	First source point coords.
x2, y2, z2	:	Second source point coordinates
x3, y3	:	Centroid coordinates.
z3	:	Processed heights (centroid z value).
Weight1	:	First source data weight.
Weight2	:	Second source data weight.

The weights depend on the source, the data capture method and implementation, the method of calculation etc. In this work because two sources are used the first source (aerial photography) was assumed to have Weight1 = 1.0. The second source (SPOT data), after extensive statistical analysis was estimated to have Weight2 = 0.10 (see § 5.5.3).

E.6.1. PROCEDURE Height_Calculations.

The aim of the procedure is to calculate the second source height value. In this procedure are applied the weights in order to estimate the centroid z coordinate (simulated second source height value).

E.6.1.1. Calculation of the Distances of the four first source neighbour points:

```
Distance[m,n] = SQRT(SQR(x2[q]- x1[m,n]) + SQR(y2[q] - y1[m,n]))
```

E.6.1.2. Calculation of the height average of the first source (4 neighbour points):

```
Average = (z1[m,n] + z1[m,n+1] + z1[m+1,n+1] + z1[m+1,n]) / 4
```

E.6.1.3. Calculation of the centroid z coordinate:

```
z3[m,n] = (( Weight1 * Average) / Length) + (Weight2 * z2 / Distance)) /
                    ((Weight1  / Length) + ( Weight2 / Distance))
```

E.6.2. PROCEDURE Case_Quadrants.

This procedure defines the digital elevation matrix quadrant. It is also checks whether any second source point lies in any cell of the first source elevation matrix.

STEPS:

E.6.2.1. Calls the PROCEDURE Height_Calculations.

E.6.2.2. Defines and allocates the first source elevation matrix through a CASE statement

E.6.2.3. Checks which of the second source points lie in the first source defined elevation matrix and in which cell.

IF the second source point lies in the first source defined matrix THEN
WRITE to the output file :
Number_of_Row, Number_of_Column, Height_Difference
ELSE WRITE to Superfluous_Points_File : Point_Number2[q].

E.7. PROCEDURE Processing_First_Source_Data.

This procedure merge the second source data (less reliable), with the first source data (more reliable), in order that the second source data be equivalent in terms of reliability with the first source data.

This procedure includes two other procedures.

E.7.1. PROCEDURE Processed_ Heights.

E.7.2. PROCEDURE Average_Heights_Estimation.

The main part of the procedure Processing_First_Source_Data, allocates the DEM source grid according to the quadrant. Furthermore it calls the procedure Processed_Heights and finally the procedure Average_Heights_Estimation.

E.7.1. PROCEDURE Processed_Heights.

Declarations:

Points_Length[s1,m,n]	}	
Points_Length[s2,m,n+1]	}	The distance between the second
Points_Length[s3,m+1,n+1]	}	source data point and the four first
Points_Length[s4,m+1,n]	}	source neighbour points.
Proces_z1[s1,m,n]	}	
Proces_z1[s2,m,n+1]	}	The new z values for the first data
Proces_z1[s3,m+1,n+1]	}	source taking into account the second
Proces_z1[s4,m+1,n]	}	source z values.

s1 = 1.

$$Points\_Length[s1,m,n] = \left((x2[q] - x1[m,n])^2 + (y2[q] - y1[m,n])^2\right)^{1/2}$$

IF Points_Length[s1,m,n] = 0, that means the second source point lie exactly in the same position as the first source data point (just in case) THEN

Proces_z1[s1,m,n] = Weight1 * z1[m,n] + Weight2 * z2[q] ELSE

Proces_z1[s1,m,n] = [((Weight1 * z1[m,n] + Weight2 * z2[q])) / Points_length[s1,m,n]] / ((Weight1 + Weight2) / Points_Length[s1,m,n])

s2 = 2.

$$Points\_Length[s2,m,n+1] = \left((x2[q] - x1[m,n+1])^2 + (y2[q] - y1[m,n+1])^2\right)^{1/2}$$

IF Points_Length[s2,m,n+1] = 0, that means the second source point lie exactly in the same position as the first source data point (just in case) THEN

Proces_z1[s2,m,n+1] = Weight1 * z1[m,n+1] + Weight2 * z2[q] ELSE

Proces_z1[s2,m,n+1] = [((Weight1 * z1[m,n+1] + Weight2 * z2[q])) / Points_length[s2,m,n+1]] / ((Weight1 + Weight2) / Points_Length[s2,m,n+1])

s3 = 3.

$$Points\_Length[s3,m+1,n+1] = \left((x2[q] - x1[m+1,n+1])^2 + (y2[q] - y1[m+1,n+1])^2\right)^{1/2}$$

IF Points_Length[s3,m,n+1] = 0, that means the second source point lie exactly in the same position as the first source data point (just in case) THEN

Proces_z1[s3,m+1,n+1] = Weight1 * z1[m+1,n+1] + Weight2 * z2[q] ELSE

Proces_z1[s3,m,n+1] = [((Weight1 * z1[m+1,n+1] + Weight2 * z2[q])) / Points_length[s3,m+1,n+1]] / ((Weight1 + Weight2) / Points_Length[s3,m+1,n+1])

s4 = 4.

$$Points\_Length[s4,m+1,n] = \left((x2[q] - x1[m+1,n])^2 + (y2[q] - y1[m+1,n])^2\right)^{1/2}$$

IF Points_Length[s4,m+1,n] = 0, that means the second source point lie exactly in the same position as the first source data point (just in case) THEN

Proces_z1[s4,m+1,n] = Weight1 * z1[m+1,n] + Weight2 * z2[q] ELSE

Proces_z1[s4,m+1,n] = [((Weight1 * z1[m+1,n] + Weight2 * z2[q])) / Points_length[s4,m+1,n]] / ((Weight1 + Weight2) / Points_Length[s4,m+1,n])

E.7.2. PROCEDURE Average_Heights_Estimation.

This procedure treats the case whether a second source data point in each first source cell lies.

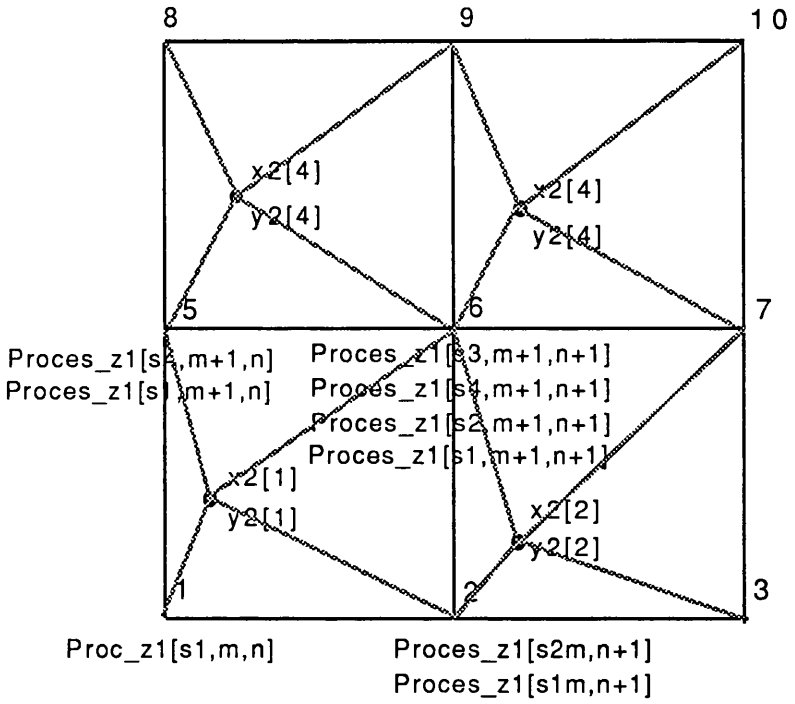

Figure E.1. Example of a first source point affected by four second source neighbouring points.

Furthermore if a point does not lie in a cell the program skips this cell. The situation is complicated because the number of Proc_z1 is varied according to whether or not a point lies in the neighbour cell, as we can see in figures E.2 and E3.

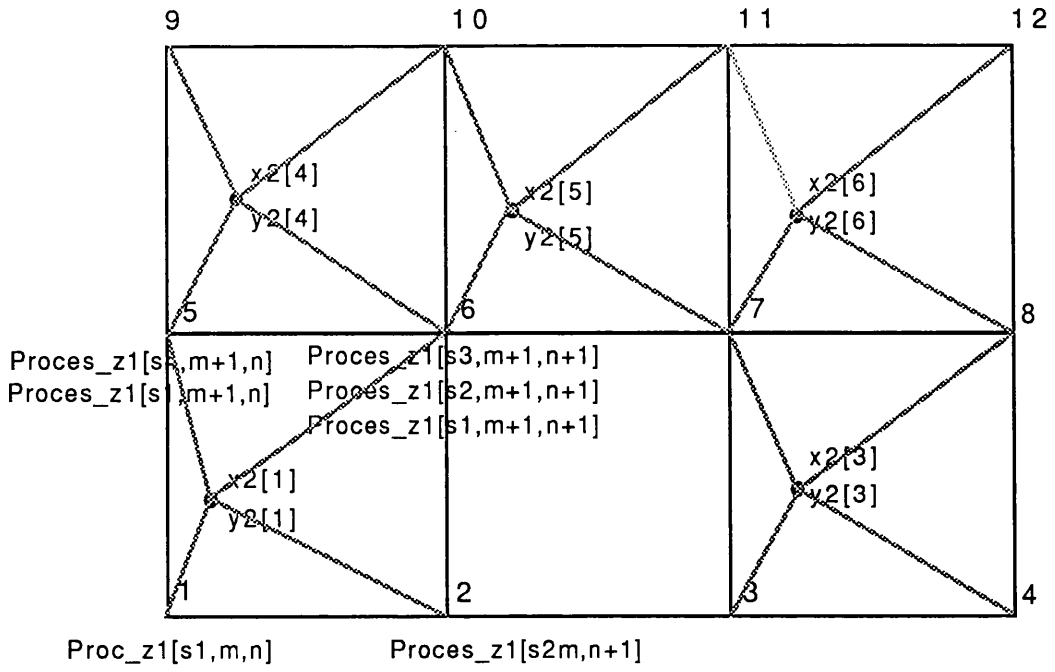

Figure E.2. Example of a first source point affected by three second source neighbouring points.

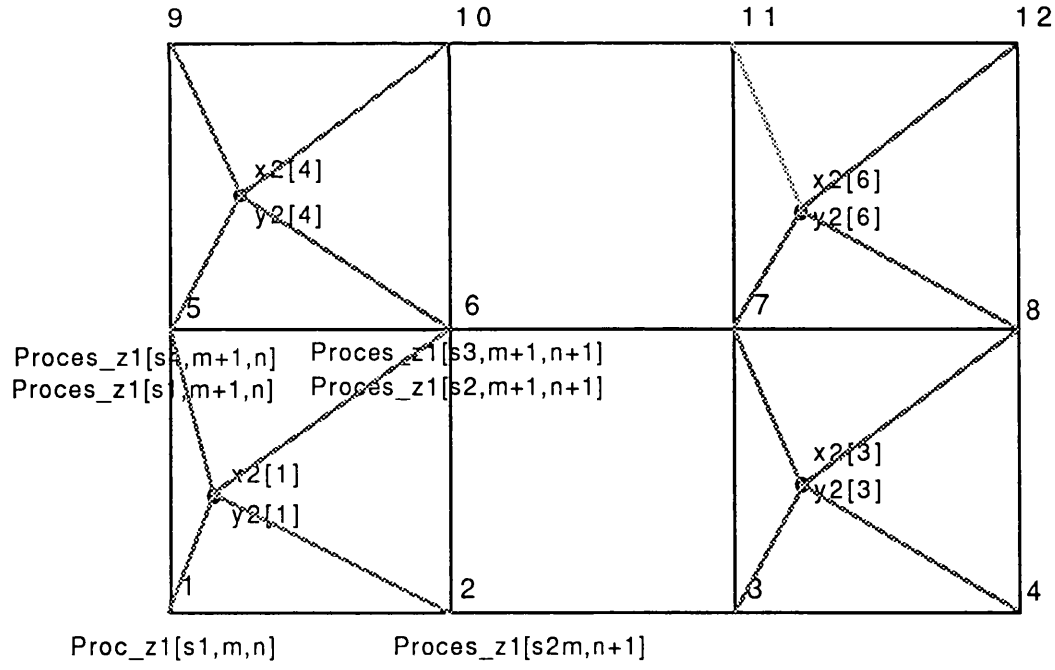

Figure E.3. Example of a first source point affected by two second source neighbouring points.

The first source data are captured in 30 m grid spacing, while the second source data are captured in 100 m grid spacing. That means that in every 3.33 cells of the aerial photography data matrix, lies a SPOT point.

All the above cases use the procedure Average_Heights_Estimation which calculates the averages according to the number of Proces_z1 which appears in every case.

APPENDIX F.

The data skipping program.

F. The elevation data skipping program. Algorithm description.

A Pascal program was written to skip data from a dense data file in order to be able to produce data with a different grid interval.

The program asks the user for:

1. The input data file name.
2. The output data file name.
3. The total number of points.
4. The number of lines which the user wants to skip.

F.1. PROCEDURE Give_Prompts.

Give the prompts to the user to specify the input and output filenames and the other mentioned input values.

F.2. PROCEDURE Read_Input_File.

The aim of this procedure is to read the input data from a sequential file (Point_Number, x,y,z coords).

F.3. PROCEDURE Write_Output_File.

The purpose of the procedure is to skip the lines according to the user specification and write the new derived data to the output file.

Note: One restriction of this simple algorithm is that it will work only when the output number of rows and number of columns is an integer multiple of the input number of rows, columns and the output grid interval is an integer multiple of the input grid interval. This is possible when the modulo reduction (the remainder left by integer division) of the number of rows and the number columns of the data by the number of points (lines) to be skipped is zero. This is necessary in order to have resulting data in a normal grid.

APPENDIX G

The IFF structure.

G. IFF structure.

This section is not intended to cover all the entries in IFF structure but to identify the most important entries by giving a brief information for each entry. The order in which IFF entries occur within each level is given below. An entry printed in bold type is obligatory. The entries are presented in order except if otherwise refer. Bold type entries are used in the creation of the IFF text form files transferred from count number string of spatial coordinates format (output from the analytical plotter) through a written transferring Pascal program (see § 6.6.6).

1. Entries at file level.

Coordinate RAnge - RA - records the maximum extent of the data in the IFF file (X-min, X-max, Y-min, Y-max).

HIstory - HI - records statistics each time IFF file is updated(date, time, username, program, function, elapsed, cpu, status).

Sector Header SH - is from necessity a complex entry. It contains information defining the position and size of the sectors into which the data are divided.

In addition it references information which is not directly accessible to the user (IFF junction structure).

End Job - EJ - End of data (file) marker (does not have any contents).

2. Entries at Map Level.

Map Header - MH - user specific data about the IFF file - map specific information -(eg which format of data is present).

Map Descriptor - MD - holds map projection information (Map Area MA, Grid Representation GR, SCale SC, Projection Status PS and Auxiliary Grid AG.

End Map marker - EM - last entry of a map flagging the end (does not have any contents).

3. Entries at section Level.

New Section identification - NS -is used to flag a new digitising session.

Cubic Coefficients for coordinate transformation - CC.

Corner points for coordinate transformation - CP - four points in the order NW, SW, SE and NE.

4. Entry at Layer Level.

New Overlay (layer) - NO - includes layer number and status.

End Overlay - EO - End overlay marker.

There is no specific order for the following entries, which historically occur within layers but outsides features. They are regarded as obsolete.

Transmitted Comment - TC - a text string is used to label the following feature.

CHaracter data - CH - is the literal character entry.

Character Size - CS - it contains two identifying numbers (the character height and character spacing).

Symbol Select - SS - is the numeric identifier of a symbol within a symbol library.

Symbol Library select - SL - is the numeric identifier of a symbol library.

5. Entries at Feature Level.

Ancillary Code - AC - it can be an optional text field, or an integer, or a real value which does not have text.

start of New Feature - NF - starts a new feature , it contains two identifying numbers (the feature serial number and the feature internal sequence number).

Feature Status - FS - contains data which describes the feature containing it (feature code, flag data, feature type or process code, ephemeral used independent data).

ROtation entry - RO - angle at which an oriented symbol or a text is to be drawn.

Text height / line THickness entry - TH - line thickness or text size (ie. 0 when follow X,Y,Z coords).

Text Status entry - TS -introduces a text component, and contains data which describes the text following it.

TeXt entry - TX - holds the text for a text feature.

2 dimensional point string entry - ST - (planimetric coordinates X,Y).

3 dimensional point string entry - ZS - (spatial coordinates X,Y and Z).

Coordinate Block - CB - entry which allows the description of other per-point attributes in addition to the X, Y, Z coords).

End of Feature - EF - entry flags the end of a feature, and balances the NF entry at the start of the feature.

The following entries can occur anywhere in a file:

VOid - VO- is used to replace a series of deleted IFF entries. Since it is not possible to 'compress' an IFF file, a deleted entry or series of entries is overwritten with a void area of the requisite size.

Junction Block - JB -defines a series of junctions (IFF junction structure).

Junction Pointer - JP - is a pointer back to a JB entry (IFF junction structure).

APPENDIX H.

Software used for DEM creation and display.

H. Software used for DEM creation and display.

The software for DEM creation and display (in the Department of Photogrammetry and Surveying UCL) was produced by Laser-Scan Laboratories Ltd running on a VAX/VMS microcomputer. The main software categories, for data preparation, creation, manipulation and viewing of DEMs , are as follows:

H.1. DTMPREPARE package.
- H.1.1. IFROMTEXT module.
- H.1.2. ITOTEXT module.

H.2. DTMCREATE and displaying package.
- H.2.1. DEM creation.
  - H.2.1.1. TRIANG module.
  - H.2.1.2. TRIDER module.
  - H.2.1.3. TRIGRID module.
- H.2.2. 3-Dimensional view
  - H.2.2.1. DTIVIEW module (isometrics, perspectives).
- H.2.3. Contour generation software.
  - H.2.3.1. DTICONTOUR module.
- H.2.4. Used Contour display software.
  - H.2.4.1. LITES2 package.
  - H.2.4.2. ROVER module.

The DTMCREATE package and output devices are shown in the figure H.1.

H.1. The DTMPREPARE package.

Prepares the Laser-Scan IFF (Internal Feature Format) vector data for DEM creation using the package DTMCREATE.

H.1.1. The IFROMTEXT module.

Transfers IFF text files, in ASCII form (*.TEXT files), to IFF format in binary form (*.IFF files), in order to be in acceptable form for processing by the

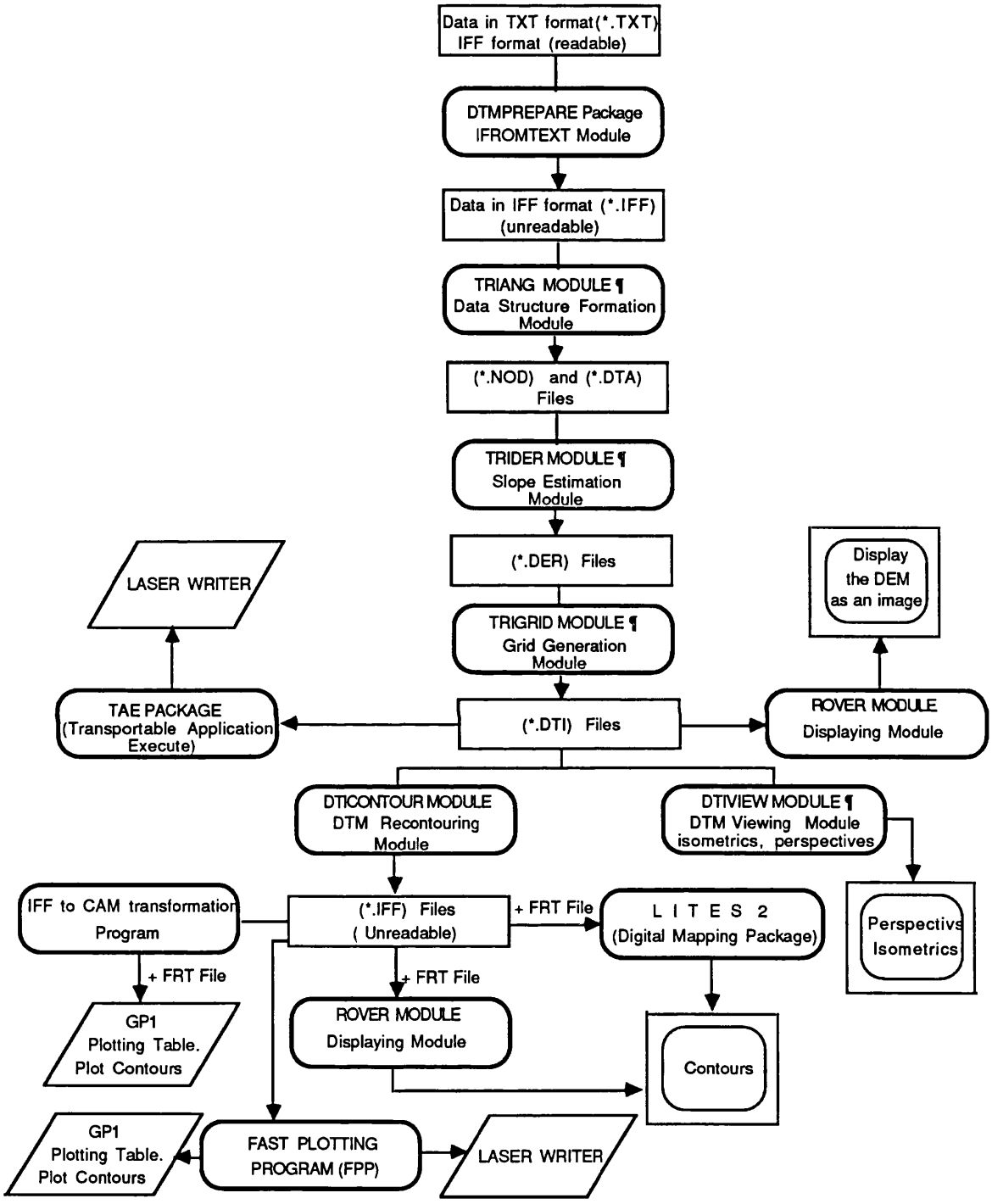

Figure H.1. Packages for DEM creation and output devices at UCL.

DTMCREATE package.

H.1.2. The ITOTEXT module.

Transfers IFF format files, in binary form (*.IFF files), to IFF text files in ASCII form (*.TXT). An output file in binary form can be for example an output file from DTICONTOUR module.

H.2. The DTMCREATE and displaying package.

DTMCREATE is a semi-interactive DEM package, which provides tools for production, validation, manipulation and viewing of matrix data, particularly of elevation (height) data, derived from IFF vector data.

H.2.1. DEM creation.

H.2.1.1. The TRIANG Module.

Is the main data structuring formation module in the DTMCREATE package. In the TRIANG a TIN (Triangular Irregular Network) is produced. TINs have the properties of stability, equilateralness (the set of triangles are as equilateral as possible with minimum line strength) and non intersection.

The purpose of TRIANG is to extract heighted data from IFF (Internal Feature Format) files and existing DTI (Digital Terrain Image) files, to produce a triangular data structure. From the neighbours surrounding the point, a system of triangles can be built (McGullah, 1980) which uniquely segment the map area using the Delauney (1934) Triangulation method (carried out on input data files in IFF format). This provides a structure that relates every point with its Thiessen neighbours (Brassel, 1979) in the complete data set. The Thiessen polygon formation is carried out by choosing an arbitrary starting point and, where necessary creating, a set of imaginary guaranteed neighbours outside the data to be polygonised. The triangulation is optimum in the sense that it has the most equilateral set of triangles possible for the data set under consideration. This does

not necessarily imply that locally the triangles will be very equilateral. Spot heights, contours and structural features are output to two files. The output file *.DTA holds data in scaled integer form and *.NOD data structure itself with a list of nodes and Thiessen neighbours.

The module offers the choice between an idealised Delaunay triangulation (more suited to large scale geological surface estimation) or constrained Delaunay triangulation for complex geological applications, such as contour interpolation.

In the triangulation procedure with the TRIANG module, extrapolation techniques are needed so the triangulation can be extended over the whole area. This is achieved by assigning the 'plausible' height values to imaginary points placed at the perimeter of the region. Poor choice of points lead to poor relief configuration at a later stage and poor edge matching.

When initially triangulated these points have locations but no z values.

TRIANG offers the user four different interpolation options to estimate suitable heights for these points:

1. FIXED option . This allows the surface to decline to some fixed value at all the way around the triangulation area at some distance from the main triangular grid coverage. The user specifies the Z value. TRIANG inserts the specified value and a zero partial derivative at each imaginary point. By the edge of the triangulation area the surface will be a horizontal plane with the desired surface height. This option is suitable if the edges of the area are all at the same level (sea level).

2. TREND option applies a linear trend surface fitted through all the data points in the interpolation area. The derivatives of the imaginary points will reflect the general trend of relief in the triangulation area. So if there is a trend of decreasing height in a certain direction then this trend will be reflected in the values assigned to the imaginary points. This option is the default as it is the 'safe option'.

3. BOX. A distance-weighted interpolation is employed based on points which fall in an 'expanding box' search. The box expands outwards from the imaginary point until 'sufficient' points, defined by a threshold value, have been included in the interpolation function. The function can be specified as : weighted, linear, quadratic, or quartic which determines the order of the curve to be fitted in the interpolation process.

4. SHELL. This option uses a similar interpolation function but the number of points integrated in the interpolation procedure depends upon the Thiessen neighbour shells. The first shell consists of first shell nearest neighbours. Three shells are generally sufficient in this interpolation.

The BOX method is more suited to randomly distributed points, like spot heights, and sets a distance limit on points to be included in the interpolation. The SHELL method seems to be appropriate where points are more evenly distributed.

At the triangulation stage it is also possible to introduce structural features like breaklines and cliffs, river- or ridge-strings.

The data used in the project consisted mainly of spot heights, captured in a regular pattern (grid) with pre-specified grid interval. The interpolation option which is chosen to assign heights to the created imaginary points, is the BOX option with the function QUARTIC (see commands used in the project).

H.2.1.2. The TRIDER Module.

Slope derivative estimation module. It takes the *.DTA and *.NOD files from TRIANG generated Thiessen neighbour node data estimation, or edited output from TRIEDIT and calculates the slope derivatives at the nodes, (data points created in the triangulation), to allow more accurate interpolation at the gridding stage. The derivatives are used in some interpolation options to give a strong fit. It outputs to a *.DER file. TRIDER is also used to provide z-values for the imaginary points generated around the edge of the triangulation by TRIANG.

H.2.1.3. The TRIGRID Module.

The actual grid generation module. It takes as input the triangulation created by TRIANG, node and data files (*.DTA, *.NOD files), or edited output from TRIEDIT together with slope derivatives and the imaginary point information file produced by TRIDER (*.DER file) and maps the triangulation onto a user specified grid (the user can produce a grid at different resolutions). Before the process of grid creation (initialised by a FILEIN command) TRIGRID allows the user to modify parameters that will control the final appearance of the model depending on the input data type and the desired output resolution.

TRIGRID offers two types of interpolation from the triangular form to the DEM grid: an option using linear 'patch' techniques, or a smooth 'patch' interpolation (patch, because the interpolation takes place in small area at a time).

Smooth patch estimation tends to give a more rounded smooth appearance to a DEM surface than given by linear facets. If smooth patch interpolation is selected, individual triangle interpolation limits are applied. The smooth patch option fits a mathematical surface to each triangle using the partial derivatives and the vertice values. The aim of a smooth patch option is to ensure both a continuous surface and at least continuous first order derivatives. This option was applied in the interpolation of SPOT data.

Linear facet interpolation, by definition, does not need to apply interpolation as interpolation is restricted to the triangle facet plane. Grid heights are estimated using linear interpolation across the triangle facet planes. The linear approach has the advantage that it is faster and does not produce values outside those at the vertices of the triangle. It is appropriate as a means of initial check viewing or in cases where the surface is particularly well defined by spot heights.

Many different size grids can be generated from a single TIN. Both the area to be covered by the final DEM and the number of grid squares it contains, ie. the resolution, must be specified. The resolution of the DEM should locally be made to match the density of the points. It is pointless to generate a grid with a resolution much finer than the source of triangular grid.

The processing data is stored in a *.DTI file. The grid area may fully or partially cover the area of triangulation. TRIGRID offers 3 DTI data types: WORD LONGWORD and REAL. By default a *.DTI file type WORD (16 bit integer post values) is generated. It also offers 3 DTI header types: TED4, UHL1 and LSLA. By default the DTI file is given the LSLA type header. The LSLA type DTI header contains only the matrix X and Y extent, Z range and the X and Y grid interval.

H.2.2. 3-D views.

Display techniques enable a quick check to be made on DEM correctness or existence of blunders. Moreover the 3-D views are very useful for illustration and communication with both persons familiar with the subject and others.

H.2.2.1. The DTIVIEW Module.

Displays part or all of *.DTI file on the screen as an isometric or perspective view for validation or display purposes.

Once the output data file is in *.DTI format a Laser writer output is possible through the TAE software (Transportable Application Executive).

Once the grid has been calculated the array of points are written out to a so-called 'MIKE' type DTI files, which are compatible with the DEM viewing module DTIVIEW, which represents by wire frame 3-D isometric and perspective views. The 3-D views are based on the projection of height profiles onto the picture plane by a variety of oblique transformations.

DTIVIEW has the facility to superimpose contours onto the isometric display which has been produced from spot heights.

Isometric views.

The isometric projection, which is the common form of the parallel or orthographic projection is used. The image of each point is specified by a perpendicular line to the picture plane from the point.

Perspective views.

In the perspective view parallel lines project as converging lines in most cases. Image points on the picture plane are fixed by a 'line of sight' from each object point (X, Y, Z) to converge to a central focus , or view-point on the opposite side of the picture plane.

H.2.3. Contour generation software.

H.2.3.1. The DTICONTOUR Module.

DTICONTOUR is one module of the TVES (Terrain Visualisation and Exploitation Package). The TVES package is an advanced DEM manipulation, validation and editing package. It is a Bilinear hardcopy contouring module. It creates and smooths contours, which are generated via a triangular or rectangular grid, by curve fitting, using linear interpolation techniques. Contour smoothing may be optionally applied using a least squares filter.

The triangle is used as the basic data structure, which has the advantage that there can be no ambiguity as to where a contour goes, because of the fact that a contour entering a triangle must also leave it. It is essential by using the DTICONTOUR options to ensure that the contour interval is specified relative to the target measurement system. The basic method consists firstly of systematically scanning the boundary edges of the DTI in an anticlockwise manner for the start of the contour. DTICONTOUR then follows the contour throughout the data window and finds the points at which the contour crosses a DTI row or column and the row and column diagonals, until it hits the boundary again. This is repeated for each of the 'open' contours at this height. The interior of the DTI array is then scanned to see if there are any 'closed' contours of this height and these are followed as for the 'open' ones.

DTICONTOUR takes as input the data created by TRIGRID (*.DTI file). The processed contour is output to an *.IFF file, for viewing in the LITES2 package, the Module ROVER , or the Kern GP1 plotting table for off line plotting. Off line plotting on the GP1 can be done in two ways:

1. Passing the IFF file through the IFFTOKERN.FOR program + FRT file (Feature Representation Table), in order to transfer from IFF format to Kern CAM format.

2. Passing the IFF file through the FPP (Fast Plotting Package) + FRT file.

Once the output data file is in *.IFF format a Laser Writer output is possible through FPP (Fast Plotting Package) + FRT file.

In this project contour maps at scale 1:25,000 and 1:50,000 from the two sources were produced in 20 m grid interval. The contour smoothing facility is not used because the main goal was to produce interpolated angular contours rather than smoothed contours. Smoothed contours look better but they have the drawback of additional errors which involve during the smoothing procedure.

H.2.4. The contour display software.

H.2.4.1. The LITES2 package.

Is a digital mapping package, but it can be used in order to display the contours derived by the DTICONTOUR module from interpolated heights. Output data from DTICONTOUR is in IFF format which is the only format accepted by LITES2.

H.2.4.2. The ROVER Module.

ROVER is one nodule of the TVES package. It is a display module for data validation and visualisation. It displays both grid based and vector geographic data (combined raster and vector data). It reads the raster or grid information from a *.DTI file and represents the areas in the same form. In that representation the third dimension (height information) appears in a different colour. The ROVER module can be used to display the *.IFF file created by the DTICONTOUR or *.DTI file created by the TRIGRID module, etc.

H.3. List of DTMCREATE and displaying commands used in the project.

TRIANG module. ! Triangulation structuring Module.

```
TRIANG
ENABLE DIAGNOSTICS                ! Enables diagnostic printout.
WINDOW  xmin ymin  xmax ymax      ! Limits of the area to be
                                    triangulated.
ZLIMITS  Zmin Zmax                ! Approximate min and max z
                                    values in the input data file(s).
                                  ! The following commands have
                                    significance when random data
                                    are used.
ASSIGN BREAKLINE_LAYER 161
ASSIGN CLOSED_CLIFF_LAYER 27
ASSIGN RIVER_LAYER 64
ASSIGN RIVER_FC 64
ASSIGN CLOSED_CLIFF_FC 27
ASSIGN BREAKLINE_FC 161
ENABLE GRAPHICS                   ! To get the formed triangulation
                                    on the graphical display.
FILEOUT  Filename                 ! Output Files name create and
                                    open (*.NOD and  *.DTA)
FRT                               ! Feature Representation Table
                                    name.
FILEIN  Filename                  ! Input File name, to be opened for
                                    data input(IFF Format).
GO                                ! Starts the triangulation.
                                    (Initiates the processing of the
                                    data).
```

TRIDER Module. ! Slope Derivative Estimation Module at each data point in the triangulation. Also provides z values for the imaginary points generated around the edge of the triangulation by TRIANG. Once TRIDER has been used to generate a slope derivative file many subsequent runs of TRIGRID may be made to produce DEM grids at differing resolutions.

TRIDER

ENABLE DIAGNOSTICS	! Enables diagnostic printout.
ZLIMITS zmin. zmax	! Min and max limits height estimation of imaginary points.
ENABLE GRAPHICS	! To get the formed slope derivatives on the graphical display.
IMAGINARY BOX QUARTIC 0.0	! TRIDER provides four interpolation options. Of those, the following two were suitable for the current experiment: BOX - interpolate heights on the basis of known heights found using an expanding hollow box search. This option provides a very smooth edge around the data area and SHELLNEIGHBOUR - interpolate heights from nodes in expanding shells of neighbours. Four interpolation techniques are provided for the BOX and SHELLNEIGHBOUR interpolation options: UNWEIGHTED, LINEAR, QUADRATIC, or QUARTIC. To keep the imaginary points close to the grid a parameter 0.0 is chosen. From the interpolation options the QUADRATIC or the QUARTIC degree are the more suitable, as the highest degree function. This is decided because of the test area roughness (average slope 40%) and "random appearance"of the systematic error in the SPOT data.
FILEIN Filename	! Input File names (*.NOD and *.DTA)
GO	! Starts the Slope Derivatives estimation.

TRIGRID Module. ! Takes the triangulation created by TRIANG and the Slope Derivative file produced by TRIDER. and forms the triangulation on the user specified grid.

```
TRIGRID
ENABLE DIAGNOSTICS                ! Enables diagnostic printout.
WINDOW  xmin ymin  xmax ymax      ! Specifies the limits of the
                                    triangulation area to be gridded.
SIDELENGTH x y-sidelength         ! The spacing between DEM posts
                                    (nodes) along x axis (columns)
                                    and y axis (rows). From the
                                    SIDELENGTH the software
                                    estimates the number of the
                                    rows and the number of the
                                    columns of the DEM.
FILEIN  Filename                  !  Input File name (*.DER).
FILEOUT  Filename                 !  Output File name (*.DTI)
ENABLE GRAPHICS                   ! To display the formed
                                    Triangulation on the user
                                    specified grid.
ENABLE SMOOTH                     ! Enables grid point estimation by
                                    smooth patches. Smooth patch
                                    estimation tends to give a more
                                    rounded smooth appearance to a
                                    DEM surface than given by linear
                                    facets. If smooth patch
                                    interpolation is selected,
                                    individual triangle interpolation
                                    limits are applied. Linear facet
                                    interpolation, by definition, does
                                    not need to apply interpolation as
                                    interpolation is restricted to the
                                    triangle facet plane (default).
                                    This option applied for the
                                    interpolation of the SPOT data.
DISABLE SMOOTH                    ! Disables grid point estimation by
                                    smooth patches. Grid heights are
                                    instead estimated using linear
                                    interpolation across the triangle
                                    facet planes.
ENABLE TRACE                      ! Trace along original data strings
                                    for up-hill/ down hill side of line
                                    information.
DATA_TYPE REAL                    ! The output DEM posts as real
                                    (floating point). The DTI file to be
                                    created can not be used for
                                    display, while it can be used for
                                    retrieving the interpolated height
                                    values through the DTI2TEXT
                                    module. By default data type
                                    WORD (integer height values) are
                                    generated.
GO                                ! Starts the Triangulation.
```

DTIVIEW Module. ! For producing a perspective or isometric views of a DEM for validation or display purposes. DTI data should be type WORD.

DTIVIEW

FILE input_Filename	!	Input file (*.DTI) created by TRIGRID.
WINDOW xmin ymin xmax ymax	!	Specifies an area of interest in the input DEM. (Matrix coverage SW, NE).
ENABLE GRAPHICS	!	To display the Perspective or isometric view.
ENABLE FISHNET	!	Enable of producing a fishnet representation (drawing of terrain view as a grid rather than a series of profiles along just one DEM axes) when the ISOMETRIC or PERSPECTIVE command is given. Default is not enable.
ENABLE IFF_OUTPUT filename	!	IFF file which contains vector data. This enable a terrain view to be subsequently plotted on a device such a plotter, edited in LITES2, or manipulated using IFF utilities.
IFF WINDOW xmin ymin xmax ymax	!	To enable the registration of the IFF data to the DEM.
SHOW IFF	!	Checks the IFF range and IFF window.
SAMPLE row column	!	eg. 3 3 It gives a quick look. (Default 1 1)
LUT file specification	!	Select a colour table.
COLOURS number	!	Defines the number of colours used to display an isometric or perspective view on a colour graphics device.
LABEL SIZE character_size	!	Specifies the character size of text output to the screen using the DRAW LABEL command.
LABEL POSITION screen_x screen_y	!	Defines the position of a label on the graphics screen.
DRAW LABEL user specified text	!	Outputs a text string to the display screen of a graphics device.

THETA rotation_angle	!	Defines the amount of rotation applied to the y-axis of an isometric view (ie the tilt of an isometric view).
PHI rotation_angle	!	Defines the amount of rotation applied to the terrain view in the x axis.
DIRECTION direction	!	Defines the direction of view (default WEST)
ZSCALE scale_factor	!	Defines the vertical exaggeration that is applied to all DEM heights when generating a profile, or an isometric, or a perspective view (default 1.0 ,no exaggeration applied).
HEIGHT height_of_view	!	Defines the height above sea level of the view point. The parameter is used when generating a perspective view (default 300m).
ZLIMITS lower_height upper_height	!	Allocates the display colours only to height values that lie within the specified height range.
ZSTEP height_interval	!	Defines the height interval used when displaying an isometric or perspective view on a colour graphics device.
ISOMETRIC	!	Generate an isometric terrain view.
SHOW VIEW	!	Displays the current values of all viewing parameters controlling the form of an isometric or perspective view.
LEGEND SIZE scale_factor	!	Defines the size of the legend.
LEGENDPOSITION screen_x screen_y	!	Generates a legend on the graphics screen.
DRAW LEGEND	!	The legend relates the colours in the terrain view, to their DTM height values.

DTICONTOUR Module. ! A TVES package contouring module. It is a bilinear contour utility, using data contained in a DTI file. Contour smoothing may be optionally applied using a least square filter.

```
DTICONTOUR
FILEIN Filename                    ! Input File name (*.DTI).
WINDOW xmin ymin xmax ymax         ! Matrix window (area to be
                                     contoured).
ZLIMITS Real1 Real2                ! Minimum Maximum Z value in
                                     the input data.
FILEOUT Filename                   ! Output File name (*.IFF) in
                                     binary form.
ENABLE LABELLING                   ! Enable the generation of contour
                                     and spot height label features.
INTERVAL interval                  ! Specifies the height interval
                                     between successive contours
                                     (used interval 20 m).
INDEX_INTERVAL interval            ! Specifies the height interval
                                     between successive index contours
                                     (used interval 100 m).
SET SPOT_FC feature_code           ! Set IFF feature code of spot height
                                     features to the specified value.
SET CONTOUR_FC feature_code        ! Set IFF feature code of contour
                                     features to the specified value.
ENABLE SPOT_HEIGHTS                ! Causes DTICONTOUR to output any
                                     single point spot height features
                                     to the IFF file.
SET SPOT_LABEL_FC feature_code     ! Set IFF feature code of label
                                     features for Spot heights to the
                                     specified value.
LABEL MODULUS height               ! Specifies the height modulus for
                                     index contour labelling.
LABEL INDEX_MODULUS height         ! A real value specifies the height
                                     modulus for index contour
                                     labelling (used height 100.0 m).
LABEL INTEGER                      ! Specifies that contour labels are
                                     to be displayed as integer
                                     numbers.
LABEL MAX CURVE real               ! A real value in the range 0.0 to
                                     1.0 which determines the
                                     maximum rate of change of
                                     curvature along along a line
                                     before that section of line is
                                     considered to be unsuitable for
                                     labelling. Default 0.7 (used value
                                     0.4).
ENABLE FRAME                       ! Enable to output a frame feature
                                     to the IFF file.
SHOW DEFAULTS                      ! Shows current status of
                                     DTICONTOUR defaults.
GO                                 ! Do the contouring.
```

ROVER Module ! Is a TVES package displaying module. It plots contours from an IFF file, output from DTICONTOUR module, or an image generated from TRIGRID module (*.DTI).

ROVER

FRT file specification ! Feature Representation Table filename.

IFF input_filename ! File created from DTICONTOUR module (*.IFF). The module can accepts also (*.DTI) files created from the TRIGRID module or elsewhere (NE1.FOR program).

LABEL COLOUR overlay_colour ! Selects the colour of user labelling.

LABEL SIZE character_size ! Specifies the character size of text output to the screen using the DRAW LABEL command.

LABEL POSITION screen_x screen_y! Defines the position of a label on the graphics screen.

DRAW LABEL user specified text ! Outputs a text string to the display screen of a graphics device.

DISPLAY ! Is the raster drawing command that will output grid information contained in a IFF file, to the graphics screen in colour coded form.

APPENDIX I.

Estimation of the semivariance and variogram values for the Aix En Provence test area.

I. Estimation of the semivariance values for the Aix En Provence test area.

Three main terms (semivariance, semivariogram and variogram) are used by scientists in geostatistics and in photogrammetry. Although in practice these terms are often presumed to be synonymous, in reality they are not the same. Because a little confusion arises the following definitions are provided to simplify and to standardise the use of these three terms.

The semivariogram or semivariance is estimated from the following formula (see also § 7.3.1):

$$\gamma(h) = \Sigma_{i}^{n-h} \left(H(i)-H(i+h)\right)^2 / 2n$$

The "semi" refers to the factor 1/2, but some authors sloppily call it variogram.

The semivariogram, γ, is a graph (and/or formula) describing the expected difference in value between pairs of samples with a given relative orientation. In the calculation procedure only the "experimental" semivariogram $\gamma^*(h)$ is used. The experimental semivariogram γ^* bears the same relationship to γ that a histogram does to a probability distribution. In the following estimation the experimental semivariogram term is used.

The aerial photography derived elevation measurements cover an area of 87 sqkm in a 30 m regular grid. The area has not a canonical geometrical shape (see figure 5.3). The normal shape area has E-W size of 12420 m by N-S size 6900 m (231 rows x 415 columns). The minimum elevation is 191.7 m and the maximum is 1011.0 m. For this area the experimental variogram values are calculated as follows:

Consider that we have elevation data in a regular grid. In this project each regular grid node contains a height value. This is a two-dimensional problem, so that the h according to the semivariogram definition depends on the distance between the pair of samples, and their relative orientation in a two-dimensional plane.

In order to construct an experimental semivariogram a direction is chosen (ie. east-west direction). The grid interval is constant (30 m for the aerial photography data), so that we calculate the values for the experimental semivariogram, γ *, for distances which are multiple of this. At zero we know that γ *(0) is equal to zero. At 30 m we need to find all pairs of samples at a separation of 30 m in the East-West direction.

The calculation as defined says: take each pair; measure the difference in height value between the two samples; square them; add up all the squares; divide this sum by twice the number of pairs.

This procedure gives a single point $\gamma^*(30)$ which can be plotted on a graph of the experimental semivariogram (γ^*) versus the distance between the samples (h).

Then we consider a distance between samples of 2 x 30 m. This procedure gives a second point; an estimation of the semivariogram value $\gamma^*(60)$ which we can plot again on the graph. The question now arises of where to stop. We could obviously continue up to 12420 m (the length of the area). In practice we rarely go past about half of the total sampled extent (6210 m).

The calculated semivariogram values correspond to the total test area in the East-West and North-South direction. The distance between samples for which the semivariogram value is estimated is $(12420 \times 6900)^{1/2} = 7110$ m.

In case that the diagonal semivariogram values are estimated the intervals will be multiples of $30*\sqrt{2} = 42.43$ m.

The distance between samples (lags) appear in the second column. The number of pairs appear in the third column and the semivariance (experimental semivariogram) values appear in the fourth column. The fifth column includes the variogram values which are the values of the fourth column multiplied by 2. The sixth, seventh and eighth column contain the natural logarithms of the distance

(lag), semivariance and variogram respectively.

The semivariogram values of elevations representing all the Aix En Provence test area appear in figure 7.2.

StatWorks™ Data

	Distance h (m)	Number of pairs	Semivariance	Variogram	Ln Distance	Ln semivar	Ln Variogram
1	30	381524	51.695	103.3900	3.4012	3.9454	4.6385
2	60	570030	135.219	270.4380	4.0943	4.9069	5.6000
3	90	757250	238.760	477.5200	4.4998	5.4755	6.1686
4	120	1506798	388.792	777.5840	4.7875	5.9630	6.6562
5	150	1313148	560.477	1120.9540	5.0106	6.3288	7.0219
6	180	1867156	737.800	1475.6000	5.1930	6.6037	7.2968
7	210	1860108	928.144	1856.2880	5.3471	6.8332	7.5263
8	240	2222432	1131.868	2263.7360	5.4806	7.0316	7.7248
9	270	3133056	1374.154	2748.3080	5.5984	7.2256	7.9187
10	300	2570086	1626.024	3252.0480	5.7038	7.3939	8.0870
11	330	3287854	1877.620	3755.2400	5.7991	7.5378	8.2309
12	360	3094234	2130.932	4261.8640	5.8861	7.6643	8.3575
13	390	3983424	2416.748	4833.4960	5.9661	7.7902	8.4833
14	420	3966320	2711.830	5423.6600	6.0403	7.9054	8.5985
15	450	3772720	2988.356	5976.7120	6.1092	8.0025	8.6956
16	480	5003546	3308.032	6616.0640	6.1738	8.1041	8.7973
17	510	4980222	3644.060	7288.1200	6.2344	8.2009	8.8940
18	540	4957006	3978.541	7957.0820	6.2916	8.2887	8.9818
19	570	5112696	4294.924	8589.8480	6.3456	8.3652	9.0583
20	600	4919124	4596.275	9192.5500	6.3969	8.4330	9.1261
21	630	6285576	4968.151	9936.3020	6.4457	8.5108	9.2040
22	660	6088154	5306.320	10612.6400	6.4922	8.5767	9.2698
23	690	6230506	5674.541	11349.0820	6.5367	8.6437	9.3369
24	720	6206022	6003.738	12007.4760	6.5793	8.7001	9.3933
25	750	7205586	6368.676	12737.3520	6.6201	8.7591	9.4523
26	780	6998906	6744.982	13489.9640	6.6593	8.8166	9.5097
27	810	6801724	7079.663	14159.3260	6.6970	8.8650	9.5581
28	840	7779568	7464.444	14928.8880	6.7334	8.9179	9.6111
29	870	7244380	7801.800	15603.6000	6.7685	8.9621	9.6553
30	900	8375490	8201.766	16403.5320	6.8024	9.0121	9.7053
31	930	8007014	8554.918	17109.8360	6.8352	9.0543	9.7474
32	960	7809906	8883.962	17767.9240	6.8669	9.0920	9.7852
33	990	8591236	9290.136	18580.2720	6.8977	9.1367	9.8299
34	1020	9212084	9631.867	19263.7340	6.9276	9.1728	9.8660
35	1050	9164136	10033.082	20066.1640	6.9565	9.2136	9.9068
36	1080	9292486	10356.863	20713.7260	6.9847	9.2454	9.9386
37	1110	9081918	10742.869	21485.7380	7.0121	9.2820	9.9751
38	1140	9999506	11133.313	22266.6260	7.0388	9.3177	10.0108
39	1170	9479016	11451.559	22903.1180	7.0648	9.3459	10.0390
40	1200	10539616	11872.969	23745.9380	7.0901	9.3820	10.0752
41	1230	9870980	12133.307	24266.6140	7.1148	9.4037	10.0969
42	1260	10444560	12551.285	25102.5700	7.1389	9.4376	10.1307
43	1290	10864988	12904.842	25809.6840	7.1624	9.4654	10.1585
44	1320	10351866	13202.943	26405.8860	7.1854	9.4882	10.1813
45	1350	11221966	13633.619	27267.2380	7.2079	9.5203	10.2134
46	1380	10722898	13846.136	27692.2720	7.2298	9.5358	10.2289
47	1410	11733516	14279.157	28558.3140	7.2513	9.5666	10.2597
48	1440	11680688	14583.786	29167.5720	7.2724	9.5877	10.2808
49	1470	11944580	14829.101	29658.2020	7.2930	9.6043	10.2975
50	1500	12013622	15286.656	30573.3120	7.3132	9.6347	10.3279
51	1530	12116614	15521.634	31043.2680	7.3330	9.6500	10.3431
52	1560	12941606	15938.542	31877.0840	7.3524	9.6765	10.3696
53	1590	11854892	16091.739	32183.4780	7.3715	9.6861	10.3792
54	1620	12524780	16495.868	32991.7360	7.3902	9.7109	10.4040
55	1650	13052112	16796.725	33593.4500	7.4085	9.7289	10.4221
56	1680	12560710	16985.781	33971.5620	7.4265	9.7401	10.4333
57	1710	13795294	17409.242	34818.4840	7.4442	9.7648	10.4579
58	1740	12295442	17511.153	35022.3060	7.4616	9.7706	10.4637
59	1770	14241210	17920.983	35841.9660	7.4787	9.7937	10.4869
60	1800	13737190	18181.180	36362.3600	7.4955	9.8081	10.5013
61	1830	13253816	18333.873	36667.7460	7.5121	9.8165	10.5097

StatWorks™ Data

	Distance h (m)	Number of pairs	Semivariance	Variogram	Ln Distance	Ln semivar	Ln Variogram
62	1860	14297720	18796.143	37592.2860	7.5283	9.8414	10.5346
63	1890	12984744	18801.552	37603.1040	7.5443	9.8417	10.5348
64	1920	15570962	19250.277	38500.5540	7.5601	9.8653	10.5584
65	1950	14100630	19387.950	38775.9000	7.5756	9.8724	10.5656
66	1980	14872682	19587.021	39174.0420	7.5909	9.8826	10.5758
67	2010	14633660	19965.458	39930.9160	7.6059	9.9018	10.5949
68	2040	14439272	20051.264	40102.5280	7.6207	9.9060	10.5992
69	2070	15436040	20460.776	40921.5520	7.6353	9.9263	10.6194
70	2100	14689166	20573.301	41146.6020	7.6497	9.9317	10.6249
71	2130	14757650	20737.207	41474.4140	7.6639	9.9397	10.6328
72	2160	16274758	21105.809	42211.6180	7.6779	9.9573	10.6505
73	2190	15010712	21116.282	42232.5640	7.6917	9.9578	10.6509
74	2220	15838408	21517.910	43035.8200	7.7053	9.9766	10.6698
75	2250	15238024	21620.477	43240.9540	7.7187	9.9814	10.6745
76	2280	16209312	21866.580	43733.1600	7.7319	9.9927	10.6859
77	2310	16515868	22040.568	44081.1360	7.7450	10.0006	10.6938
78	2340	15517842	22202.647	44405.2940	7.7579	10.0080	10.7011
79	2370	16203350	22475.735	44951.4700	7.7706	10.0202	10.7133
80	2400	15994234	22609.407	45218.8140	7.7832	10.0261	10.7193
81	2430	17320432	22833.844	45667.6880	7.7956	10.0360	10.7291
82	2460	16451916	23011.905	46023.8100	7.8079	10.0438	10.7369
83	2490	16366472	23175.294	46350.5880	7.8200	10.0508	10.7440
84	2520	16410502	23315.682	46631.3640	7.8320	10.0569	10.7500
85	2550	17435018	23561.303	47122.6060	7.8438	10.0674	10.7605
86	2580	17089902	23766.215	47532.4300	7.8555	10.0760	10.7692
87	2610	16873456	23895.077	47790.1540	7.8671	10.0814	10.7746
88	2640	16655208	24092.078	48184.1560	7.8785	10.0896	10.7828
89	2670	18031548	24269.631	48539.2620	7.8898	10.0970	10.7901
90	2700	17089890	24339.274	48678.5480	7.9010	10.0998	10.7930
91	2730	17577934	24671.656	49343.3120	7.9121	10.1134	10.8066
92	2760	17249762	24751.107	49502.2140	7.9230	10.1166	10.8098
93	2790	17849786	25043.489	50086.9780	7.9338	10.1284	10.8215
94	2820	17408058	25113.829	50227.6580	7.9445	10.1312	10.8243
95	2850	17659740	25307.925	50615.8500	7.9551	10.1389	10.8320
96	2880	17803028	25435.782	50871.5640	7.9655	10.1439	10.8371
97	2910	18057352	25579.723	51159.4460	7.9759	10.1496	10.8427
98	2940	19424614	25940.584	51881.1680	7.9862	10.1636	10.8567
99	2970	17264594	25916.700	51833.4000	7.9963	10.1626	10.8558
100	3000	18530670	26196.224	52392.4480	8.0064	10.1734	10.8665
101	3030	17184764	26235.973	52471.9460	8.0163	10.1749	10.8680
102	3060	18993336	26504.360	53008.7200	8.0262	10.1851	10.8782
103	3090	19074200	26832.733	53665.4660	8.0359	10.1974	10.8905
104	3120	17548350	26773.024	53546.0480	8.0456	10.1952	10.8883
105	3150	18637530	27111.387	54222.7740	8.0552	10.2077	10.9009
106	3180	18336622	27117.211	54234.4220	8.0646	10.2079	10.9011
107	3210	18868126	27377.353	54754.7060	8.0740	10.2175	10.9106
108	3240	19065894	27596.830	55193.6600	8.0833	10.2255	10.9186
109	3270	18457092	27527.198	55054.3960	8.0925	10.2229	10.9161
110	3300	19572640	27962.785	55925.5700	8.1017	10.2386	10.9318
111	3330	18104680	27888.363	55776.7260	8.1107	10.2360	10.9291
112	3360	18916694	28202.870	56405.7400	8.1197	10.2472	10.9403
113	3390	18812666	28273.884	56547.7680	8.1286	10.2497	10.9428
114	3420	19041470	28268.776	56537.5520	8.1374	10.2495	10.9427
115	3450	19594876	28641.486	57282.9720	8.1461	10.2626	10.9558
116	3480	19113360	28504.294	57008.5880	8.1548	10.2578	10.9510
117	3510	18951404	29785.536	59571.0720	8.1634	10.3018	10.9949
118	3540	18747482	28811.640	57623.2800	8.1719	10.2685	10.9617
119	3570	18940330	28899.397	57798.7940	8.1803	10.2716	10.9647
120	3600	19793482	29145.050	58290.1000	8.1887	10.2800	10.9732
121	3630	19633356	28980.745	57961.4900	8.1970	10.2744	10.9675
122	3660	19350000	29258.002	58516.0040	8.2052	10.2839	10.9771

StatWorks™ Data

	Distance h (m)	Number of pairs	Semivariance	Variogram	Ln Distance	Ln semivar	Ln Variogram
123	3690	19827444	29317.063	58634.1260	8.2134	10.2859	10.9791
124	3720	18914020	29362.494	58724.9880	8.2215	10.2875	10.9806
125	3750	19261980	29542.050	59084.1000	8.2295	10.2936	10.9867
126	3780	19086514	29414.629	58829.2580	8.2375	10.2892	10.9824
127	3810	20249386	29738.859	59477.7180	8.2454	10.3002	10.9934
128	3840	19090230	29694.398	59388.7960	8.2532	10.2987	10.9919
129	3870	19611132	29831.856	59663.7120	8.2610	10.3033	10.9965
130	3900	19124540	29823.715	59647.4300	8.2687	10.3031	10.9962
131	3930	19289752	29829.937	59659.8740	8.2764	10.3033	10.9964
132	3960	19940906	30134.545	60269.0900	8.2840	10.3134	11.0066
133	3990	19478410	29998.520	59997.0400	8.2915	10.3089	11.0021
134	4020	19891994	30090.942	60181.8840	8.2990	10.3120	11.0051
135	4050	19106660	30170.230	60340.4600	8.3065	10.3146	11.0078
136	4080	20148048	30217.887	60435.7740	8.3139	10.3162	11.0093
137	4110	19287064	30262.284	60524.5680	8.3212	10.3177	11.0108
138	4140	19085690	30203.720	60407.4400	8.3285	10.3157	11.0089
139	4170	19910998	30318.505	60637.0100	8.3357	10.3195	11.0127
140	4200	19928182	30366.740	60733.4800	8.3428	10.3211	11.0143
141	4230	19614742	30381.089	60762.1780	8.3500	10.3216	11.0147
142	4260	19231338	30319.517	60639.0340	8.3570	10.3195	11.0127
143	4290	18843412	30282.108	60564.2160	8.3640	10.3183	11.0115
144	4320	20216552	30462.192	60924.3840	8.3710	10.3242	11.0174
145	4350	19998888	30317.484	60634.9680	8.3779	10.3195	11.0126
146	4380	19580970	30386.377	60772.7540	8.3848	10.3217	11.0149
147	4410	19143982	30225.594	60451.1880	8.3916	10.3164	11.0096
148	4440	19827042	30226.377	60452.7540	8.3984	10.3165	11.0096
149	4470	19872376	30378.880	60757.7600	8.4051	10.3215	11.0147
150	4500	18868504	30156.052	60312.1040	8.4118	10.3141	11.0073
151	4530	19820440	30288.191	60576.3820	8.4185	10.3185	11.0117
152	4560	18683762	30024.335	60048.6700	8.4251	10.3098	11.0029
153	4590	19998134	30202.700	60405.4000	8.4316	10.3157	11.0088
154	4620	19238886	30041.761	60083.5220	8.4381	10.3103	11.0035
155	4650	18872364	29923.603	59847.2060	8.4446	10.3064	10.9996
156	4680	19541148	30013.261	60026.5220	8.4511	10.3094	11.0025
157	4710	19736296	29844.340	59688.6800	8.4574	10.3038	10.9969
158	4740	19556612	29829.488	59658.9760	8.4638	10.3033	10.9964
159	4770	18737000	29684.258	59368.5160	8.4701	10.2984	10.9915
160	4800	18674130	29611.854	59223.7080	8.4764	10.2959	10.9891
161	4830	19805334	29727.959	59455.9180	8.4826	10.2998	10.9930
162	4860	18899666	29468.348	58936.6960	8.4888	10.2911	10.9842
163	4890	19523988	29453.209	58906.4180	8.4949	10.2906	10.9837
164	4920	18654640	29330.310	58660.6200	8.5011	10.2864	10.9795
165	4950	19200824	29343.498	58686.9960	8.5071	10.2868	10.9800
166	4980	19109670	29257.129	58514.2580	8.5132	10.2839	10.9770
167	5010	18353910	29097.246	58194.4920	8.5192	10.2784	10.9715
168	5040	19000678	29099.433	58198.8660	8.5252	10.2785	10.9716
169	5070	19090960	28998.172	57996.3440	8.5311	10.2750	10.9681
170	5100	19105752	28943.566	57887.1320	8.5370	10.2731	10.9663
171	5130	18949452	28863.151	57726.3020	8.5429	10.2703	10.9635
172	5160	17660742	28760.579	57521.1580	8.5487	10.2668	10.9599
173	5190	19008310	28723.015	57446.0300	8.5545	10.2655	10.9586
174	5220	18589378	28754.723	57509.4460	8.5603	10.2666	10.9597
175	5250	18298038	28568.238	57136.4760	8.5660	10.2601	10.9532
176	5280	18592006	28575.666	57151.3320	8.5717	10.2603	10.9535
177	5310	18027620	28419.411	56838.8220	8.5773	10.2548	10.9480
178	5340	18824792	28485.282	56970.5640	8.5830	10.2571	10.9503
179	5370	18110408	28443.376	56886.7520	8.5886	10.2557	10.9488
180	5400	18381382	28262.121	56524.2420	8.5942	10.2493	10.9424
181	5430	17971762	28295.823	56591.6460	8.5997	10.2505	10.9436
182	5460	18172466	28244.820	56489.6400	8.6052	10.2487	10.9418
183	5490	17936376	28213.624	56427.2480	8.6107	10.2476	10.9407

StatWorks™ Data

	Distance h (m)	Number of pairs	Semivariance	Variogram	Ln Distance	Ln semivar	Ln Variogram
184	5520	17724020	28217.701	56435.4020	8.6161	10.2477	10.9409
185	5550	17539036	27978.376	55956.7520	8.6216	10.2392	10.9323
186	5580	17795626	28122.245	56244.4900	8.6269	10.2443	10.9375
187	5610	17926534	27983.332	55966.6640	8.6323	10.2394	10.9325
188	5640	17648366	28054.964	56109.9280	8.6376	10.2419	10.9351
189	5670	17423416	27999.303	55998.6060	8.6429	10.2399	10.9331
190	5700	17063140	27778.104	55556.2080	8.6482	10.2320	10.9252
191	5730	17799004	27994.992	55989.9840	8.6535	10.2398	10.9329
192	5760	17060756	27742.857	55485.7140	8.6587	10.2307	10.9239
193	5790	17307460	27839.169	55678.3380	8.6639	10.2342	10.9273
194	5820	17056922	27746.038	55492.0760	8.6691	10.2308	10.9240
195	5850	17216610	27790.184	55580.3680	8.6742	10.2324	10.9256
196	5880	17000798	27823.343	55646.6860	8.6793	10.2336	10.9268
197	5910	17059976	27564.571	55129.1420	8.6844	10.2243	10.9174
198	5940	16383592	27672.936	55345.8720	8.6895	10.2282	10.9214
199	5970	17009400	27651.290	55302.5800	8.6945	10.2274	10.9206
200	6000	16187302	27664.684	55329.3680	8.6995	10.2279	10.9211
201	6030	16274318	27733.304	55466.6080	8.7045	10.2304	10.9235
202	6060	16578658	27434.060	54868.1200	8.7095	10.2195	10.9127
203	6090	16069240	27629.619	55259.2380	8.7144	10.2266	10.9198
204	6120	16516676	27522.357	55044.7140	8.7193	10.2228	10.9159
205	6150	15580208	27576.453	55152.9060	8.7242	10.2247	10.9179
206	6180	16073388	27526.611	55053.2220	8.7291	10.2229	10.9161
207	6210	15746524	27444.692	54889.3840	8.7339	10.2199	10.9131
208	6240	16000050	27671.920	55343.8400	8.7387	10.2282	10.9213
209	6270	15986030	27341.166	54682.3320	8.7435	10.2161	10.9093
210	6300	15036282	27615.473	55230.9460	8.7483	10.2261	10.9193
211	6330	15346028	27311.495	54622.9900	8.7531	10.2151	10.9082
212	6360	15527016	27552.018	55104.0360	8.7578	10.2238	10.9170
213	6390	15043480	27599.830	55199.6600	8.7625	10.2256	10.9187
214	6420	15408082	27279.562	54559.1240	8.7672	10.2139	10.9070
215	6450	14384218	27591.196	55182.3920	8.7718	10.2253	10.9184
216	6480	15204026	27266.011	54532.0220	8.7765	10.2134	10.9065
217	6510	14821012	27511.866	55023.7320	8.7811	10.2224	10.9155
218	6540	14100416	27446.482	54892.9640	8.7857	10.2200	10.9131
219	6570	15075028	27305.650	54611.3000	8.7903	10.2148	10.9080
220	6600	14113234	27714.416	55428.8320	8.7948	10.2297	10.9229
221	6630	14589526	27234.923	54469.8460	8.7994	10.2123	10.9054
222	6660	14011106	27399.698	54799.3960	8.8039	10.2183	10.9114
223	6690	13753858	27302.353	54604.7060	8.8084	10.2147	10.9079
224	6720	13607510	27136.311	54272.6220	8.8128	10.2086	10.9018
225	6750	14081780	27712.720	55425.4400	8.8173	10.2296	10.9228
226	6780	13799380	27000.458	54000.9160	8.8217	10.2036	10.8968
227	6810	13358164	27467.968	54935.9360	8.8261	10.2208	10.9139
228	6840	13349354	27141.380	54282.7600	8.8305	10.2088	10.9020
229	6870	13293726	27182.401	54364.8020	8.8349	10.2103	10.9035
230	6900	13085382	27504.462	55008.9240	8.8393	10.2221	10.9153
231	6930	12985532	26772.895	53545.7900	8.8436	10.1951	10.8883
232	6960	12750321	27257.230	54514.4600	8.8479	10.2131	10.9062
233	6990	12904814	26933.096	53866.1920	8.8522	10.2011	10.8943
234	7020	12510837	27020.491	54040.9820	8.8565	10.2044	10.8975
235	7050	12322440	26933.300	53866.6000	8.8608	10.2011	10.8943
236	7080	12304027	26755.708	53511.4160	8.8650	10.1945	10.8877
237	7110	12310902	27089.431	54178.8620	8.8693	10.2069	10.9000